Insights into the evolution of cellular and regulatory processes in mixoplankton

Dissertation

zur Erlangung des Akademischen Grades eines
Doktors der Naturwissenschaften
-Dr. rer. nat.-
im Fachbereich 2 Biologie/Chemie der Universität Bremen

vorgelegt von

Konstantinos Anestis

Bremen, 2022

Datum des Kolloquiums: 31.03.2022

1. **Gutachter:** Dr. Fabrice Not

Station Biologique de Roscoff, CNRS/Sorbonne Université

2. **Gutachter:** Prof. Per Juel Hansen

Marine Biology Section, University of Copenhagen

Table of Contents

Versicherung an Eides Statt

Ich, Konstantinos Anestis,

versichere an Eides Statt durch meine Unterschrift, dass ich die vorstehende Arbeit selbständig und ohne fremde Hilfe angefertigt und alle Stellen, die ich wörtlich dem Sinne nach aus Veröffentlichungen entnommen habe, als solche kenntlich gemacht habe, mich auch keiner anderen als der angegebenen Literatur oder sonstiger Hilfsmittel bedient habe.
Ich versichere an Eides Statt, dass ich die vorgenannten Angaben nach bestem Wissen und Gewissen gemacht habe und dass die Angaben der Wahrheit entsprechen und ich nichts verschwiegen habe.
Die Strafbarkeit einer falschen eidesstattlichen Versicherung ist mir bekannt, namentlich die Strafandrohung gemäß § 156 StGB bis zu drei Jahren Freiheitsstrafe oder Geldstrafe bei vorsätzlicher Begehung der Tat bzw. gemäß § 161 Abs. 1 StGB bis zu einem Jahr Freiheitsstrafe oder Geldstrafe bei fahrlässiger Begehung.

Bremen, den 7 Januar 2022

Konstantinos Anestis

Acknowledgements

There are many people I would like to thank for making this thesis possible.

Firstly, I would like to thank my supervisor Uwe John for his support and guidance. Thank you Uwe for all your feedback and effort.

Many thanks to Aditee Mitra for creating the MixITiN consortium and offering me the opportunity to be a member of this amazing network.

Many thanks to Per Juel Hansen for always welcoming me at your lab and sharing your excitement for science with me. I look forward to working with you again in the future.

Thank you Vivi Pitta and Xabier Irigoien for your hospitality during my secondments.

Thank you Sylke for always having time for my questions and for your precious advice. I learned so much from you and it has been just amazing working with you!

Thanks to Gurjeet Kohli and Elisabeth Varga. It was a pleasure collaborating with you.

Special thanks to my MixITiN fellow colleagues, for not only sharing our excitement for science but also supporting each other in difficult times. Thanks to Anna, Lisa, Claudia, Andreas, Nikola, Gui, Mena and Jon.

Thanks Maira for being an amazing colleague but also an extremely good friend. Ti voglio tanto bene!

Thank you Joost for accepting my invitation to write the review together. We also managed to write together so many reports for the project and we still talk to each other (that's an achievement).

Thanks to all the members of the working group for always being supportive and compassionate. Thanks to Antonia, Nancy, Cora, Sabrina, Stephanie, Kerstin and Anne.

Special thanks to my beloved office mate Claudia, for being a genuine friend and always being there when I needed to share personal and PhD related difficulties.

Thanks to Thanasis for being the best friend in the world.

Finally, thanks to my friends and family for your support.

I hope I didn't forget anyone.

Summary

Mixoplankton are key organisms in marine ecosystems, due to their ability to combine the two nutrition strategies of phototrophy and phagotrophy. Their dual mode of nutrition has major impact on trophic food webs and general biogeochemical cycles. Processes that are related to phagotrophy and phototrophy include the production of toxins for subsequent prey lysis and uptake, and the ability to sequester plastids (kleptoplasts) from photosynthetic prey. The studies presented in this thesis aim to (i) explore the processes of phagotrophy and phototrophy in marine protists in an evolutionary context, (ii) to extend our knowledge on the underlying mechanisms of toxin biosynthesis in the mixoplanktonic species *Prymnesium parvum*, (iii) to investigate the physiology and driving factors of phagotrophy in *P. parvum* under different treatments, (iv) to elucidate the molecular mechanisms involved in functionality of kleptoplasts in the ciliate *Strombidium* cf. *basimorphum*.

As a prerequisite for the subsequent experimental studies, a meticulous literature review was performed in order to gain better understanding of the evolutionary aspects of mixotrophy. Current literature evidences support the idea that mixoplankton are ideal organisms for studying processes such as the establishment of permanent plastids. Such evidences include the transfer of photosynthesis related genes from prey and/or endosymbionts to the host.

In this thesis, the transcriptomes of nine different *P. parvum* strains, known to produce different types of the toxin prymnesin, were generated and analyzed for the presence of polyketide synthase genes (PKSs). The toxic and mixotrophic *P. parvum* harbors numerous polyketide synthases and their abundance is independent of the toxin content of the corresponding strains. The evolutionary origin of PKSs in *P. parvum* was assessed using phylogenetics. Moreover, the functional and structural annotations of the PKS encoding transcripts for all nine *P. parvum* strains are reported. The expression pattern of genes associated with increasing toxin content is shown, and indicates a general downregulation of genes involved in metabolic processes. As a result, these molecular trade-offs suggest higher metabolic rates in strains with lower toxin content.

Different treatments of salinity and phosphorus availability (P) were used in order to investigate physiological and transcriptomic responses in *P. parvum* strain UIO223. The increased growth rates observed in cells growing under low salinity were depicted in the gene expression

data, with upregulation of genes involved in catabolic processes under low salinity. Additionally, incubations of *P. parvum* with the cryptophyte prey *Teleaulax acuta* showed that phagotrophy in *P. parvum* was enhanced under P starvation suggesting that phagotrophy in *P. parvum* might serve as a mechanism for compensating macronutrient limitation. However, prey mortality was significantly higher under low salinity, showing that salinity and P differently influence the processes of cell lysis and uptake. Genes involved in endocytosis were upregulated under both low salinity and phosphorus starved monocultures of *P. parvum*, highlighting the evolutionary conservation of prey uptake mechanisms even in absence of prey. Toxin content in *P. parvum* showed a considerable increase at high cell density conditions, suggesting the occurrence of cell density dependent mechanisms that regulate toxin production.

Single-cell transcriptomics were used to study the genetic mechanisms involved in the establishment of plastidic endosymbiosis in *Strombidium* cf. *basimorphum.* The ciliate retains prey genetic material from its cryptophyte prey, and the presence of genes related to transcription and translation suggests that the prey nuclei remain transcriptionally active within the ciliate. It can be thus suggested that the sequestration of prey nuclei in *S.* cf. *basimorphum* is an effective mechanism to achieve longer retention times for the kleptoplasts, which can be used for performing photosynthesis.

Zusammenfassung

Wegen ihrer Fähigkeit die beiden Ernährungsstrategien von Phototrophie und Phagotrophie zu vereinen sind Mixoplankton Spezies Schlüsselorganismen in marinen Ökosystemen. Der duale Modus ihrer Ernährung hat großen Einfluss auf Trophienetzwerke und globale biochemische Kreisläufe. Prozesse, die mit Phagotrophie und Phototrophie zusammenhängen, sind unter Anderem die Produktion von Toxinen zur Lyse und Aufnahme von Beuteorganismen und die Fähigkeit, Plastiden von photosynthetischer Beute (Kleptoplasten) zu beschlagnahmen und selbst zu nutzen. Die in dieser Dissertation gezeigten Studien zielen darauf ab (i) die Prozesse der Phagotrophie und Phototrophie in einem evolutionären Kontext zu erkunden, (ii) das Wissen über die der Toxinproduktion zu Grunde liegender Mechanismen der mixoplanktonischen Spezies *Prymnesium parvum* zu erweitern, (iii) die antreibenden Faktoren für die Phagotrophie in *P. parvum* zu untersuchen und (iv) die molekularen Mechanismen, die in der Funktionalität von Kleptoplasten des Ciliaten *Strombidium* cf. *basimorphum* involviert sind, zu studieren.

Als Voraussetzung für die nachfolgenden experimentellen Studien wurde eine akribische Literaturuntersuchung durchgeführt, um ein besseres Verständnis über die evolutionären Aspekte der Mixotrophie zu bekommen. Aktuelle Studien unterstützen die Annahme, dass Mixoplankton Spezies ideale Organismen zur Untersuchung von Prozessen wie die Etablierung permanenter Plastiden, sind. Diese Studien beinhalten unter Anderem den Transfer von Genen, die mit Photosynthese in Verbindung stehen, von Beute oder Endosymbionten auf den Wirtsorganismus.

In dieser Dissertation wurden die Transkriptome von neun verschiedenen *P. parvum* Stämmen, die verschiedene Typen des Toxins Prymnesin produzieren, sequenziert und analysiert und auf die Anwesenheit von Polyketidsynthasegenen (PKSs) hin untersucht. Die toxische und mixotrophe Spezies *P. parvum* hat mehrere Polyketidsynthasen und ihre Menge ist unabhängig vom Toxingehalt der korrespondierenden Stämme. Außerdem werden hier die funktionellen und strukturellen Annotationen der PKS-codierenden Transkripte aller neun *P. parvum*-Stämme gezeigt. Das Expressionsmuster der Gene, die mit gesteigertem Toxingehalt assoziiert sind, werden gezeigt, welche auf eine generelle Herabregelung von Genen, die in metabolische Prozesse involviert sind, hindeuten. Umgekehrt suggeriert dieser molekulare trade-off einen aktiveren Metabolismus in Stämmen mit geringerem Toxingehalt.

Um die physiologischen und transkriptomischen Reaktionen des *P. parvum* Stammes UIO223 zu untersuchen, wurden verschiedene Behandlungen mit Salinität und Verfügbarkeit von Phosphor (P) ausgeführt. Die erhöhten Wachstumsraten, die bei Zellen, die in reduzierter Salinität kultiviert wurden, konnten auch in den Daten der Genexpressionsanalysen als vermehrte Expression von Genen katabolischer Prozesse wiedergegeben werden. Außerdem hat die Inkubation von *P. parvum* mit dem Beuteorganismus *Teleaulax acuta*, ein Cryptophyt, gezeigt, dass Phagotrophie unter P-Mangel erhöht stattfand. Dies deutet darauf hin, dass Phagotrophie in *P. parvum* möglicherweise ein Mechanismus zur Kompensation von limitierten Makronährstoffen ist. Im Gegensatz dazu war die Beutemortalität signifikant höher bei geringerer Salinität, was zeigt, dass Salinität und P die Prozesse von Zelllyse und -aufnahme unterschiedlich beeinflussen. Gene, die mit Endozytose assoziiert sind, waren sowohl unter geringer Salinität und P-hungernden Monokulturen vermehrt exprimiert. Dies zeigt die evolutionäre Konservierung von Mechanismen zur Beuteaufnahme selbst bei Abwesenheit von Beuteorganismen. Bei hoher Zelldichte von *P. parvum* wurde ein besonders hoher Toxingehalt festgestellt, was auf das Auftreten von Zelldichte-abhängigen Prozessen in der Toxinregulation hindeutet.

Trancriptomics von einzelnen Zellen wurde genutzt, um die genetischen Mechanismen, die in der Etablierung von plastidischen Endosymbionten in *Strombidium* cf. *basimorphum* zu studieren. Der Ciliat behält genetisches Material von Beuteorganismen seiner Cryptophytenbeute und die Anwesenheit von Genen, die im Zusammenhang mit Transkription und Translation stehen, deutet darauf hin, dass die Nuclei der Beuteorganismen im Ciliaten transkriptionell aktiv bleiben. Deshalb kann vermutet werden, dass die Beschlagnahmung von Nuclei aus Beuteorganismen in *S.* cf. *basimorphum* ein effektiver Mechanismus zur längeren Retention von Kleptoplastiden ist, welche zur Photosynthese genutzt werden können.

List of abbreviations

ACP	Acyl carrier protein
ANOVA	Analysis of Variance
AT	Acyltransferase
BLAST	Basic Local Alignment Search Tool
Chl-*a*	Chlorophyll-*a*
CM	Constitutive mixoplankton
CRO	Enoyl-CoA hydratase/isomerase
DEG	Differentially expressed gene
DH	Dehydratase
DNA	Deoxyribonucleic acid
EGT	Endosymbiont gene transfer
ER	Enoyl reductase
eSNCM	Endosymbiotic specialist non-constitutive mixoplankton
FAS	Fatty acid synthase
GNCM	Generalist non-constitutive mixoplankton
GP	Gene Orthology
HMG	Hydroxymethylglutaryl-coenzyme A synthase
KEGG	The Kyoto Encyclopedia of Genes and Genomes
KR	Ketoreductase
KS	Ketosynthase
MT	Methyltransferase
N	Nitrogen
NCBI	National Center for Biotechnology Information
NCM	Non-constitutive mixoplankton
NRPS	Non-ribosomal polyketide synthase
ORF	Open reading frame
P	Phosphorus

PCR	Polymerase chain reaction
PKS	Polyketide synthase
POC	Particulate organic carbon
PON	Particulate organic nitrogen
pSNCM	Plastidic specialist non-constitutive mixoplankton
qPCR	Quantitative PCR
RNA	Ribonucleic acid
rRNA	Ribosomal RNA
TE	Thioesterase

Introduction

1. Mixoplankton and functional classification

Marine protists have been traditionally divided into two functional categories, phyto- and protozooplankton, based on their mode of nutrient uptake. Phytoplankton perform photosynthesis to fix carbon (phototrophs/producers) whereas protozooplankton feed on other organisms (heterotrophs/consumers), a process known as phagotrophy. Many marine protists can combine these two modes of nutrition and thus use both phototrophy and phagotrophy to cover their cellular nutrient requirements (Flynn et al., 2019). This mode of nutrition is defined as mixotrophy, and is not only restricted to marine protists, but is also widespread on land and in multicellular metazoa (Serôdio et al., 2014; Selosse et al., 2017). Well-known examples of mixotrophic plants and metazoa include the carnivorous plants that feed on insects, jellyfish and sea slugs that either use endosymbionts or acquires plastids for performing photosynthesis.

The increasing focus on the study of mixotrophic plankton is due to the realization of the impact of mixotrophy in food webs and biogeochemical cycles. New studies have highlighted the considerable prevalence of mixotrophy in aquatic ecosystems, with major implications for the existent knowledge of species interactions and dynamics within plankton (Stoecker et al., 2009; Flynn et al., 2013). Mixotrophic species comprise different specific nutrition strategies, underscoring the need for a comprehensive nomenclature and functional classification. The first functional categories for mixotrophic plankton were suggested by Mitra et al., (2016) and were later modified by Flynn et al., 2019 who suggested the use of the term mixoplankton to describe "*planktonic protists that express, or have potential to express phototrophy and phagotrophy*".

The functional classification of mixoplankton is centered around the way the cell performs photosynthesis (Figure 1). Mixotrophic protists (i.e. mixoplankton), as defined by Mitra et al., (2016) and Flynn et al., (2019), are separated into two general categories: the constitutive mixoplankton (CM) and the non-constitutive mixoplankton (NCM). A CM has an inherent capability for photosynthesis, while it can additionally perform phagotrophy to supplement their nutrition. Non-constitutive mixoplankton acquire their photosynthetic ability through external means. Photosynthetic ability in NCM can be acquired by: 1) stealing chloroplasts of (any) prey (generalist non-constitutive mixoplankton, GNCM); 2) stealing chloroplasts from a specific type

of prey (plastidic specialist non-constitutive mixoplankton pSNCM) or 3) harboring photosynthetically active endosymbionts (endosymbiotic specialist non-constitutive mixoplankton, eSNCM).

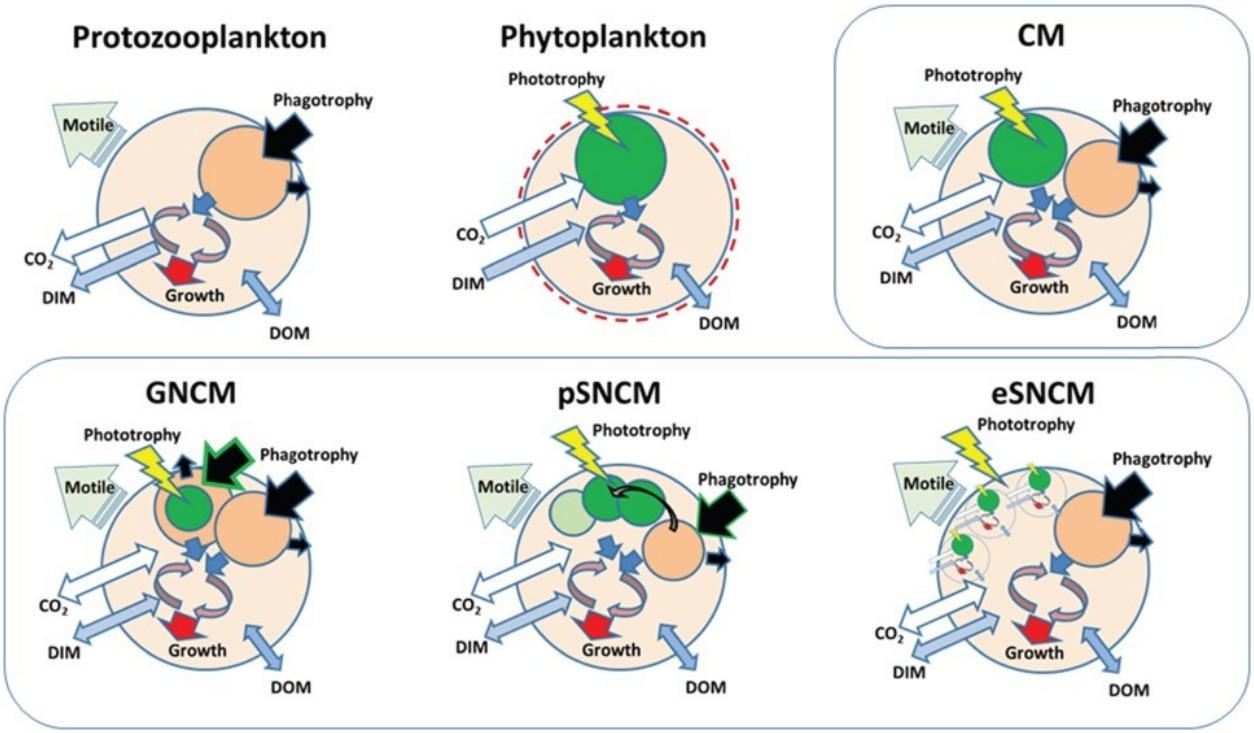

Figure 1 Schematics showing the distinct differences between different protist plankton physiologies. The protozooplankton are osmo–phagotrophic; they are incapable of phototrophy. The phytoplankton are photo-osmo mixotrophic; they are incapable of phagotrophy. The constitutive mixoplankton (CM) and non-constitutive mixoplankton (NCMs) are all photo-, osmo- and phago-mixotrophic. However, some mixoplankton have life stages that are not photo- and phagotrophic, with nutrition aligning with that of "phytoplankton" or "protozooplankton". The generalist GNCMs acquire phototrophy from many phototroph prey types; pSNCMs are plastidic specialists acquiring phototrophy from specialist prey type(s); eSNCMs are endosymbiotic acquiring phototrophy by harbouring specific phototrophic prey. Note: illustrations are not to scale; in particular, eSNCMs are in relative terms ca. 10 to 100 times larger than the others (From Kevin J. Flynn *et al.*, 2019 with original legend).

The classification of mixoplankton into functional types can be challenging, as both phagotrophy and phototrophy need to be described within the same organism (Beisner et al., 2019; Hansen et al., 2019). To identify phagotrophic potential in an organism often requires meticulous experimentation (Anderson et al., 2017; Beisner et al., 2019). Such attempts are made even more complex by the fact that phagotrophy may be expressed only under specific abiotic and biotic conditions. Additional tools such as transcriptomics and genomics-based approaches and

subsequent gene-based predictive models can help to evaluate the potential for mixotrophy (Burns et al., 2018).

2. Constitutive mixoplankton

Constitutive mixoplankton are prevalent in many eukaryotic microalgal lineages (e.g. green algae, euglenophytes, cryptophytes, chrysophytes, haptophytes, and dinoflagellates) and could be easily considered as the perfect organisms, capable to dominate their occurring communities by taking full advantage of their mixotrophic capacity. However, this mixed way of nutrition incurs trade-offs related to the sustenance of structures which are involved in both processes (Raven, 1997). As a result, the equilibrium between the two processes of phagotrophy and phototrophy can be variable and heavily dependent on both biotic and abiotic factors. Resources (micro- and macronutrients) are required for sustaining the functionality of both photosynthetic and phagotrophic machineries (Raven, 1984, 1997). Such energetic costs have inevitably impact on important physiological parameters, such as growth rate, given that these resources could be alternatively allocated towards other processes related to cell proliferation (Flynn and Mitra, 2009; Ward et al., 2011).

An increasing number of studies, from both laboratory and field experiments, have stressed the important influence of biotic and abiotic factors on the expression of phagotrophy by constitutive mixoplankton. We could thus refer to a gradient of mixotrophy (Figure 2), which is characterized by flexibility in the relative contribution of phototrophy and phagotrophy, which in turn, is dependent on parameters such as light, nutrient and prey availability (Andersen et al., 2015).

Responses of constitutive mixoplankton to changing light availability and intensity are species specific, even though certain patterns have been observed at ecosystem level. Upon saturating light intensities, increased growth rates may be observed when prey is present (Li et al., 1999). However, the degree to which constitutive mixoplankton rely on photosynthesis or phagotrophy can be highly variable, with often either one or the other trophic mode being dominant (Keller et al., 1994; Skovgaard, 1996; Flöder et al., 2006). Research on the effect of nutrient availability has mainly focused, for non-carbon elements, on nitrogen and phosphorus. Mixotrophy in conditions of low dissolved nutrients availability can be beneficial as it represents an alternative

option to uptake nutrients, i.e. via prey ingestion. For example, under nutrient deficiency, *Nephroselmis pyriformis* can grow normally when provided with bacteria (Anderson et al., 2018a). In other cases, dissolved nutrient limitation can actually be applied in order to investigate the potential for phagotrophy, as a number of species actually perform phagotrophy only when the availability of dissolved nutrients is limiting (Smalley et al., 2003; Johnson, 2015; Chan et al., 2019; González-Olalla et al., 2019).

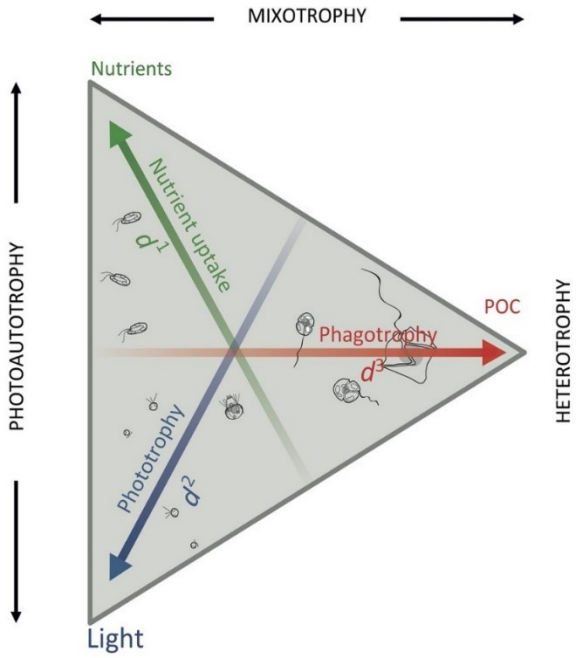

Figure 2 Conceptual illustration of the trophic continuum from photosynthesis over mixotrophy to pure heterotrophy. The trophic continuum is defined by the allocation into three harvesting traits: nutrient uptake, photosynthesis and phagotrophy, each leading to uptake of dissolved inorganic nutrients, CO_2 and particulate organic matter. A specific organisms' trophic strategy is defined as a point within the triangle: an organism in the middle will invest equally into all three traits, an organism somewhere along the left side will be a pure phototroph and an organism at the right tip would be a pure heterotroph. On each arrow depicting the traits is indicated how the affinity towards the trait scales with organism size *d*. (from Andersen et al., 2015; original figure legend)

3. Non-constitutive mixoplankton

Non-constitutive mixoplankton (NCM) acquire the photosynthetic ability either via sequestration of plastids from prey or by harboring photosynthetic symbionts. NCM are found within the groups of Rhizaria (especially Foraminifera and Acantharea), Alveolates (ciliates and dinoflagellates) and Katablepharids. The phylogenetic placement of NCM suggests that heterotrophic protists (including NCM) have originated from photosynthetic protists, and have secondary lost the ability to photosynthesize (Figure 3).

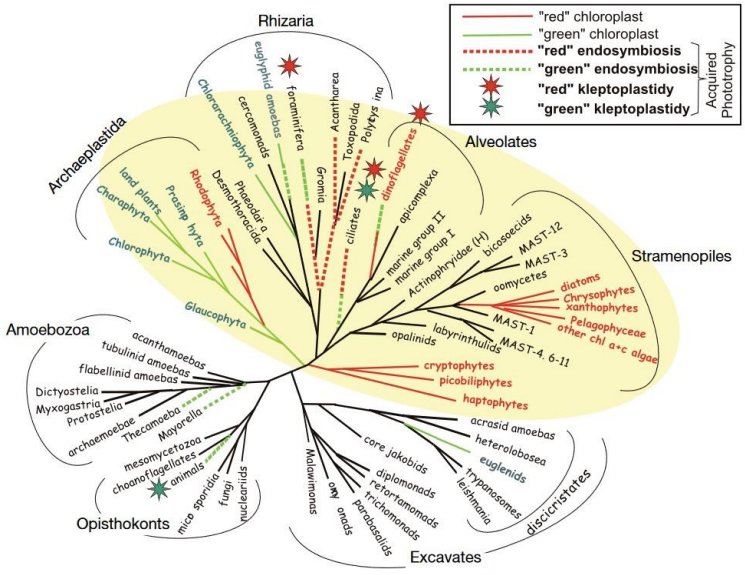

Figure 3 Synthetic tree of eukaryotic life based on recent phylogenetic/genomic data (modified from Stoecker et al., 2007). Acquired endosymbiosis and organelle retention based on both red and green plastids are concentrated in a mega-division including all permanent phototrophic protists plus pseudo-heterotrophic lineages (from Stoecker et al., 2009; original figure legend).

3.1 Kleptoplasty

Kleptoplasty is the process of plastid acquisition from prey and it is common among various protists taxa including dinoflagellates, ciliates, and Foraminifera (Stoecker et al., 2009; Pillet and Pawlowski, 2013; Park et al., 2014). The kleptoplast can origin either from a wide range of prey or restricted to a certain group. The retention time of a kleptoplast can vary from few days to months and can be affected from both the control the host has on the plastid and the inherent stability of the plastid itself (Green et al., 2005).

Control over the functionality of the plastids can be achieved by either the transfer of photosynthetic genes from the prey to the host or the additional sequestration of the prey nucleus, which is known as kleptokaryon (Figure 4; Hansen et al., 2013, 2016). Photosynthesis related genes, which are specifically involved in the maintenance of the chloroplasts have been found in the kleptoplastidic dinoflagellates of the genus *Dinophysis* (Hongo et al., 2019). Such photosynthetic genes in *Dinophysis* are of various phylogenetic origin, highlighting the complexity of species interactions in time. Moreover, the degree of gene transfer from the prey to the host can be variable among species and extensive gene transfer can lead to considerable retention time of the kleptoplast, up to 22 months (Hehenberger et al., 2019). The presence of a transcriptionally active kleptokaryon can be an optimal strategy for transcribing photosynthesis related genes when

those are completely missing in the genome of the host (Onuma et al., 2020; Altenburger et al., 2021).

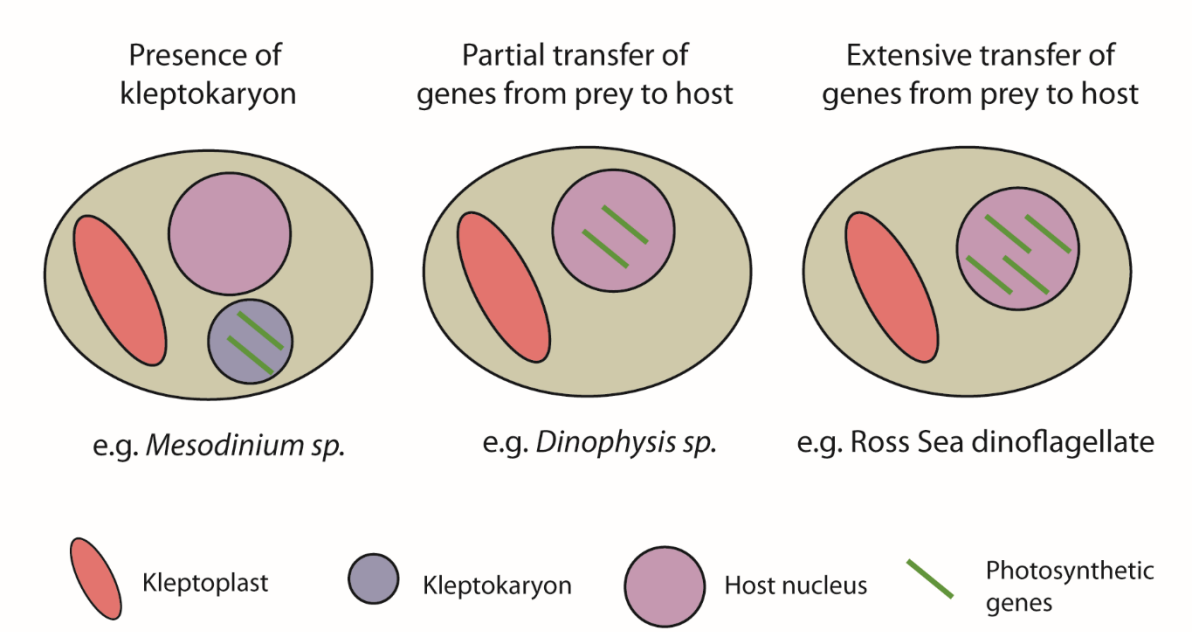

Figure 4 Graphical illustration of different strategies, developed to elongate the retention time of kleptoplasts (original artwork).

4. *Prymnemsiun parvum:* a toxic and bloom forming mixotrophic haptophyte

The haptophyte species *Prymnesium parvum* is a cosmopolitan single-cell eukaryote with length that ranges from 8 to 16 μm and width from 4 to 10 μm. *Prymnesium parvum* belongs to the class of haptophytes, which are characterized by certain morphological features, such as the presence of a haptonema, a needle-like structure that is likely used for attachment to surfaces or prey capture (Figure 5). While *P. parvum* can grow as autotroph, it can also feed on a wide range of prey, from bacteria to fish larvae (Skovgaard and Hansen, 2003; Tillmann, 2003), thus classifying it as a constitutive mixotroph. The benefits of mixotrophy in *P. parvum* are considered to be related to the acquisition of nutrients such as phosphorus, and thus being a survival strategy under dissolved nutrient limitation.

Moreover, *P. parvum* is known for frequent worldwide harmful algal blooms (defined below), with negative impact on fishing and aquaculture industries (Roelke et al., 2016). *P. parvum* can grow in a wide range of salinities, from 0.5 to 45 and it is thus present in both freshwater and marine ecosystems (Edvardsen and Paasche, 1998; Barone et al., 2010). Factors that induce the

formation of blooms by this species include fresh-water inflow, salinity or even the mediation of viruses that interact with components of their cellular membrane (Roelke et al., 2011; Wagstaff et al., 2017, 2018).

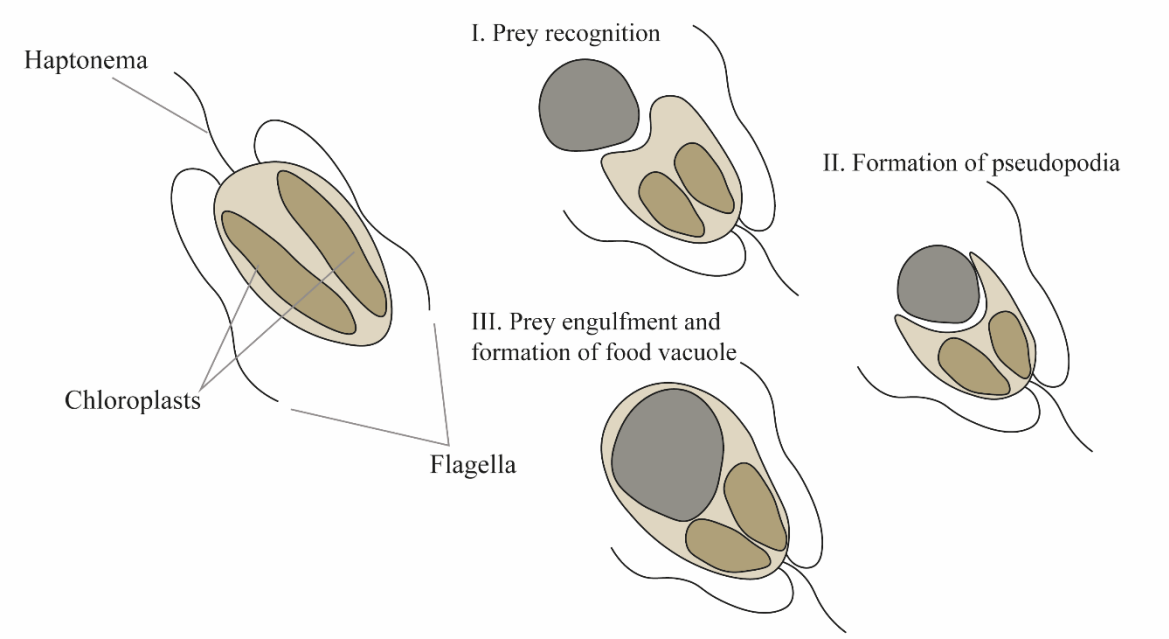

Figure 5 Graphical illustration of *Prymnesium parvum* morphological features and stages of phagotrophy (original artwork).

The toxicity of *P. parvum* is attributed to the production of large ladder-frame polyether compounds known as prymnesins (Igarashi et al., 1999). Prymnesins belong to the group of polyketides, an extremely diverse group of compounds produced by a wide range of organisms, ranging from prokaryotes to unicellular algae and higher eukaryotes (Wright and Cembella, 1998; Staunton and Weissman, 2001). Prymnesins were first characterized back in 1999 and reported as prymnesin -1 and -2 (Igarashi et al., 1999). Recently, a new B-type of prymnesin was isolated and structurally characterized (Rasmussen et al., 2016), and high-resolution mass spectrometric analyses demonstrated the existence of an additional third type of prymnesin, altogether leading to the classification of three prymnesin types, the A-, B- and C-types (Rasmussen et al., 2016). The three types differ in the size of the backbone: the A-type being the longest with 91 carbons, followed by B-type and C-type with 85 and 83 carbons, respectively (Figure 6). Within each prymnesin type there is large structural diversity, such as variances in chlorination, saturation and

attached sugar moieties, and altogether 51 prymnesin congeners have been reported (Binzer et al., 2019).

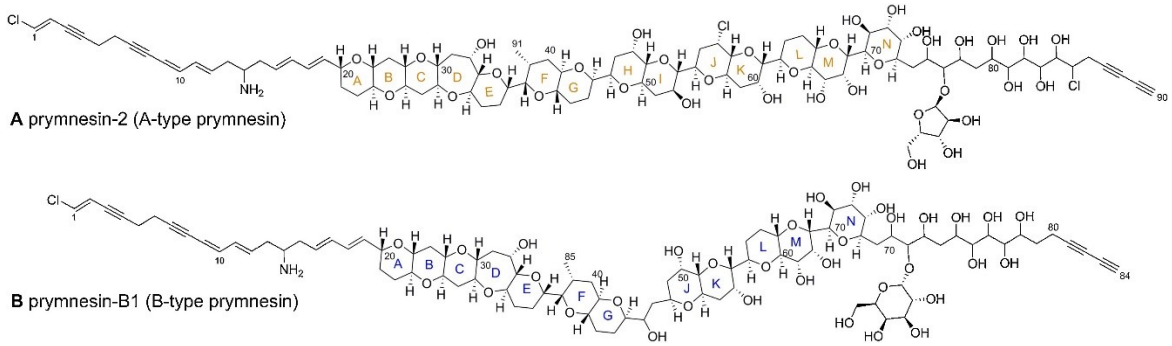

Figure 6 Chemical structure of A- and B- type prymnesins (from Binzer et al., 2019).

4.1 Harmful algal blooms

The term harmful algal bloom (HAB) refers to the rapid proliferation of organisms traditionally classified as phytoplankton, with negative effects on humans and their occurring ecosystems (Figure 7; Smayda, 1997). The driving factors behind HABs can be of both anthropogenic and natural origin (Lewitus et al., 2012). One of the most discussed cause of HABs is eutrophication, which is often caused by the inflow of dissolved nutrients (nitrogen and phosphorus) that are subsequently used by phytoplankton (both prokaryotic and eukaryotic) for rapid growth (Heisler et al., 2008; Flynn et al., 2018). The subsequent degradation of the formed biomass leads to decrease in oxygen availability in the water (hypoxia), which can have lethal consequences for co-occurring species. Consequences of climate change, such as alternation in the water temperature and nutrient inflow due to rain intensity changes and to ice melting (Meire et al., 2017) have been suggested as the reasons behind the increased occurrence of HABs (Anderson et al., 2012; Gobler et al., 2017; Gobler, 2020).

Many HAB species are known to be mixotrophic. In eutrophic ecosystems, mixoplankton growth can be affected by both the increased dissolved nutrients concentration and the availability of particulate organic nutrients in the form of algal and bacterial prey (Burkholder et al., 2008). Under such conditions, mixoplankton seem to have an advantage as they can make use of all possible forms of resources. Studying the role of mixotrophy in such bloom conditions can provide

substantial insights about the functional role of mixotrophy in marine ecosystems. Most of the knowledge in this field comes from culture grazing experiments, highlighting the need to conduct more field studies under bloom conditions.

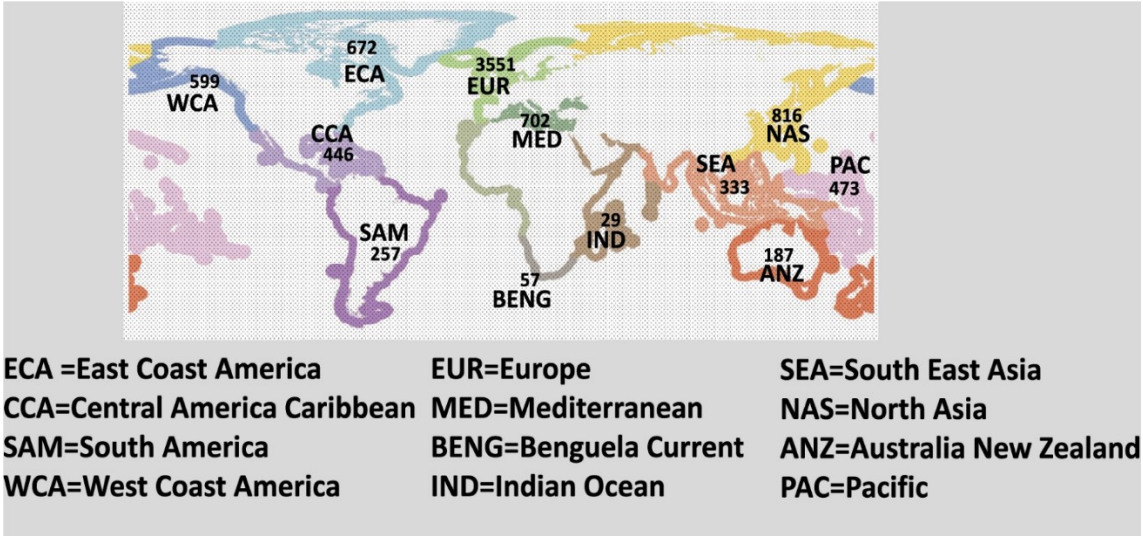

Figure 7 Harmful algal bloom events according to Harmful Algae Event Database (http://haedat.iode.org) in twelve geographic regions (from Hallegraeff et al., 2021).

4.2 Toxin production and potential molecular mechanisms of biosynthesis

Apart from the negative impact of HABs, due to their uncontrollable proliferation and subsequent depletion of oxygen in the water, most HAB species are also known to produce toxic compounds, known as phycotoxins (Table 1). Production and accumulation of toxins at higher trophic levels is common during HABs. The economic losses due to the production of toxins can be considerable (Hallegraeff et al., 2021b) and the accumulation of toxins in shellfish can have poisoning effects on humans and animals that consumed contaminated seafood (James et al., 2010) or fish. Among the best-known examples of toxin producing groups are dinoflagellates, diatoms and haptophytes, which are responsible for the production of a wide range of toxic substances and can have severe effects on human health (Anderson et al., 2021).

The exact genetic basis of most toxin biosynthesis remains not well known, except for saxitoxins (Stücken et al., 2011; Orr et al., 2013; Akbar et al., 2020) and domoic acid (Brunson et al., 2018; Haroardóttir et al., 2019), where substantial progress have been made in the last years. For polyether toxins (polyketides), the carbon backbone of such toxic compounds is putatively

synthesized by a group of genes, collectively called polyketide synthase genes (PKSs) (Rein and Borrone, 1999), which are evolutionarily related to fatty acid synthases (FASs) (Kohli et al., 2016). The standard core structure of PKSs and FASs consists of a ketosynthase domain (KS), which catalyzes the condensation of the acyl units in synergy with an acyltransferase (AT) and an acyl carrier protein (ACP) (Cane et al., 1998; Jenke-Kodama et al., 2005). After the condensation, further structure modifications can occur by other domains such as dehydratase (DH), enoyl reductase (ER) and ketoreductase (KR) (Figure 8). These domains can respectively produce a double bond, a fully-reduced methylene or a hydroxy group (Weissman, 2015). The biosynthesis of a polyketide is terminated by the presence of a thioesterase domain (TE), which hydrolyzes the polyketide compound from the ACP.

Table 1 The main chemical groups of phycotoxins, source organisms, algal class and impact (from Blossom, 2018 with information from Hallegraeff, 1993; Anderson et al., 2011; Rasmussen et al., 2016).

Structural group	Toxin group	Producer organism	Algal class	Syndrome/impact
Tetrahydropurines				
	Saxitoxin	*Alexandrium spp.* *Amphanizominon*	Dinophagellates Cyanobacteria	Paralytic shellfish poisoning (PSP)
Secondary amines				
	Domoic acid	*Pseudo-nitzschia spp.*	Diatoms	Amnesic shellfish poisoning (ASP)
	Azaspiracid	*Azadinium spinosum*	Dinoflagellates	Azaspiracid shellfish poisoning (AZP)
Macrolytic imines				
	Gymnodymine	*Alexandrium peruvianum*	Dinoflagellates	
	Spirolide	*Alexandrium ostenfeldii*	Dinoflagellates	
Ladder-frame polyether				
	Brevetoxin	*Karenia brevis*	Dinoflagellates	Neurotoxic shellfish poisoning (NSP) Ichthyotoxic
	Cuguatoxin	*Gambierdiscus toxicus*		Ciguatera fish poisoning
Linear or macrocyclic polyethers				
	Okadaic acid	*Diniphysis spp.*	Dinoflagellates	Diarrhetic shellfish poisoning (DSP)
	Dinophysistoxins	*Dinophysis spp.*	Dinoflagellates	
	Goniodomin A	*Alexandrium*	Dinoflagellates	
Linear superchain polyethers				
	Karlotoxin	*Karlodinium*	Dinoflagellate	Ichthyotoxic
Supersized ladder-like polyethers				
	Prymnesin	*Prymnesium parvum*	Haptophytes	Ichthyotoxic
Unknown ichthyotoxins				
	Unknown	*Pseudochattonella spp.*	Dictyochophytes	Ichthyotoxic
	Unknown	*Heterosigma akashiwo*	Raphidophytes	

PKSs are grouped into three categories, based on their structural organization and function:

- Type I PKSs can be either iterative or modular. Iterative type I PKSs possess all catalytic domains in a single protein, and can elongate a chain in a repeated way. Modular type I PKSs occur as distinct modules, where each module contains all the

prerequisite domains needed for catalyzing the condensation reaction, leading to the elongation of the polyketide chain by two carbon atoms.

- Type II PKSs consist of distinct catalytic domains, which function independently and iteratively.
- Type III PKSs also function in an iterative manner and consist of self-contained homodimeric enzymes with each monomer catalyzing a specific function. Type III PKSs differ from the other PKS types due to their ability to perform condensation without using acyl carrier proteins (Ferrer et al., 1999).

Known bloom-forming haptophytes include *Chrysochromulina leadbeateri*, *Prymnesium polylepis*, *Prymnesium parvum* and *Phaeocystis spp.*. Transcriptomic surveys of 12 strains of haptophytes have revealed the presence of type I PKSs (Kohli et al., 2016). Only a subset of strains are known to produce toxins, and given the involvement of PKSs in variable biosynthetic pathways, no direct connection of PKSs to toxic product was feasible. The *Chrysochromulina* genus contains species that produce ichthyotoxic compounds of unknown structure, but presumably similar to prymnesins. The only available transcriptomic study comes for the species *Chrysochromulina polylepis*, where thirteen putative PKSs were found based on expressed sequence tags (John et al., 2010). In comparison to dinoflagellates, few detailed studies have been conducted concerning the potential involvement of PKSs in toxin biosynthesis in haptophytes (Freitag et al., 2011; Beszteri et al., 2012).

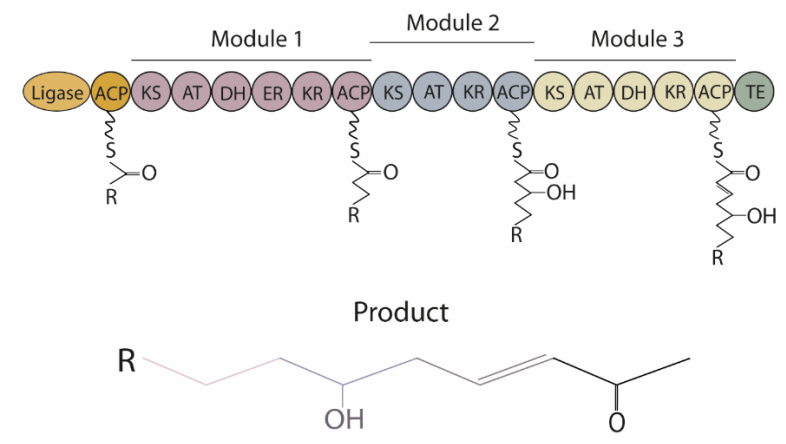

Figure 8 Example of a structure and mode of function of a modular type I polyketide synthase. KS = ketoacyl synthase, KR = ketoreductase, ER = enoyl reductase, ACP = acyl carrier protein, DH = dehydratase, TE = thioesterase, AT = acyltransferase.

5. Plastid retention in oligotrich ciliates

The group of oligotrichs (subclass Oligotrichia) consists of both heterotrophic and mixotrophic species. Plastid retention in this group has been observed within the genera of *Cyrtostrombidium*, *Laboea*, *Strombidium* and *Tontonia* (Stoecker et al. 2009), and around 30 species of marine oligotrich ciliates are known to be kleptoplastidic. Species of the *Strombidium* genus account for about half of the known oligotrich kleptoplastidic ciliates. Oligotrich ciliates are currently thought to be all prey generalists (GNCM), since several species can retain plastids from different algal lineages including chlorophytes, haptophytes, cryptophytes and heterokonts (Laval-Peuto and Febvre, 1986; Johnson and Beaudoin, 2019). The sequestered plastid are able to perform photosynthesis and substantially contribute to the energy budget of the cell (Maselli et al., 2020; Hughes et al., 2021). The photosynthetic efficiency depends on the availability of light (Stoecker et al., 1998) and the total number of sequestered plastids (McManus et al., 2018).

Outline of the thesis

Mixoplankton present a wide variety of nutrition modes and the dynamics between phototrophy and phagotrophy is still an open question. To understand the ecological implications of mixoplankton, it is important to study mixotrophy-related physiological processes, as they could provide explanations about the evolutionary context in which mixotrophy is favored and advantageous. Apart from the impact of mixoplankton in the global biogeochemical cycles, the spectrum of species interactions observed within mixoplanktonic species can provide substantial insights about the evolution of life in the oceans as we know it today.

The fundamental difference between constitutive (CM) and non-constitutive mixoplankton (NCM) lies in the strategies they have developed to sustain their growth, as the group of CM have an innate ability to perform photosynthesis and occasionally use phagotrophy, whereas the NCM complement their heterotrophic lifestyle by acquiring photosynthesis by endosymbiosis or kleptoplasts. **My objective for Publication I was to get a deep understanding of mixotrophy in an evolutionary context, supported by detailed cellular and regulatory processes related to mixotrophy in CM and NCM**. In **Publication I,** I performed a detailed review of the current literature on major evolutionary trajectories of prey uptake, plastid establishment and finally endosymbiosis concepts and discussed it under the perspective of mixotrophy. The evolution of the two fundamental traits of phagotrophy and photosynthesis for mixotrophy are explored in detail and indicate the plasticity of these traits with regards to their loss and acquisition of these processes during time. Theories on the evolution and establishment of permanent plastids are addressed, as well as the current supporting evidences about mixoplankton species being evolutionary intermediates towards pure phototrophs. Moreover, in an effort to link ecology and evolution, the occurrence of general patterns observed in the ecophysiology of mixoplankton and different environmental conditions are discussed.

Toxin production by mixoplanktonic species is considered to support phagotrophy, as the produced toxins mediate feeding via prey lysis. The haptophyte *Prymnesium parvum* is an ecologically important species due to its ability to form blooms with considerable ecological and economic consequences and produce the lytic toxins, prymnesins. **Within Publication II, my objective has been to explore the molecular mechanisms underlying toxin biosynthesis in *P. parvum*.** Prymnesins are chemically classified as polyketides, thus indicates the involvement of

polyketide synthase genes (PKSs). Additionally, inducible toxin production requires the investment of energy (cost) and thus I have studied if certain metabolic trade-offs might occur and could be related to toxin production. In **Publication II,** I generated and explored the transcriptomes of nine *P. parvum* strains that are known to produce different types of prymnesins. The studied transcriptomes were screened for the presence of PKSs and their evolutionary origin was assessed via phylogenetics. The transcriptomic data was combined with physiological parameters such as the total cellular prymnesin contents and growth rates in an effort to understand potential metabolic trade-offs related to the toxin production.

The prevalence of mixotrophy in the environment is influenced by both biotic and abiotic factors. The abiotic factors include, among others, the availability of dissolved nutrients such as phosphorus (P) and nitrogen (N). **In Publication III, I aimed to make a step forward towards disentangling the relationship among mixotrophy, toxin production and bloom formation in *P. parvum.*** A single *P. parvum* strain (UIO223) was used to study the effect of different salinities and phosphorus availabilities on cell growth, phagotrophy and toxin production. For this purpose, I generated and analyzed the transcriptomes of *P. parvum* under different combinations of salinity (salinity of 5 vs salinity of 30), P (P-replete vs P-deplete) and cell density (middle exponential vs late exponential/stationary). Moreover, the obtained dataset included physiological parameters such as growth rates, toxin content, phagotrophy and elemental stoichiometry.

In contrast to CM, which have permanent plastids and use phagotrophy as additional source of nutrients, the NCM are heterotrohic and can perform photosynthesis only via their interactions with photosynthetic prey. Thus, the acquisition of photosynthesis by these primary heterotrophic organisms suggests the potential presence of mechanisms involved in the maintenance of the kleptoplasts and assurance of their longevity within the cell. Such mechanisms might involve the transfer of photosynthesis related genes from the prey to the host nuclei and/or the retention of transcriptionally active prey genetic material. **In Publication IV, my aim was to gain an understanding of the cellular and regulatory underlying mechanisms involved the establishment and of plastidic endosymbiosis in NCMs.** Therefore, I studied the genetic relationship between the kleptoplastidic ciliate *Strombidium* cf. *basimorphum* and its cryptophyte prey *Teleaulax amphioxeia*. For this purpose, I used single-cell transcriptomics to investigate the possible retention of prey genetic material in the ciliate, as well as understanding the function of the prey transcriptome within the host.

List of publications

List of publications and declaration of contribution

I. J.S. Mansour and **K. Anestis** (2021). Eco-evolutionary perspectives on mixoplankton. Frontiers in Marine Science.

The candidate has equally co-authored the publication.

II. **K. Anestis**, G.S. Kohli, S. Wohlrab, E. Varga, T.O. Larsen, P.J. Hansen, U. John (2021). Polyketide synthase genes and molecular trade-offs in the ichthyotoxic species *Prymnesium parvum*. Science of the Total Environment.

The candidate designed the study in collaboration with SW and UJ. The candidate performed the experiments, generated the transcriptomic data, performed the data analysis and wrote the manuscript.

III. **K. Anestis**, S. Wohlrab, E. Varga, P.J. Hansen, U. John. Distinct physiological and transcriptomic responses in *Prymnesium parvum* under different salinity, phosphorus and cell density conditions. In submission.

The candidate design the study in collaboration with SW and UJ. The candidate performed the experiments, generated the transcriptomic data, performed the data analysis and prepared the manuscript.

IV. M. Maselli, **K. Anestis**, K. Klemm, P.J. Hansen, U. John (2021). Retention of prey genetic material by the kleptoplastidic ciliate *Strombidium* cf. *basimorphum*. Frontiers in Microbiology.

The candidate performed the part referring to single-cell transcriptome data generation and analysis.

Publication I

Eco-evolutionary perspectives on mixoplankton

frontiers in Marine Science

REVIEW
published: 26 May 2021
doi: 10.3389/fmars.2021.666160

Eco-Evolutionary Perspectives on Mixoplankton

Joost Samir Mansour[1†‡] *and Konstantinos Anestis*[2,3*†‡]

[1]*CNRS and Sorbonne University, UMR7144 Adaptation and Diversity in Marine Environment (AD2M) Laboratory, Ecology of Marine Plankton Team, Station Biologique de Roscoff, Roscoff, France,* [2]*Department of Ecological Chemistry, Alfred-Wegener-Institute Helmholtz Centre for Polar and Marine Research, Bremerhaven, Germany,* [3]*Faculty of Biology/Chemistry, University of Bremen, Bremen, Germany*

Mixotrophy, i.e., the capability of both phototrophy and phagotrophy within a single organism, is a prominent trophic mode in aquatic ecosystems. Mixotrophic strategies can be highly advantageous when feeding or photosynthesis alone does not sustain metabolic needs. In the current review, we discuss the functional types of mixotrophic marine protists (herein mixoplankton) within the context of evolution. Permanent plastids have been established in large due to gene transfer from prey and/or endosymbionts to the host cell. In some kleptoplastidic mixoplankton, prior gene transfers and active transcription of plastid related genes in the host can help maintain and extend retention of the current kleptoplast. In addition to kleptoplasts, the prey nucleus is also sometimes retained and actively transcribed to help maintain and even replicate the kleptoplasts. Endosymbiotic relations vary considerably in the extent to which hosts affect symbionts. For example, some endosymbionts are heavily modified to increase photosynthetic efficiency, or are controlled in their cell division. It can be proposed that many kleptoplasts and endosymbionts are in fact *en route* to becoming permanent plastids. Conditions such as increased temperature and limiting nutrients seem to favor phagotrophy in mixoplankton. However, responses of mixoplankton to changing environmental conditions like light irradiance, temperature, nutrient, and prey availability are variable and species-specific. Studying mixotrophs with temporary plastids could elucidate past and future evolutionary mechanisms and dynamics of processes such as phagotrophy and the establishment of (secondary) permanent plastids.

Keywords: evolution, mixotrophy, endosymbiosis, plankton, kleptoplasty, plastids

OPEN ACCESS

Edited by:
Viola Liebich,
Bremen Society for Natural Sciences, Germany

Reviewed by:
Elisabeth Hehenberger,
GEOMAR Helmholtz Center for Ocean Research Kiel, Germany
Patricia M. Glibert,
University of Maryland Center for Environmental Science (UMCES), United States

***Correspondence:**
Konstantinos Anestis
kanestis@awi.de

[†]*These authors have contributed equally to this work*

[‡]***ORCID:***
Joost Samir Mansour
orcid.org/0000-0002-9505-1673
Konstantinos Anestis
orcid.org/0000-0002-8208-6789

Specialty section:
This article was submitted to Marine Biology, a section of the journal Frontiers in Marine Science

Received: *09 February 2021*
Accepted: *29 April 2021*
Published: *26 May 2021*

Citation:
Mansour JS and Anestis K (2021) Eco-Evolutionary Perspectives on Mixoplankton. Front. Mar. Sci. 8:666160. doi: 10.3389/fmars.2021.666160

INTRODUCTION TO MIXOTROPHY

All living organisms need resources (micronutrients and macronutrients) in order to sustain their structure, basic cellular functions, and their overall existence. Various strategies (e.g., phototrophy, phagotrophy, chemotrophy, or osmostrophy) have evolved in order to acquire these important resources. The two most well-known strategies for nutrient acquisition distinguish organisms into two functional categories, those that make use of light to fix carbon (phototrophs/primary producers) and those that feed on others (heterotrophs/consumers). However, there is a third category to consider – mixotrophs. As indicated by the name, mixotrophy refers to a mixed trophic mode, thereby combining both phototrophic and heterotrophic modes of nutrition in order to fulfill cellular nutrient requirements.

We focus here on marine mixotrophic protists, but mixotrophy is an important trait for organisms both on land, and in water (Selosse et al., 2017). A well-known land example being the carnivorous plants that feed on insects. In aquatic ecosystems, mixotrophy is much more prevalent and widespread than initially thought. It can be found in a plethora of different organisms, from unicellular eukaryotes to multicellular metazoa such as jellyfishes or sea slugs that use endosymbionts or acquired plastids for photosynthesis (Cruz et al., 2013; Selosse et al., 2017). Plankton research has traditionally been based on the division of plankton between photosynthetic phytoplankton and heterotrophic zooplankton. The increasing focus on mixotrophy has changed the perception of plankton dynamics and interactions within plankton communities (Flynn et al., 2013). As more examples of mixotrophic marine organisms became known, it was realized that mixotrophy is not a rare occurrence in aquatic ecosystems, but fairly common (Mitra et al., 2014; Caron, 2017).

Mixoplankton

In the last decades, mixotrophic protists were referred to using definitions combining the two contradicting terms of phytoplankton and phagotrophy. The term mixotroph was used for photosynthetic organisms that take up dissolved organic carbon by osmotrophy, as well as for those using phagotrophy (Burkholder et al., 2008; Sforza et al., 2012). An emerging need to formally define mixotrophic protists (Flynn et al., 2013) with regards to their nutritional mode led to the first efforts to categorize mixotrophs in groups with distinct features. In an attempt to group protists based on their nutritional mode and function, Mitra et al. (2016) proposed a comprehensive terminology. Following the definitions of functional groups for mixotrophic protists, Flynn et al. (2019) suggested the use of the term *mixoplankton* – "*planktonic protists that express, or have potential to express, phototrophy and phagotrophy*" – as is the nomenclature we herein follow.

The functional classification of mixoplankton is based on how the cell incorporates photosynthesis. Mixotrophic protists (i.e., mixoplankton), as defined by Mitra et al. (2016) and Flynn et al. (2019), are functionally distinguished between *constitutive mixoplankton* (*CM*) and *non-constitutive mixoplankton* (*NCM*). A CM has an inherent capability for both phototrophy and phagotrophy. *Constitutive mixoplankton* are found in most eukaryotic microalgal lineages (e.g., green algae, euglenophytes, cryptophytes, chrysophytes, haptophytes, and dinoflagellates; **Figure 1**). *Non-constitutive mixoplankton*, which are defined by the need to acquire their photosynthetic ability through external means, are found mostly among ciliates, dinoflagellates, Foraminifera, and Radiolaria (**Figure 1**). Phototrophic activity in NCM can broadly be achieved in three ways which further divide NCM into sub-groups: (1) stealing chloroplasts of (any) prey (*generalist non-constitutive mixoplankton*, *GNCM*); (2) stealing chloroplasts from specific prey (*plastidic specialist non-constitutive mixoplankton pSNCM*); and (3) harboring photosynthetically active endosymbionts (*endosymbiotic specialist non-constitutive mixoplankton*, *eSNCM*; acquired phototrophy reviewed in Stoecker et al., 2009). Even though, we currently make a functional separation between GNCM and pSNCM, it is possible that some pSNCM lean more toward GNCM. Often very few data are available to support the GNCM assumption, making GNCM appear as pSNCM. The main differences between GNCM and pSNCM definitions rest simply on the rate of success in utilizing plastids from prey, and on the observed specificity of the prey from which plastids can be acquired.

Similar to the distinction of GNCM and pSNCM, the classification of mixoplankton into functional types is greatly influenced by current knowledge or lack thereof. Often the metabolic contribution of predation vs. photosynthesis is poorly understood (Anschütz and Flynn, 2020). By default, an organism would be either phototroph or heterotroph, while to identify a mixotroph both phagotrophic and phototrophic capabilities need to have been identified (Beisner et al., 2019; Hansen et al., 2019; Ferreira and Calbet, 2020). Considering the relative ease to identify a photosynthetic organism (by fluorescence signal of plastid pigments, and/or optical and electron microscopy to characterize the cell) it is tempting to immediately classify it as a (pure) phototroph (Anderson et al., 2017; Beisner et al., 2019). In contrast, phagotrophy rarely has clear external identifiers, instead it requires meticulous experimentation to identify phagotrophic potential in an organism (Anderson et al., 2017; Beisner et al., 2019). Even then, the absence of observed phagotrophy might just imply that not all conditions were met–time, type or state of prey, or state of the potential predator. Transcriptomics and genomics-based approaches and subsequent gene-based predictive models can help indicate mixotrophic potential (Burns et al., 2018). Identification of genetic potential for both phototrophy and phagotrophy does not forego the need for physiological experimentation and knowledge of photosynthetic and feeding rates. When the potential for a nutritional mode is observed, one could expect this potential to be used or otherwise lost over evolutionary time. Though, a nutritional mode might only be used under certain conditions. An organism could rely on (yet unobserved) instances of e.g., phagotrophy in space or time, which can be exceedingly difficult confirm.

The different functional groups of mixoplankton possess traits, such as phagotrophy and acquired photosynthesis that play a major part in evolutionary processes. Studying mixotrophy in its different forms offers an opportunity to gain a better understanding of major ecological and evolutionary processes that have been crucial in the creation of life as we know it today. Mixotrophy has not only been pivotal in the past with visible effects still identifiable today (such as the establishment of permanent organelles through endosymbiosis), but also it is still a prevalent biological phenomenon with a considerable fraction of marine plankton identified as mixoplankton (Flynn et al., 2019; Schneider et al., 2020; **Figure 1**). In mixotrophic organisms, we may have a glimpse of how life used to look in the past, and how things could change in the future. In the following sections, we address evolutionary theories and their relation to different functional types of mixoplankton, to gain a general overview of the possible role of mixotrophy as a transient

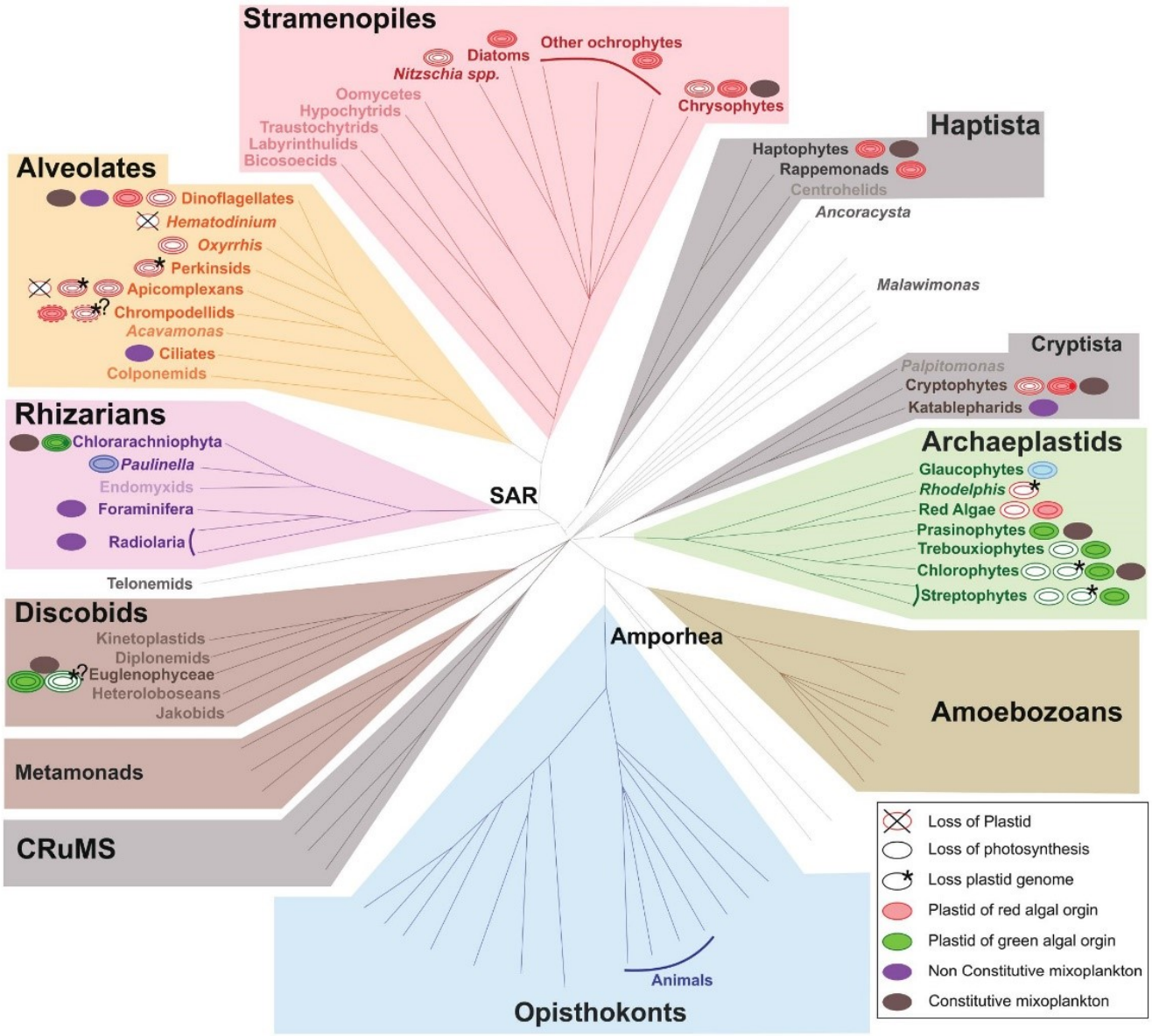

FIGURE 1 | Distribution of (non-)photosynthetic plastids and mixoplankton among eukaryotes. The schematic representation of the eukaryotic tree of life shows the distribution of plastids and protist mixoplankton among major taxonomic lineages. The tree topology is based on (Keeling and Burki, 2019). Dashed gray lines of certain deep branches indicate yet unclear relationships. Mixoplankton indicated with a purple non-constitutive mixoplankton (NCM) or dark gray constitutive mixoplankton (CM) circle is attributed if at least one member of the lineage can be indicated as such, this does not exclude that other taxa in the lineage use trophic modes such as purely heterotrophic (phagotrophic) or phototrophic. The focus here is on mixoplankton, hence kleptoplasty and photosymbiosis in animals is not indicated. Plastids and their origins are indicated by a circle, primary plastids are bounded by two membranes, while secondary, tertiary, or alternatively quaternary plastids (complex plastids) are bounded either by three or four membranes as schematically shown by the number of circular lines. Non-photosynthetic plastids are shown in white, and the number and color of circular lines corresponds to the photosynthetic plastids from which they were derived. The primary plastids, arising from a single primary endosymbiosis, of Archaeplastida including glaucophytes (bright blue), red algae (red), green algae, and land plants (green) are bounded by two membranes (two circular lines). The plastid of *Paulinella chromatophora* (Rhizaria) represents an example of another independent primary endosymbiosis, and is also depicted bound by two membranes (dark blue). Complex plastids of red algal origin can be found in Stramenopiles (plastids bounded by four membranes), Alveolata (plastids bounded by three or four membranes), haptophytes and cryptophytes (both containing plastids bounded by four membranes). Both photosynthetic and non-photosynthetic plastids can be found among Stramenopiles, dinoflagellates, chrompodellids, and cryptophytes. Plastids present in Apicomplexa and perkinsid taxa, as well as *Oxhhrris* are all non-photosynthetic (uncertain number of membranes). Chlorarachniophyta (Rhizaria; plastids bounded by four membranes) and Euglenophyceae (Discobits, Excavata; plastids bounded by three membranes) arose *via* two independent secondary endosymbioses of green algae. Evidence for the loss of photosynthesis and retention of non-photosynthetic plastids exists among Euglenophyceae (white circle, three green circular lines). Nucleomorphs, leftover nuclei of endosymbionts, are present between the second and the third plastid membranes of Chlorarachniophyta (dark green dot) and cryptophytes (dark red dot). Complete plastid loss (crossed circles) is found in some Apicomplexa and dinoflagellates, while genome-less non-photosynthetic plastids occur among perkinsids, and *Rhodelphis* (asterisk) and likely also among chrompodellids and Euglenophyceae (asterisks with question marks). The outermost fourth membrane of chrompodellids is indicated by a dashed circular line, because it is yet uncertain if colpodellids have three of four membranes. Figure modified from Keeling and Burki (2019) with permission from Elsevier. Plastid details are mainly derived from Hadariová et al. (2018) and Sibbald and Archibald (2020), see also **Supplementary Table 1**.

state between stable evolutionary states. Given the driving force of a changing environment in protist evolution, we further discuss environmental factors that have an impact on mixoplankton and could explain their current prevalence and success.

EVOLUTION OF PLASTIDS IN RELATION TO MIXOTROPHY

Eukaryotic life as we know it today is very likely only possible due to phagocytosis (Yutin et al., 2009). Many eukaryotic cells still possess the mechanisms for phagocytosis, that is, the engulfment and internalization of particles with a diameter bigger than 0.4 μm (Haas, 2007). Phagocytosis facilitated the evolution of permanent plastids. However, how and when phagocytosis first evolved remains a major question in evolutionary biology (as discussed in Mills, 2020) and many theories have been proposed about explaining its connection to eukaryogenesis and organellogenesis (Sagan, 1967; Martin and Müller, 1998; Cavalier-Smith, 2002; Lane, 2005; Koonin, 2010; Martijn and Ettena, 2013; Booth and Doolittle, 2015; Hampl et al., 2019). These theories are mainly orientated toward the evolution of mitochondria and will not be treated in further detail here. Phylogenetic analyses have shown the high diversity of the molecular systems involved in phagocytosis and indicate that from early phagocytosis-like engulfment modern-type phagocytosis has independently evolved within many lineages (Yutin et al., 2009). Regardless of how and when phagocytosis first appeared, it is a trait retained by a considerable portion of marine unicellular life and plays a crucial role in ecosystem dynamics (without it, there would be no microbial loop).

The primary source of photosynthesis in eukaryotes is generally agreed upon to be established by the uptake and permanent retention of a photosynthetic cyanobacterium by a eukaryote – "primary endosymbiosis" (Schimper, 1883; Mereschkowsky, 1905; Cavalier-Smith, 1987; Zimorski et al., 2014). In essence, this resulted in the first mixotroph, capable of ingestion and photosynthesis. This primary endosymbiosis gave rise to Archaeplastida, and subsequent evolution of the plastids found in both plants and algae (with exception of the recent primary plastid acquisition of Paulinella, **Box 1**; **Figure 1**; Rodríguez-Ezpeleta et al., 2005; Adl et al., 2012; Jackson and Reyes-Prieto, 2014). For discussions on the monophyly, or polyphyly of Archaeplastida, see e.g., Larkum et al., 2007; Howe et al., 2008; Kim and Maruyama, 2014. Subsequent events of secondary and tertiary symbioses (uptake of eukaryotic alga with a primary plastid and secondary plastid, respectively) in eukaryotic algae have spread chloroplasts throughout the (eukaryotic) tree of life (see also Keeling, 2013 and references therein). To this day, it remains unresolved how many independent secondary and tertiary endosymbiotic events have occurred (Sibbald and Archibald, 2020).

Endosymbiont Gene Transfer for the Establishment of Permanent Plastids

Endosymbiosis has indisputably played a critical role in the evolution of eukaryotes and cellular plastids (reviewed in Keeling, 2013). However, the distinction between endosymbionts and permanent plastids or organelles has become constantly more blurred (Theissen and Martin, 2006; Keeling et al., 2015). In the current review, endosymbionts are considered "*organisms non-permanently and autonomously living within their host – they keep their organellar integrity and are spatially separated from the host*." The symbiosis can be beneficial for both host and symbiont, and the endosymbionts are often still viable outside of their host. To be able to discuss endosymbionts in the context of mixoplankton classifications and ecology this definition of an endosymbiont should be considered. The reader, though, needs to be aware that the difference between an endosymbiont and a permanent organelle is all but clear-cut – with various examples discovered that bridge somewhere between the two concepts.

In the evolutionary context, a permanent plastid is the result of endosymbiosis and is stably maintained in the host organism over long periods of evolutionary time. A permanent plastid is not established simply through the engulfment of another alga. For the establishment of permanent plastids (organellogenesis), it is considered a prerequisite that genes for plastid functioning are transferred (from the endosymbiont) and integrated into the host nucleus, conjointly with a reduction of the endosymbiont plastid genome, and the establishment of a protein-targeting system to move nuclear-encoded proteins into the plastid (Larkum et al., 2007; Zimorski et al., 2014; Archibald, 2015). The transfer of genes from the endosymbiont to the host nucleus is known as EGT (Timmis et al., 2004). EGT allows the establishment of a genetic connection between the functions of host and symbiont. Before plastid retention, maintenance, and continuity are achieved EGT or gene loss can total up to 90% of the endosymbiont genome (Archibald, 2015; Qiu et al., 2017). In effect, most of the transferred genes are not involved in processes associated with photosynthesis or plastid maintenance, but in other essential biosynthetic pathways. Loss of such genes creates increased metabolic integration in the host.

BOX 1 | Paulinella.

The case of the photosynthetic euglyphid testate amoeba *Paulinella chromatophora* (Cercozoa, Rhizaria) is an interesting one. First discovered in 1894 by Robert Lauterborn, *P. chromatophora* was found to have one or two kidney-shaped intracellular symbionts per cell, and unlike its sister species does not seem to feed on cyanobacteria but relies solely on photosynthesis (Nowack et al., 2008). The symbionts, now called chromatophores or cyanelles, were found to be related to *Synechoccous/Prochlorococcus* and function as "normal" plastids (Kies and Kremer, 1979; Marin et al., 2005; Yoon et al., 2006). Furthermore, the cyanelles have a significantly reduced genome, though less than canonical plastids, and also divide synchronously with the host (Kies and Kremer, 1979; Marin et al., 2005; Yoon et al., 2006). Besides the phylogenetic origin, the different origin of cyanelles is further supported by the distinct protein targeting mechanisms used by cyanelles and plastids of Archeaeplastida (Marin et al., 2005; Nowack and Grossman, 2012; Nowack, 2014). With evidence of endosymbiont gene transfer (EGT) and protein trafficking, the cyanelle can be considered an organelle, though at a more recent evolutionary stage than canonical plastids, due to its relatively large genome and the thick wall still surrounding it (Nakayama and Ishida, 2009; Nowack, 2014). *Paulinella chromatophora* is now considered the most recent and only known case of independent primary plastid acquisition, other than the Archaeplastida plastids, making it a model organism for understanding the evolution of primary endosymbiotic events.

Why EGT to the Hosts' Nuclear Genome?

Incorporation of genes into the nuclear genome could impart the selective advantage of decreased mutation by moving the genetic material away from the reactive oxygen species producing plastids (Allen and Raven, 1996). For organellar genes, which are present in relatively small copy numbers, detrimental mutations would spread quickly. Nuclear genes have the advantage of sexual recombination, which could aid in the repair of mutations (whereas there are no repair mechanisms in organelles) and improve fitness in ever-changing environments. The advantage of less genetic material at the plastid site is proposed to further enhance the plastids metabolic efficiency by limiting the volume occupied by DNA and ribosomes (Cavalier-Smith, 1987; Timmis et al., 2004).

Why Keep Genes in the Plastid?

A hypothesis proposed by Allen (1993), known as the co-location (of gene and gene product) for redox reaction (CoRR) hypothesis, attempts to explain why any genes are left in the plastids at all. The underlying concept behind this hypothesis is that core regulatory plastid genes have an advantage by remaining in the plastid genome. In prokaryotes, which are the origin of plastids, the redox state can regulate gene expression. The close spatial contact of genes and their product in the same intercellular compartment permits immediate feedback and regulation after a change in redox state in the light reaction centers of chloroplasts, or the mitochondrial oxidative phosphorylation system (Allen, 2017). Indeed, genes found in the organelles are essential for the proper functioning of the electron transport chain of the photosynthetic reaction centers of chloroplasts or the oxidative phosphorylation pathway in mitochondria (Pfannschmidt et al., 1999; Allen and Martin, 2016; Allen, 2017). For example, as shown in extracted chloroplasts, *in vitro*, there is direct and rapid redox control of chloroplast transcription at the plastoquinone site, more rapid than possible by comparable nuclear genes (Pfannschmidt et al., 1999). Björkholm et al. (2015) further proposed that selective pressure on highly hydrophobic membrane proteins caused these genes to remain in plastid genomes.

How Are Imported Gene Products Targeted to Their Destination?

Crucial for the establishment of permanent plastids is the targeting of nuclear-encoded genes toward the plastid. von Heijne (1986) hypothesized that the hydrophobicity of nuclear precursor products would pose issues in endo-cellular protein transfer among cellular components. Due to hydrophobicity, protein targeting to the plastid could be misdirected toward the wrong cellular compartment (i.e., the endoplasmic reticulum; Björkholm et al., 2015). As a result, transport of proteins would be the main obstacle for effective EGT. Yet, many examples exist of nuclear-encoded hydrophobic proteins directed to the plastids. Proteins of the light-harvesting chlorophyll *b* or fucoxanthin chlorophyll *a/c* are all hydrophobic and need to move across several membranes before reaching the thylakoids (Allen and Raven, 1996). In effect, it is not only that genes need to be transferred to the host nucleus, but also maybe more importantly, transporter and protein-targeting systems need to be established. Arguably, this is the most complex and critical step toward the establishment of permanent plastids (Cavalier-Smith, 1999; Bodył et al., 2009).

Briefly, in early evolution, protein targeting could have been achieved by early forms of the complex TIC and TOC plastid translocons of the inner and outer chloroplast membranes, respectively (Bodył et al., 2009). The subunits of TIC-TOC translocons suggest a diverse origin, with genes involved from both prokaryotic (mainly cyanobacterial) and eukaryotic origin (reviewed in Reumann et al., 2005). Further targeting mechanisms involve the transit peptides on most nucleus-encoded proteins, which serve as a signal for import to a specific cellular component. Proteins can be targeted to, and recognized by, the plastid before being post-translationally imported through the TIC-TOC translocons. Additionally, this allows import through an endomembrane system involving the endoplasmic reticulum and Golgi system, further facilitating flexibility to target multiple cellular locations (Bodył et al., 2009). Whether the initial system and driver of plastid evolution revolved around a TIC-TOC-like system or an endomembrane system is not generally agreed upon (Cavalier-Smith, 2006; Bhattacharya et al., 2007; Bodył et al., 2009).

What Are the Actual Origins of Imported Nuclear Genes?

Recently, the interestingly coined "shopping bag model" hypothesized that nuclear genes for plastid proteins encompass varying phylogenetic origins, and builds on the fact that protists readily take up cytosolic DNA into their nucleus (Larkum et al., 2007; Howe et al., 2008). This DNA can remain for significant periods of time. DNA from lysed plastids will thus not unlikely result in integrations of plastid DNA into the nuclear genome. Before the final establishment of a permanent plastid, there could thus have been genetic contributions of many different origins over time. Transient relations like kleptoplasty, where a plastid is only temporarily retained (more in section "Temporary plastids: On their way to becoming permanent?"), could result in DNA entering the host nucleus. The kleptoplastic dinoflagellate *Dinophysis*, or likewise the Ross Sea dinoflagellate, which itself does not harbor a permanent plastid, does harbor genes of diverse phylogenetic origin encoding for plastid-related proteins (Hehenberger et al., 2019; Hongo et al., 2019).

If a stable plastid were to be established, the genetics underlying the plastid machinery would finally be a mixture of the current stably established plastid and from previously acquired DNA. Cases of such chimeric genomes can be found in a great diversity of taxa (Dorrell et al., 2017). Certain dinoflagellates, for example, express isoforms for plastid-targeted proteins from several different phylogenetic origins, proteins such as cysteine synthase and psbU (*Karlodinium*, Patron et al., 2006), or isoprenoid and heem biosynthesis (*Dinophysis*, Hongo et al., 2019). Likewise, for the diatom genome, Morozov and Galachyants (2019), and earlier cases discussed in Dagan and Martin (2009)

and Deschamps and Moreira (2012), illustrated supposed ancient gene transfers from green algae, in addition to genetic information from the current red algal plastid.

Eukaryotic cells readily take up DNA into the nucleus. Obviously, though, not all foreign DNA is integrated, nor do all endosymbionts become permanent plastids. The conversion of an endosymbiont to permanent organelle is a long evolutionary process that requires specific and complex protein transport mechanisms. The simple transfer of genes is not enough. The apparent complexity of the needed protein transport mechanisms makes it that plastids are less likely to become permanent and be sustained, than is endosymbiosis or temporal plastid retention in the host.

Secondary Loss of Trophic Functions

Photosynthesis

The acquisition of photosynthetic ability is considered to be well established in (plankton) evolution, yet, it is by no means always permanent (Cavalier-Smith, 1987). Secondary reduction of photosynthetic plastids has been recorded many times. When heterotrophy is retained, phototrophy may not be essential to a cell's survival anymore. Consequently, the loss of a plastid can occur when the ecological situation changes and the functions of the plastid are no longer entirely needed, or even potentially detrimental (Williams and Keeling, 2003; Burki, 2016). Transcriptomic surveys of heterotrophic and mixotrophic chrysophytes have revealed genetic adaptations to a gradual loss of chloroplasts (Beisser et al., 2017; Graupner et al., 2018). The gene expression in these cases tends to be downregulated for photosynthesis-related processes. The gradual reduction of plastids, both in genome and size, leads to the formation of non-photosynthetic structures that could be described as "cryptic" plastids (reviewed in Hadariová et al., 2018).

Non-photosynthetic plastids are not uncommon and have been recorded across the eukaryotic tree, from Alveolata and Stramenophiles to cryptophytes, Euglenopycae, red and green algae, as well as (parasitic) land plants (Hadariová et al., 2018; **Figure 1**). For example, several diatoms, mostly of the genus *Nitzschia*, are apochlorotic, that is with non-photosynthetic plastids (Li and Volcani, 1987). Though the plastids are genomically reduced and no longer photosynthetically active, transcriptomics show that the plastids still play an indispensable role in among others glycolysis and gluconeogenesis (Kamikawa et al., 2017). The reduced chloroplasts–the apicoplasts–of plasmodium parasites no longer function for photosynthesis but carry out other biosynthetic processes for which the cell is dependent on the plastids (McFadden and Yeh, 2017; Janouskovec et al., 2019). Likewise, the recently described phagotrophic genus *Rhodelphis* was found to still host cryptic plastids involved in heem synthesis (Gawryluk et al., 2019). Here, the involvement in the heem synthesis pathway is likely the reason the plastids have not been entirely lost.

Even though reduction of plastids has been reported in many taxa, the complete loss of a plastid seems more difficult due to the importance of the plastid in many biochemical/metabolic pathways (Barbrook et al., 2006). Though it is rare, cases of complete plastid loss have been suggested for taxa belonging to oomycetes, ciliates, and dinoflagellates (Saldarriaga et al., 2001; Archibald, 2008; Reyes-Prieto et al., 2008). In the case of ciliates, the presence of proteins of plastid-origin suggests gene transfer from either algal prey or a putative photosynthetic history; however, in most cases evidence of a plastid harboring ancestor is not clear (Reyes-Prieto et al., 2008). Complete plastid loss is only unambiguously defined for several apicomplexan group parasites, e.g., *Cryptosporidium* and *Hematodinium* (Abrahamsen et al., 2004; **Figure 1**). While apicomplexans are evolutionarily descended from a mixotroph through the primary endosymbiotic event, the current parasitic live style could have been a major cause for the loss of dependency on the photosynthetic functions of the plastid (Archibald, 2015). *Hematodinium*, and also Amoebophrya, independently retain limited functions from their ancestral plastidic pathways, but as they live and fulfill their metabolic needs from their hosts the plastid would be redundant and is lost entirely (Gornik et al., 2015; John et al., 2019). Interestingly, free-living organisms tend to retain their plastid, possibly indicating that replacing lost metabolic pathways is more challenging (Janouskovec et al., 2017). Some cases are also known for dinoflagellates where, over evolutionary time, plastid loss is followed by the replacement with another (Keeling, 2013). This shows the relevant adaptability and evolutionary transitions between nutritional modes as a response to changing environmental factors.

Phagocytosis

In essence, all eukaryotic microalgal lineages (e.g., cryptophytes, haptophytes, Euglenophyceae, Stramenopiles, or dinoflagellates) have the capacity of predation, though it may have been lost in species of each lineage. Phagocytosis was lost on multiple occasions, proposed as owing to the lack of need for this mode of nutritional uptake, i.e., when photosynthetic plastids were acquired. Indeed, extant red algae or glaucophyptes harboring primary plastids, as well as diatoms, have lost their phagotrophic ability (Raven et al., 2009). Phagocytosis is most often kept in those taxa harboring secondary or tertiary plastids – many of which are mixoplankton. The fact that it is specifically those species with secondary and tertiary plastid that retain phagotrophy has been hypothesized to be an artifact of time (Kim and Maruyama, 2014). That is to say, these secondary plastids species are younger and current selective pressures keep these species mixotrophic, whereas this might not have been the case after the establishment of primary plastids.

Temporary Plastids: On Their Way to Becoming Permanent?

> *"The mitochondria and plastids we see today may, accordingly, have only been the luckiest of a longstanding series of doomed endosymbionts who were saved by transfer of genes to the nucleus."* – Keeling et al. (2015)

GNCM and pSNCM: Stolen Plastids

Unlike a permanent plastid, a stolen plastid or kleptoplast is transient. Kleptoplasty refers to the acquisition of solely the plastid from a plastid-containing prey. Kleptoplasty is a relatively common phenomenon that has been observed in various protists taxa including dinoflagellates, ciliates, and Foraminifera (Stoecker et al., 2009; Pillet and Pawlowski, 2013; Park et al., 2014). An exceptional case of animal kleptoplasty is of sacoglossan sea slugs (Pierce et al., 2003) and some flatworms (Van Steenkiste et al., 2019). The critical aspect of the kleptoplasty definition is that plastids remain only transiently functional within the kleptoplastic host. Depending on the taxa, the stolen plastids exhibit a wide range of origins and varying retention times. Retention time can be from days to months, after which the photosynthetic activity is lost and/or the plastid digested. Both the ability of the host to control the upkeep of the plastid, and the inherent stability of the original plastid can affect the retention time (Green et al., 2005). Even though kleptoplasts can have a positive impact on the energy budget of the host, there are also "side effects" due to the functioning of kleptoplasts. The host has to deal with the stress invoked due to the generation of reactive oxygen species as well as maintain the plastid with the perspective of assuring its functionality (Uzuka et al., 2019).

Studies of the *Dinophysis-Mesodinium*-Cryptophyta complex have contributed substantially to our understanding of the dynamics of kleptoplasty and the route toward a potential tertiary plastid establishment. Kleptoplastidic *Mesodinium* sp. (ciliate) does not only steal the plastid (kleptoplasts) from its cryptophyte prey but also the nucleus (kleptokaryon; Hansen et al., 2013, 2016). The kleptoplastids significantly contribute to the energetic budget of the cell with a large proportion of the total carbon needs (Hansen et al., 2013). The ability to retain fully functional plastids for a long period of time is in large part due to the additional retention of the prey nucleus (Johnson et al., 2007; Kim et al., 2017). The kleptokaryon becomes enlarged, and recent advances in transcriptomic and genomic data from both the ciliate and cryptophyte suggest that the sequestered nucleus is transcriptionally active and could account for approximately half of the total transcriptome of the ciliate (Altenburger et al., 2020). The kleptokaryon expresses genes responsible for both the maintenance of chloroplasts and the biosynthesis of metabolites for which *Mesodinium* lacks the genetic toolkit (Lasek-Nesselquist et al., 2015; Kim et al., 2016). This allows *Mesodinium* to replicate and exploit the plastids for a few months before being degraded (Smith and Hansen, 2007; Hansen et al., 2013). Interestingly, no photosynthesis-related genes were found to be transcribed by the genome of the ciliate (Altenburger et al., 2020). Instead, differential gene expression analysis indicates *Mesodinium* alters the gene expression of the kleptokaryon compared to when the nucleus is in its original host (Lasek-Nesselquist et al., 2015; Kim et al., 2016).

Kleptoplasts and kleptokaryon usage have also been observed in the (freshwater) dinoflagellate *Nusuttodinium aeruginosum* (Onuma and Horiguchi, 2015). The nucleus of cryptomonad origin undergoes extensive remodeling, accompanied by the enlargement of the kleptoplast (Onuma et al., 2020). The remodeling includes polyploidization, upregulated gene expression of pathways that involve among others, metabolism, gene translation, and DNA replication, as well as downregulation of certain genes like those involved in motility. In both *Mesodinium rubrum* and *Nusuttodinium aeroginosum* the transcriptional regulation of the kleptokaryon is no longer affected by light-regime. These transcriptional changes, and especially polyploidization, are common ground among kleptoplastic organisms and are also seen in permanently established plastids (Bendich, 1987). This suggests that polyploidization and transcriptional regulation could be a prerequisite in plastid evolution and prospective organelles. These modifications are also observed in the permanent diatom endosymbiont of *Durinskia baltica* – made possible by its polyploidy – the diatom nucleus can undergo karyostenosis during cell division (Tippit and Pickett Heaps, 1976; Yamada et al., 2019).

Dinophysis (Dinoflagellata) are known to sequester plastids of cryptophyte origin, but not the nucleus (Park et al., 2014). The difference to other kleptoplastidic organisms is that in this case the acquisition is indirect and solely after the consumption of *Mesodinium* sp. (note that *Mesodinium* sp. itself has a kleptoplast; Park et al., 2014; Hansen et al., 2016). Several *Dinophysis* nuclear transcripts are involved in photosynthesis-related processes including plastid maintenance or pigment biosynthesis (Hongo et al., 2019). Even though the acquired plastids originate from a cryptophyte, genes involved in their maintenance originate from: haptophytes, dinoflagellates, chlorarachniophytes, cyanobacteria, and cryptophytes (Hongo et al., 2019). This indicates the complexity of gene transfer to the nuclear genome of the host and gives an idea about their evolutionary past, and previous interactions, and also advocates for the "shopping bag" hypothesis (see section "Endosymbiont gene transfer for the establishment of permanent plastids"). The aforementioned NCM highlight different methods for the control of acquired plastids. The first one involves the acquisition of the prey nucleus, which is actively expressed and allows extended use and even replication of the kleptoplasts, without EGT of plastid related genes (the case of *Mesodinium*). The second strategy does involve EGT. Host-encoded genes facilitate extended use of the plastid, and possible plastid division, instead of a kleptokaryon (the case of *Dinophysis*; Rusterholz et al., 2017). The incapability to enslave the nucleus of the prey could have resulted in stronger selective forces for EGT. Yet, both strategies ultimately yield an increased survival in absence of food (Hansen et al., 2013), and could potentially evolve host-governed organelles.

A recent study by Hehenberger et al. (2019) has provided substantial insights into the fine lines between temporary and permanent plastids. The kleptoplastic Antarctic Ross Sea dinoflagellate belongs to the Kareniaceae lineage, but unlike its sister taxa, it does not have permanent plastids (Gast et al., 2007). The unusual long retention (up to 22 months) of the kleptoplast in the host suggests the presence of genes to stabilize the plastid (Sellers et al., 2014). Transcriptomic analysis of the Ross Sea dinoflagellate revealed host-encoded genes for

kleptoplast-targeted proteins (Hehenberger et al., 2019). This includes photosynthesis related genes that are also found in permanent plastids harboring relatives of the Ross Sea dinoflagellate. Interestingly, such plastid-targeted genes appear to come from various phylogenetic sources, the majority of which do not share origin with the kleptoplast, indicating ancestral establishment of plastid-targeting mechanisms. The early establishment of such mechanisms would facilitate the further usage and possible integration of subsequent plastids (of different origin), such as the haptophyte kleptoplast of the Ross Sea dinoflagellate. A critical factor for the permanent integration of the kleptoplast, as indicated in Hehenberger et al. (2019), is the level of transcriptional regulation of the host on plastid-targeted nuclear genes. The Ross Sea dinoflagellate only has transcriptional regulation for a subset of plastid-related genes, as depicted by the response (or lack thereof) to different light and temperature conditions. Indications of the establishment of transcriptional regulation mechanisms, which are important for the control of modern-day plastids, would suggest progress toward permanent plastid integration.

eSNCM: Plastids Through Photosymbiosis

The internalization of a phototroph by a heterotrophic organism characterizes one of the first steps toward a permanent plastid (section "Endosymbiont gene transfer for the establishment of permanent plastids"). Many extant examples exist of such endosymbioses, without *per se* being permanent plastids (reviewed in Stoecker et al., 2009). Upon entering a host cell an endosymbiont is encapsulated in a vacuole-like unit called a symbiosome. Endosymbionts can (most of the time) divide within the host, foregoing the need for continuous replenishment of photosymbionts. Well-known endosymbioses are cnidarians, like corals, with dinoflagellate endosymbionts. Other (photo)endosymbioses include among others: marine Rhizaria, bivalves, and gastropods with dinoflagellate symbionts; Acantharia with haptophytes and a dinoflagellate (*Noctiluca scintillans*) with green prasinophyte algal symbionts (*Pedimonas noctilucae*; Anderson, 2012; Decelle et al., 2015; Clavijo et al., 2018).

In a photosymbiosis (or other endosymbiosis), where the symbiont provides energy or photosynthates, a prerequisite for a stable relation is that the interaction is beneficial to the host. The host must be dependent on the symbiont, otherwise, the symbiont would be expendable and the relation forfeited. The relation would thus naturally be driven toward exploitation of the symbiont by the host (Keeling and McCutcheon, 2017). For the symbiosis to be evolutionarily viable to the endosymbiont it needs to be able to reproduce itself. Indeed, many photosymbionts have been extracted and cultured from their host systems, illustrating that they are capable of independent existence and reproduction (Trench and Thinh, 1995; Probert et al., 2014). However, this is not always the case, thus creating an evolutionary dead-end for the symbiont.

In the Acantharia-*Phaeocystis* symbiosis, the Acantharia host cell recruits environmental *Phaeocystis* as endosymbionts. The acquisition of symbionts is suspected to be purely horizontal, and symbionts need to be reacquired for each individual. The symbionts *in hospite* are modified in several physiological aspects, among which are an increased number and volume of plastids, and more dense thylakoids, thereby increasing the photosynthetic efficiency (Decelle et al., 2019). The symbiosome of mature symbionts intrudes into the symbiont cell, further indicating a permanent change of the endosymbiont (Uwizeye et al., 2020). These modifications are thought to be a major reason as to why the symbionts are not viable after extraction from the host. The modifications made to the symbiont in this symbiosis show several similarities to the plastid acquisition of *Paulinella*, possibly representing steps toward more complete plastid integration. Genomic or transcriptomic studies of this symbiosis are still lacking; hence it remains unknown if there have been EGT events. Evidence of EGT could show further integration and hijacking of the functions of the symbiont besides the already observed modifications.

In endosymbiotic dinotoms – dinoflagellates in symbiosis with diatoms – like other endosymbioses, the symbiotic diatom is surrounded by a membrane, a symbiosome that separates it spatially from the cytosol of the host (Tomas et al., 1973; Jeffrey and Vesk, 1976). It should be noted that in this endosymbiosis, the diatom is not fully intact as it loses its silica frustule during uptake, and unlike a permanent plastid, genome reduction and EGT are lacking, and major cellular components of the diatom remain (Hehenberger et al., 2016; Yamada et al., 2019). The symbionts of endosymbiotic dinotoms, e.g., *Durinksia kwazulunatalensis*, *D. baltica*, and *Glenodinium foliaceum*, are structurally and transcriptionally autonomous from the host dinoflagellate and can replicate independently, yet DNA replication of the diatom endosymbiont seems to coincide closely with the cell division of the host (Figueroa et al., 2009; Yamada et al., 2019). This allows permanent retention of the diatom symbiont and vertical symbiont transfer. In contrast, in the kleptoplastidic dinotom *Durinskia capensis*, an internalized diatom gradually loses most of its organelles leaving only the plastids until those are also degraded (Yamada et al., 2019). The diatoms cannot be permanently retained as no nucleus control mechanisms are developed in the host, thus converting them into temporary kleptoplasts that will need to be reobtained in subsequent generations. The synchronized karyokinesis of host and endosymbiont, as in *D. baltica* or *D. kwazulunatalensis*, seems critical for the development of a more stable relationship between host and endosymbiont.

NCM as a Transition to Permanent Plastids

Bodył (2018) hypothesized that red algal derived secondary plastids, like those of dinoflagellates, evolved not necessarily by phagocytotic uptake, but *via* kleptoplastidy. In fact, it can be proposed that many of the previously explored kleptoplastidic and endosymbiotic relations are in effect new plastids *en route* to becoming permanent plastids, a "work in progress" situation. The establishment of permanent plastids is preceded by genomic reduction, and increased control of the host on its symbiont to the point that the symbiont is no longer able to reproduce *in hospite* nor *ex hospite* once released from the host. Progressively there would be increased genetic integration (EGT) of

photosynthetic genes from the transient symbiont/kleptoplast associations (see targeting-ratchet model in Keeling, 2013). *Dinophysis* and *Mesodinium* both use a kleptoplast obtained from the same source, though EGT has yet only occurred in *Dinophysis*. Apart from EGT, the Ross Sea dinoflagellate exemplifies the importance of establishing transcriptional regulation mechanisms for transferred genes. The acantharian symbiont *Phaeocytis* has already been suggested to possibly be a form of kleptoplasty instead of symbiosis, due to the restrictions in proliferation and modifications on the symbiont (Decelle et al., 2012, 2019). Similar modifications are observed for the kleptoplast of *Nusuttodinium*. Dinotoms have varying levels of endosymbiont integration and karyokinesis in concert with their own (Yamada et al., 2019). Considering the insights into gene transfer, metabolic connectivity and protein-targeting between plastid/endosymbiont and host, we could hypothesize that kleptoplastic or endosymbiotic mixotrophs are an evolutionary intermediate toward a permanent plastid (**Figure 2**; Keeling, 2013; Keeling and McCutcheon, 2017; Hehenberger et al., 2019). However, this is not to say that all these systems are heading in the same direction, but could offer a chance to compare potential stages of evolving systems.

Alternatively, temporary plastids could be an advantageous adaptation as opposed to permanent organelles. Unlike genetic adaptation, and thus the establishment of permanent plastids, temporary plastids could allow for more plasticity within an environmental range. This could be thought of in light of Acantharia that acquire and maintain locally adapt *Phaeocystis* symbionts as directed by the environment (Decelle et al., 2012; Mars Brisbin et al., 2018). Corals can also shuffle their symbiont populations when stress events mandate it (Lewis and Coffroth, 2004; LaJeunesse et al., 2009, 2010). This allows the host to better adapt to changing environments by shuffling and swapping symbionts. Additionally, acquired plastids possibly impose less energy investment and could be converted into host biomass, whereas this is not possible for permanent plastids (Flynn and Hansen, 2013).

WHY, WHEN, AND HOW TO MIXOTROPH

Protists are often limited in their growth capabilities, pure phototrophs by nutrients or light, and pure phagotrophs by prey availability. This holds particularly true in oligotrophic

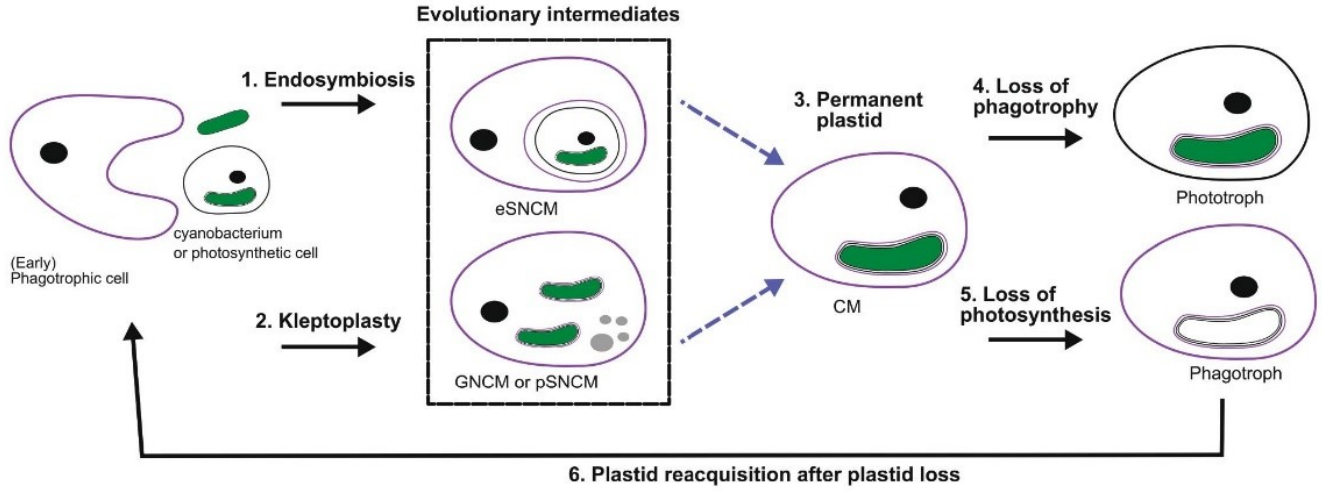

FIGURE 2 | Perspective of protist plastid evolution and the role of mixotrophy. Conceptual illustration of plastid evolution depicting non-constitutive mixoplankton as hypothetical intermediate stages to permanent plastids. The cell nucleus is shown as a black circle, kleptokaryons as gray circles, and photosynthetic plastids in green. For the initial primary plastid acquisition, the plastid came from a cyanobacterium (green oval; see also "Box 1 *Paulinella*" for a possible exception), the acquired primary plastid would be bound by only two membranes as depicted in the photosynthetic cell on the left. While complex permanent plastids gained by secondary or tertiary endosymbiosis are bound by three or four membranes, respectively as illustrated by the number of lines around the plastid. In secondary and higher plastid acquisition, the photosynthetic cell can be either a CM or phototroph with primary, secondary or higher-order plastid. Illustrated here is secondary plastid acquisition with the host membrane in purple. Blue dashed lines are the hypothetical route toward permanent plastid retention. (1) Uptake of a photosynthetic alga and internalization of the entire organism as a symbiont (in a symbiosome) e.g., Radiolaria, *Noctiluca*. (2) Kleptoplasty shows the phagotrophic uptake of photosynthetic algae (prey), keeping the chloroplasts temporarily functional. The photosynthetic prey can be with primary, secondary (or higher) plastids. For example, the kleptoplastic ciliates like *Strombidium* sp. In some cases, the prey nucleus (gray circles) is also retained e.g., *Mesodinium rubrum* (which feeds on secondary plastid holding cryptophytes), and *Nusuttodinium aeroginosum*. (3) The establishment of permanent plastids. Primary plastids by uptake of a cyanobacterium, with the plastid bound by only two membranes, e.g., as retained in most Archaeplastida including glaucophytes, red and green algae, as well as land plants and the more recent primary plastid of *Paulinella chromatophora*. Secondary plastids bound by three or more membranes are found in Euglenophycaea, haptophytes, cryptophytes, and SAR organisms. Tertiary plastid acquisitions have only been clearly documented in Dinoflagellates. (4) Indicated here is the secondary loss of phagotrophy, we assume all pure phototrophs lost phagotrophy somewhere along their phylogeny e.g., diatoms. (5) Loss of photosynthesis, though only in rare cases is the plastid completely lost, the non-photosynthetic plastid is depicted lacking green color. Evidence for such primary plastid loss is found in e.g., *Rhodelphis* sp., *Helicosporidium* sp. Loss of photosynthesis after secondary (or higher) permanent plastid acquisition can be found, for example, in some Euglenophycaea, Stramenopiles like apochlorotic diatoms, dinoflagellates, cryptophytes, perkinsids, and Apicomplexa like *Cryptosporidium*. Complete plastid loss can, for example, be seen in *Polytoma* sp., *Cryptosporidium*, and *Hematodinium* (see also **Figure 1**). (6) Plastid reacquisition after loss of phototrophy is only known in dinoflagellates.

ecosystems, where mixotrophy proved to be more beneficial (Stoecker et al., 2017). In such nutrient poor environments, mixotrophy can thus be especially widespread. Since mixoplankton can meet their metabolic demands through a mixture of photosynthesis and prey ingestion, they can supplement one nutrient source with another.

Trade-Offs

Even though mixotrophy offers flexibility in nutrient and energy acquisition, mixoplankton are not prevailing everywhere. Therefore, certain trade-offs (benefits and costs) to mixed nutrition seem apparent (Raven, 1997). Both phototrophy and phagotrophy involve mechanisms and structures that incur costs. In the case of a phototroph, this is primarily the maintenance of the photosynthetic machinery. For phagotrophs, it includes costs related to all the required mechanisms for the internalization of food particles and/or production of secondary metabolites, like toxins that mediate prey capture. Investments into the photosynthetic (or phagotrophic) machinery involve nutrient costs, estimated as up to 50% (or 10%) of the cell's nutrient currency (e.g., carbon, nitrogen, and phosphorus; Raven, 1984, 1997). Resources used to maintain chloroplasts could have otherwise been used for other processes, like growth or reproduction. This is likewise the case for traits associated with, for example, phagotrophy, dissolved nutrient uptake, prey detection, capture or defense (Andersen et al., 2015). This inevitably has an impact on the growth rate, as "costs" are to be paid in order to make use of each of these processes. Costs that are also incurred by the fundamentals such as DNA, RNA, and ribosome maintenance and multiplication (Flynn and Mitra, 2009; Stoecker et al., 2009; Ward et al., 2011).

Besides the basic trade-offs in cell maintenance, more plastid-specific trade-offs have also been researched. Giovanardi et al. (2017) showed more tightly compressed thylakoids in plastids of mixotrophic *Neochloris oleoabundans* than in autotrophically grown samples, thereby the compressed thylakoids would lose on fluidity. It has been hypothesized that more appressed thylakoids would preserve or delay the degradation of the photosystems (Giovanardi et al., 2017). However, in turn, decreased fluidity could impair plasticity for stressors such as temperature change (Mansour et al., 2018).

Along with phototrophy come high-affinity nutrient transporters for the import of dissolved nutrients into the cell. An increase in nutrient uptake sites for dissolved nutrients, facilitates higher affinity and an increase in nutrient uptake. Simultaneously, these sites could also be costly due to being potential entry points for viruses (Menge and Weitz, 2009). From that perspective, a lower affinity to dissolved nutrients could mitigate viral entry. For mixotrophs, the loss of these sites and the involved costs would be minimized when nutrient uptake can be achieved and supplemented through phagotrophy. Predation, in turn, requires encounters with other cells, which could also incur indirect costs due to increased encounters with potential predators (Broglio et al., 2001; Kiørboe, 2011). Phagotrophy would further exclude a rigid cell wall and thereby limit protection, as in diatoms with rigid cell walls but having lost phagotrophic capability.

Mixotrophic Gradient Under Changing Biotic and Abiotic Factors

An increasing number of both field and laboratory studies have contributed to our understanding of the dynamics and different aspects of mixotrophy. A mixotrophic lifestyle is often flexible. The biological investment in phagotrophy or phototrophy can vary depending on the prevailing biotic and abiotic environmental conditions. The reliance on either photosynthesis or prey consumption can be partial or complete. We thus refer to a gradient of mixotrophy, toward either more phototrophy or phagotrophy, considering their relative contribution to an organism's metabolic needs (**Figure 3**). This mixotrophic spectrum is further affected by the degree of investment into nutrient uptake (Andersen et al., 2015), to which previously discussed potential trade-offs apply. How mixotrophy and mixotrophic communities change in response to environmental changes is a current scientific challenge (González-Olalla et al., 2019). Environmental conditions discussed here include light irradiance, temperature, and nutrients in the perspective of feeding and growth.

Light

The ability to photosynthesize prerequisites the availability of light in order to grow. Irradiance generally increases growth up to a point of saturation, though often the highest growth rates are achieved if prey is available (Li et al., 1999). There are, however, exceptions of mixoplankton that rely mainly on either photosynthesis (e.g., *Gymnodinium resplendens*; Skovgaard, 2000) or phagotrophic feeding (e.g., *Fragilidium* sp. or *Ochromonas*; Skovgaard, 1996; Flöder et al., 2006). In these cases, mixotrophy seems to be a survival strategy for when a single trophic mode does not suffice (Keller et al., 1994; Flöder et al., 2006; Anderson et al., 2018), for example, during long polar winters (Stoecker and Lavrentyev, 2018).

Under low light conditions, two different isolates of *Ochromonas* showed contrasting physiological responses. Whereas one isolate moved toward an increased focus on photosynthesis by compensating the lower light intensity with more cellular chlorophyll *a*, the other isolate substituted the focus on photosynthesis with an increased rate of bacterivory (Wilken et al., 2020), as is similarly seen for *Heterocapsa rotundata* (Millette et al., 2017). Increased irradiance has been shown to cause a positive feedback chain for *Karlodinium veneficum*, where higher light increased photosynthesis as well as feeding rate; the increased phagotrophy in turn increased photosynthetic capacity (Li et al., 1999). In contrast, the feeding rate of *M. rubrum* is not affected by irradiance (Smith and Hansen, 2007). *Karlodinium veneficum*, and some other dinoflagellates, cannot grow (or are only sustained) in the dark even when prey is available, that is to say, it is an obligate phototroph. Other dinoflagellate species, or chrysophytes such as *Ochromonas* sp., can grow in constant darkness if supplied with food (Caron et al., 1993; Ok et al., 2019). Thus, predation can, but does not always, compensate for the inability to use chloroplasts in the dark. Fischer et al. (2017) investigated the effect of light on the success of mixotrophic flagellates, and showed

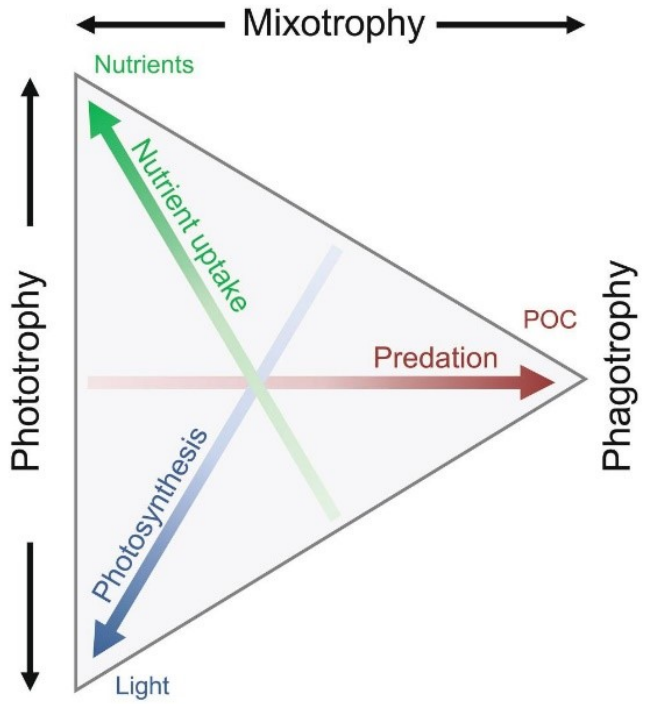

FIGURE 3 | Conceptual illustration of the trophic continuum from phototrophy over mixotrophy to pure phagotrophy. The mixotrophic spectrum is defined by the allocation into three traits: nutrient uptake, photosynthesis, and predation/phagotrophy, leading to the uptake of dissolved inorganic nutrients, CO_2, and particulate organic matter. A specific organisms' trophic strategy is defined as a point within the triangle: an organism somewhere along the left side will be a pure phototroph, an organism at the right tip would be a pure heterotroph, and any organism somewhere between these two extremes is a mixotroph. Redrawn and modified from Andersen et al. (2015), with permission from Oxford University Press.

that mixotrophic bacterivorous flagellates prevail in high light and low nutrients conditions. Oppositely, pure heterotrophs and pure autotrophs prevail in low-light and nutrient-rich ecosystems.

Nutrients

Research has mostly focused on the availability of non-carbon elements such as nitrogen and phosphorus. When one or both of these nutrients are inadequate mixotrophy can be vital, as prey ingestion is the only alternative to obtain missing nutrients. Many examples are recorded of species feeding on either bacteria or eukaryotic prey under short- or long-term starvations of nitrogen and phosphorus. *Nephroselmis pyriformis*, for example, can achieve normal growth even when nutrient-limited by compensation *via* bacterivory (Anderson et al., 2018). Other seemingly non-phagotrophic species can be induced to perform phagotrophy by nutrient-limited treatments, e.g., in dinoflagellates (Smalley et al., 2003; Johnson, 2015), haptophytes (Chan et al., 2019), and cryptophytes (González-Olalla et al., 2019). The use of diluted media to provoke starvation indicates the complexity in understanding in detail the principal factors that could induce phagotrophy and identify mixotrophy.

Nutrients that are usually found in low concentrations, such as iron, micronutrients, and vitamins are mostly understudied (Anderson et al., 2018), but can have major effects on growth rates (Reich et al., 2020). It is believed that (N)CM obtain micro-nutrients mainly through the ingestion of prey (Hansen et al., 2019). However, there remains a lot to learn about nutrient acquisition dynamics in NCM, and the role of endosymbionts in acquiring dissolved nutrients.

Temperature

The general theory of metabolism in ecology suggests a shift to heterotrophy when temperature increases (Allen et al., 2005; Rose and Caron, 2007; Franzè and Lavrentyev, 2014). As in many biological systems, the relation of phagotrophy and temperature is Gaussian, and delimited by an organism's temperature tolerance. Higher temperature implies higher metabolic rates and concomitantly an increased need for energy, and possible stress incurrence. Studies have indeed shown higher ingestion rates in response to temperature increase in many species (Princiotta et al., 2016; Cabrerizo et al., 2019; Ok et al., 2019). This validates the applicability of the general theory of metabolism in marine protists. A combined increase of phagotrophy and a decrease in photosynthetic capacity with higher temperatures strongly decreased the relative contribution of phototrophy in mixotrophic *Ochromonas* sp., allowing growth rates to keep increasing under temperatures where photosynthetic growth rate already declined (Wilken et al., 2013). This effect of temperature on the autotrophic, mixotrophic, and heterotrophic growth of *Ochromonas* sp. has highlighted the trade-offs in its trophic strategy and temperature tolerance. The increased temperature can be considered as a stressor that needs to be alleviated by reduced photosynthetic activity, and/or compensated for with nutrients from phagotrophy (Cabrerizo et al., 2019). This might be achieved by using nutrients from phagotrophy to repair or maintain photosystems.

Role of Mixotrophy in a Future Scenario

We found the physiological research on mixoplankton is generally biased toward CM. Yet, within this group there is already a large taxonomic and physiological diversity resulting in ambiguous responses to environmental factors. Especially among dinoflagellates – which can be CM, NCM, pure phagotrophs, or pure phototrophs – there is a wide spectrum of responses to food availability and abiotic conditions (Hansen, 2011). Efforts to understand the effects of varying conditions, such as nutrients, light irradiance, temperature, and prey availability have given diverse results, thus making it difficult to highlight general patterns.

Changing environmental conditions can shift mixoplankton toward a higher prevalence of either phototrophy or phagotrophy (**Figure 4**). Such shifts have apparent effects on the plankton community composition and the energy transfer between trophic levels (Rose and Caron, 2007; O'Connor et al., 2009). Though not unambiguous, the general trends seem to show mostly a phagotrophic increase with increased temperature. Decreased nutrients can induce or promote phagotrophy, oppositely,

phototrophy seems preferred when sufficient nutrients are available. Whereas light is directly fueling phototrophy, it can promote both phototrophy and phagotrophy. In some cases, limiting inorganic nutrients is a critical factor for expressing mixotrophy, while in other cases mixotrophy is a de-facto state independent of nutrient regime (Johnson, 2015). The combination of low nutrients and high light is suggested to favor mixotrophy, as it is suboptimal for either pure phagotrophy or phototrophy (Mitra et al., 2014; Hansen et al., 2019). Seasonally such conditions can already show increased mixoplankton abundance, e.g., in summer (mature ecosystem states; Hansen et al., 2019). It has also been proposed that polar regions, characterized by extremes in solar irradiance and nutrient-limitation, select for mixotrophy (Stoecker and Lavrentyev, 2018). The *grand écart* hypothesis proposed by Selosse et al. (2017) further attempts to explain the ubiquity of mixotrophy. The open ocean ecosystem is usually limited in non-carbon elements, and summer stratification limits the recycling of sinking particles or nutrients back into the water column and upper layers. The biological carbon pump further exports carbon and other nutrients from the upper photic layers. This results in light being available in the upper layers, while other essential nutrients are separated toward deeper layers. This imbalance in resources (light and nutrients) favors and selects for mixotrophs that can supplement the lack of resources by feeding.

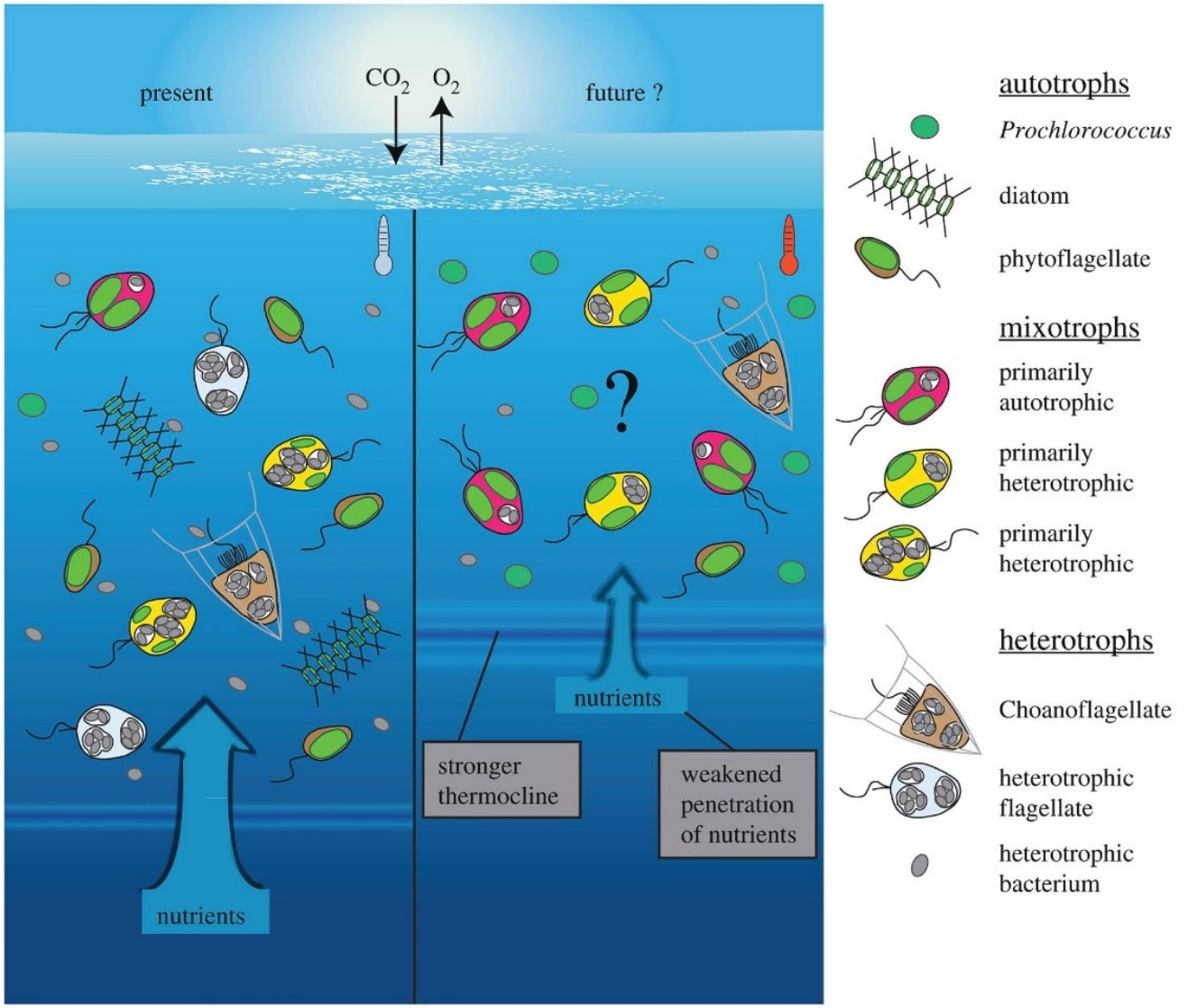

FIGURE 4 | Conceptual depiction of plankton community shift under a climate change scenario in the open ocean. Future changes involve warmer, more oligotrophic water and higher light irradiance, due to stronger water stratification and a shallower mixed layer depth (right). Protists with photosynthetic ability contain plastids (green), while phagotrophic ability is indicated by food vacuoles containing bacterial prey (gray). The limiting nutrients in this future scenario are expected to favor more nutrient competitive species like *Prochlorococcus* (cyanobacteria), while no generalized effects can yet be accurately predicted for mixoplankton. Generally, the flexibility in nutritional modes by mixoplankton renders them more competitive than pure phototrophs or heterotrophs, thus a general increase in relative mixoplankton abundance could be expected. Species-specific responses could shift over the mixotrophic continuum either toward more heterotrophy (in red) or more photosynthesis (in yellow). Reprinted from Wilken et al. (2019), with permission from Royal Society.

CONCLUSION

Phagotrophy rests at the origin of the different functional types of mixoplankton. The complete digestion of prey, the retention of prey organelles, or whole cells as endosymbionts indicates the diversity of responses after phagocytosis of "external" material. Constitutive mixoplankton benefits from having alternative ways of nutrient acquisition that each can be exploited under certain conditions. In non-constitutive mixoplankton, undigested organelles can either be perceived as the inability of the host to degrade (or digest) the organelles (incidental retention), or as the active retention of them for further use (deliberate retention). The longevity of an organelle within the host as well as the level of usage, integration, and connectivity is species-specific and variable (Gast et al., 2007; Stoecker et al., 2009; Yamada et al., 2019). The broad diversity in exploitation and handling of acquired organelles, as well as the acquisition and/or loss of phagocytosis or photosynthesis, is indicative of the adaptation of organisms to environmental conditions over their evolutionary history.

Mixotrophs with temporary plastids could depict evolutionary intermediates of permanent plastids (**Figure 2**). In species with temporary plastids, evolutionary force could still drive toward fixing phototrophic potential. That is, of course, given that the trade-offs for having potential for both photosynthesis and phagotrophy do not pose too strong a counterforce. With ever-changing environmental conditions, even seasonally, temporary plastids can give more flexibility by allowing a change to better-adapted plastids and are thereby more beneficial. Conversely, when either organic matter or light is constantly available, maintaining phagotrophy as well as photosynthesis can be costly. When the costs for maintaining multiple structures do not offset the benefits, evolution might be driven toward permanent plastids in lieu of temporary plastids, or toward pure heterotrophy. It is thus interesting to note that mixoplankton have been associated with oligotrophic environments (Mitra et al., 2014; Hansen et al., 2019), as the imbalance in resource availability "forces" more efficient use and alternative means of resource acquisition.

So far, eco-physiological studies to understand the role of environmental conditions in the prevalence of mixotrophy are mostly done on cultures. Many taxa thus remain understudied due to difficulties in culturing them. This is especially true for fragile protists and grazers (often NCM), where the successful isolation of both the predator and the prey is required. Field experiments are thus especially needful as the effects of parameters such as light, temperature, prey, and nutrients availability can be tested on understudied uncultured taxa. New technologies including single-cell genomics (Labarre et al., 2020), transcriptomics (Cooney et al., 2020), and chemical imaging (Decelle et al., 2020) allow us to study the biological role of individual cells. The potential of such techniques could reinforce the study of rare and unculturable NCM taxa. Comparative genomics has already helped to better understand how temporary plastids become permanent (Sibbald and Archibald, 2020). Combined knowledge from comparative genomics and new eco-physiological studies on mixotrophs could give further insights in the evolutionary fate of extant temporary plastids and NCM, as well as resolve evolutionary histories and their early intermediates. Jointly, knowledge of the evolutionary fate of such trophic dynamics shaping traits will assist in predictions of oceanic ecosystems.

AUTHOR CONTRIBUTIONS

All authors listed have made a substantial, direct and intellectual contribution to the work, and approved it for publication.

FUNDING

This work was supported by European Union's Horizon 2020 research and innovation programme under grant agreement No. 766327.

ACKNOWLEDGMENTS

We thank the MixITiN consortium (www.mixotroph.org) for helpful comments and criticism on early versions of the manuscript, in particular Fabrice Not, Uwe John, Maira Maselli, Lisa Schneider, Claudia Traboni, Kevin Flynn, and Aditee Mitra. We also want to thank the editor and the reviewers of the manuscript for their constructive comments.

SUPPLEMENTARY MATERIAL

The Supplementary Material for this article can be found online at: https://www.frontiersin.org/articles/10.3389/fmars.2021.666160/full#supplementary-material

REFERENCES

Abrahamsen, M. S., Templeton, T. J., Enomoto, S., Abrahante, J. E., Zhu, G., Lancto, C. A., et al. (2004). Complete genome sequence of the apicomplexan, *Cryptosporidium parvum*. *Science* 304, 441–445. doi: 10.1126/science.1094786

Adl, S. M., Simpson, A. G. B., Lane, C. E., Lukeš, J., Bass, D., Bowser, S. S., et al. (2012). The revised classification of eukaryotes. *J. Eukaryot. Microbiol.* 59, 429–493. doi: 10.1111/j.1550-7408.2012.00644.x

Allen, J. F. (1993). Control of gene expression by redox potential and the requirement for chloroplast and mitochondrial genomes. *J. Theor. Biol.* 165, 609–631. doi: 10.1006/jtbi.1993.1210

Allen, J. F. (2017). The CoRR hypothesis for genes in organelles. *J. Theor. Biol.* 434, 50–57. doi: 10.1016/j.jtbi.2017.04.008

Allen, A. P., Gillooly, J. F., and Brown, J. H. (2005). Linking the global carbon cycle to individual metabolism. *Funct. Ecol.* 19, 202–213. doi: 10.1111/j.1365-2435.2005.00952.x

Allen, J. F., and Martin, W. F. (2016). Why have organelles retained genomes? *Cell Syst.* 2, 70–72. doi: 10.1016/j.cels.2016.02.007

Allen, J. F., and Raven, J. A. (1996). Free-radical-induced mutation vs redox regulation: costs and benefits of genes in organelles. *J. Mol. Evol.* 42, 482–492. doi: 10.1007/BF02352278

Altenburger, A., Cai, H., Li, Q., Drumm, K., Kim, M., Zhu, Y., et al. (2020). Limits to the cellular control of sequestered cryptophyte prey in the marine

ciliate *Mesodinium rubrum*. *ISME J.* 15, 1056–1072. doi: 10.1038/s41396-020-00830-9

Andersen, K. H., Aksnes, D. L., Berge, T., Fiksen, Ø., and Visser, A. (2015). Modelling emergent trophic strategies in plankton. *J. Plankton Res.* 37, 862–868. doi: 10.1093/plankt/fbv054

Anderson, O. R. (2012). Living together in the plankton: a survey of marine protist symbioses. *Acta Protozool.* 52, 1–10. doi: 10.4467/16890027AP.13.006.1085

Anderson, R., Charvet, S., and Hansen, P. (2018). Mixotrophy in chlorophytes and haptophytes—effect of irradiance, macronutrient, micronutrient and vitamin limitation. *Front. Microbiol.* 9:1704. doi: 10.3389/FMICB.2018.01704

Anderson, R., Jürgens, K., and Hansen, P. J. (2017). Mixotrophic phytoflagellate bacterivory field measurements strongly biased by standard approaches: a case study. *Front. Microbiol.* 8:1398. doi: 10.3389/fmicb.2017.01398

Anschütz, A. A., and Flynn, K. J. (2020). Niche separation between different functional types of mixoplankton: results from NPZ-style N-based model simulations. *Mar. Biol.* 167, 1–21. doi: 10.1007/s00227-019-3612-3

Archibald, J. M. (2008). Plastid evolution: remnant algal genes in ciliates. *Curr. Biol.* 18, R663–R665. doi: 10.1016/j.cub.2008.06.031

Archibald, J. M. (2015). Endosymbiosis and eukaryotic cell evolution. *Curr. Biol.* 25, R911–R921. doi: 10.1016/j.cub.2015.07.055

Barbrook, A. C., Howe, C. J., and Purton, S. (2006). Why are plastid genomes retained in non-photosynthetic organisms? *Trends Plant Sci.* 11, 101–108. doi: 10.1016/j.tplants.2005.12.004

Beisner, B. E., Grossart, H. P., and Gasol, J. M. (2019). A guide to methods for estimating phago-mixotrophy in nanophytoplankton. *J. Plankton Res.* 41, 77–89. doi: 10.1093/plankt/fbz008

Beisser, D., Graupner, N., Bock, C., Wodniok, S., Grossmann, L., Vos, M., et al. (2017). Comprehensive transcriptome analysis provides new insights into nutritional strategies and phylogenetic relationships of chrysophytes. *PeerJ* 5:e2832. doi: 10.7717/peerj.2832

Bendich, A. J. (1987). Why do chloroplasts and mitochondria contain so many copies of their genome? *Bioessays* 6, 279–282. doi: 10.1002/bies.950060608

Bhattacharya, D., Archibald, J. M., Weber, A. P. M., and Reyes-Prieto, A. (2007). How do endosymbionts become organelles? Understanding early events in plastid evolution. *Bioessays* 29, 1239–1246. doi: 10.1002/bies.20671

Björkholm, P., Harish, A., Hagström, E., Ernst, A. M., and Andersson, S. G. E. (2015). Mitochondrial genomes are retained by selective constraints on protein targeting. *Proc. Natl. Acad. Sci. U. S. A.* 112, 10154–10161. doi: 10.1073/pnas.1421372112

Bodył, A. (2018). Did some red alga-derived plastids evolve via kleptoplastidy? A hypothesis. *Biol. Rev. Camb. Philos. Soc.* 93, 201–222. doi: 10.1111/brv.12340

Bodył, A., Mackiewicz, P., and Stiller, J. W. (2009). Early steps in plastid evolution: current ideas and controversies. *Bioessays* 31, 1219–1232. doi: 10.1002/bies.200900073

Booth, A., and Doolittle, W. F. (2015). Eukaryogenesis, how special really? *Proc. Natl. Acad. Sci. U. S. A.* 112, 10278–10285. doi: 10.1073/pnas.1421376112

Brisbin, M. M., Mesrop, L. Y., Grossmann, M. M., and Mitarai, S. (2018). Intra-host symbiont diversity and extended symbiont maintenance in photosymbiotic Acantharea (clade F). *Front. Microbiol.* 9:1998. doi: 10.3389/fmicb.2018.01998

Broglio, E., Johansson, M., and Jonsson, P. R. (2001). Trophic interaction between copepods and ciliates: effects of prey swimming behavior on predation risk. *Mar. Ecol. Prog. Ser.* 220, 179–186. doi: 10.3354/meps220179

Burkholder, J. A. M., Glibert, P. M., and Skelton, H. M. (2008). Mixotrophy, a major mode of nutrition for harmful algal species in eutrophic waters. *Harmful Algae* 8, 77–93. doi: 10.1016/j.hal.2008.08.010

Burki, F. (2016). Mitochondrial evolution: going, going, gone. *Curr. Biol.* 26, R410–R412. doi: 10.1016/j.cub.2016.04.032

Burns, J. A., Pittis, A. A., and Kim, E. (2018). Gene-based predictive models of trophic modes suggest asgard archaea are not phagocytotic. *Nat. Ecol. Evol.* 2, 697–704. doi: 10.1038/s41559-018-0477-7

Cabrerizo, M. J., González-Olalla, J. M., Hinojosa-López, V. J., Peralta-Cornejo, F. J., and Carrillo, P. (2019). A shifting balance: responses of mixotrophic marine algae to cooling and warming under UVR. *New Phytol.* 221, 1317–1327. doi: 10.1111/nph.15470

Caron, D. A. (2017). Acknowledging and incorporating mixed nutrition into aquatic protistan ecology, finally. *Environ. Microbiol. Rep.* 9, 41–43. doi: 10.1111/1758-2229.12514

Caron, D. A., Sanders, R. W., Lim, E. L., Marrasé, C., Amaral, L. A., Whitney, S., et al. (1993). Light-dependent phagotrophy in the freshwater mixotrophic chrysophyte *Dinobryon cylindricum*. *Microb. Ecol.* 25, 93–111. doi: 10.1007/BF00182132

Cavalier-Smith, T. (1987). The simultaneous symbiotic origin of mitochondria, chloroplasts, and microbodies. *Ann. N. Y. Acad. Sci.* 503, 55–71. doi: 10.1111/j.1749-6632.1987.tb40597.x

Cavalier-Smith, T. (1999). Principles of protein and lipid targeting in secondary symbiogenesis: euglenoid, dinoflagellate, and sporozoan plastid origins and the eukaryote family tree. *J. Eukaryot. Microbiol.* 46, 347–366. doi: 10.1111/j.1550-7408.1999.tb04614.x

Cavalier-Smith, T. (2002). The phagotrophic origin of eukaryotes and phylogenetic classification on protozoa. *Int. J. Syst. Evol. Microbiol.* 52, 297–354. doi: 10.1099/00207713-52-2-297

Cavalier-Smith, T. (2006). Origin of mitochondria by intracellular enslavement of a photosynthetic purple bacterium. *Proc. Biol. Sci.* 273, 1943–1952. doi: 10.1098/rspb.2006.3531

Chan, Y. F., Chiang, K. P., Ku, Y., and Gong, G. C. (2019). Abiotic and biotic factors affecting the ingestion rates of mixotrophic nanoflagellates (Haptophyta). *Microb. Ecol.* 77, 607–615. doi: 10.1007/s00248-018-1249-2

Clavijo, J. M., Donath, A., Serôdio, J., and Christa, G. (2018). Polymorphic adaptations in metazoans to establish and maintain photosymbioses. *Biol. Rev. Camb. Philos. Soc.* 93, 2006–2020. doi: 10.1111/brv.12430

Cooney, E. C., Okamoto, N., Cho, A., Hehenberger, E., Richards, T. A., Santoro, A. E., et al. (2020). Single cell transcriptomics of *Abedinium* reveals a new early-branching dinoflagellate lineage. *Genome Biol. Evol.* 12, 2417–2428. doi: 10.1093/gbe/evaa196

Cruz, S., Calado, R., Serôdio, J., and Cartaxana, P. (2013). Crawling leaves: photosynthesis in sacoglossan sea slugs. *J. Exp. Bot.* 64, 3999–4009. doi: 10.1093/jxb/ert197

Dagan, T., and Martin, W. (2009). Seeing green and red in diatom genomes. *Science* 324, 1651–1652. doi: 10.1126/science.1175765

Decelle, J., Colin, S., and Foster, R. A. (2015). "Photosymbiosis in marine planktonic protists" in *Marine Protists*. eds. S. Ohtsuka, T. Suzaki, T. Horiguchi, N. Suzuki and F. Not (Tokyo, Japan: Springer), 465–500.

Decelle, J., Probert, I., Bittner, L., Desdevises, Y., Colin, S., de Vargas, C., et al. (2012). An original mode of symbiosis in open ocean plankton. *Proc. Natl. Acad. Sci. U. S. A.* 109, 18000–18005. doi: 10.1073/pnas.1212303109

Decelle, J., Stryhanyuk, H., Gallet, B., Veronesi, G., Schmidt, M., Balzano, S., et al. (2019). Algal remodeling in a ubiquitous planktonic photosymbiosis. *Curr. Biol.* 29, 968–978. doi: 10.1016/j.cub.2019.01.073

Decelle, J., Veronesi, G., Gallet, B., Stryhanyuk, H., Benettoni, P., Schmidt, M., et al. (2020). Subcellular chemical imaging: new avenues in cell biology. *Trends Cell Biol.* 30, 173–188. doi: 10.1016/j.tcb.2019.12.007

Deschamps, P., and Moreira, D. (2012). Reevaluating the green contribution to diatom genomes. *Genome Biol. Evol.* 4, 683–688. doi: 10.1093/gbe/evs053

Dorrell, R. G., Gile, G., McCallum, G., Méheust, R., Bapteste, E. P., Klinger, C. M., et al. (2017). Chimeric origins of ochrophytes and haptophytes revealed through an ancient plastid proteome. *elife* 6:e23717. doi: 10.7554/eLife.23717

Ferreira, G. D., and Calbet, A. (2020). Caveats on the use of rotenone to estimate mixotrophic grazing in the oceans. *Sci. Rep.* 10:3899. doi: 10.1038/s41598-020-60764-2

Figueroa, R. I., Bravo, I., Fraga, S., Garcés, E., and Llaveria, G. (2009). The life history and cell cycle of *Kryptoperidinium foliaceum*, a dinoflagellate with two eukaryotic nuclei. *Protist* 160, 285–300. doi: 10.1016/j.protis.2008.12.003

Fischer, R., Giebel, H.-A., Hillebrand, H., and Ptacnik, R. (2017). Importance of mixotrophic bacterivory can be predicted by light and loss rates. *Oikos* 126, 713–722. doi: 10.1111/oik.03539

Flöder, S., Hansen, T., and Ptacnik, R. (2006). Energy-dependent bacterivory in *Ochromonas minima*—a strategy promoting the use of substitutable resources and survival at insufficient light supply. *Protist* 157, 291–302. doi: 10.1016/j.protis.2006.05.002

Flynn, K. J., and Hansen, P. J. (2013). Cutting the canopy to defeat the "selfish gene"; conflicting selection pressures for the integration of phototrophy in mixotrophic protists. *Protist* 164, 811–823. doi: 10.1016/j.protis.2013.09.002

Flynn, K. J., and Mitra, A. (2009). Building the "perfect beast": modelling mixotrophic plankton. *J. Plankton Res.* 31, 965–992. doi: 10.1093/plankt/fbp044

Flynn, K. J., Mitra, A., Anestis, K., Anschütz, A. A., Calbet, A., Ferreira, G. D., et al. (2019). Mixotrophic protists and a new paradigm for marine ecology: where does plankton research go now? *J. Plankton Res.* 41, 375–391. doi: 10.1093/plankt/fbz026

Flynn, K. J., Stoecker, D. K., Mitra, A., Raven, J. A., Glibert, P. M., Hansen, P. J., et al. (2013). Misuse of the phytoplankton-zooplankton dichotomy: the need to assign organisms as mixotrophs within plankton functional types. *J. Plankton Res.* 35, 3–11. doi: 10.1093/plankt/fbs062

Franzè, G., and Lavrentyev, P. J. (2014). Microzooplankton growth rates examined across a temperature gradient in the Barents Sea. *PLoS One* 9:e86429. doi: 10.1371/journal.pone.0086429

Gast, R. J., Moran, D. M., Dennett, M. R., and Caron, D. A. (2007). Kleptoplasty in an antarctic dinoflagellate: caught in evolutionary transition? *Environ. Microbiol.* 9, 39–45. doi: 10.1111/j.1462-2920.2006.01109.x

Gawryluk, R. M. R., Tikhonenkov, D. V., Hehenberger, E., Husnik, F., Mylnikov, A. P., and Keeling, P. J. (2019). Non-photosynthetic predators are sister to red algae. *Nature* 572, 240–243. doi: 10.1038/s41586-019-1398-6

Giovanardi, M., Poggioli, M., Ferroni, L., Lespinasse, M., Baldisserotto, C., Aro, E. M., et al. (2017). Higher packing of thylakoid complexes ensures a preserved photosystem II activity in mixotrophic *Neochloris oleoabundans*. *Algal Res.* 25, 322–332. doi: 10.1016/j.algal.2017.05.020

González-Olalla, J. M., Medina-Sánchez, J. M., and Carrillo, P. (2019). Mixotrophic trade-off under warming and UVR in a marine and a freshwater alga. *J. Phycol.* 55, 1028–1040. doi: 10.1111/jpy.12865

Gornik, S. G., Cassin, A. M., MacRae, J. I., Ramaprasad, A., Rchiad, Z., McConville, M. J., et al. (2015). Endosymbiosis undone by stepwise elimination of the plastid in a parasitic dinoflagellate. *Proc. Natl. Acad. Sci. U. S. A.* 112, 5767–5772. doi: 10.1073/pnas.1423400112

Graupner, N., Jensen, M., Bock, C., Marks, S., Rahmann, S., Beisser, D., et al. (2018). Evolution of heterotrophy in chrysophytes as reflected by comparative transcriptomics. *FEMS Microbiol. Ecol.* 94, 1–11. doi: 10.1093/femsec/fiy039

Green, B. J., Fox, T. C., and Rumpho, M. E. (2005). Stability of isolated algal chloroplasts that participate in a unique mollusc/kleptoplast association. *Symbiosis* 40, 31–40.

Haas, A. (2007). The phagosome: compartment with a license to kill. *Traffic* 8, 311–330. doi: 10.1111/j.1600-0854.2006.00531.x

Hadariová, L., Vesteg, M., Hampl, V., and Krajčovič, J. (2018). Reductive evolution of chloroplasts in non-photosynthetic plants, algae and protists. *Curr. Genet.* 64, 365–387. doi: 10.1007/s00294-017-0761-0

Hampl, V., Čepička, I., and Eliáš, M. (2019). Was the mitochondrion necessary to start eukaryogenesis? *Trends Microbiol.* 27, 96–104. doi: 10.1016/j.tim.2018.10.005

Hansen, P. J. (2011). The role of photosynthesis and food uptake for the growth of marine mixotrophic dinoflagellates. *J. Eukaryot. Microbiol.* 58, 203–214. doi: 10.1111/j.1550-7408.2011.00537.x

Hansen, P. J., Anderson, R., Stoecker, D. K., Decelle, J., Altenburger, A., Blossom, H. E., et al. (2019). "Mixotrophy among freshwater and marine protists," in *Encyclopedia of Microbiology*. ed. T. M. Schmidt (Amsterdam, Netherlands: Elsevier Ltd.), 199–210.

Hansen, P. J., Nielsen, L. T., Johnson, M., Berge, T., and Flynn, K. J. (2013). Acquired phototrophy in *Mesodinium* and *Dinophysis*—a review of cellular organization, prey selectivity, nutrient uptake and bioenergetics. *Harmful Algae* 28, 126–139. doi: 10.1016/j.hal.2013.06.004

Hansen, P. J., Ojamäe, K., Berge, T., Trampe, E. C. L., Nielsen, L. T., Lips, I., et al. (2016). Photoregulation in a kleptochloroplastidic dinoflagellate, *Dinophysis acuta*. *Front. Microbiol.* 7:785. doi: 10.3389/fmicb.2016.00785

Hehenberger, E., Burki, F., Kolisko, M., and Keeling, P. J. (2016). Functional relationship between a dinoflagellate host and its diatom endosymbiont. *Mol. Biol. Evol.* 33, 2376–2390. doi: 10.1093/molbev/msw109

Hehenberger, E., Gast, R. J., and Keeling, P. J. (2019). A kleptoplastidic dinoflagellate and the tipping point between transient and fully integrated plastid endosymbiosis. *Proc. Natl. Acad. Sci. U. S. A.* 116, 17934–17942. doi: 10.1073/pnas.1910121116

Hongo, Y., Yabuki, A., Fujikura, K., and Nagai, S. (2019). Genes functioned in kleptoplastids of *Dinophysis* are derived from haptophytes rather than from cryptophytes. *Sci. Rep.* 9, 1–11. doi: 10.1038/s41598-019-45326-5

Howe, C. J., Barbrook, A. C., Nisbet, R. E. R., Lockhart, P. J., and Larkum, A. W. D. (2008). The origin of plastids. *Philos. Trans. R. Soc. B Biol. Sci.* 363, 2675–2685. doi: 10.1098/rstb.2008.0050

Jackson, C. J., and Reyes-Prieto, A. (2014). The mitochondrial genomes of the glaucophytes gloeochaete wittrockiana and cyanoptyche gloeocystis: multilocus phylogenetics suggests amonophyletic archaeplastida. *Genome Biol. Evol.* 6, 2774–2785. doi: 10.1093/gbe/evu218

Janouskovec, J., Gavelis, G. S., Burki, F., Dinh, D., Bachvaroff, T. R., Gornik, S. G., et al. (2017). Major transitions in dinoflagellate evolution unveiled by phylotranscriptomics. *Proc. Natl. Acad. Sci. U. S. A.* 114, E171–E180. doi: 10.1073/pnas.1614842114

Janouskovec, J., Paskerova, G. G., Miroliubova, T. S., Mikhaiiov, K. V., Birley, T., Aieoshin, V. V., et al. (2019). Apicomplexan-like parasites are polyphyletic and widely but selectively dependent on cryptic plastid organelles. *elife* 8:e49662. doi: 10.7554/eLife.49662

Jeffrey, S. W., and Vesk, M. (1976). Further evidence for a membrane-bound endosymbiont within the dinoflagellate *Peridinium foliaceum*. *J. Phycol.* 12, 450–455. doi: 10.1111/j.1529-8817.1976.tb02872.x

John, U., Lu, Y., Wohlrab, S., Groth, M., Janouškovec, J., Kohli, G. S., et al. (2019). An aerobic eukaryotic parasite with functional mitochondria that likely lacks a mitochondrial genome. *Sci. Adv.* 5, 1–12. doi: 10.1126/sciadv.aav1110

Johnson, M. D. (2015). Inducible mixotrophy in the dinoflagellate *Prorocentrum minimum*. *J. Eukaryot. Microbiol.* 62, 431–443. doi: 10.1111/jeu.12198

Johnson, M. D., Oldach, D., Delwiche, C. F., and Stoecker, D. K. (2007). Retention of transcriptionally active cryptophyte nuclei by the ciliate *Myrionecta rubra*. *Nature* 445, 426–428. doi: 10.1038/nature05496

Kamikawa, R., Moog, D., Zauner, S., Tanifuji, G., Ishida, K. I., Miyashita, H., et al. (2017). A non-photosynthetic diatom reveals early steps of reductive evolution in plastids. *Mol. Biol. Evol.* 34, 2355–2366. doi: 10.1093/molbev/msx172

Keeling, P. J. (2013). The number, speed, and impact of plastid endosymbioses in eukaryotic evolution. *Annu. Rev. Plant Biol.* 64, 583–607. doi: 10.1146/annurev-arplant-050312-120144

Keeling, P. J., and Burki, F. (2019). Progress towards the tree of eukaryotes. *Curr. Biol.* 29, R808–R817. doi: 10.1016/j.cub.2019.07.031

Keeling, P. J., and McCutcheon, J. P. (2017). Endosymbiosis: the feeling is not mutual. *J. Theor. Biol.* 434, 75–79. doi: 10.1016/j.jtbi.2017.06.008

Keeling, P. J., McCutcheon, J. P., and Doolittle, W. F. (2015). Symbiosis becoming permanent: survival of the luckiest. *Proc. Natl. Acad. Sci. U. S. A.* 112, 10101–10103. doi: 10.1073/pnas.1513346112

Keller, M. D., Shapiro, L. P., Haugen, E. M., Cucci, T. L., Sherr, E. B., and Sherr, B. F. (1994). Phagotrophy of fluorescently labeled bacteria by an oceanic phytoplankter. *Microb. Ecol.* 28, 39–52. doi: 10.1007/BF00170246

Kies, L., and Kremer, B. P. (1979). Function of cyanelles in the thecamoeba *Paulinella chromatophora*. *Naturwissenschaften* 66, 578–579. doi: 10.1007/BF00368819

Kim, M., Drumm, K., Daugbjerg, N., and Hansen, P. J. (2017). Dynamics of sequestered cryptophyte nuclei in *Mesodinium rubrum* during starvation and refeeding. *Front. Microbiol.* 8:423. doi: 10.3389/fmicb.2017.00423

Kim, G. H., Han, J. H., Kim, B., Han, J. W., Nam, S. W., Shin, W., et al. (2016). Cryptophyte gene regulation in the kleptoplastidic, karyokleptic ciliate *Mesodinium rubrum*. *Harmful Algae* 52, 23–33. doi: 10.1016/j.hal.2015.12.004

Kim, E., and Maruyama, S. (2014). A contemplation on the secondary origin of green algal and plant plastids. *Acta Soc. Bot. Pol.* 83, 331–336. doi: 10.5586/asbp.2014.040

Kiørboe, T. (2011). How zooplankton feed: mechanisms, traits and trade-offs. *Biol. Rev.* 86, 311–339. doi: 10.1111/j.1469-185X.2010.00148.x

Koonin, E. V. (2010). The origin and early evolution of eukaryotes in the light of phylogenomics. *Genome Biol.* 11:209. doi: 10.1186/gb-2010-11-5-209

Labarre, A., Obiol, A., Wilken, S., Forn, I., and Massana, R. (2020). Expression of genes involved in phagocytosis in uncultured heterotrophic flagellates. *Limnol. Oceanogr.* 65, S149–S160. doi: 10.1002/lno.11379

LaJeunesse, T. C., Smith, R. T., Finney, J., and Oxenford, H. (2009). Outbreak and persistence of opportunistic symbiotic dinoflagellates during the 2005 Caribbean mass coral "bleaching" event. *Proc. R. Soc. B Biol. Sci.* 276, 4139–4148. doi: 10.1098/rspb.2009.1405

LaJeunesse, T. C., Smith, R., Walther, M., Pinzón, J., Pettay, D. T., McGinley, M., et al. (2010). Host-symbiont recombination versus natural selection in the response of coral-dinoflagellate symbioses to environmental disturbance. *Proc. Biol. Sci.* 277, 2925–2934. doi: 10.1098/rspb.2010.0385

Lane, N. (2005). *Power, Sex, Suicide: Mitochondria and the Meaning of Life*. Oxford, United Kingdom: Oxforsd University Press.

Larkum, A. W. D., Lockhart, P. J., and Howe, C. J. (2007). Shopping for plastids. *Trends Plant Sci.* 12, 189–195. doi: 10.1016/j.tplants.2007.03.011

Lasek-Nesselquist, E., Wisecaver, J. H., Hackett, J. D., and Johnson, M. D. (2015). Insights into transcriptional changes that accompany organelle sequestration from the stolen nucleus of *Mesodinium rubrum*. *BMC Genomics* 16:805. doi: 10.1186/s12864-015-2052-9

Lewis, C. L., and Coffroth, M. A. (2004). The acquisition of exogenous, algal symbionts by an octocorat after bleaching. *Science* 304, 1490–1492. doi: 10.1126/science.1097323

Li, A., Stoecker, D. K., and Adolf, J. E. (1999). Feeding, pigmentation, photosynthesis and growth of the mixotrophic dinoflagellate *Gyrodinium galatheanum*. *Aquat. Microb. Ecol.* 19, 163–176. doi: 10.3354/ame019163

Li, C. W., and Volcani, B. E. (1987). Four new apochlorotic diatoms. *Br. Phycol. J.* 22, 375–382. doi: 10.1080/00071618700650441

Mansour, J. S., Pollock, F. J., Díaz-Almeyda, E., Iglesias-Prieto, R., and Medina, M. (2018). Intra- and interspecific variation and phenotypic plasticity in thylakoid membrane properties across two *Symbiodinium* clades. *Coral Reefs* 37, 841–850. doi: 10.1007/s00338-018-1710-1

Marin, B., Nowack, E. C. M., and Melkonian, M. (2005). A plastid in the making: evidence for a second primary endosymbiosis. *Protist* 156, 425–432. doi: 10.1016/j.protis.2005.09.001

Martijn, J., and Ettena, T. J. G. (2013). From archaeon to eukaryote: the evolutionary dark ages of the eukaryotic cell. *Biochem. Soc. Trans.* 41, 451–457. doi: 10.1042/BST20120292

Martin, W., and Müller, M. (1998). The hydrogen hypothesis for the first eukaryote. *Nature* 392, 37–41. doi: 10.1038/32096

McFadden, G. I., and Yeh, E. (2017). The apicoplast: now you see it, now you don't. *Int. J. Parasitol.* 47, 137–144. doi: 10.1016/j.ijpara.2016.08.005

Menge, D. N. L., and Weitz, J. S. (2009). Dangerous nutrients: evolution of phytoplankton resource uptake subject to virus attack. *J. Theor. Biol.* 257, 104–115. doi: 10.1016/j.jtbi.2008.10.032

Mereschkowsky, C. (1905). Über natur und ursprung der chromatophoren im pflanzenreiche. *Biol. Cent.* 25, 593–604. (English translation in Martin, W., Kowallik, K. V. (1999). Annotated English translation of Mereschkowsky's 1905 paper `Uber Natur und Ursprung der Chromatophoren im Pflanzenreiche '. Eur. J. Phycol. 34, 287–295).

Millette, N. C., Pierson, J. J., Aceves, A., and Stoecker, D. K. (2017). Mixotrophy in *Heterocapsa rotundata*: a mechanism for dominating the winter phytoplankton. *Limnol. Oceanogr.* 62, 836–845. doi: 10.1002/lno.10470

Mills, D. B. (2020). The origin of phagocytosis in earth history. *Interface Focus* 10:20200019. doi: 10.1098/rsfs.2020.0019

Mitra, A., Flynn, K. J., Burkholder, J. M., Berge, T., Calbet, A., Raven, J. A., et al. (2014). The role of mixotrophic protists in the biological carbon pump. *Biogeosciences* 11, 995–1005. doi: 10.5194/bg-11-995-2014

Mitra, A., Flynn, K. J., Tillmann, U., Raven, J. A., Caron, D., Stoecker, D. K., et al. (2016). Defining planktonic protist functional groups on mechanisms for energy and nutrient acquisition: incorporation of diverse mixotrophic strategies. *Protist* 167, 106–120. doi: 10.1016/j.protis.2016.01.003

Morozov, A. A., and Galachyants, Y. P. (2019). Diatom genes originating from red and green algae: implications for the secondary endosymbiosis models. *Mar. Genomics* 45, 72–78. doi: 10.1016/j.margen.2019.02.003

Nakayama, T., and Ishida, K. I. (2009). Another acquisition of a primary photosynthetic organelle is underway in *Paulinella chromatophora*. *Curr. Biol.* 19, R284–R285. doi: 10.1016/j.cub.2009.02.043

Nowack, E. C. M. (2014). *Paulinella chromatophora*—rethinking the transition from endosymbiont to organelle. *Acta Soc. Bot. Pol.* 83, 387–397. doi: 10.5586/asbp.2014.049

Nowack, E. C. M., and Grossman, A. R. (2012). Trafficking of protein into the recently established photosynthetic organelles of *Paulinella chromatophora*. *Proc. Natl. Acad. Sci. U. S. A.* 109, 5340–5345. doi: 10.1073/pnas.1118800109

Nowack, E. C. M., Melkonian, M., and Glöckner, G. (2008). Chromatophore genome sequence of *Paulinella* sheds light on acquisition of photosynthesis by eukaryotes. *Curr. Biol.* 18, 410–418. doi: 10.1016/j.cub.2008.02.051

O'Connor, M. I., Piehler, M. F., Leech, D. M., Anton, A., and Bruno, J. F. (2009). Warming and resource availability shift food web structure and metabolism. *PLoS Biol.* 7:e1000178. doi: 10.1371/journal.pbio.1000178

Ok, J. H., Jeong, H. J., Lim, A. S., You, J. H., Kang, H. C., Kim, S. J., et al. (2019). Effects of light and temperature on the growth of *Takayama helix* (Dinophyceae): mixotrophy as a survival strategy against photoinhibition. *J. Phycol.* 55, 1181–1195. doi: 10.1111/jpy.12907

Onuma, R., Hirooka, S., Kanesaki, Y., Fujiwara, T., Yoshikawa, H., and Miyagishima, S. (2020). Changes in the transcriptome, ploidy, and optimal light intensity of a cryptomonad upon integration into a kleptoplastic dinoflagellate. *ISME J.* 14, 2407–2423. doi: 10.1038/s41396-020-0693-4

Onuma, R., and Horiguchi, T. (2015). Kleptochloroplast enlargement, karyoklepty and the distribution of the cryptomonad nucleus in *Nusuttodinium* (= *Gymnodinium*) *aeruginosum* (Dinophyceae). *Protist* 166, 177–195. doi: 10.1016/j.protis.2015.01.004

Park, M. G., Kim, M., and Kim, S. (2014). The acquisition of plastids/phototrophy in heterotrophic dinoflagellates. *Acta Protozool.* 53, 39–50. doi: 10.4467/16890027AP.14.005.1442

Patron, N. J., Waller, R. F., and Keeling, P. J. (2006). A tertiary plastid uses genes from two endosymbionts. *J. Mol. Biol.* 357, 1373–1382. doi: 10.1016/j.jmb.2006.01.084

Pfannschmidt, T., Nilsson, A., and Allen, J. F. (1999). Photosynthetic control of chloroplast gene expression. *Nature* 397, 625–628. doi: 10.1038/17624

Pierce, S. K., Massey, S. E., Hanten, J. J., and Curtis, N. E. (2003). Horizontal transfer of functional nuclear genes between multicellular organisms. *Biol. Bull.* 204, 237–240. doi: 10.2307/1543594

Pillet, L., and Pawlowski, J. (2013). Transcriptome analysis of foraminiferan *Elphidium margaritaceum* questions the role of gene transfer in kleptoplastidy. *Mol. Biol. Evol.* 30, 66–69. doi: 10.1093/molbev/mss226

Princiotta, S. D. V., Smith, B. T., and Sanders, R. W. (2016). Temperature-dependent phagotrophy and phototrophy in a mixotrophic chrysophyte. *J. Phycol.* 52, 432–440. doi: 10.1111/jpy.12405

Probert, I., Siano, R., Poirier, C., Decelle, J., Biard, T., Tuji, A., et al. (2014). *Brandtodinium* gen. nov. and *B.nutricula* comb. Nov. (Dinophyceae), a dinoflagellate commonly found in symbiosis with polycystine radiolarians. *J. Phycol.* 50, 388–399. doi: 10.1111/jpy.12174

Qiu, H., Lee, J. M., Yoon, H. S., and Bhattacharya, D. (2017). Hypothesis: gene-rich plastid genomes in red algae may be an outcome of nuclear genome reduction. *J. Phycol.* 53, 715–719. doi: 10.1111/jpy.12514

Raven, J. A. (1984). A cost-benefit analysis of photon absorption by photosynthetic unicells. *New Phytol.* 98, 593–625. doi: 10.1111/j.1469-8137.1984.tb04152.x

Raven, J. A. (1997). Phagotrophy in phototrophs. *Limnol. Oceanogr.* 42, 198–205. doi: 10.4319/lo.1997.42.1.0198

Raven, J. A., Beardall, J., Flynn, K. J., and Maberly, S. C. (2009). Phagotrophy in the origins of photosynthesis in eukaryotes and as a complementary mode of nutrition in phototrophs: relation to darwin's insectivorous plants. *J. Exp. Bot.* 60, 3975–3987. doi: 10.1093/jxb/erp282

Reich, H. G., Rodriguez, I. B., LaJeunesse, T. C., and Ho, T. Y. (2020). Endosymbiotic dinoflagellates pump iron: differences in iron and other trace metal needs among the Symbiodiniaceae. *Coral Reefs* 39, 915–927. doi: 10.1007/s00338-020-01911-z

Reumann, S., Inoue, K., and Keegstra, K. (2005). Evolution of the general protein import pathway of plastids (review). *Mol. Membr. Biol.* 22, 73–86. doi: 10.1080/09687860500041916

Reyes-Prieto, A., Moustafa, A., and Bhattacharya, D. (2008). Multiple genes of apparent algal origin suggest ciliates may once have been photosynthetic. *Curr. Biol.* 18, 956–962. doi: 10.1016/j.cub.2008.05.042

Rodríguez-Ezpeleta, N., Brinkmann, H., Burey, S. C., Roure, B., Burger, G., Löffelhardt, W., et al. (2005). Monophyly of primary photosynthetic eukaryotes: green plants, red algae, and glaucophytes. *Curr. Biol.* 15, 1325–1330. doi: 10.1016/j.cub.2005.06.040

Rose, J. M., and Caron, D. A. (2007). Does low temperature constrain the growth rates of heterotrophic protists? Evidence and implications for algal blooms in cold waters. *Limnol. Oceanogr.* 52, 886–895. doi: 10.4319/lo.2007.52.2.0886

Rusterholz, P. M., Hansen, P. J., and Daugbjerg, N. (2017). Evolutionary transition towards permanent chloroplasts?—division of kleptochloroplasts in starved cells of two species of *Dinophysis* (Dinophyceae). *PLoS One* 12:e0177512. doi: 10.1371/journal.pone.0177512

Sagan, L. (1967). On the origin of mitosing cells. *J. Theor. Biol.* 14, 225–IN6. doi: 10.1016/0022-5193(67)90079-3

Saldarriaga, J. F., Taylor, F. J. R., Keeling, P. J., and Cavalier-Smith, T. (2001). Dinoflagellate nuclear SSU rRNA phylogeny suggests multiple plastid losses and replacements. *J. Mol. Evol.* 53, 204–213. doi: 10.1007/s002390010210

Schimper, A. F. W. (1883). Uber die entwicklung der chlorophyllkorner und farbkorper. *Bot. Zeit.* 41, 105–114.

Schneider, L., Anestis, K., Mansour, J., Anschütz, A., Gypens, N., Hansen, P., et al. (2020). A dataset on trophic modes of aquatic protists. *Biodivers. Data J.* 8:e56648. doi: 10.3897/bdj.8.e56648

Sellers, C. G., Gast, R. J., and Sanders, R. W. (2014). Selective feeding and foreign plastid retention in an Antarctic dinoflagellate. *J. Phycol.* 50, 1081–1088. doi: 10.1111/jpy.12240

Selosse, M. A., Charpin, M., and Not, F. (2017). Mixotrophy everywhere on land and in water: the grand écart hypothesis. *Ecol. Lett.* 20, 246–263. doi: 10.1111/ele.12714

Sforza, E., Cipriani, R., Morosinotto, T., Bertucco, A., and Giacometti, G. M. (2012). Excess CO_2 supply inhibits mixotrophic growth of *Chlorella protothecoides* and *Nannochloropsis salina*. *Bioresour. Technol.* 104, 523–529. doi: 10.1016/j.biortech.2011.10.025

Sibbald, S. J., and Archibald, J. M. (2020). Genomic insights into plastid evolution. *Genome Biol. Evol.* 12, 978–990. doi: 10.1093/gbe/evaa096

Skovgaard, A. (1996). Mixotrophy in Fragilidium subglobosum (Dinophyceae): growth and grazing responses as functions of light intensity. *Mar. Ecol. Prog. Ser.* 143, 247–253. doi: 10.3354/meps143247

Skovgaard, A. (2000). A phagotrophically derivable growth factor in the plastidic dinoflagellate *Gyrodinium resplendens* (Dinophyceae). *J. Phycol.* 36, 1069–1078. doi: 10.1046/j.1529-8817.2000.00009.x

Smalley, G. W., Coats, D. W., and Stoecker, D. K. (2003). Feeding in the mixotrophic dinoflagellate *Ceratium furca* is influenced by intracellular nutrient concentrations. *Mar. Ecol. Prog. Ser.* 262, 137–151. doi: 10.3354/meps262137

Smith, M., and Hansen, P. J. (2007). Interaction between *Mesodinium rubrum* and its prey: importance of prey concentration, irradiance and pH. *Mar. Ecol. Prog. Ser.* 338, 61–70. doi: 10.3354/meps338061

Stoecker, D. K., Hansen, P. J., Caron, D. A., and Mitra, A. (2017). Mixotrophy in the marine plankton. *Annu. Rev. Mar. Sci.* 9, 311–335. doi: 10.1146/annurev-marine-010816-060617

Stoecker, D. K., Johnson, M. D., De Vargas, C., and Not, F. (2009). Acquired phototrophy in aquatic protists. *Aquat. Microb. Ecol.* 57, 279–310. doi: 10.3354/ame01340

Stoecker, D. K., and Lavrentyev, P. J. (2018). Mixotrophic plankton in the polar seas: a pan-Arctic review. *Front. Mar. Sci.* 5:292. doi: 10.3389/fmars.2018.00292

Theissen, U., and Martin, W. (2006). The difference between organelles and endosymbionts. *Curr. Biol.* 16, R1016–R1017. doi: 10.1016/j.cub.2006.11.020

Timmis, J. N., Ayliff, M. A., Huang, C. Y., and Martin, W. (2004). Endosymbiotic gene transfer: organelle genomes forge eukaryotic chromosomes. *Nat. Rev. Genet.* 5, 123–135. doi: 10.1038/nrg1271

Tippit, D. H., and Heaps, J. D. P. (1976). Apparent amitosis in the binucleate dinoflagellate *Peridinium balticum*. *J. Cell Sci.* 21, 273–289. doi: 10.1242/jcs.21.2.273

Tomas, R. N., Cox, E. R., and Steidinger, K. A. (1973). *Peridinium balticum* (Levander) Lemmermann, and unusual dinoflagelate with a mesocaryotic and an eucaryotic nucleus. *J. Phycol.* 9, 91–98. doi: 10.1111/j.0022-3646.1973.00091.x

Trench, R. K., and Thinh, L. V. (1995). *Gymnodinium linucheae* sp. Nov.: the dinoflagellate symbiont of the jellyfish *Linuche unguiculata*. *Eur. J. Phycol.* 30, 149–154. doi: 10.1080/09670269500650911

Uwizeye, C., Brisbin, M. M., Gallet, B., Chevalier, F., Lekieffre, C., Schieber, N., et al. (2020). Cytoklepty in the plankton: a host strategy to optimize the bioenergetic machinery of endosymbiotic algae. bioRxiv. [Preprint]. doi: 10.1101/2020.12.08.416644

Uzuka, A., Kobayashi, Y., Onuma, R., Hirooka, S., Kanesaki, Y., Yoshikawa, H., et al. (2019). Responses of unicellular predators to cope with the phototoxicity of photosynthetic prey. *Nat. Commun.* 10:5606. doi: 10.1038/s41467-019-13568-6

Van Steenkiste, N. W. L., Stephenson, I., Herranz, M., Husnik, F., Keeling, P. J., and Leander, B. S. (2019). A new case of kleptoplasty in animals: marine flatworms steal functional plastids from diatoms. *Sci. Adv.* 5:eaaw4337. doi: 10.1126/sciadv.aaw4337

von Heijne, G. (1986). Why mitochondria need a genome. *FEBS Lett.* 198, 1–4. doi: 10.1016/0014-5793(86)81172-3

Ward, B. A., Dutkiewicz, S., Barton, A. D., and Follows, M. J. (2011). Biophysical aspects of resource acquisition and competition in algal mixotrophs. *Am. Nat.* 178, 98–112. doi: 10.1086/660284

Wilken, S., Choi, C. J., and Worden, A. Z. (2020). Contrasting mixotrophic lifestyles reveal different ecological niches in two closely related marine protists. *J. Phycol.* 56, 52–67. doi: 10.1111/jpy.12920

Wilken, S., Huisman, J., Naus-Wiezer, S., and Van Donk, E. (2013). Mixotrophic organisms become more heterotrophic with rising temperature. *Ecol. Lett.* 16, 225–233. doi: 10.1111/ele.12033

Wilken, S., Yung, C. C. M., Hamilton, M., Hoadley, K., Nzongo, J., Eckmann, C., et al. (2019). The need to account for cell biology in characterizing predatory mixotrophs in aquatic environments. *Philos. Trans. R. Soc. Lond. Ser. B Biol. Sci.* 374:20190090. doi: 10.1098/rstb.2019.0090

Williams, B. A. P., and Keeling, P. J. (2003). Cryptic organelles in parasitic protists and fungi. *Adv. Parasitol.* 54, 9–68. doi: 10.1016/S0065-308X(03)54001-5

Yamada, N., Bolton, J. J., Trobajo, R., Mann, D. G., Dąbek, P., Witkowski, A., et al. (2019). Discovery of a kleptoplastic 'dinotom' dinoflagellate and the unique nuclear dynamics of converting kleptoplastids to permanent plastids. *Sci. Rep.* 9:10474. doi: 10.1038/s41598-019-46852-y

Yoon, H. S., Reyes-Prieto, A., Melkonian, M., and Bhattacharya, D. (2006). Minimal plastid genome evolution in the *Paulinella* endosymbiont. *Curr. Biol.* 16, 670–672. doi: 10.1016/j.cub.2006.08.018

Yutin, N., Wolf, M. Y., Wolf, Y. I., and Koonin, E. V. (2009). The origins of phagocytosis and eukaryogenesis. *Biol. Direct* 4, 1–26. doi: 10.1186/1745-6150-4-9

Zimorski, V., Ku, C., Martin, W. F., and Gould, S. B. (2014). Endosymbiotic theory for organelle origins. *Curr. Opin. Microbiol.* 22, 38–48. doi: 10.1016/j.mib.2014.09.008

Conflict of Interest: The authors declare that the research was conducted in the absence of any commercial or financial relationships that could be construed as a potential conflict of interest.

Supplementary information

Supplementary Table 1: Information on the type of mixotrophy documented in at least one member of the taxa presented in Figure 1. The group of mixotrophs include constitutive mixoplankton (CM) and non-constitutive mixoplankton (NCM), which is further divided to photosymbiotic and kleptoplastidic.

Taxa	Lower taxa	CM	NCM	NCM Photosymbiosis	NCM Kleptoplastidic	Reference
Rhizarians						
Chlorarachniophyta		Y	N	N	N	Archibald (2005)
Paulinella		N	N	N	N	Gabr et al. (2020)
Endomyxids						
Foraminifera		N	Y	Y	Y	Decelle et al. (2015)
Acantharia		N	Y	Y	N	Decelle et al. (2015)
Polycistine	Collodaria	N	Y	Y	N	Decelle et al. (2015)
Polycistine	Spummellaria	N	Y	Y	N	Decelle et al. (2015)
Polycistine	Nassellaria	N	Y	Y	N	Decelle et al. (2015)
Discobids						
Kinetoplastids		N	N	N	N	NA
Diplonemids		N	N	N	N	NA
Euglenids		Y	N	N	N	Yamaguchi et al. (2012)
Heteroloboseans		N	N	N	N	NA
Jakobids		N	N	N	N	NA
Metamonads						
Oxymonads						NA
Parabasalids						NA
Diplomonads						NA
CRuMS						
Mantamonads		N	N	N	N	NA
Rigifilids		N	N	N	N	NA
Diphylleida		N	N	N	N	NA
Opisthokonts						
Funghi						NA
Animals						NA
Choanoflagellates		N	N	N	N	NA
Amoebozoans						
Amoebozoans						NA
Archaeplastids						
Glaucophytes		N	N	N	N	NA
Rhodelphis		N	N	N	N	Gawryluk et al. (2019)
Red algae		N	N	N	N	NA
Green algae	Tracheophytes	N	N	N	N	NA
Green algae	Charophytes	N	N	N	N	NA
Green algae	Chlorophytes	Y	N	N	N	Anderson et al. (2018)
Green algae	Trebouxiophytes	N	N	N	N	Summerer et al. (2008)

Green algae	Prasinophytes	Y	N	N	N	Bock et al. (2021)
Cryptista						
Katablepharids		N	Y	Y	N	Okamoto et al. (2006)
Palpitomonas		N	N	N	N	NA
Cryptophytes		Y	N	N	N	
Haptista						
Haptophytes		Y	N	N	N	Anderson et al. (2018)
Rappemonads		N	N	N	N	NA
Centrohelids		N	N	N	N	NA
Stramenopiles						
Ochrophytes	Diatoms	N	N	N	N	Schneider et al. (2020)
Ochrophytes	Bolidophytes	N	N	N	N	Schneider et al. (2020)
Ochrophytes	Chrysophytes	Y	N	N	N	Rottberger et al. (2013)
Ochrophytes	Phaeophytes	N	N	N	N	Schneider et al. (2020)
Ochrophytes	Pelagophytes	N	N	N	N	Schneider et al. (2020)
Ochrophytes	Eustigmatophytes	N	N	N	N	Schneider et al. (2020)
Oomycetes		N	N	N	N	Judelson, H. S. (2012)
Thraustochytrids		N	N	N	N	Leyland et al. (2017)
Labyrinthulids		N	N	N	N	Raghukumar (2002).
Bicosoecids		N	N	N	N	Sibbald, S. J., and Archibald, J. M. (2020)
Hyphochytrids		N	N	N	N	Beakes et al. (2014)
Alveolates						
Dinoflagellates		Y	Y	Y	Y	Decelle et al. (2015)
Syndiniales		N	N	N	N	NA
Oxyhrris		N	N	N	N	Schneider et al. (2020)
Perkinsids		N	N	N	N	NA
Apicomplexa		N	N	N	N	NA
Apicomplexa	Cryptosporidia	N	N	N	N	NA
Apicomplexa	Gregarines	N	N	N	N	NA
Chrompodellids	Piridium	N	N	N	N	NA
Chromerida	Vitrella	N	N	N	N	NA
Chromerida	Chromera	N	N	N	N	NA
Chrompodellids	Platyproteum	N	N	N	N	NA
Acavamonas						NA
Ciliates		N	Y	N	Y	Decelle et al. (2015)
Colponemida		N	N	N	N	Tikhonenkov et al. (2020)

Supplementary Table 2: Information on the type of plastid found in at least one member of the taxa presented in Figure 1.

Taxa	Lower taxa	plastid type-1	plastid type-2	plastid type-3	Notes	Reference
Rhizarians						
Chlorarachniophyta		Green 4			+ nucleomorph	Ota and Vaulot (2012)
Paulinella		Primary (recent?)				Hadariová et al. (2018)
Endomyxids		None				NA
Foraminifera		None				NA
Acantharia		None				NA
Polycistine	Collodaria	None				NA
Polycistine	Spummellaria	None				NA
Polycistine	Nassellaria	None				NA
Discobids						
Kinetoplastids		None				Sibbald and Archibald (2020)
Diplonemids		None				Sibbald and Archibald (2020)
Euglenids		Green 3	Green 3/Non-photo			Maruyama et al. (2011)
Heteroloboseans		None				Sibbald and Archibald (2020)
Jakobids		None				Sibbald and Archibald (2020)
Metamonads						
Metamonads		None				Sibbald and Archibald (2020)
CRuMS						
CruMS		None				Sibbald and Archibald (2020)
Opisthokonts						
Opisthokonts		None				Hadariová et al. (2018)
Amoebozoans						
Amoebozoans		None				Hadariová et al. (2018)
Archaeplastids						
Glaucophytes		Primary (2)				Hadariová et al. (2018)
Rhodelphis		Green 2/Non-photo/Genome-less				Gawryluk et al. (2019)
Red algae		Red 2	Red 2/Non photo			Hadariová et al. (2018)
Green algae	Tracheophytes	Green 2	Green 2 / Non-photo	Green 2/Non-photo/Genome-less	Rafflesia no plastid genome	Sibbald and Archibald (2020)
Green algae	Charophytes	Green 2				Hadariová et al. (2018)
Green algae	Chlorophytes	Green 2	Green 2/Non-photo	Green 2/Non-photo/Genome-less	Polytoma non-photo, Polytomella no genome	Sibbald and Archibald (2020)
Green algae	Trebouxiophytes	Green 2	Green 2/Non-photo			Sibbald and Archibald (2020)

Green algae	Prasinophytes	Green 2				Hadariová et al. (2018)
Cryptista						
Katablepharids		None				Okamoto et al. (2006)
Palpitomonas		None				Sibbald and Archibald (2020)
Cryptophytes		Red 4	Red 4/Non-photo		+ nucleomorph	Sibbald and Archibald (2020)
Haptista						
Haptophytes		Red 4				Hadariová et al. (2018)
Rappemonads		Red 4				Kim et al. (2011)
Centrohelids		None				Sibbald and Archibald (2020)
Stramenopiles						
Ochrophytes	Diatoms	Red 4	Red 4/Non-photo		Nitzschia spp. non-photo	Kamikawa et al. (2017)
Ochrophytes	Bolidophytes	Red 4				Sibbald and Archibald (2020)
Ochrophytes	Chrysophytes	Red 4	Red 4/Non-photo			Sibbald and Archibald (2020)
Ochrophytes	Phaeophytes	Red 4				Sibbald and Archibald (2020)
Ochrophytes	Pelagophytes	Red 4				Sibbald and Archibald (2020)
Oomycetes		None				Judelson, H. S. (2012)
Thraustochytrids		None				Leyland et al. (2017)
Labyrinthulids		None				Raghukumar (2002).
Bicosoecids		None				Sibbald and Archibald (2020)
Hyphochytrids		None				Beakes et al. (2014)
Alveolates						
Dinoflagellates		Red 3	Red 3/Non-photo			Hadariová et al. (2018)
Syndiniales	*Hematodinium*	Lost				Gornik, S. G., Febrimarsa, Cassin, A. M., MacRae et al. (2015).
Oxyhrris		Red 3/Non-photo			number membranes on cryptic plastid uncertain	Slamovits and Keeling (2008)
Perkinsids		Red 4/Non-photo/Genome-less				Hadariová et al. (2018)
Apicomplexa		Red 4/Non-photo	Lost	Red 4/ Non-photo/Genome-less	Genome loss in gregarines	Sibbald and Archibald (2020)
Chrompodellids	Others	Red 4?	Red 4?/Non-photo/Genome-less		"chrompodellids" (chromerids + colpodellids); chromerids 4 membranes, colpdellids uncertain	Sibbald and Archibald (2020)

Chrompodellids	Piridium	Red 4?/Non-photo	Mathur et al. (2019)
Chrompodellids	Platyproteum	Red 4?/Non-photo	Mathur et al. (2019)
Chromerida		Red 4	Sibbald and Archibald (2020)
Acavamonas		None	NA
Ciliates		None	NA
Colponemida		None	NA

Publication II

Polyketide synthase genes and molecular trade-offs in the ichthyotoxic species *Prymnesium parvum*

Science of the Total Environment 795 (2021) 148878

Contents lists available at ScienceDirect

Science of the Total Environment

journal homepage: www.elsevier.com/locate/scitotenv

Polyketide synthase genes and molecular trade-offs in the ichthyotoxic species *Prymnesium parvum*

Konstantinos Anestis [a], Gurjeet Singh Kohli [a], Sylke Wohlrab [a,b], Elisabeth Varga [c], Thomas Ostenfeld Larsen [d], Per Juel Hansen [e], Uwe John [a,b,*]

[a] Ecological Chemistry, Alfred Wegener Institute for Polar and Marine Research, Am Handelshafen 12, 27570, Bremerhaven, Germany
[b] Helmholtz Institute for Functional Marine Biodiversity, Ammerländer Heerstraße 231, 26129 Oldenburg, Germany
[c] Department of Food Chemistry and Toxicology, Faculty of Chemistry, University of Vienna, Währinger Straße 40, 1090 Vienna, Austria
[d] Department of Biotechnology and Biomedicine, Technical University of Denmark, Søltofts Plads 221, 2800 Kongens Lyngby, Denmark
[e] Marine Biology Section, University of Copenhagen, Strandpromenaden 5, 3000 Helsingør, Denmark

HIGHLIGHTS

- The ichthyotoxic species *Prymnesium parvum* produces the lytic toxins, prymnesins.
- Nine *P. parvum* strains with various toxin contents were studied for the presence of polyketide synthase genes.
- Numerous polyketide synthase genes and their functional domain organization are reported for all nine strains.
- Gene expression analysis highlights the occurrence of molecular trade-offs related to cellular toxin content.

GRAPHICAL ABSTRACT

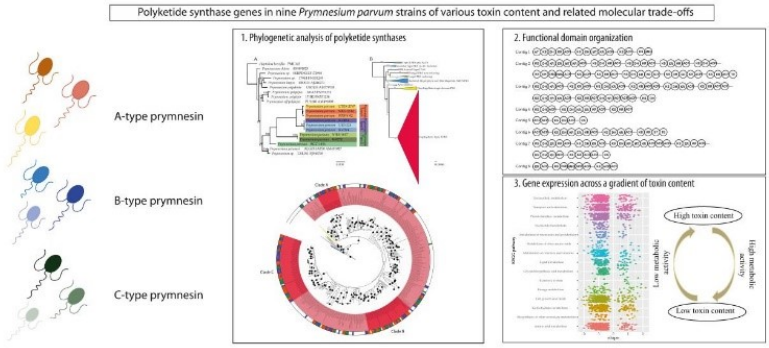

ARTICLE INFO

Article history:
Received 15 April 2021
Received in revised form 18 June 2021
Accepted 2 July 2021
Available online 6 July 2021

Editor: Daniel Wunderlin

Keywords:
Prymnesins
Harmful algae
Algal toxins
HABs
Haptophyte
Polyketides

ABSTRACT

Prymnesium parvum is a bloom forming haptophyte that has been responsible for numerous fish kill events across the world. The toxicity of *P. parvum* has been attributed to the production of large polyketide compounds, collectively called prymnesins, which based on their structure can be divided into A-, B- and C-type. The polyketide chemical nature of prymnesins indicates the potential involvement of polyketide synthases (PKSs) in their biosynthesis. However, little is known about the presence of PKSs in *P. parvum* as well as the potential molecular trade-offs of toxin biosynthesis. In the current study, we generated and analyzed the transcriptomes of nine *P. parvum* strains that produce different toxin types and have various cellular toxin contents. Numerous type I PKSs, ranging from 37 to 109, were found among the strains. Larger modular type I PKSs were mainly retrieved from strains with high cellular toxin levels and eight consensus transcripts were present in all nine strains. Gene expression variance analysis revealed potential molecular trade-offs associated with cellular toxin quantity, showing that basic metabolic processes seem to correlate negatively with cellular toxin content. These findings point towards the presence of metabolic costs for maintaining high cellular toxin quantity. The detailed analysis of PKSs in *P. parvum* is the first step towards better understanding the molecular basis of the biosynthesis of prymnesins and contributes to the development of molecular tools for efficient monitoring of future blooms.

* Corresponding author at: Ecological Chemistry, Alfred Wegener Institute for Polar and Marine Research, Am Handelshafen 12, 27570 Bremerhaven, Germany.
E-mail addresses: kanestis@awi.de (K. Anestis), gurukohli@gmail.com (G.S. Kohli), sylke.wohlrab@awi.de (S. Wohlrab), elisabeth.varga@univie.ac.at (E. Varga), tol@bio.dtu.dk (T.O. Larsen), pjhansen@bio.ku.dk (P.J. Hansen), uwe.john@awi.de (U. John).

1. Introduction

Worldwide blooms of the haptophyte *Prymnesium parvum* occur frequently, and negatively impact fishing and aquaculture industries (Roelke et al., 2011, 2016). *P. parvum* is a cosmopolitan species, that owing to its high plasticity, can be found in freshwater, brackish and marine ecosystems (Granéli et al., 2012). Historically, much of the knowledge on the toxic effects of *P. parvum* on other organisms have been derived from simple bioassay studies, and not via quantitative measurements of the causative toxins. Nutrient availability and the elemental composition in the water have been shown to influence the cellular and extracellular levels of the toxins. In general, nutrient deplete conditions induce higher toxicity in the bioassays. For example, toxicity towards fish erythrocytes was highly enhanced with phosphorous limitation (Beszteri et al., 2012), whereas high light availability and high temperature seem to reduce the toxic effects of prymnesins (Qin et al., 2020; Taylor et al., 2021). *P. parvum* belongs to the constitutive mixoplankton (Flynn et al., 2019), and can feed on bacteria and other protists. The release of toxins by *P. parvum* mediates feeding through the immobilization and lysis of its prey (Skovgaard and Hansen, 2003; Tillmann, 2003). However, attempts to demonstrate enhanced feeding under nitrogen and phosphorous limitation have not been successful (Skovgaard et al., 2003; Lundgren et al., 2016).

The toxicity of *P. parvum* has been attributed to its ability to produce large ladder-frame polyether compounds known as prymnesins (Igarashi et al., 1999). Prymnesins belong to the group of polyketides, an extremely diverse group of compounds produced by a wide range of organisms, from prokaryotes, unicellular algae to higher eukaryotes (Wright and Cembella, 1998; Staunton and Weissman, 2001). Prymnesins were first characterized back in 1999 and reported as prymnesin −1 and −2 (Igarashi et al., 1999). Recently, a new B-type of prymnesin was isolated and structurally characterized by NMR (Rasmussen et al., 2016), and high-resolution mass spectrometric analyses demonstrated the existence of an additional third type of prymnesin, altogether leading to the classification of three prymnesin types, the A-, B- and C-types (Rasmussen et al., 2016). The three types differ in the size of the backbone: the A-type being the longest with 91 carbons, followed by B-type and C-type with 85 and 83 carbons, respectively. Within each type there is a huge structural diversity due to variances in chlorination, saturation and attached sugar moieties, and altogether 51 prymnesin congeners have been reported so far (Binzer et al., 2019). The chemical diversity of polyketides is reflected by a plethora of associated biological functions including anticancer and immunosuppressive properties (Martínez Andrade et al., 2018).

The carbon chain of polyketide compounds is synthesized by polyketide synthases (PKSs) (Rein and Borrone, 1999). PKS related genes share a common evolutionary history with fatty acid synthases (FASs) (Kohli et al., 2016). Both PKSs and FASs have a standard core structure, where the ketosynthase domain (KS) catalyzes the condensation of the acyl units in synergy with an acyltransferase (AT) and an acyl carrier protein (ACP) (Cane et al., 1998; Jenke-Kodama et al., 2005). After the condensation of an acyl unit, the product can be subject to further modifications by the presence of other domains such as dehydratase (DH), enoyl reductase (ER) and ketoreductase (KR). These domains can respectively produce a double bond, a fully-reduced methylene or a hydroxy group (Weissman, 2015). As a result, the organization of these domains has a different effect on the product's final structure. The biosynthesis of a polyketide is terminated by the presence of a thioesterase domain (TE), which hydrolyzes the polyketide compound from the ACP.

Type I PKSs can be iterative, possessing all the catalytic domains in a single protein, and can elongate a chain in a repeated way, functioning like fatty acid synthases in animals and fungi. Modular type I PKSs occur as distinct modules, where each module contains all the prerequisite domains needed for catalyzing the condensation reaction, leading to the elongation of the polyketide chain by two carbon units. In type II PKSs, each catalytic domain is a distinct protein and they function independently and iteratively to type II FASs in bacteria and plants (Cane et al., 1998; Jenke-Kodama et al., 2005). Type III PKSs also function in an iterative manner and consist of self-contained homodimeric enzymes with each monomer catalyzing a specific function. Type III PKSs differ from the other PKS types due to their ability to perform condensation without using acyl carrier proteins (Ferrer et al., 1999).

The role of polyketide synthases in the biosynthesis of marine secondary metabolites has driven extensive studies to elucidate their presence in marine protists and their evolutionary history (e.g. John et al., 2008; Monroe and Dolah, 2008; Kohli et al., 2016). Genome- and transcriptome-based studies on dinoflagellates have shed light on the diversity and presence of PKSs in this potentially toxic and phylogenetically diverse group. The majority of PKS transcripts from dinoflagellates belong to type I PKSs, alongside sequences from other protists. Both modular and single mono-functional domains are present, with the latter showing similar structure to type II PKSs (Monroe and Dolah, 2008). Large modular type I PKSs have been found in many dinoflagellate species including the ciguatoxin-producing *Gambierdiscus polynesiensis*, palytoxin-like producing *Ostreopsis* species and the brevetoxin producing *Karenia brevis* (Kohli et al., 2017; Van Dolah et al., 2017; Verma et al., 2019). Diatoms are another diverse group of marine protists with the potential to be toxic. The *Pseudo-nitzschia* genus is known for the production of the neurotoxin domoic acid and the combination of transcriptomic and biochemical approaches has led to the identification of the complete biosynthetic pathway of domoic acid (Brunson et al., 2018; Haroardóttir et al., 2019). The lack of tools to genetically manipulate the majority of toxin producing organisms has also been an obstacle in incorporating functional genomics in the study of the molecular mechanisms involved in polyketides' biosynthesis (Kohli et al., 2016; Lauritano et al., 2019).

In haptophytes, transcriptomic surveys of 12 strains indicated the presence of type I PKSs (Kohli et al., 2016). However, not all strain screened in this study are toxin producing and given the involvement of PKSs in a wide range of biosynthetic pathways, no direct connection to toxin production was feasible. The *Chrysochromulina* genus contains species that produce ichthyotoxic compounds of unknown structure, but presumably similar to prymnesins. The only available transcriptomic study comes for the species *Chrysochromulina polylepis*, where thirteen putative PKSs were found based on expressed sequence tags (John et al., 2010). In comparison to dinoflagellates, few detailed studies have been conducted concerning the potential involvement of PKSs in toxin biosynthesis in haptophytes (Freitag et al., 2011; Beszteri et al., 2012).

In the current study, we compared the prymnesin profile, the transcriptomes with a focus on the presence of PKSs, and the corresponding expressed metabolic and cellular functions of nine *P. parvum* strains. Given the existence of three different prymnesin types, we chose three strains for each of the prymnesin types, A, B and C. The PKS transcripts derived from the transcriptomes were analyzed through phylogenetics of the KS domain to assess the relationship between prymnesin type and PKS genes to get insights into PKSs evolution within haptophytes and *P. parvum* in particular. Furthermore, we measured the cellular toxin content of all nine strains, relating patterns between toxin types and cellular toxin contents with the presence of PKS genes. Moreover, we investigated gene expression pattern of cellular, metabolic and regulative processes in relation to the cellular toxin and composition to understand the potential molecular and metabolic trade-offs of toxin production in *P. parvum*.

2. Materials and methods

2.1. Cultures

Nine strains of *P. parvum* were obtained from various culture collections, and further information on the year and site of isolation is provided in the Supplementary information. All strains were grown at

17 °C using standard K-medium prepared with sterile filtered North Sea seawater of a salinity of 30. All strains were grown with a light:dark cycle of 16:8 h and a light intensity of 80 μmol photons·m^{-2}·s^{-1}. Prior to establishing the experimental cultures, the cells were rendered axenic using a cocktail of antibiotics (165 μg ml^{-1} ampicillin, 33,3 μg ml^{-1} gentamicin, 100 μg ml^{-1} streptomycin, 1 μg ml^{-1} chloramphenicol, 10 μg ml^{-1} ciprofloxacin). The antibiotic treatment lasted 4 days and was performed a second time after one week. The axenicity of the cultures was validated by fluorescence microscopy after staining with 4′,6-diamidino-2-phenylindole (DAPI).

2.2. Toxin extraction, quantification and correlation analysis

Toxin extraction and quantification were performed according to the protocol described in Svenssen et al., 2019, with small modifications. In general, the biomass on each filter was extracted two times with 20 mL MeOH each for 30 min using an ultrasonic batch. The samples were centrifuged in between at 4300 ×*g* for 15 min at 4 °C. The combined extract (40 mL) was evaporated to dryness using a CentriVap Benchtop Vacuum Concentrator (Labconco Corporation, Kansas City/MO, USA) at 35 °C. Reconstitution was performed with 1 mL methanol:H_2O (90:10, v:v) and short-time ultrasonic bath treatment. The solution was centrifuged to separate residues from the glass fiber filters, and the supernatant was transferred to an HPLC-glass vial. HPLC-FLD measurements were performed after derivatization with the AccQ-Tag Fluor Reagent Kit (Waters Cooperation, Milford/MA, USA) with a 1200 HPLC system (Agilent Technologies, Waldbronn, Germany) using fumonisins B_1 and B_2 as external calibrants due to the lack of standards. Prymnesins and fumonisins share a primary amine group as structural feature important for the derivatization process using AccQ-Fluor. The obtained results are an approximation of the prymnesin content in the samples. HPLC-HRMS-measurements were performed to confirm the presence of prymnesins and identify the specific prymnesin analogues using a 1290 UHPLC system coupled to a 6550 iFunnel QTOF LC/MS (both from Agilent Technologies). Chromatographic separation was achieved with a Kinetex F5 (2.1 × 100 mm, 2.6 μm, Phenomenex, Aschaffenburg, Germany) column using a water-acetonitrile gradient (eluent A: H_20, eluent B: acetonitrile: H_2O (90:10, v:v)). The mass spectrometer was operated in the positive ionization mode in a scanning range of *m/z* 50 to 1700 with 3 scans per second. The total amount of extracted prymnesins was divided by the total number of harvested cells in order to obtain the concentration of prymnesins per cell.

A linear model was used in order to test for a potential effect of growth rates on toxin contents and the toxin data were therefore power transformed (x^0.25) to achieve a normal distribution of the residuals. All analysis were performed with the R base packages.

2.3. RNA extraction, library generation and assembly analysis

Cells for RNA extraction were harvested at the same time point as for toxin extraction (initial exponential phase and cell concentration of ~100,000 cells mL^{-1}) by centrifugation at 1500 ×*g* for 10 min and the obtained pellet was transferred to 1 mL of TriReagent mixed with glass beads. RNA isolation was performed as described in Wohlrab et al. (2017). Libraries for sequencing were prepared using the Truseq Stranded mRNA Samples Prep LS Protocol (Illumina, San Diego, USA). The reads were trimmed using the CLC Genomics Workbench with the default settings. Trinity (v2.8.4) was used for assembling, with a set-up minimum contig length of 300 bp (Haas et al., 2013). The total contigs were clustered together with a similarity threshold of 98% using CD-hit (Fu et al., 2012) while contigs containing homopolymer stretches were removed using an in-house script. The quality of the assemblies was assessed using BUSCO and reference datasets for both Stramenopiles and Alveolates (Waterhouse et al., 2017).

The assemblies were screened for the presence of NRPS, PKS and FAS transcripts using HMMER (Finn et al., 2011) and an in-house HMM database with an applied E-value cutoff of ≤$10e^{-10}$ as described in Kohli et al., 2016. The sequences coding for PKS domains were afterward further analyzed using Pfam (Punta et al., 2012) and conserved domain searches (Marchler-bauer et al., 2017) to get the structure of PKSs and NRPS/PKS contigs. The annotation of the contig domains, protein alignments and phylogenetic analyses were all performed with the Geneious software (Kearse et al., 2012). The sequences were aligned using MAFFT (Katoh et al., 2002), while phylogenetic analysis was carried out using RaxML (Stamatakis, 2006) and selected the LG model of rate heterogeneity with 1000 bootstraps (Le and Gascuel, 2008). The reference assembly was annotated using Trinotate v3.0.2 and the top blastx hit with e-value ≤$10e^{-9}$ was selected in order to increase the accuracy of protein assignment. The resulting PFAM domains were assigned to KEGG Orthologies which were further used for the gene expression analysis.

The gene expression variance analysis was done in the R environment using the 'variancePartition' package (Hoffman and Schadt, 2016). The read counts were normalized based on the total number of reads per sample and further variance stabilizing transformation with the Deseq2 package (Love et al., 2014), as recommended by Hoffman and Schadt (2016).

3. Results and discussion

3.1. Strain phylogeny and toxin content

The transcriptome derived 18S rDNA sequences were used to construct a phylogenetic tree. In this way, we validated that no cross-contamination occurred during the experiments and subsequent extractions. The phylogenetic placement of the strains (Fig. 1) is in accordance with the findings from which have used the internal transcribed spacer (ITS) of the rRNA operon and supports the concept of the monophyletic origin of the prymnesin-type based on the producing strains of a given phylogenetic clade. The strains have been isolated from different areas of the world and no clear pattern was observed between their geographic distribution and phylogenetic placement.

In the current study, the cellular toxin contents varied among the nine strains of *P. parvum*. We confirmed the presence of described prymnesin analogues (Supplementary information), which have been previously detected. It is yet unknown, if and at which level the different analogues contribute to the potential toxic effects. Comparison of toxic effects of *P. parvum* strains on a fish species (*Oncorhynchus mykiss*) and a microalga (*Teleaulax acuta*) gave no correlation with strains low in toxicity towards the microalga being highly toxic towards fish (Blossom et al., 2014); however these strains produced different types of prymnesins. In the current study, toxin contents were at the same level for A-type producing strains, which contained 0.045 to 0.076 fmol of toxin per cell. In B-type producing strains, two of them contained the highest amounts of toxin in this study, with an average of 0.63 fmol per cell for K-0081 and 0.533 fmol per cell for K-0374. Among the C-type producing strains, strains K-0252 and NIES-1017 contained very low, almost undetectable amounts of prymnesins, while RCC-1436 contained the highest amount of prymnesins. In a previous study, Svenssen et al. (2019) developed an indirect method for estimating the prymnesin content of B-type producing strains, and showed that the majority of the toxin is found intracellular rather than being released into the medium. In the same study, strains K-0081 and K-0374 were selected for prymnesin B-type quantification. The amount of cellular toxin content varied from our finding, with K-0081 containing ~5 times more prymnesin than K-0374. These findings highlight the importance of the applied and well controlled culturing methods as probably one of the essential drivers for toxin production and allelopathy in *P. parvum*. The cellular toxin content could be indicative for the potential allelopathy of *P. parvum*; therefore, sensitive but also ecological relevant bioassays should be used in order to elucidate the relation between these two parameters: cellular toxin content and expressed extra cellular lytic toxicity.

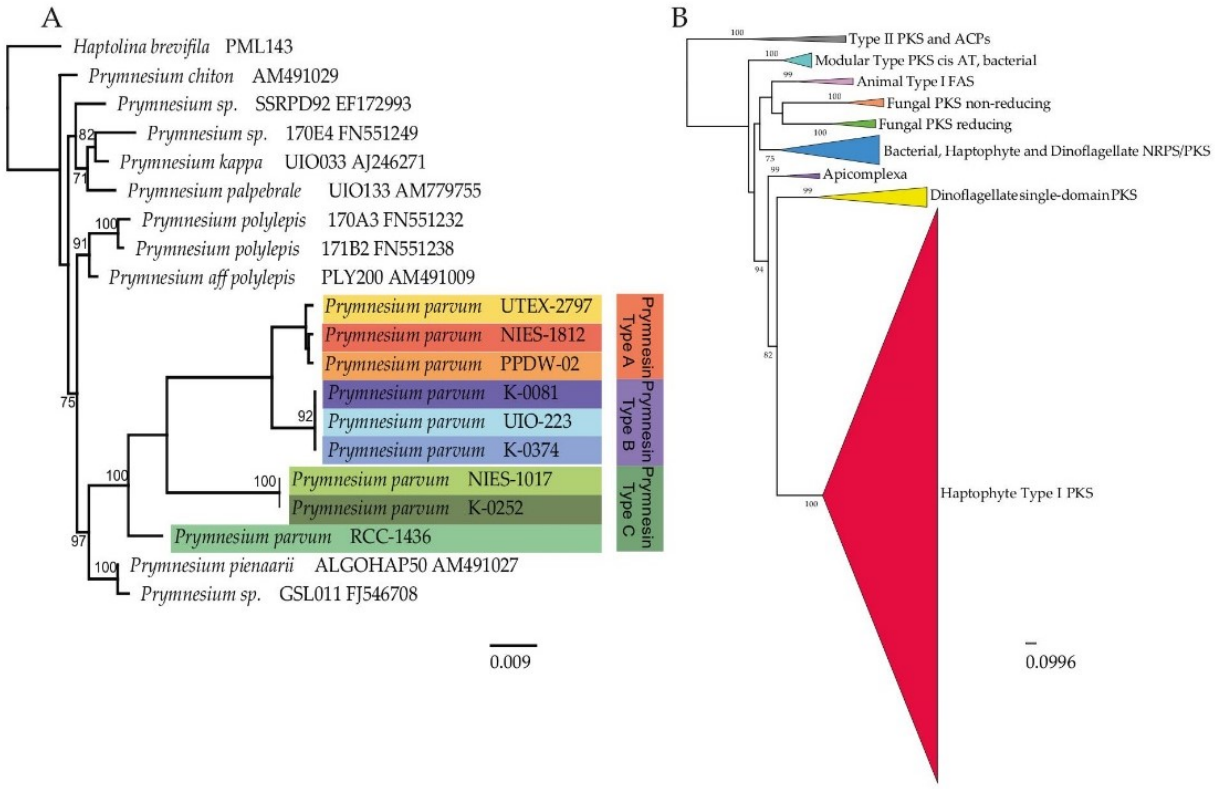

Fig. 1. Phylogeny of 18S rRNA extracted from the transcriptomes of all nine *P. parvum* strains (A). Phylogenetic analysis of type I polyketide synthases (PKSs) and non-ribosomal polyketide synthetases/synthase (NRPSs) ketoacyl synthase (KS) domains. The alignment included 412 KS sequences, out of which 208 belong to the nine *P. parvum* strains. KS domains with an identity of ≥98% were excluded in order to avoid redundancy and to improve the alignment. RaxML with 1000 bootstraps was used for the construction of the phylogenetic tree.

3.2. De novo transcriptomic assembly

On average 149 ± 34 million reads were generated for every strain (Table 1). The raw read sequences have been deposited at NCBI (National Center for Biotechnology Information) under the BioProject PRJNA718746. Strain specific de novo transcriptomes were assembled. After clustering all contigs with a similarity of 98% and a minimum length of 300 bp, the number of contigs varied among the strains, from 56,645 to 80,915 (Table 1). According to BUSCO (Benchmarking Universal Single-Copy Orthologs), the completeness of the assemblies was evaluated using as reference a total of 171 highly conserved proteins belonging to Stramenopiles and Alveolates (Waterhouse et al., 2017). The percentage of total proteins with a match in either complete single or duplicated copy varied with an average of 78.06 ± 2.56. Previous studies of haptophytes transcriptomic PKS surveys have not analyzed their completeness according to recent tools and thus a direct comparison is not possible (e.g. John et al., 2010; Beszteri et al., 2012). The reference assembly used for the gene expression variance analysis had a BUSCO completeness of 81.5%. The total number of transcripts was 186,144 and KEGG orthologies were assigned for 44,408.

3.3. Type I modular polyketide synthase encoding transcripts

Modular type I PKSs consist of consecutive modules, each of them catalyzing the addition of an extender unit (acyl group) to the growing polyketide product. The sequence of the domains on each module and their combination decides the nature of the final chemical structure of the produced compound. As a result, the functional annotation and domain organization of modular Type I PKSs can be an important step towards correlating which gene clusters that encodes the enzymes making a given carbon backbone. Our analyses revealed the presence of a plethora of PKS-related contigs in all strains of *P. parvum*. The

Table 1
Transcriptomes overview and number of PKS domains retrieved per strain.

	Type A			Type B			Type C		
	NIES-1812	PPDW02	UTEX-2797	K-0081	UIO-223	K-0374	K-0252	NIES-1017	RCC-1436
Assembled reads	134,628,014	173,930,042	108,806,618	174,294,139	177,225,633	116,245,080	124,143,170	129,669,753	209,186,155
Total contigs ≥ 300 bp	59,570	64,714	61,656	60,561	54,645	80,915	60,981	58,249	63,379
BUSCO % completeness	70.85	74.91	83.76	80.81	77.12	73.80	81.92	84.13	75.28
GC content (%)	56.3	55.7	56.9	56.8	56.3	55.8	56.9	57	55.3
Total PKS related transcripts	109	96	91	37	67	68	64	83	61
Total multi-domain transcripts	49	47	35	25	46	41	33	42	25
#KS domains	112	100	84	68	77	83	67	89	56
#KR domains	25	35	19	50	29	28	14	23	12
#DH domains	23	25	11	32	31	21	18	20	6
#ER domains	6	8	6	11	8	5	5	5	4
#ACP domains	62	69	42	70	51	52	31	49	31
Complete modules at longest transcript	3	3	3	10	6	4	3	2	2

total number of PKS-related contigs varied from 37 to 109. The KS domain catalyzes the condensation of carbon units and is highly conserved, thus making it the most suitable one for phylogenetic purposes (John et al., 2008). Therefore, the resulting KS domains of *P. parvum* were phylogenetically analyzed in order to identify type I PKS transcripts. Additional KS domains from other haptophytes, or corresponding outgroup species (Kohli et al., 2016), were used to check for common clades found within haptophytes (Fig. 1). The KS domains were divided based on whether they coded the full or partial domain and their presence on multi- or single-domain contigs (Supplementary information). In general, full KS domains in multi-modular transcripts accounted for 24.6–72.6% of the total KS domains. The partial KS domains in multi-modular transcripts had a relative contribution ranging from 12.3–33.3%, while KS domains in single-domain transcripts accounted for 15.1–55.3% of the total KS domains.

The resulting phylogeny is in its general topology in accordance with previous studies that involved KS domains from a wide range of protists (John et al., 2008; Kohli et al., 2016). The *P. parvum* ketoacyl synthase (KS) domains fell into a well-supported haptophyte specific group (Fig. 2). Within this group, the *P. parvum* KS domains dominated in three clades. Two of those clades, A and C, were well supported with both of them having a bootstrap value of 100. In clade A, all KS domain sequences belonged to *P. parvum*, while in clade C there was a KS domain belonging to *Chrysochromulina brevifilum*, another prymnesiophyte. All KS domains we examined for the amino acid sequence of their active sites and the level of conservation. In principle, active sites are conserved among the sequences with some exceptions, which presented clade specific patterns. In type I PKSs, conserved active site residues seem to be important for the functionality of the KS domains (Kwon et al., 1998). In clade A, the amino acid sequence QGLGS was found in all KS domains and is divergent to the expected HGTGT motif. Moreover, in clade C, some KSs possessed NTACS instead of the expected DTACS. However, the active site C, which is responsible for the decarboxylative condensation, was maintained in all sequences. The divergent active site residues could attribute different function to enzymes, something indicated by the formation of distinct clades by the corresponding KS sequences (Eichholz et al., 2012).

Besides having *P. parvum* specific KS clades, no clear relation to the prymnesin type produced by the strains was found. Moreover, KS domains belonging to the same modular PKS contigs were not only found in the *P. parvum* dominated ones, but also fell into mixed haptophyte clades. The high number of KS domains and the corresponding other functional domains found in *P. parvum* and other species indicate a relaxed selection pressure leading to highly diverse domains driven by evolutionary processes such as gene duplications and domain shuffling (Beedessee et al., 2019). Moreover, no clear pattern was observed in terms of the total number of retrieved KS domains and the level of cellular toxin content. Nonetheless, a high number of modular PKS genes was found in the highly toxic strain K-0081 and most KS domains (84%) made part of modular PKS transcripts.

Modular type I PKSs have been detected in many marine protists and can have considerable gene length as indicated by their products (John et al., 2008). In the current study, larger transcripts were found in strain K-0081, with a 41,957 nt long transcript (K0081_21_c0_g1_i7_frame3) encoding for a 10-module type I PKS. When further assembled, the total

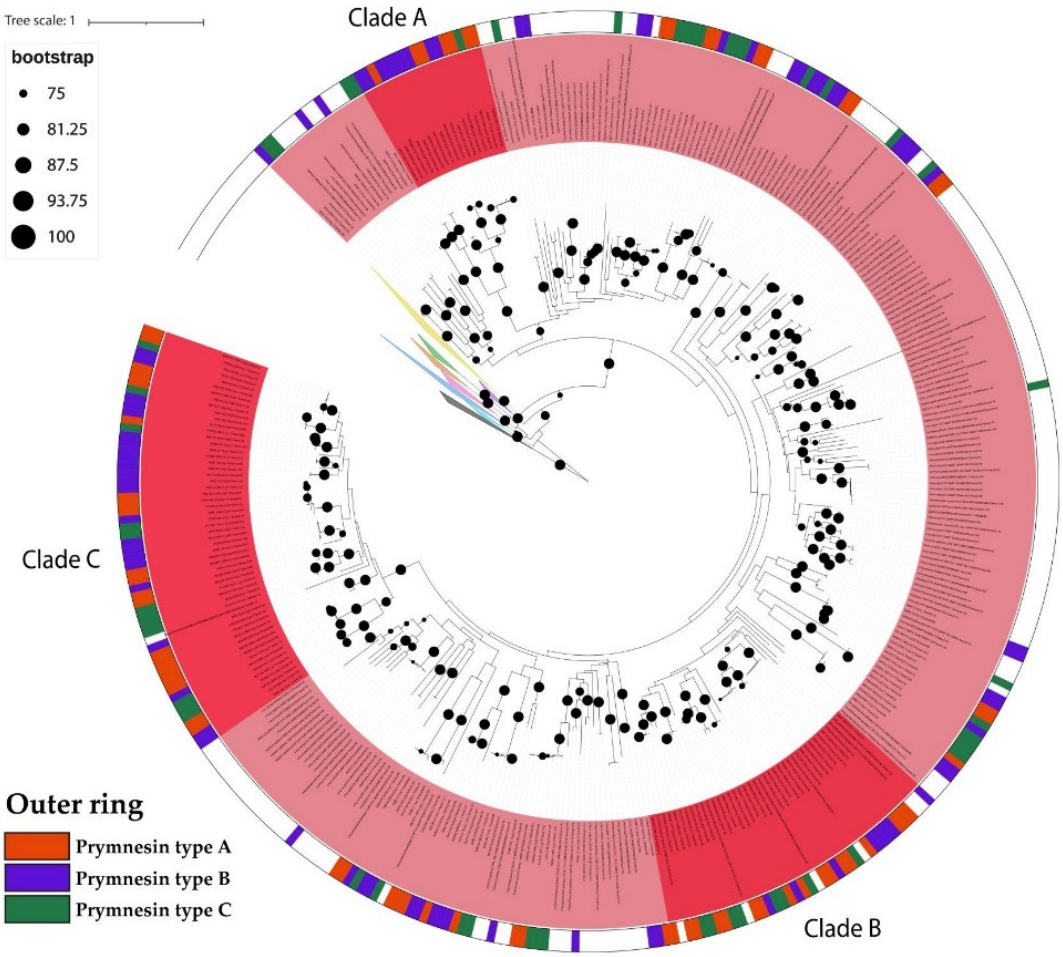

Fig. 2. Detailed phylogeny of type I polyketide synthases (PKSs) and non-ribosomal polyketide synthases (NRPS) ketoacyl synthase (KS) domains. Outgroups correspond to those indicated in Fig. 1. The outer ring represents the prymnesin type that is produced by the corresponding strain. In clades A, B and C, *P. parvum* ketoacyl synthase (KS) domains dominated.

length of the contig was 49,007 nt and 11 modules as it assembled with K0081_21_c0_g3_i1_frame1r and had an overlap of 1473 nt and two mismatches. In total, we identified the presence of eight consensus modular type I PKS contigs in all nine strains (Fig. 3B). The identification of the consensus contigs was based upon the identity of the KS domains of the corresponding transcripts and the overall domain organization of the contigs (Fig. 3B). However, not the same contig length was found in all strains. In general, long modular type I PKS contigs were retrieved from the highly toxic B strains and smaller contigs from the other strains aligned to them. All PKSs retrieved by each strain and their functional domain organizations can be found at the Supplementary information.

Genome wide studies to mine PKSs from microalgae has led to the description of large modular type I PKSs, up to 14 modules long (Sasso et al., 2012). In *Ostreococcus* sp., PKSs account for 1.5% of the genome, illustrating the increased fitness the products of these genes attribute to their holders (John et al., 2008). The diversity of polyketides is not only restricted in their biosynthetic mechanisms, but also in their function. For example, in *Chlamydomonas reinhardtii* a type I PKS gene with an estimated mass of 2.3 MDa is involved in zygospore maturation (Heimerl et al., 2018). High number of KS encoding transcripts, 115 and 121 for ichthyotoxic *Ostreopsis* sp. and *K. brevis* respectively, have been discovered (Van Dolah et al., 2017; Verma et al., 2019). Larger contigs and a higher number of modular PKS transcripts were retrieved from a highly toxic strain of *Gambierdiscus* sp. compared to a non-toxic one (van Dolah et al., 2020). In this case, the longest PKS transcript consisted of seven modules and could predict a part of the polyether backbone of the produced ciguatoxin. In another study, PKS transcripts were higher expressed in a toxic strain of *G. balechii* as compared to a non-toxin one (Wu et al., 2020). Other studies have suggested no differences in terms of total number of PKSs transcripts when toxic and non-toxic species or strains of the same species were used, suggesting their constitutive presence in the genome of the organisms (Verma et al., 2019; Vingiani et al., 2020).

The functional annotation of the modular type I PKSs in *P. parvum* resulted in the expected PKS domains, but also revealed the presence of some additional ones (Fig. 3B). Such 'unusual' PKS domains have previously been found in toxigenic dinoflagellates such as *Gambierdiscus* sp. and *K. brevis* (Kohli et al., 2015, Van Dolah et al., 2017). The presence

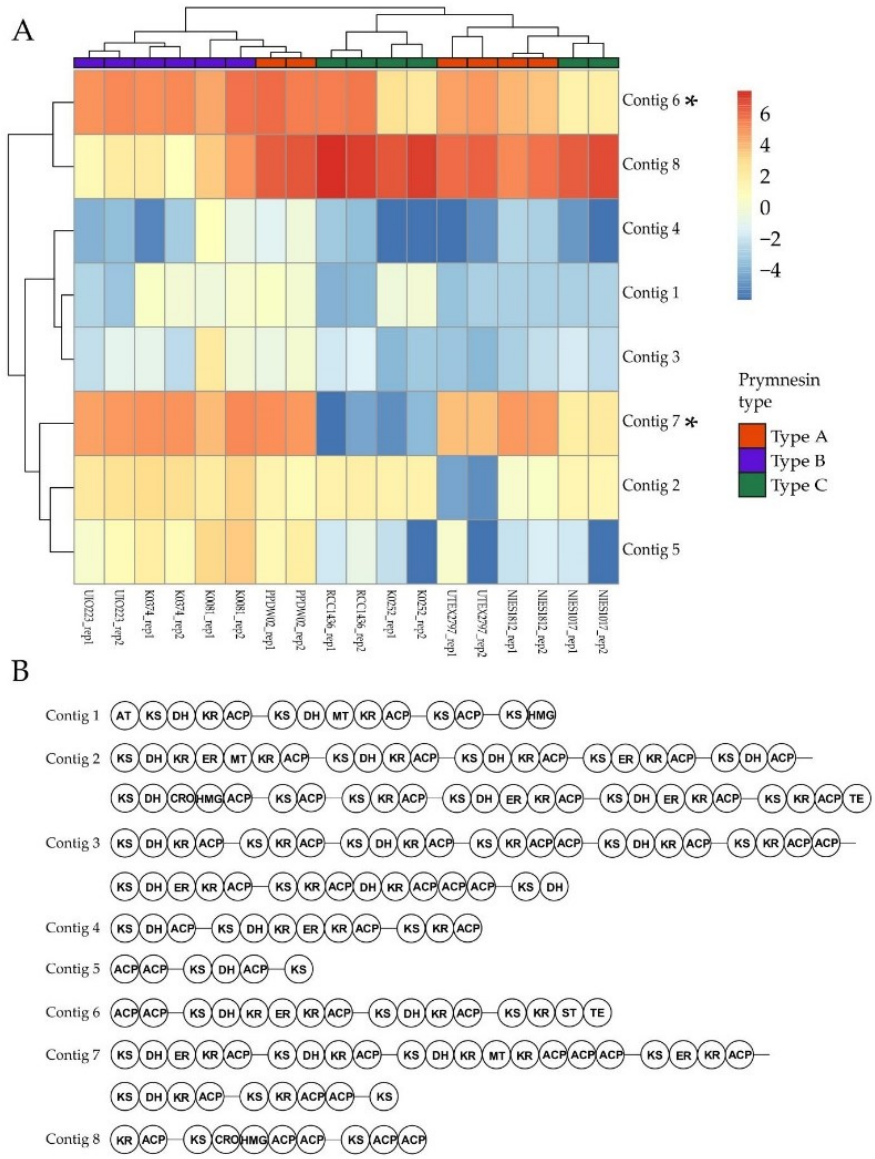

Fig. 3. Heatmap of log2TPM gene expression of 8 consensus modular type I PKS contigs (A) and their domain organization (B). KS = ketoacyl synthase, KR = ketoreductase, ER = enoyl reductase, ACP = acyl carrier protein, DH = dehydratase, TE = thioesterase, AT = acyltransferase, HMG = hydroxymethylglutaryl-coenzyme A synthase, CRO = enoyl-CoA hydratase/isomerase, MT = methyltransferase. The * symbol indicates the contigs for which the cellular toxin content explained >70% of their gene expression variance.

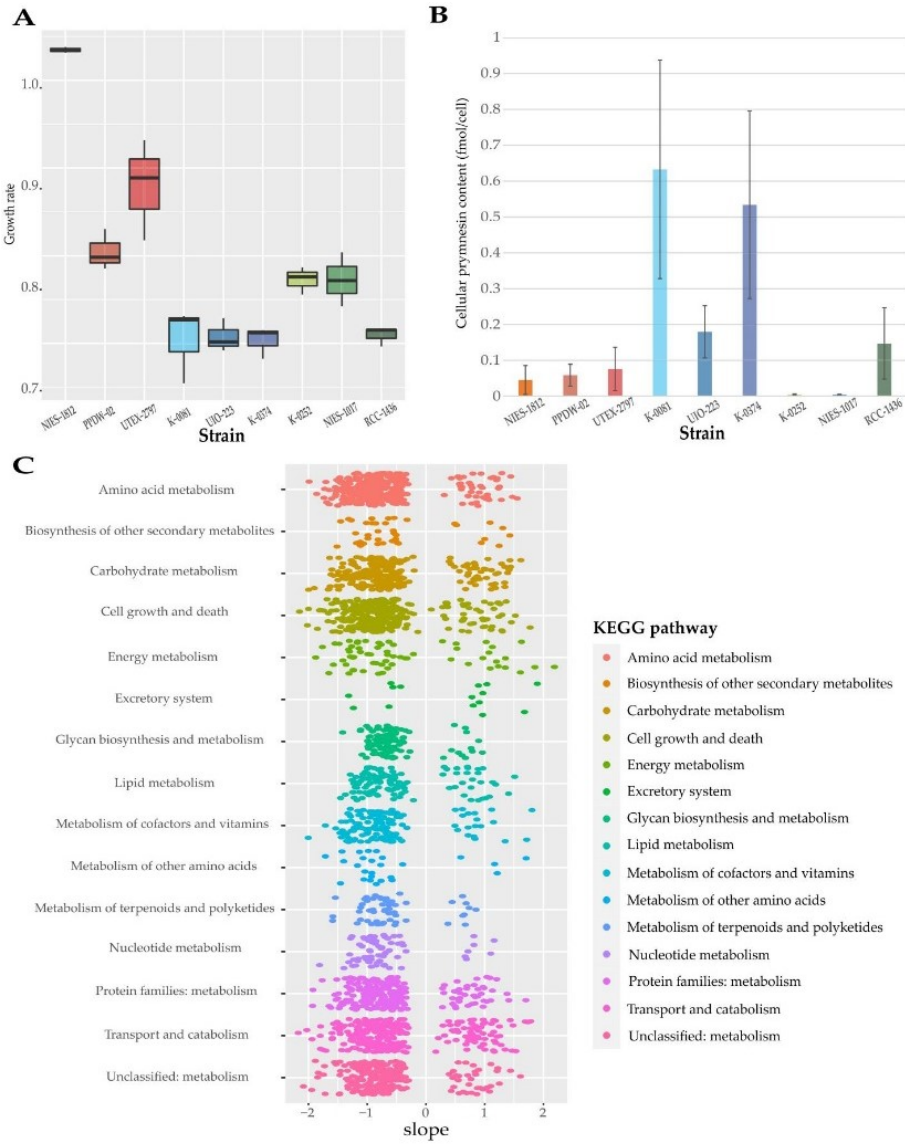

Fig. 4. Growth rates (d^{-1}) of the nine *P. parvum* strains (A) and their corresponding cellular toxin content expressed as fmol/cell (B). Chart of transcripts for which gene expression variance was explained by the cellular toxin content (C). The x axis indicates the slope of the correlation with <0 showing a negative correlation and >0 a positive correlation.

of such 'unusual' PKS domains in distinct genera could be a result of either convergent evolution or horizontal gene transfer (Orr et al., 2013). Independently of the events that led to this result, secondary metabolism (which PKSs make part of) is subject to increased evolution which is driven by environmental pressures and selection based on the fitness the product attributes to an organism (Pichersky and Gang, 2000). A methyltransferase domain (MT) belonging to the methyltrasf_12 family was detected in three modular contigs. This domain belongs to the CL0063 clan and contains member proteins that are S-adenosylmethionine-dependent methyltransferases (SAM). S-adenosyl-L-methionine is acting as a donor of methyl groups that are added to a wide variety of substrates that include lipids and nucleic acids (Martin and McMillan, 2003). In PKSs, this domain catalyzes the addition of methyl branches (Piel, 2010). An enoyl-CoA hydratase/isomerase domain was also found and showed high similarity to the crotonase superfamily proteins and the CL0127 clan. This superfamily contains multiple enzymes with the ability to perform processes such as dehalogenation, hydration or isomerization. This domain was usually followed by a hydroxymethylglutaryl-coenzyme A synthase. This enzyme is member of the thiolase-like superfamily and the CL0046 clan. Members of this protein family are involved in both the degradation and biosynthesis of fatty acid synthases. Finally, a sulfotransferase domain was found in a modular contig and was followed by a thioesterase (TE) domain. This sulfotransferase domain belongs to the CL0023 clan and catalyzes the addition of a sulfo group to the substrate.

The identification of 'unusual' PKS domains highlights the complexity of haptophyte derived polyketides and the involvement of domains with variable effect on the final product. The study of these additional domains is limited and further investigations would contribute substantially to our understanding of chemical compounds biosynthesized by protists. This is especially important, as marine natural products can have a wide range of medical applications which would include antibiotics and anticancer medicines (Martínez Andrade et al., 2018; Lauritano et al., 2020).

Non-ribosomal peptide synthases (NRPS) catalyse the incorporation of amino acids to the final product. Hybrid PKS/NRPS products involve the addition of both acetate groups and amino acids. Three different PKS/NRPS hybrids were found in the current study, but they were not present in the transcriptomes of all strains. The phylogenetic analysis of the KS domains from PKS/NRPS hybrids supports their bacterial origin.

The expression pattern of the found modular PKS transcripts as transcripts per million (TPM) was further analyzed (Fig. 3A). The expression variance of two consensus contigs was found to be explained by the cellular toxin content, rendering them alongside their phylogeny as potential candidate genes in the biosynthesis of prymnesins. Moreover, the contigs clustered together in the case of B-type prymnesin producing strains, while there was a mixed clustering for the A- and C-types producing ones. Single-domain contigs from low toxin content strains showed high KS similarity and clustered with modular contigs, which indicates lower expression in low toxin content strains and the requirement of deeper sequencing in order to obtain full length transcripts.

3.4. Gene expression variance and potential ecological implications

The gradient of toxin content across the nine strains studied here was used as a parameter in order to search for molecular trade-offs involved in toxin production. The production of complex and large toxic compounds such as prymnesins may come at a considerable cost via the investment of carbon and energy resources, which, could instead be allocated to cell proliferation. We decomposed the total variance in the gene expression matrix into partial variances explained by the factors 'toxin content' and 'prymnesin type'. The number of transcripts with a KEGG annotation for which the toxin content explained the majority of the expression variance was 6335. The further exploration of these transcripts was done only for the ones that are involved in metabolic pathways. The general pattern revealed a downregulation of the cell's metabolism as a trade-off for high cellular toxin contents (Fig. 4C). For all KEGG metabolic pathways, 1892 transcripts showed a negative correlation to toxin content, while 631 transcripts showed a positive correlation.

Trade-offs of cellular toxin content and growth rates have been studied in the paralytic shellfish toxin (PST) producing dinoflagellates of the genus *Alexandrium* (Blossom et al., 2019). In this study, strains with higher cellular PST contents had lower growth rates compared to strains with low cellular PST content. Our study indicated similar patterns in *P. parvum:* strains with high prymnesin content had lower growth rates compared to strains with low cellular prymnesin content (Fig. 4A; B). Although differences in growth rates could only explain 15% of the observed variability in toxin contents, the negative correlation was statistically significant ($p = 0.043$). The fact that growth rate explained 15% of the toxin variability highlights that multiple factors influence toxin production.

Prymnesin production seems to be constitutive in all *P. parvum* strains studied up to date, indicating the importance of toxin production in this species (Binzer et al., 2019). Within natural populations, the presence of strains of various toxicity attributes different advantages in individual and collective level (Tillmann and Hansen, 2009). Highly toxic strains play an important role to the success of the given species as they often have a broad impact on competitors and grazers (Donk and Ianora, 2011). The advantage of toxigenic strains with regard to grazing and competition has been shown for several species (John et al., 2002; Tillmann and Hansen, 2009) and a mutual facilitation of toxic strains for non-toxic ones has been postulated (John et al., 2015). However, if both toxic and non-toxic strains of a given species co-occur in populations, it may not always be to the benefit of the toxic strains, if the non-toxic strains are not affected by the released toxins. This has, in fact, been shown in experiments with a mixture of toxic and non-toxic *P. parvum* strains in the presence of a competitor; the non-toxic strains increased in relative abundance during the incubation (Driscoll et al., 2013). Initially, the highly toxic strains produced and released toxic compounds, which eliminated competitors and thus attributed a competitive advantage of the species. Within the context of the theory of the "public goods", non-toxic or low toxic strains (also described as "cheaters") are benefited by the elimination of competition as they have easier access to nutrients (Driscoll and Pepper, 2010; John et al., 2015). In the same study, the increase in frequency of low toxic strains highlights the fine balance and trade-offs between high and low toxicity. The growth advantage of low toxic strains would imply their later dominance in a community and the elimination of slowly growing strains. However, an important parameter to take into account is grazing, as low toxic strains will be preferred for consumption (Selander et al., 2006; Tillmann et al., 2007).

4. Conclusion

The study of the molecular basis of toxin biosynthesis is challenging due to the diversity of both chemical structures and involved genes. A plethora of polyketide synthase genes were found in *P. parvum* and this is the first step for future studies to elucidate the mechanisms involved in the study of prymnesins. Eight modular type I PKSs were present in the transcriptomes in all nine strains, while the expression of two contigs was explained by the cellular prymnesin content. The expression variance analysis suggests the downregulation of basic metabolic processes as a potential trade-off for high cellular toxin content. This work contributes to the developments of molecular tools for monitoring harmful blooms of the ichthyotoxic species *P. parvum* by providing a detailed analysis of a group of genes potentially involved in the production of prymnesins.

CRediT authorship contribution statement

Konstantinos Anestis: Conceptualization, Methodology, Formal analysis, Investigation, Data Curation, Writing – Original Draft, Writing – Review & Editing, Visualization **Gurjeet Singh Kohli:** Conceptualization, Methodology, Writing – Review & Editing **Sylke Wohlrab:** Methodology, Writing – Review & Editing, Visualization **Elisabeth Varga:** Methodology, Investigation, Writing – Review & Editing, Funding acquisition **Thomas Ostenfeld Larsen:** Writing – Review & Editing **Per Juel Hansen:** Writing – Review & Editing, Funding acquisition **Uwe John:** Conceptualization, Methodology, Writing – Review & Editing, Supervision, Funding acquisition.

Declaration of competing interest

The authors declare no conflict of interest. The funders had no role in the design of the study; in the collection, analyses, or interpretation of data; in the writing of the manuscript, or in the decision to publish the results.

Acknowledgements

E.V. thanks Franz Berthiller of the University of Natural Resources and Life Sciences, Vienna (BOKU) for the access to the Agilent 6550 iFunnel QTOF LC/MS system.

Funding

This work has been funded by European Union's Horizon 2020 research and innovation programme under grant agreement No. 766327. E.V. received funding of the Austrian Science Fund (FWF) through an Erwin-Schrödinger fellowship [J3895-N28].

Appendix A. Supplementary data

Supplementary data to this article can be found online at https://doi.org/10.1016/j.scitotenv.2021.148878.

References

Beedessee, G., Hisata, K., Roy, M.C., Van Dolah, F.M., Satoh, N., Shoguchi, E., 2019. Diversified secondary metabolite biosynthesis gene repertoire revealed in symbiotic dinoflagellates. Sci. Rep. 9, 1–12. https://doi.org/10.1038/s41598-018-37792-0.

Beszteri, S., Yang, I., Jaecksch, N., Tillmann, U., Frickenhaus, S., Glöckner, G., et al., 2012. Transcriptomic response of the toxic prymnesiophyte *Prymnesium parvum* (N. Carter) to phosphorus and nitrogen starvation. Harmful Algae 18, 1–15. https://doi.org/10.1016/j.hal.2012.03.003.

Binzer, S.B., Svenssen, D.K., Daugbjerg, N., Alves-de-Souza, C., Pinto, E., Hansen, P.J., et al., 2019. A-, B- and C-type prymnesins are clade specific compounds and chemotaxonomic markers in *Prymnesium parvum*. Harmful Algae 81, 10–17. https://doi.org/10.1016/J.HAL.2018.11.010.

Blossom, H.E., Rasmussen, S.A., Andersen, N.G., Larsen, T.O., Nielsen, K.F., Hansen, P.J., 2014. *Prymnesium parvum* revisited: relationship between allelopathy, ichthyotoxicity, and chemical profiles in 5 strains. Aquat. Toxicol. 157, 159–166. https://doi.org/10.1016/j.aquatox.2014.10.006.

Blossom, H.E., Markussen, B., Daugbjerg, N., Krock, B., Norlin, A., Hansen, P.J., 2019. The cost of toxicity in microalgae: direct evidence from the dinoflagellate *Alexandrium*. Front. Microbiol. 10, 1065. https://doi.org/10.3389/fmicb.2019.01065.

Brunson, J.K., McKinnie, S.M.K., Chekan, J.R., McCrow, J.P., Miles, Z.D., Bertrand, E.M., et al., 2018. Biosynthesis of the neurotoxin domoic acid in a bloom-forming diatom. Science 361, 1356–1358. https://doi.org/10.1126/science.aau0382.

Cane, D.E., Walsh, C.T., Khosla, C., 1998. Harnessing the biosynthetic code: combinations, permutations, and mutations. Science 282, 63–68. https://doi.org/10.1126/science.282.5386.63.

Donk, E. Van, Ianora, A., 2011. Induced defences in marine and freshwater phytoplankton: a review. Hydrobiologia 668, 3–19. https://doi.org/10.1007/s10750-010-0395-4.

Driscoll, W.W., Pepper, J.W., 2010. Theory for the evolution of diffusible external goods. Evolution 64, 2682–2687. https://doi.org/10.1111/j.1558-5646.2010.01002.x.

Driscoll, W.W., Espinosa, N.J., Eldakar, O.T., Hackett, J.D., 2013. Allelopathy as an emergent, exploitable public good in the bloom-forming microalga *Prymnesium parvum*. Evolution 67, 1582–1590. https://doi.org/10.1111/evo.12030.

Eichholz, K., Beszteri, B., John, U., 2012. Putative monofunctional type I polyketide synthase units: a dinoflagellate-specific feature? PLoS One 7, e48624. https://doi.org/10.1371/journal.pone.0048624.

Ferrer, J.L., Jez, J.M., Bowman, M.E., Dixon, R.A., Noel, J.P., 1999. Structure of chalcone synthase and the molecular basis of plant polyketide biosynthesis. Nat. Struct. Biol. 6, 775–784. https://doi.org/10.1038/11553.

Finn, R.D., Clements, J., Eddy, S.R., 2011. HMMER web server: interactive sequence similarity searching. Nucleic Acids Res. 39, W29–W37. https://doi.org/10.1093/nar/gkr367.

Flynn, K.J., Mitra, A., Anestis, K., Anschütz, A.A., Calbet, A., Ferreira, G.D., et al., 2019. Mixotrophic protists and a new paradigm for marine ecology: where does plankton research go now? J. Plankton Res. 41, 375–391. https://doi.org/10.1093/plankt/fbz026.

Freitag, M., Beszteri, S., Vogel, H., John, U., Freitag, M., Beszteri, S., et al., 2011. Effects of physiological shock treatments on toxicity and polyketide synthase gene expression in *Prymnesium parvum* (Prymnesiophyceae). Eur. J. Phycol. 46, 193–201. https://doi.org/10.1080/09670262.2011.591438.

Fu, L., Niu, B., Zhu, Z., Wu, S., Li, W., 2012. CD-HIT: accelerated for clustering the next-generation sequencing data. Bioinformatics 28, 3150–3152. https://doi.org/10.1093/bioinformatics/bts565.

Granéli, E., Edvardsen, B., Roelke, D.L., Hagström, J.A., 2012. The ecophysiology and bloom dynamics of *Prymnesium spp*. Harmful Algae 14, 260–270. https://doi.org/10.1016/j.hal.2011.10.024.

Haas, B.J., Papanicolaou, A., Yassour, M., Grabherr, M., Blood, P.D., Bowden, J., et al., 2013. De novo transcript sequence reconstruction from RNA-seq using the Trinity platform for reference generation and analysis. Nat. Protoc. 8, 1494–1512. https://doi.org/10.1038/nprot.2013.084.

Haroardóttir, S., Wohlrab, S., Hjort, D.M., Krock, B., Nielsen, T.G., John, U., et al., 2019. Transcriptomic responses to grazing reveal the metabolic pathway leading to the biosynthesis of domoic acid and highlight different defense strategies in diatoms. BMC Mol. Biol. 20, 1–14. https://doi.org/10.1186/s12867-019-0124-0.

Heimerl, N., Hommel, E., Westermann, M., Meichsner, D., Lohr, M., Hertweck, C., et al., 2018. A giant type I polyketide synthase participates in zygospore maturation in *Chlamydomonas reinhardtii*. Plant J. 95, 268–281. https://doi.org/10.1111/tpj.13948.

Hoffman, G.E., Schadt, E.E., 2016. variancePartition: interpreting drivers of variation in complex gene expression studies. BMC Bioinforma. 17, 17–22. https://doi.org/10.1186/s12859-016-1323-z.

Igarashi, T., Satake, M., Yasumoto, T., 1999. Structures and partial stereochemical assignments for prymnesin-1 and prymnesin-2: potent hemolytic and ichthyotoxic glycosides isolated from the red tide alga *Prymnesium parvum*. J. Am. Chem. Soc., 8499–8511 https://doi.org/10.1021/ja991740e.

Jenke-Kodama, H., Sandmann, A., Müller, R., Dittmann, E., 2005. Evolutionary implications of bacterial polyketide synthases. Mol. Biol. Evol. 22, 2027–2039. https://doi.org/10.1093/molbev/msi193.

John, U., Tillmann, U., Medlin, L.K., 2002. A comparative approach to study inhibition of grazing and lipid composition of a toxic and non-toxic clone of *Chrysochromulina polylepis* (Prymnesiophyceae). Harmful Algae 1, 45–57. https://doi.org/10.1016/S1568-9883(02)00005-7.

John, U., Beszteri, B., Derelle, E., Van de Peer, Y., Read, B., Moreau, H., et al., 2008. Novel insights into evolution of protistan polyketide synthases through phylogenomic analysis. Protist 159, 21–30. https://doi.org/10.1016/j.protis.2007.08.001.

John, U., Beszteri, S., Glöckner, G., Singh, R., Medlin, L., Cembella, A.D., et al., 2010. Genomic Characterisation of the Ichthyotoxic Prymnesiophyte *Chrysochromulina polylepis*, and the Expression of Polyketide Synthase Genes in Synchronized Cultures. vol. 45, pp. 215–229. https://doi.org/10.1080/09670261003746193.

John, U., Tillmann, U., Hülskötter, J., Alpermann, T.J., Wohlrab, S., Van de Waal, D.B., 2015. Intraspecific facilitation by allelochemical mediated grazing protection within a toxigenic dinoflagellate population. Proc. R. Soc. B Biol. Sci. 282. https://doi.org/10.1098/rspb.2014.1268.

Katoh, K., Misawa, K., Kuma, K.I., Miyata, T., 2002. MAFFT: a novel method for rapid multiple sequence alignment based on fast Fourier transform. Nucleic Acids Res. 30, 3059–3066. https://doi.org/10.1093/nar/gkf436.

Kearse, M., Moir, R., Wilson, A., Stones-havas, S., Sturrock, S., Buxton, S., et al., 2012. Geneious Basic: an integrated and extendable desktop software platform for the organization and analysis of sequence data. Bioinformatics 28, 1647–1649. https://doi.org/10.1093/bioinformatics/bts199.

Kohli, G.S., John, U., FIgueroa, R.I., Rhodes, L.L., Harwood, D.T., Groth, M., Bolch, C.J.S., Murray, S.A, 2015. Polyketide synthesis genes associated with toxin production in two species of *Gambierdiscus* (Dinophyceae). BMC Genomics 16, 1–10. https://doi.org/10.1186/s12864-015-1625-y.

Kohli, G.S., John, U., Van Dolah, F.M., Murray, S.A., 2016. Evolutionary distinctiveness of fatty acid and polyketide synthesis in eukaryotes. ISME J. 10, 1877–1890. https://doi.org/10.1038/ismej.2015.263.

Kohli, G.S., Campbell, K., John, U., Smith, K.F., Fraga, S., Rhodes, L.L., et al., 2017. Role of modular polyketide synthases in the production of polyether ladder compounds in Ciguatoxin-producing *Gambierdiscus polynesiensis* and *G. excentricus* (Dinophyceae). J. Eukaryot. Microbiol. 64, 691–706. https://doi.org/10.1111/jeu.12405.

Kwon, H., Smith, W.C., Scharon, A.J., Hwang, S.H., Kurth, M.J., Shen, B., 1998. C-O bond formation by polyketide synthases. Science 297, 1327–1330. https://doi.org/10.1126/science.1073175.

Lauritano, C., Ferrante, M.I., Rogato, A., 2019. Marine natural products from microalgae: an -omics overview. Mar. Drugs 17, 1–18. https://doi.org/10.3390/md17050269.

Lauritano, C., Martínez, K.A., Battaglia, P., Granata, A., de la Cruz, M., Cautain, B., et al., 2020. First evidence of anticancer and antimicrobial activity in Mediterranean mesopelagic species. Sci. Rep. 10, 1–8. https://doi.org/10.1038/s41598-020-61515-z.

Le, S.Q., Gascuel, O., 2008. An improved general amino acid replacement matrix. Mol. Biol. Evol. 25, 1307–1320. https://doi.org/10.1093/molbev/msn067.

Love, M.I., Huber, W., Anders, S., 2014. Moderated estimation of fold change and dispersion for RNA-seq data with DESeq2. Genome Biol. 15, 1–21. https://doi.org/10.1186/s13059-014-0550-8.

Lundgren, V.M., Glibert, P.M., Granéli, E., Vidyarathna, N.K., Fiori, E., Ou, L., et al., 2016. Metabolic and physiological changes in Prymnesium parvum when grown under, and grazing on prey of, variable nitrogen:phosphorus stoichiometry. Harmful Algae 55, 1–12. https://doi.org/10.1016/J.HAL.2016.01.002.

Marchler-bauer, A., Bo, Y., Han, L., He, J., Lanczycki, C.J., Lu, S., et al., 2017. CDD/SPARCLE: functional classification of proteins via subfamily domain architectures. Nucleic Acids Res. 45, 200–203. https://doi.org/10.1093/nar/gkw1129.

Martin, J.L., McMillan, F.M., 2003. SAM (dependent) I AM: the S-adenosylmethionine-dependent methyltransferase fold. Curr. Opin. Struct. Biol. 13, 140. https://doi.org/10.1016/S0959-440X(02)00008-8.

Martínez Andrade, K.A., Lauritano, C., Romano, G., Ianora, A., 2018. Marine microalgae with anti-cancer properties. Mar. Drugs 16. https://doi.org/10.3390/md16050165.

Monroe, E.A., Dolah, F.M. Van, 2008. The toxic dinoflagellate Karenia brevis encodes novel type I-like polyketide synthases containing discrete catalytic domains. Protist 159, 471–482. https://doi.org/10.1016/j.protis.2008.02.004.

Orr, R.J.S., Stüken, A., Murray, S.A., Jakobsen, K.S., 2013. Evolution and distribution of saxitoxin biosynthesis in dinoflagellates. Mar. Drugs 11, 2814–2828. https://doi.org/10.3390/md11082814.

Pichersky, E., Gang, D.R., 2000. Genetics and biochemistry of secondary metabolites in plants: an evolutionary perspective. Trends Plant Sci. 5, 439–445. https://doi.org/10.1016/S1360-1385(00)01741-6.

Piel, J., 2010. Biosynthesis of polyketides by trans-AT polyketide synthases. Nat. Prod. Rep. 27, 996–1047. https://doi.org/10.1039/b816430b.

Punta, M., Coggill, P.C., Eberhardt, R.Y., Mistry, J., Tate, J., Boursnell, C., et al., 2012. The Pfam protein families database. Nucleic Acids Res. 40, 290–301. https://doi.org/10.1093/nar/gkr1065.

Qin, J., Hu, Z., Zhang, Q., Xu, N., Yang, Y., 2020. Toxic effects and mechanisms of *Prymnesium parvum* (Haptophyta) isolated from the Pearl River Estuary, China. Harmful Algae 96, 101844. https://doi.org/10.1016/j.hal.2020.101844.

Rasmussen, S.A., Meier, S., Andersen, N.G., Blossom, H.E., Duus, J.Ø., Nielsen, K.F., et al., 2016. Chemodiversity of ladder-frame prymnesin polyethers in *Prymnesium parvum*. J. Nat. Prod. 79, 2250–2256. https://doi.org/10.1021/acs.jnatprod.6b00345.

Rein, K.S., Borrone, J., 1999. Polyketides from dinoflagellates: origins, pharmacology and biosynthesis. Comp. Biochem. Physiol. 124, 117–131. https://doi.org/10.1016/s0305-0491(99)00107-8.

Roelke, D.L., Grover, J.P., Brooks, B.W., Joanglass, Davidbuzan, Southard, G.M., et al., 2011. A decade of fish-killing *Prymnesium parvum* blooms in Texas: roles of in flow and salinity. J. Plankton Res. 33, 243–253. https://doi.org/10.1093/plankt/fbq079.

Roelke, D.L., Barkoh, A., Brooks, B.W., Grover, J.P., Hambright, K.D., Laclaire, J.W., et al., 2016. A chronicle of a killer alga in the west: ecology, assessment, and management of *Prymnesium parvum* blooms. Hydrobiologia 764, 29–50. https://doi.org/10.1007/s10750-015-2273-6.

Sasso, S., Pohnert, G., Lohr, M., Mittag, M., Hertweck, C., 2012. Microalgae in the postgenomic era: a blooming reservoir for new natural products. FEMS Microbiol. 36, 761–785. https://doi.org/10.1111/j.1574-6976.2011.00304.x.

Selander, E., Thor, P., Toth, G., Pavia, H., Ety, S., 2006. Copepods induce paralytic shellfish toxin production in marine dinoflagellates. Proc. R. Soc. B Biol. Sci. 273, 1673–1680. https://doi.org/10.1098/rspb.2006.3502.

Skovgaard, A., Hansen, P.J., 2003. Food uptake in the harmful alga *Prymnesium parvum* mediated by excreted toxins. Limnol. Oceanogr. 48, 1161–1166. https://doi.org/10.4319/lo.2003.48.3.1161.

Skovgaard, A., Legrand, C., Hansen, P., Granéli, E., 2003. Effects of nutrient limitation on food uptake in the toxic haptophyte *Prymnesium parvum*. Aquat. Microb. Ecol. 31, 259–265. https://doi.org/10.3354/ame031259.

Stamatakis, A., 2006. RAxML-VI-HPC: maximum likelihood-based phylogenetic analyses with thousands of taxa and mixed models. Bioinformatics 22, 2688–2690. https://doi.org/10.1093/bioinformatics/btl446.

Staunton, J., Weissman, K.J., 2001. Polyketide biosynthesis: a millennium review. Nat. Prod. Rep. 18, 380–416. https://doi.org/10.1039/a909079g.

Svenssen, D.K., Binzer, S.B., Medić, N., Hansen, P.J., Larsen, T.O., Varga, E., 2019. Development of an indirect quantitation method to assess ichthyotoxic b-type prymnesins from *Prymnesium parvum*. Toxins 11, 1–15. https://doi.org/10.3390/toxins11050251.

Taylor, R.B., Hill, B.N., Langan, L.M., Chambliss, C.K., Brooks, B.W., 2021. Sunlight concurrently reduces *Prymnesium parvum* elicited acute toxicity to fish and prymnesins. Chemosphere 263, 127927. https://doi.org/10.1016/j.chemosphere.2020.127927.

Tillmann, U., 2003. Kill and eat your predator: a winning strategy of the planktonic flagellate *Prymnesium parvum*. Aquat. Microb. Ecol. 32, 73–84. https://doi.org/10.3354/ame032073.

Tillmann, U., Hansen, P.J., 2009. Allelopathic effects of *Alexandrium tamarense* on other algae: evidence from mixed growth experiments. Aquat. Microb. Ecol. 57, 101–112. https://doi.org/10.3354/ame01329.

Tillmann, U., John, U., Cembella, A., 2007. On the allelochemical potency of the marine dinoflagellate *Alexandrium ostenfeldii* against heterotrophic and autotrophic protists. J. Plankton Res. 29, 527–543. https://doi.org/10.1093/plankt/fbm034.

Van Dolah, F.M., Kohli, G.S., Morey, J.S., Murray, S.A., 2017. Both modular and single-domain Type I polyketide synthases are expressed in the brevetoxin-producing dinoflagellate, *Karenia brevis* (Dinophyceae). J. Phycol. 53, 1325–1339. https://doi.org/10.1111/jpy.12586.

van Dolah, F.M., Morey, J.S., Milne, S., Ung, A., Anderson, P.E., Chinain, M., 2020. Transcriptomic analysis of polyketide synthases in a highly ciguatoxic dinoflagellate, *Gambierdiscus polynesiensis* and low toxicity *Gambierdiscus pacificus*, from French Polynesia. PLoS One 15, 1–21. https://doi.org/10.1371/journal.pone.0231400.

Verma, A., Kohli, G.S., Harwood, D.T., Ralph, P.J., Murray, S.A., 2019. Transcriptomic investigation into polyketide toxin synthesis in Ostreopsis (Dinophyceae) species. Environ. Microbiol. 21, 4196–4211. https://doi.org/10.1111/1462-2920.14780.

Vingiani, G.M., Stalberga, D., De Luca, P., Ianora, A., De Luca, D., Lauritano, C., 2020. De novo transcriptome of the non-saxitoxin producing Alexandrium tamutum reveals new insights on harmful dinoflagellates. Mar. Drugs 18, 386. https://doi.org/10.3390/MD18080386.

Waterhouse, R.M., Seppey, M., Sim, F.A., Ioannidis, P., 2017. BUSCO applications from quality assessments to gene prediction and phylogenomics. Mol. Biol. Evol. 35, 543–548. https://doi.org/10.1093/molbev/msx319.

Weissman, K.J., 2015. Uncovering the structures of modular polyketide synthases. Nat. Prod. Rep. 32, 436–453. https://doi.org/10.1039/c4np00098f.

Wohlrab, S., Selander, E., John, U., 2017. Predator cues reduce intraspecific trait variability in a marine dinoflagellate. BMC Ecol. 17, 1–9. https://doi.org/10.1186/s12898-017-0119-y.

Wright, J.L.C., Cembella, A., 1998. Ecophysiology and biosynthesis of polyether marine biotoxins. In: G. Anderson, D.M., Cembella, A.D. (Eds.), Physiological Ecology of Harmful Algal Blooms. Hallegraef (Springer-Verlag), pp. 427–451.

Wu, Z., Luo, H., Yu, L., Lee, W.H., Li, L., Mak, Y.L., et al., 2020. Characterizing ciguatoxin (CTX)- and non-CTX-producing strains of *Gambierdiscus balechii* using comparative transcriptomics. Sci. Total Environ. 717, 137184. https://doi.org/10.1016/j.scitotenv.2020.137184.

Supplementary information

Table S1: Information on the *Prymnesium parvum* strains including the site and year of isolation.

Strain	Isolation site	Year of isolation
NIES-1812	Yufu island, Okinawa, Japan	2004
PPDW02	on-shore aquaculture, Northern Territory, Australia	2009
UTEX-2797	Texas Colorado River, Texas, USA	2002
K-0081	Flade So, Thy, Denmark	1985
UIO-223	Bjerknes, Norway	2008
K-0374	Norway	1989
K-0252	Norman Bay, Victoria, Australia	2000
NIES-1017	Jogashima Miura, Misaki Kanagawa, Japan	1997
RCC-1436	France, Atlantic Ocean	1977

Figure S1: Contribution of retrieved per strain ketosynthase domains based on their presence on modular contigs and completeness.

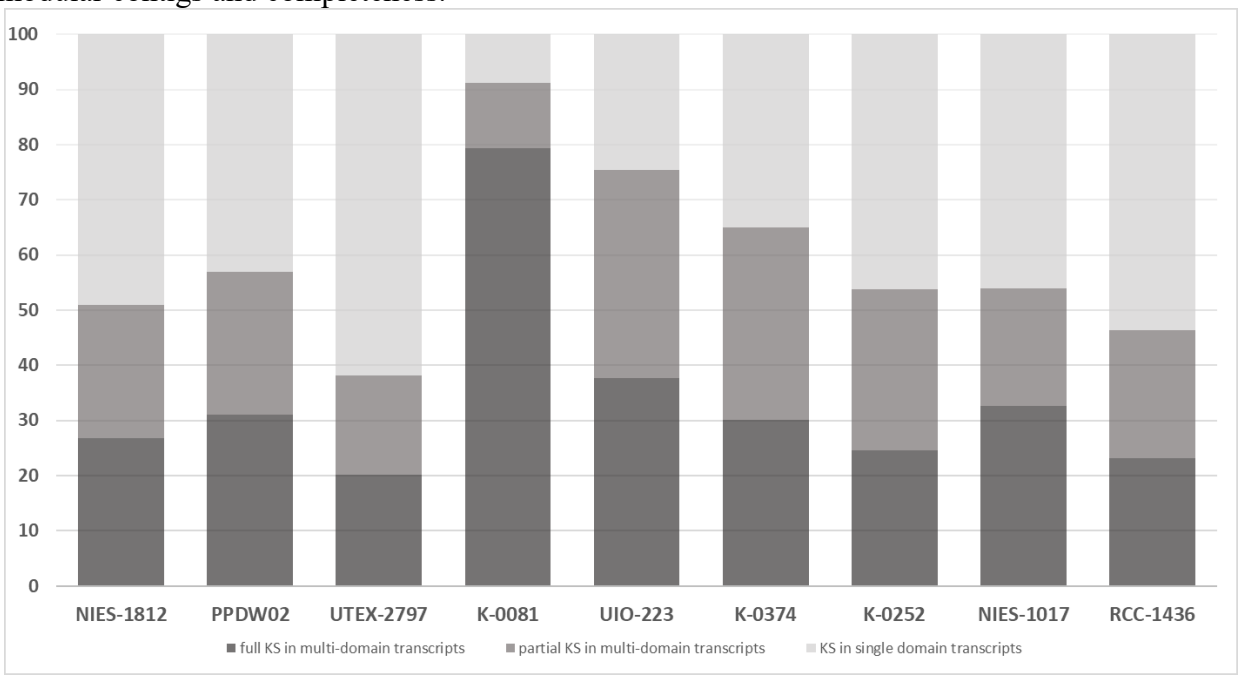

Table S2: Contigs encoding for polyketide synthases retrieved from *Prymnesium parvum* strain K-0081, the corresponding domain order and contig length in amino acids.

Contig	Domain order	Length (aa)
K0081_104_c0_g1_i14_frame2	PP-PP-KS-DH-KR-ER-KR-PP-KS-DH-KR-PP-KS-KR-ST-TE(p)	17296
K0081_11312_c0_g2_i2_frame1	HMG_CoA-PP-PP-KS-PP-PP	11190
K0081_11768_c0_g1_i2_frame1r	NRPS-PP-KS-KR(p)	4134
K0081_13506_c0_g1_i1_frame2	KS(p)	310
K0081_16604_c0_g1_i2_frame3r	KS(p)-DH(p)	1224
K0081_1838_c0_g1_i1_frame1	KR(p)-PP-PP-KS	2621
K0081_21_c0_g1_i4_frame1	DH-KR(p)-PP(p)-KS	3740
K0081_21_c0_g1_i7_frame3	KS-DH-KR(p)-ER-MT-KR(p)-PP- KS-DH-KR-PP-KS-DH-KR-PP-KS-ER-KR-PP-KS-DH(p)-PP-KS-DH-CRO-HMG_CoA-PP-KS-PP-KS-KR-PP-KS-DH-ER-KR-PP(p)-KS-DH-ER-KR	41957
K0081_21_c0_g3_i1_frame1r	ER-KR-PP(p)-KS-KR-PP-ST-TE(p)-AAT	8520
K0081_2779_c0_g1_i2_frame1r	KS(p)	1009
K0081_3627_c0_g2_i1_frame2	PP-KS(p)	827
K0081_36368_c0_g1_i1_frame1	KS	1870
K0081_37739_c0_g1_i1_frame3	KS(p)	889
K0081_39373_c0_g1_i1_frame2	KS	1975
K0081_402_c0_g1_i3_frame1	DH(p)-KR-PP-KS-KR-PP-PP-KS-DH-ER-KR-PP-KS-DH-KR-PP-KS-DH-KR(p)-MT-KR(p)-PP(p)-PP	21185
K0081_411_c0_g2_i1_frame3	KS(p)	730
K0081_4346_c0_g2_i4_frame3	AT(p)-KS-DH-KR-PP-KS-DH-MT-KR-PP-KS-PP-KS-CRO-HMG_CoA-PP(p)	18635
K0081_465_c0_g1_i1_frame2	PP-KS-KR-PP-PP-KS-DH-ER-KR-PP-KS-KR-PP-DH-KR(p)-PP-PP-PP(p)-KS-DH(p)	18395
K0081_465_c0_g2_i1_frame1	KS(p)-DH-PP-KS-DH-KR(p)-ER(p)-KR(p)-PP-KS-KR-PP	9757
K0081_465_c0_g3_i1_frame3	PP(p)-KS-ER-KR(p)-PP-KS-DH-KR-PP-KS-KR(p)-PP-PP-KS	13471
K0081_46630_c0_g1_i1_frame2	KR(p)-PP-KS	2401
K0081_5344_c0_g1_i2_frame2	NRPS-PP-KS-DH-KR-PP-KS-DH-ER-KR	11321
K0081_54169_c0_g1_i1_frame1	PP-KS(p)	719
K0081_5452_c1_g2_i1_frame3r	KS	1326
K0081_5527_c0_g1_i1_frame3	KR-PP-KS(p)	2063
K0081_5709_c0_g2_i1_frame1	PP-PP-KS-DH-PP-KS	4126
K0081_5709_c0_g2_i2_frame3	KS(p)	483
K0081_677_c0_g3_i2_frame1	KS-AT-KR(p)-DH-KS-KS(p)	9123
K0081_70253_c0_g1_i1_frame1	KS(p)	1462
K0081_873_c0_g1_i2_frame1	KS(p)-KR-PP-KS-KR(p)	6045
K0081_873_c0_g1_i4_frame1	DH-KR-PP-KS-KR-PP-PP-KS-DH-KR-PP(p)	10746
K0081_873_c0_g1_i5_frame1	KS(p)-DH-KR(p)-PP-KS-KR-PP-KS-DH-KR(p)-PP-KS-KR-PP-PP-KS-DH-KR-PP(p)	21474
K0081_9468_c0_g4_i1_frame2r	KS(p)	858

Table S3: Contigs encoding for polyketide synthases retrieved from *Prymnesium parvum* strain K-0374, the corresponding domain order and contig length in amino acids.

Contig	Domain order	Length (aa)
K0374_10018_c0_g1_i1_frame2	KS(p)-PP(p)	927
K0374_10580_c0_g1_i1_frame2	KS(p)	438
K0374_11288_c0_g1_i1_frame3	DH-PP-KS(p)	1935
K0374_12648_c0_g1_i1_frame2	KS(p)	848
K0374_1267_c0_g1_i1_frame2	DH-KR-PP-KS(p)	3349
K0374_14041_c0_g1_i1_frame2r	KS(p)	791
K0374_14231_c0_g1_i1_frame2	PP(p)-KS(p)	521
K0374_15064_c0_g1_i1_frame1	KS(p)	329
K0374_17592_c0_g1_i1_frame2	KS(p)-DH(p)	1091
K0374_20917_c0_g1_i1_frame3	KS(p)	458
K0374_21_c0_g1_i1_frame2	KS(p)	1014
K0374_21067_c0_g1_i2_frame1	KS(p)	654
K0374_21725_c0_g1_i1_frame3	PP-PP-PP-KS(p)	1895
K0374_23244_c0_g1_i1_frame1	PP-KS-KR	3253
K0374_23894_c0_g1_i1_frame3	KS(p)	360
K0374_23929_c0_g1_i1_frame3r	KS(p)	1123
K0374_24050_c0_g1_i1_frame2	PP(p)-KS(p)	788
K0374_24394_c0_g1_i2_frame3	KS(p)-DH(p)	1031
K0374_27367_c0_g1_i1_frame1	KS(p)	978
K0374_29580_c0_g1_i1_frame1	KS(p)-DH-PP-KS(p)	2148
K0374_31469_c0_g1_i1_frame3	KS(p)-PP-KS(p)	1677
K0374_31469_c0_g1_i3_frame3	KS(p)-DH(p)	857
K0374_31787_c0_g1_i5_frame3	NRPS-KS-KR-DH-ER-PP-TE	11832
K0374_32154_c1_g1_i1_frame1	PP-KS-CRO	4160
K0374_323_c0_g1_i1_frame1	KS(p)-AT(p)	2150
K0374_32395_c0_g3_i4_frame1r	KR(p)-PP(p)-KS-KR-PP-ST-TE(p)-AAT	7737
K0374_32710_c1_g6_i4_frame1	KS-AT-KR-DH-KS-KS(p)	11310
K0374_32914_c4_g4_i1_frame1r	PP(p)-KS-DH-KR-PP-KS-KR(p)-PP-PP-KS	9741
K0374_33161_c0_g2_i3_frame3	PP(p)-KS-PP-KS-CRO-HMG_CoA-PP(p)	9170
K0374_33373_c0_g2_i1_frame3	ER(p)-KR(p)-PP-KS-DH-KR-PP-KS(p)	5898
K0374_33373_c0_g2_i4_frame1	KS(p)	457
K0374_33373_c1_g1_i1_frame3	KS(p)-PP-KS-DH	3253
K0374_33402_c3_g1_i1_frame1r	KS(p)	811
K0374_33574_c0_g8_i1_frame3	KS(p)-DH-KR-MT-KR-PP-PP-KS-ER-KR-PP-KS-DH-KR-PP-KS-KR-PP-PP-KS	19603
K0374_33574_c0_g9_i1_frame2	KR(p)-PP-KS	3366
K0374_33636_c4_g1_i1_frame1	ER-KR(p)-PP-KS-DH-KR-PP-KS	7674
K0374_33655_c1_g1_i1_frame1	KS(p)	365
K0374_33655_c3_g2_i1_frame1r	KR(p)-PP-KS-DH-KR-PP-KS-KR-PP-ST-TE(p)	9723
K0374_33655_c3_g2_i3_frame1r	KR(p)-PP-KS(p)	9542
K0374_33996_c1_g1_i1_frame2	KR-PP-KS-DH	4039

K0374_34010_c0_g1_i1_frame3	KS(p)-DH-ER-KR-PP-KS-KR-PP-DH-KR-PP-PP-PP-KS-DH(p)	13712
K0374_34702_c0_g1_i1_frame2	PP(p)-KS(p)	962
K0374_35005_c0_g1_i1_frame1	DH-PP-KS(p)	1933
K0374_38623_c0_g1_i1_frame1	KS(p)	820
K0374_39233_c0_g1_i1_frame1	KR(p)-PP-KS(p)	1123
K0374_41283_c0_g1_i1_frame1r	KS(p)	388
K0374_45106_c0_g1_i1_frame3r	KS(p)	1193
K0374_45248_c0_g1_i1_frame3	KS(p)-DH(p)	1071
K0374_46389_c0_g1_i1_frame3	KS(p)	540
K0374_47195_c0_g1_i1_frame3r	PP(p)-KS(p)	558
K0374_47242_c0_g1_i1_frame2r	KS(p)	488
K0374_52468_c0_g1_i1_frame1	KS(p)	2383
K0374_54355_c0_g1_i1_frame1	KS(p)	640
K0374_5633_c0_g1_i1_frame3	KS(p)	437
K0374_58448_c0_g1_i1_frame3	KS(p)	1303
K0374_59658_c0_g1_i1_frame2	PP(p)-KS(p)	583
K0374_6082_c0_g1_i1_frame1	KS(p)	456
K0374_60836_c0_g1_i1_frame1	KS(p)	450
K0374_61192_c0_g1_i1_frame1	KS(p)	351
K0374_61673_c0_g1_i1_frame1	KS(p)	343
K0374_6218_c0_g1_i1_frame3	KS(p)	555
K0374_65325_c0_g1_i1_frame2	PP(p)-KS(p)	529
K0374_65990_c0_g1_i1_frame2	KS(p)	728
K0374_66168_c0_g1_i1_frame3r	KR-PP-KS(p)	1785
K0374_67800_c0_g1_i1_frame3	KS(p)	382
K0374_7074_c0_g1_i1_frame2	PP(p)-KS(p)	658

Table S4: Contigs encoding for polyketide synthases retrieved from *Prymnesium parvum* strain UIO-223, the corresponding domain order and contig length in amino acids.

Contig	Domain order	Length (aa)
UIO223_11298_c0_g1_i1_frame1	KS(p)	495
UIO223_11845_c0_g1_i1_frame1	KS(p)-DH(p)	908
UIO223_1217_c0_g1_i1_frame2	PP-PP-PP(p)-KS-DH(p)	4000
UIO223_1217_c0_g2_i1_frame1	KR(p)-PP-PP-KS	2507
UIO223_1302_c0_g1_i1_frame1	KS(p)-DH-PP-KS-DH(p)	3292
UIO223_1302_c0_g2_i3_frame1	KS(p)-DH-PP-KS-CRO-HMG_CoA-PP(p)-KS-PP-KS-DH-ER-KR-PP(p)-KS-DH-ER-KR-PP(p)-KS-DH	21989
UIO223_13276_c0_g1_i2_frame1	KS(p)	422
UIO223_15553_c0_g1_i1_frame2	KR(p)-PP(p)-KS(p)	1554
UIO223_16640_c0_g1_i1_frame2	KS(p)	671
UIO223_18442_c0_g1_i1_frame3r	KR-PP-KS(p)	1859
UIO223_19416_c0_g1_i1_frame2	KS(p)-CRO	2514
UIO223_19416_c1_g1_i1_frame1	KS(p)-PP(p)-KS(p)	3290
UIO223_22483_c0_g1_i1_frame3	PP-KS(p)	1111
UIO223_2283_c0_g1_i6_frame2	KS-DH-ER-KR-PP(p)-KS-KR-PP-DH-KR	10046
UIO223_23238_c0_g1_i1_frame2	KS(p)-AT(p)	1493
UIO223_24235_c0_g1_i1_frame1	KS(p)	463
UIO223_24962_c0_g2_i1_frame2	KS(p)	646
UIO223_2759_c0_g1_i1_frame3	PP(p)-KS(p)	645
UIO223_2939_c0_g1_i3_frame1	KS(p)	1579
UIO223_29821_c0_g1_i1_frame2	KS-X	1648
UIO223_309_c0_g1_i1_frame3	PP-PP-KS-DH(p)	4449
UIO223_32374_c0_g1_i1_frame1r	KS(p)	493
UIO223_32476_c0_g1_i1_frame3	KS(p)-ER(p)	1937
UIO223_34765_c0_g1_i1_frame3	KS	1506
UIO223_3652_c0_g1_i1_frame1	KS(p)	3093
UIO223_40_c0_g1_i4_frame1	DH-KR-ER-KR(p)-PP-KS-DH-KR-PP-KS-KR-PP-ST-TE(p)	13489
UIO223_40_c0_g1_i5_frame1	DH-KR-PP-KS-DH(p)	4162
UIO223_40806_c0_g1_i1_frame3	KS(p)	1305
UIO223_409_c0_g1_i1_frame1	KS-AT-KR(p)-DH-KS-KS(p)	9124
UIO223_41442_c0_g1_i1_frame3	KS(p)	599
UIO223_415_c0_g1_i1_frame3	PP(p)-KS(p)	843
UIO223_415_c0_g2_i2_frame2	DH-KR-PP-KS-DH(p)	4219
UIO223_415_c0_g3_i4_frame1	KS(p)-DH-ER-KR(p)-PP-KS-DH-KR-PP-KS-DH-KR(p)-MT-KR-PP-PP-PP-KS-ER-KR-PP-KS-DH-KR-PP-KS-KR(p)-PP-PP-KS	28687
UIO223_4182_c0_g1_i1_frame1	KS(p)-KR-PP-PP-PP	2896
UIO223_4384_c0_g1_i1_frame1	KS(p)-PP-KS-DH(p)	1329
UIO223_4384_c0_g1_i3_frame1	KS(p)-DH	1603
UIO223_45007_c0_g1_i1_frame3	KS(p)-DH	1418
UIO223_49931_c0_g1_i1_frame3	KS(p)-DH-KR(p)	804
UIO223_505_c0_g1_i2_frame3	KS(p)-KR(p)	1608

UIO223_505_c0_g1_i3_frame3	KS(p)	1581
UIO223_50564_c0_g1_i1_frame1	PP(p)-KS(p)	595
UIO223_5485_c0_g2_i1_frame2	DH(p)-ER-KR(p)-PP-KS(p)	3725
UIO223_55217_c0_g1_i1_frame3	KS(p)-KS(p)	392
UIO223_58977_c0_g1_i1_frame2	KS-DH(p)	2443
UIO223_59378_c0_g1_i1_frame2	KS(p)	724
UIO223_61022_c0_g1_i1_frame3	PP(p)-KS(p)	558
UIO223_62343_c0_g1_i1_frame1	KS(p)	752
UIO223_6306_c0_g1_i2_frame3	KS(p)-KR(p)	3031
UIO223_67493_c0_g1_i1_frame3	PP-KS-DH(p)	1885
UIO223_6751_c0_g1_i2_frame2	KS(p)-DH	1605
UIO223_68334_c0_g1_i1_frame3	KS(p)-DH	1629
UIO223_71188_c0_g1_i1_frame2	KS(p)	400
UIO223_7525_c0_g1_i2_frame2r	PP(p)-KS-KR-PP-ST-TE(p)-AAT	7171
UIO223_7834_c0_g1_i2_frame2	PP-PP-KS(p)	1456
UIO223_8454_c0_g1_i1_frame3	PP-KS	1371
UIO223_93_c0_g3_i2_frame3	PP-KS-CRO	4220
UIO223_9611_c0_g1_i1_frame2	KS(p)	803
UIO223_9685_c0_g1_i1_frame2	KR-PP-PP-KS(p)	1833

Table S5: Contigs encoding for polyketide synthases retrieved from *Prymnesium parvum* strain K-0252, the corresponding domain order and contig length in amino acids.

Contig	Domain order	Length (aa)
K0252_10190_c0_g1_i2_frame2	KS	1278
K0252_11160_c0_g1_i1_frame2r	KS(p)	494
K0252_11315_c0_g1_i1_frame2	KS(p)	462
K0252_142_c0_g2_i1_frame1	KR-PP-KS-CRO-HMG_CoA-PP-PP-KS-PP-PP	15092
K0252_14305_c0_g2_i1_frame1	KS(p)	411
K0252_14959_c0_g1_i1_frame1	KS(p)	405
K0252_18194_c0_g1_i1_frame2	KS(p)	959
K0252_18924_c0_g1_i1_frame1	KS(p)-DH(p)	1398
K0252_23998_c0_g1_i1_frame1	KR(p)-PP-KS(p)	1771
K0252_24100_c0_g1_i1_frame2	KS	1500
K0252_2451_c0_g2_i1_frame1r	DH-KR-PP-KS-KR-KS-ST-TE(p)	7598
K0252_25518_c0_g1_i1_frame2	KS(p)	467
K0252_26118_c0_g1_i1_frame2	KS(p)	1448
K0252_26118_c1_g1_i1_frame3	PP-KS(p)	1296
K0252_29984_c0_g1_i1_frame3	AT(p)-KS(p)	2186
K0252_31125_c0_g1_i1_frame2	KS(p)	524
K0252_33075_c0_g1_i1_frame2r	KS(p)	345
K0252_3361_c0_g1_i1_frame3	PP-DH-ER-KR(p)	3579
K0252_3383_c0_g1_i1_frame1r	KS(p)	889
K0252_3383_c0_g2_i6_frame1	CRO-HMG_CoA-PP(p)-KS-PP-KS-DH-KR(p)-ER-KR-PP(p)-KS-KR-PP-ST-TE(p)-AAT	15838
K0252_34898_c0_g1_i1_frame3	KS(p)	868
K0252_36792_c0_g1_i1_frame2	KS(p)-DH-PP(p)	1777
K0252_38493_c0_g1_i1_frame2	KS	1169
K0252_38798_c0_g1_i1_frame3	KS(p)-DH	1416
K0252_41551_c0_g1_i1_frame1	KS(p)	613
K0252_41822_c0_g1_i1_frame1r	KS(p)	674
K0252_45368_c0_g1_i1_frame1	KS(p)-DH-KR-MT	3034
K0252_4558_c0_g1_i8_frame3r	NRPS-KS-KR-DH-ER-PP-TE	12143
K0252_45653_c0_g1_i1_frame2	KS(p)	693
K0252_46803_c0_g1_i1_frame2	KS(p)	514
K0252_47229_c0_g1_i1_frame2	KS(p)	1465
K0252_48192_c0_g1_i1_frame3	KS(p)	803
K0252_48910_c0_g1_i1_frame3	KS(p)	620

K0252_53560_c0_g1_i1_frame1	KS(p)-DH(p)	531
K0252_55690_c0_g1_i1_frame3	KS(p)-PP(p)	680
K0252_55762_c0_g1_i1_frame1	PP-KS(p)	700
K0252_58016_c0_g1_i1_frame3	KS(p)	331
K0252_5952_c0_g1_i1_frame2	KR(p)-PP-KS-PP-KS-CRO-HMG_CoA	9846
K0252_5965_c0_g1_i1_frame2r	KS(p)	679
K0252_5965_c0_g1_i2_frame2r	KS(p)-PP	2668
K0252_5991_c0_g1_i1_frame1	KS(p)-DH-PP	2888
K0252_5991_c0_g1_i2_frame1	KS(p)-DH(p)	1102
K0252_5991_c0_g1_i3_frame1	KS(p)-DH-PP	1953
K0252_60954_c0_g1_i1_frame1	PP-KS(p)	584
K0252_61268_c0_g1_i1_frame2	KS(p)	330
K0252_61329_c0_g1_i1_frame2	PP(p)-KS(p)	1084
K0252_61517_c0_g1_i1_frame3r	KS(p)	307
K0252_61779_c0_g1_i1_frame1	KS(p)-ER(p)	1736
K0252_61942_c0_g1_i1_frame2	KS(p)	890
K0252_63472_c0_g1_i1_frame3	KS(p)	338
K0252_66159_c0_g1_i1_frame2	KS(p)-DH(p)	1440
K0252_66309_c0_g1_i1_frame1	KS(p)	466
K0252_66353_c0_g1_i1_frame1r	PP(p)-KS	1756
K0252_67093_c0_g1_i1_frame2	PP-KS-DH-KR(p)	3483
K0252_68131_c0_g1_i1_frame3	KS(p)	1339
K0252_68558_c0_g1_i1_frame2	KS(p)	473
K0252_7516_c0_g1_i2_frame3	AAT-PP-PP-KS	3703
K0252_8506_c0_g1_i1_frame1r	NRPS-PP-KS-DH	5306
K0252_965_c0_g4_i1_frame1	KS-AT-KR(p)-DH-KS-KS(p)	9131

Table S6: Contigs encoding for polyketide synthases retrieved from *Prymnesium parvum* strain UTEX-2797, the corresponding domain order and contig length in amino acids.

Contig	Domain order	Length (aa)
UTEX2797_1015_c0_g1_i1_frame1	NRPS-PP-KS-KR-DH-ER-PP-TE	11904
UTEX2797_10910_c0_g1_i1_frame3	KS(p)	393
UTEX2797_10910_c0_g2_i1_frame3	KS(p)	935
UTEX2797_12242_c0_g2_i1_frame2	PP-KS(p)	725
UTEX2797_13164_c0_g1_i1_frame1	HMG_CoA-DH-ER	2207
UTEX2797_1326_c0_g1_i3_frame3	KR(p)-PP-KS-DH-KR-ER-KR-PP-KS-DH-KR-PP-KS-KR-PP-ST	15758
UTEX2797_13491_c0_g1_i1_frame3	KR-PP-PP-KS(p)	1856
UTEX2797_13601_c0_g1_i1_frame2	KS(p)	596
UTEX2797_13606_c0_g1_i1_frame1	KS(p)	1141
UTEX2797_13606_c0_g1_i2_frame2	KS(p)	1451
UTEX2797_14040_c2_g1_i1_frame1	KS(p)	589
UTEX2797_14621_c0_g1_i1_frame3	KS(p)	574
UTEX2797_14685_c0_g1_i1_frame1	KS(p)	1079
UTEX2797_16856_c0_g1_i1_frame1	PP-PP-KS-ER-KR-PP-KS-DH-KR-PP-KS-KR-PP-PP-KS	14009
UTEX2797_16856_c0_g3_i1_frame2	KR-PP-PP-KS(p)	2009
UTEX2797_177_c0_g1_i6_frame2	KR-PP-KS-CRO-HMG_CoA-PP-PP-KS-PP-PP	15210
UTEX2797_17992_c0_g1_i1_frame2	KR(p)-PP-KS	2607
UTEX2797_1818_c0_g1_i11_frame1	PP-KS-AT-PP	4085
UTEX2797_18632_c0_g1_i1_frame2	PP-KS-DH	2383
UTEX2797_1874_c0_g1_i1_frame2r	KS(p)	433
UTEX2797_19224_c0_g1_i2_frame1	KS(p)-DH(p)	889
UTEX2797_19640_c0_g1_i1_frame2	KS(p)	358
UTEX2797_20116_c0_g1_i1_frame1	KS(p)	735
UTEX2797_21763_c0_g1_i1_frame3	KS(p)	679
UTEX2797_23311_c0_g1_i1_frame2	PP(p)-KS-CRO	4661
UTEX2797_23409_c0_g1_i1_frame3	KS(p)	349
UTEX2797_23479_c0_g1_i1_frame2	KS(p)	1034
UTEX2797_23479_c0_g1_i3_frame2	KS(p)-DH	1604
UTEX2797_25871_c0_g1_i1_frame2	KS(p)	721
UTEX2797_26889_c0_g2_i1_frame1	KS(p)	704
UTEX2797_29229_c0_g1_i1_frame1	KS(p)	576
UTEX2797_30818_c0_g1_i1_frame1	KS(p)	342
UTEX2797_38270_c0_g2_i1_frame1	KR(p)-PP-KS(p)	1677
UTEX2797_39176_c0_g1_i1_frame1	KS-PP-PP	4219
UTEX2797_40649_c0_g1_i1_frame3	KS(p)	373
UTEX2797_42029_c0_g1_i1_frame2	KS(p)	1321
UTEX2797_42934_c0_g2_i1_frame2	KS(p)	367
UTEX2797_44726_c0_g1_i1_frame3	KS(p)	439
UTEX2797_44925_c0_g1_i1_frame3	KS(p)	309
UTEX2797_45314_c0_g1_i1_frame3	KS(p)	452

UTEX2797_45358_c0_g1_i1_frame2	KS(p)	911
UTEX2797_45930_c0_g1_i1_frame1	KS(p)	908
UTEX2797_46565_c0_g1_i1_frame1	KS(p)	340
UTEX2797_48349_c0_g1_i1_frame1	ER(p)-KR-PP-KS(p)	1728
UTEX2797_48651_c0_g1_i1_frame1	KS(p)	500
UTEX2797_49168_c0_g1_i1_frame3	KS(p)	380
UTEX2797_49323_c0_g1_i1_frame3	KS(p)	777
UTEX2797_50359_c0_g1_i1_frame3	KS(p)	528
UTEX2797_51645_c0_g1_i1_frame3	KS(p)	576
UTEX2797_54129_c0_g1_i1_frame1	KS(p)	570
UTEX2797_54196_c0_g1_i1_frame2	KS-PP-KS(p)	2605
UTEX2797_54231_c0_g1_i1_frame2	KS(p)-DH(p)	911
UTEX2797_54882_c0_g1_i1_frame1	KR(p)-PP-KS(p)	1287
UTEX2797_55335_c0_g1_i1_frame3	KS(p)	313
UTEX2797_55581_c0_g1_i1_frame2	KS(p)	503
UTEX2797_57808_c0_g1_i1_frame3r	KS(p)	421
UTEX2797_61700_c0_g1_i1_frame3	PP(p)-KS(p)	538
UTEX2797_62392_c0_g1_i1_frame3	KS(p)	728
UTEX2797_62661_c0_g1_i1_frame2	KS(p)	508
UTEX2797_6330_c0_g1_i6_frame2r	KS(p)-PP-PP	5409
UTEX2797_67653_c0_g1_i1_frame1	KS(p)	542
UTEX2797_68157_c0_g1_i1_frame3	KS(p)	307
UTEX2797_6903_c0_g1_i2_frame2	KS-DH-ER	3664
UTEX2797_6903_c0_g1_i6_frame2	KS-DH	3233
UTEX2797_70035_c0_g1_i1_frame2	KS(p)	331
UTEX2797_71716_c0_g1_i1_frame1	PP-KS(p)	826
UTEX2797_71836_c0_g1_i1_frame3	KS(p)	1169
UTEX2797_71944_c0_g1_i1_frame2	PP(p)-KS(p)	818
UTEX2797_72356_c0_g1_i1_frame3	KR(p)-PP-KS(p)	1336
UTEX2797_72555_c0_g1_i1_frame1	KS(p)	462
UTEX2797_72616_c0_g1_i1_frame1	KS(p)-X	1128
UTEX2797_73668_c0_g1_i1_frame1	KS(p)	311
UTEX2797_74933_c0_g1_i1_frame2	KS(p)	369
UTEX2797_75328_c0_g1_i1_frame3	KS(p)	302
UTEX2797_75742_c0_g1_i1_frame2	KS(p)	544
UTEX2797_8036_c0_g1_i1_frame3	PP-KS-KR-PP-KS(p)	4207
UTEX2797_8036_c0_g2_i1_frame1	KR(p)-PP-KS(p)	1402

Table S7: Contigs encoding for polyketide synthases retrieved from *Prymnesium parvum* strain NIES-1812, the corresponding domain order and contig length in amino acids.

Contig	Domain order	Length (aa)
NIES1812_10430_c0_g1_i1_frame2	KS(p)	636
NIES1812_1117_c0_g2_i1_frame3	PP-KS	2037
NIES1812_11318_c0_g2_i2_frame2r	KR(p)-PP-KS	2083
NIES1812_11659_c0_g3_i1_frame2	KS(p)	1274
NIES1812_12388_c0_g1_i1_frame2	PP(p)-KS(p)	514
NIES1812_12393_c0_g1_i1_frame3	KS(p)	343
NIES1812_12395_c0_g2_i1_frame3r	KS(p)	536
NIES1812_12681_c0_g1_i1_frame1r	KS-KR-PP-PP(p)	5086
NIES1812_1289_c0_g1_i2_frame2r	ER-KR-PP-KS-DH-KR-PP-KS-DH-KR	9832
NIES1812_1289_c0_g1_i3_frame2r	PP-KS-DH-KR	3805
NIES1812_13312_c0_g1_i2_frame2r	KS(p)	521
NIES1812_1473_c0_g1_i1_frame1r	KS-DH-ER(p)	3324
NIES1812_15465_c0_g1_i1_frame2r	KS(p)	561
NIES1812_15593_c0_g1_i1_frame3r	PP-KS(p)	486
NIES1812_16537_c0_g1_i1_frame3r	KS(p)-DH(p)	1063
NIES1812_17398_c0_g1_i1_frame1	KS(p)	1595
NIES1812_18228_c0_g1_i1_frame2	PP(p)-KS(p)	687
NIES1812_20152_c0_g1_i1_frame3r	PP-KS(p)	1205
NIES1812_2196_c0_g1_i4_frame2r	KR(p)-MT-KR-PP-PP-KS-ER-KR-PP-KS-DH-KR-PP-KS-KR-PP-PP	14713
NIES1812_2218_c0_g1_i1_frame1r	NRPS-KS-KR-DH-ER-PP-TE	11584
NIES1812_24566_c0_g1_i1_frame3r	KS-DH-KR-PP-KS(p)	3847
NIES1812_26741_c0_g1_i1_frame2	KS(p)	412
NIES1812_27_c0_g1_i4_frame1	PP-PP-KS-ER-KR-PP-KS-DH-KR-PP-KS-KR-PP-PP-KS	13959
NIES1812_29158_c0_g1_i1_frame3	KS(p)	383
NIES1812_3015_c0_g1_i2_frame2r	KS(p)	1294
NIES1812_3015_c0_g2_i1_frame1r	KS-DH	1519
NIES1812_3175_c0_g1_i2_frame3	PP-PP-KS-DH(p)	2959
NIES1812_32494_c0_g1_i1_frame1	KS(p)	314
NIES1812_32880_c0_g1_i1_frame1	KS(p)	358
NIES1812_33798_c0_g1_i1_frame3	PP(p)-PP-KS	1914
NIES1812_35345_c0_g1_i1_frame3r	KS(p)	404
NIES1812_3536_c0_g3_i1_frame1r	KS-AT-KR-DH-KS-KS(p)	8937
NIES1812_35995_c0_g1_i1_frame1r	KS(p)	1354
NIES1812_36974_c0_g1_i1_frame1	KS-DH(p)	1864
NIES1812_37591_c0_g1_i1_frame2r	KS(p)	432
NIES1812_37907_c0_g1_i1_frame2	KS(p)	439
NIES1812_38629_c0_g1_i1_frame3	KS(p)	443
NIES1812_38719_c0_g1_i1_frame2	KS(p)	670
NIES1812_3933_c0_g2_i4_frame3	KS-PP-PP	8059
NIES1812_39597_c0_g1_i1_frame1r	KS(p)	1080

NIES1812_39863_c0_g1_i1_frame3	PP-KS(p)	1473
NIES1812_40311_c0_g1_i1_frame2r	KS(p)	654
NIES1812_40523_c0_g1_i1_frame2r	KS(p)	336
NIES1812_41044_c0_g1_i1_frame1r	KS(p)	431
NIES1812_42475_c0_g1_i1_frame3r	KS(p)	416
NIES1812_4289_c0_g2_i1_frame2	PP-KS-KR-PP-PP-PP	4200
NIES1812_43521_c0_g1_i1_frame1r	KS(p)	990
NIES1812_43640_c0_g1_i1_frame1r	KS(p)-DH	3624
NIES1812_43673_c0_g1_i1_frame3r	KS(p)	489
NIES1812_4382_c0_g2_i3_frame3r	PP-KS-CRO-HMG_CoA-PP-KS-PP-PP	13657
NIES1812_4384_c0_g1_i4_frame1	KS(p)	987
NIES1812_43873_c0_g1_i1_frame1r	PP-KS(p)	787
NIES1812_44759_c0_g1_i1_frame1r	KS(p)	391
NIES1812_45198_c0_g1_i1_frame1	KS(p)	488
NIES1812_4546_c0_g1_i1_frame1	KS(p)-DH(p)	933
NIES1812_45470_c0_g1_i1_frame1	KS(p)	396
NIES1812_45876_c0_g1_i1_frame3r	KS(p)	424
NIES1812_47381_c0_g1_i1_frame1	PP(p)-KS(p)	655
NIES1812_4837_c0_g1_i2_frame3	KS(p)-DH	1830
NIES1812_48728_c0_g1_i1_frame1r	KS(p)	516
NIES1812_5084_c0_g1_i3_frame3r	PP-KS-DH(p)	2575
NIES1812_5084_c0_g1_i4_frame3r	PP-KS-KR-PP-KS(p)	4277
NIES1812_5084_c0_g2_i2_frame1r	KR(p)-PP(p)-KS(p)	2160
NIES1812_50924_c0_g1_i1_frame3	KS(p)	672
NIES1812_51195_c0_g1_i1_frame2	PP(p)-KS(p)	1024
NIES1812_52533_c0_g1_i1_frame2	KS(p)	503
NIES1812_54593_c0_g1_i1_frame3r	KS(p)	641
NIES1812_55136_c0_g1_i1_frame1r	KS(p)-DH(p)	800
NIES1812_5529_c0_g1_i3_frame1	PP-PP-KS(p)	1227
NIES1812_5529_c0_g2_i4_frame2r	PP-PP-KS(p)	1094
NIES1812_55429_c0_g1_i1_frame2r	KS(p)	616
NIES1812_5555_c0_g1_i1_frame1r	KR(p)-PP-KS(p)	1712
NIES1812_5617_c0_g1_i6_frame1	KS(p)-DH-ER-KR-PP-KS(p)	4804
NIES1812_57022_c0_g1_i1_frame3r	KS(p)	533
NIES1812_58322_c0_g1_i1_frame1r	PP(p)-KS	1277
NIES1812_58475_c0_g1_i1_frame3	KS(p)	546
NIES1812_58567_c0_g1_i1_frame3r	PP-KS(p)	1100
NIES1812_58915_c0_g1_i1_frame3r	KS(p)	625
NIES1812_59312_c0_g1_i1_frame2	KS(p)	937
NIES1812_6021_c0_g1_i1_frame2r	KS(p)-KR-PP-ST-TE	4682
NIES1812_61288_c0_g1_i1_frame2	KS(p)	432
NIES1812_61596_c0_g1_i1_frame1r	KS(p)	536
NIES1812_62339_c0_g1_i1_frame3r	KS(p)	629
NIES1812_6258_c0_g1_i1_frame1r	KR(p)-PP-KS(p)	1652

NIES1812_63181_c0_g1_i1_frame3r	KS(p)	309
NIES1812_6358_c0_g1_i1_frame1r	KS-PP	1703
NIES1812_64087_c0_g1_i1_frame2	KS(p)	469
NIES1812_66518_c0_g1_i1_frame3r	KS(p)-DH	1410
NIES1812_68763_c0_g1_i1_frame3	PP-KS	1478
NIES1812_69589_c0_g1_i1_frame3r	PP-KS(p)	602
NIES1812_7190_c0_g1_i1_frame2	KS-KR-PP-ST-TE-AAT	6699
NIES1812_7720_c0_g1_i1_frame1	KS(p)	329
NIES1812_7900_c0_g1_i3_frame2r	KS(p)	1463
NIES1812_7929_c0_g1_i4_frame2	KS(p)-DH	1797
NIES1812_7988_c0_g1_i1_frame2	KS(p)	508
NIES1812_8333_c0_g2_i1_frame2r	KS(p)-DH(p)	663
NIES1812_9085_c0_g1_i1_frame2	KS-PP-KS	1519
NIES1812_9085_c0_g1_i2_frame2	KS-DH(p)	1119
NIES1812_9085_c0_g2_i2_frame1r	KS(p)	686

Table S8: Contigs encoding for polyketide synthases retrieved from *Prymnesium parvum* strain NIES-1017, the corresponding domain order and contig length in amino acids.

Contig	Domain order	Length (aa)
NIES1017_11480_c0_g1_i1_frame1	KS	1234
NIES1017_123_c0_g1_i9_frame1	KS-AT-PP	4618
NIES1017_123_c0_g3_i1_frame3	KS-AT-KR-DH-KS-KS	9076
NIES1017_13034_c0_g1_i1_frame3	PP(p)-PP-PP-KS-DH	3661
NIES1017_13034_c0_g1_i3_frame1	KR(p)-PP-PP-KS	2204
NIES1017_1436_c0_g2_i4_frame1	KR-PP-KS-DH-KR-ER-KR-PP-KS-KR-PP-ST-TE-AAT	13405
NIES1017_1677_c0_g2_i2_frame1r	KS(p)-KR-PP-ST-TE	4167
NIES1017_16810_c0_g1_i1_frame2	PP-KS-DH-KR-PP-KS-DH-KR-PP-KS	10936
NIES1017_17252_c0_g1_i1_frame1	KS(p)-PP-KS-DH(p)	2760
NIES1017_17515_c0_g1_i1_frame3	KS(p)	1123
NIES1017_17770_c0_g1_i1_frame2	KS-AT-KR	4180
NIES1017_19213_c0_g1_i1_frame2	PP-KS(p)	883
NIES1017_19946_c0_g1_i1_frame3	KS(p)	449
NIES1017_20530_c0_g1_i2_frame3	KS(p)	570
NIES1017_20979_c0_g1_i1_frame2	KS(p)	1514
NIES1017_22345_c0_g1_i1_frame1r	PP(p)-KS-KR(p)	2769
NIES1017_22623_c0_g1_i1_frame2	PP-KS-HMG_CoA-DH-KS-PP	11917
NIES1017_23119_c0_g1_i1_frame3	KS(p)	537
NIES1017_23196_c0_g1_i1_frame1	KS(p)	739
NIES1017_2694_c0_g1_i1_frame1	NRPS-PP-KS-DH-KR(p)	5963
NIES1017_27225_c0_g1_i1_frame1	KR(p)-PP-KS(p)	1577
NIES1017_2742_c0_g1_i13_frame2	KR(p)-PP-KS-PP-KS-CRO	9815
NIES1017_28094_c0_g1_i1_frame3	KS(p)	405
NIES1017_28126_c0_g1_i1_frame1	KS(p)	1011
NIES1017_29011_c0_g1_i1_frame1r	KR(p)-PP-PP-KS	2964
NIES1017_29011_c1_g1_i1_frame3	PP-PP-KS(p)	1430
NIES1017_30422_c0_g1_i1_frame3	KS(p)-DH(p)	667
NIES1017_30691_c1_g1_i2_frame1	KS(p)-DH(p)	779
NIES1017_31123_c0_g1_i1_frame3	KS(p)	309
NIES1017_31149_c0_g1_i1_frame1	PP(p)-KS(p)	939
NIES1017_32504_c0_g1_i1_frame2	AT-KS-DH-KR-PP-KS(p)	5692
NIES1017_32781_c0_g1_i1_frame1	KS(p)	353
NIES1017_32795_c0_g1_i1_frame2	KS(p)	490
NIES1017_35358_c0_g1_i1_frame2	KS(p)	332
NIES1017_35566_c0_g1_i1_frame1	KS(p)	444
NIES1017_36169_c0_g1_i1_frame2	KS(p)	578
NIES1017_37624_c0_g1_i1_frame1	KS(p)	579
NIES1017_37910_c0_g1_i1_frame2	KS(p)	535
NIES1017_38771_c0_g1_i1_frame1	KS(p)	442
NIES1017_38835_c0_g1_i1_frame2	KS(p)	577
NIES1017_39008_c0_g1_i1_frame1	KS(p)	522

NIES1017_39390_c0_g1_i1_frame3	KS(p)	535
NIES1017_39894_c0_g1_i1_frame2	KS(p)	506
NIES1017_40833_c0_g1_i1_frame2	KS(p)	574
NIES1017_42046_c0_g1_i1_frame2	KS(p)	301
NIES1017_45811_c0_g1_i1_frame2	KS(p)	350
NIES1017_46630_c0_g1_i1_frame1	KS	975
NIES1017_4755_c0_g1_i4_frame2	ER(p)-KR-PP-KS-DH-ER(p)	4839
NIES1017_49297_c0_g1_i1_frame3r	KS(p)	348
NIES1017_5100_c0_g1_i3_frame1	AT-PP-PP-KS-DH(p)	3929
NIES1017_51743_c0_g1_i1_frame1	KR(p)-PP-KS	2428
NIES1017_52057_c0_g1_i1_frame1	KS(p)	922
NIES1017_52774_c0_g1_i1_frame2	KS(p)	1534
NIES1017_52785_c0_g1_i1_frame1	KS(p)	387
NIES1017_55320_c0_g1_i1_frame2	PP-KS(p)	508
NIES1017_57088_c0_g1_i1_frame2	KS(p)	361
NIES1017_58421_c0_g1_i1_frame1	KS(p)	716
NIES1017_58755_c0_g1_i1_frame2	KS(p)	361
NIES1017_59065_c0_g1_i1_frame2	KS(p)	1242
NIES1017_5915_c0_g1_i1_frame2	KS(p)-DH-PP-KS-DH	3554
NIES1017_5915_c0_g2_i1_frame2	KS(p)-DH	2277
NIES1017_5915_c0_g3_i1_frame2	KS(p)-DH-PP-KS(p)	2411
NIES1017_59437_c0_g1_i1_frame1	KS(p)	1093
NIES1017_59988_c0_g1_i1_frame2	PP-PP-KS(p)	1270
NIES1017_6001_c0_g1_i7_frame1	KR-PP-KS-CRO-HMG_CoA-PP-PP-KS-PP-PP	14490
NIES1017_60745_c0_g1_i1_frame1	KS(p)	469
NIES1017_61167_c0_g1_i1_frame2	KS(p)	352
NIES1017_65491_c0_g1_i1_frame3	DH-ER-KR-PP-KS	4298
NIES1017_66066_c0_g1_i1_frame3	PP-KS(p)	793
NIES1017_68022_c0_g1_i1_frame2	KS(p)	812
NIES1017_68256_c0_g1_i1_frame1	KS(p)-DH	1313
NIES1017_68824_c0_g1_i1_frame1	PP-KS(p)	908
NIES1017_70104_c0_g1_i1_frame1	KS(p)	300
NIES1017_809_c0_g1_i8_frame3	NRPS-PP-KS-KR-DH-ER-PP	9971
NIES1017_8984_c0_g1_i1_frame1	KR(p)-PP-KS(p)	1439
NIES1017_8984_c0_g2_i1_frame1	KS(p)-DH-KR-PP-KS(p)	3658

Table S9: Contigs encoding for polyketide synthases retrieved from *Prymnesium parvum* strain RCC-1436, the corresponding domain order and contig length in amino acids.

Contig	Domain order	Length (aa)
RCC1436_1032_c1_g1_i12_frame1	PP-KS-CRO-HMG_CoA-PP-PP-KS-PP-PP	14192
RCC1436_1032_c1_g1_i7_frame1	PP-KS-CRO(p)	14413
RCC1436_12965_c0_g1_i2_frame1	KS(p)-PP	7296
RCC1436_14526_c0_g1_i1_frame2	PP(p)-KS-TE(p)	2234
RCC1436_14526_c0_g2_i1_frame2	PP(p)-KS(p)	491
RCC1436_16596_c0_g1_i1_frame1	KS(p)	304
RCC1436_17682_c0_g1_i1_frame1	KS(p)	435
RCC1436_17682_c0_g1_i2_frame1	KS(p)-KR(p)	885
RCC1436_18259_c0_g1_i1_frame2	KS(p)	360
RCC1436_19547_c0_g1_i1_frame3	KS(p)	382
RCC1436_23033_c0_g1_i1_frame1	KS(p)	429
RCC1436_24773_c0_g1_i1_frame3	KS(p)	706
RCC1436_29084_c0_g1_i1_frame1	KS(p)	562
RCC1436_30622_c0_g1_i1_frame1	KS(p)	728
RCC1436_31848_c0_g1_i1_frame2	KS(p)	553
RCC1436_32984_c0_g1_i1_frame2	KS(p)	341
RCC1436_35624_c0_g1_i1_frame2	ER-KR-PP-KS-PP-PP(p)	7259
RCC1436_35655_c0_g1_i1_frame3	PP-KS(p)	817
RCC1436_35888_c0_g1_i1_frame3	KS(p)	1216
RCC1436_36553_c0_g1_i1_frame2	KS(p)	892
RCC1436_36752_c0_g1_i1_frame3	KS(p)-DH(p)	496
RCC1436_37518_c0_g1_i1_frame2	KS(p)	514
RCC1436_37666_c0_g1_i1_frame3	PP-KS(p)	876
RCC1436_37883_c0_g1_i1_frame2	PP-KS(p)	939
RCC1436_40704_c0_g1_i1_frame2	KS(p)	1015
RCC1436_41461_c0_g1_i1_frame1	KS(p)	1073
RCC1436_42615_c0_g1_i1_frame3	PP(p)-KS(p)	579
RCC1436_43093_c0_g1_i1_frame2	KS(p)	558
RCC1436_43228_c0_g1_i1_frame2	KS(p)	384
RCC1436_43262_c0_g1_i1_frame1	KS(p)	418
RCC1436_43277_c0_g1_i1_frame3	KS(p)	378
RCC1436_46045_c0_g1_i1_frame1	PP(p)-KS(p)	600
RCC1436_47308_c0_g1_i1_frame3	PP-KS(p)	730
RCC1436_47586_c0_g1_i1_frame3	KS(p)	391
RCC1436_47618_c0_g1_i1_frame2	KS(p)	727
RCC1436_47851_c0_g1_i1_frame1	KS(p)	591
RCC1436_4790_c0_g1_i2_frame1	KS(p)-AT(p)	1944
RCC1436_48570_c0_g1_i1_frame1	KS(p)	458
RCC1436_49540_c0_g1_i1_frame3	KS(p)	307
RCC1436_52025_c0_g1_i1_frame2	KS(p)	424
RCC1436_52251_c0_g1_i1_frame3	KS(p)-KR-PP	2381

RCC1436_53267_c0_g1_i1_frame2	KS(p)	511
RCC1436_53849_c0_g1_i1_frame3	KS(p)	310
RCC1436_54892_c0_g1_i1_frame1	KS(p)	719
RCC1436_55347_c0_g1_i1_frame3	KS(p)	498
RCC1436_6134_c0_g1_i3_frame3	KR(p)-PP-KS-KR-PP-ST	7763
RCC1436_7022_c1_g1_i6_frame3	AT-PP-PP-KS-KR-PP-KS-KR-PP-ST-TE	10443
RCC1436_7022_c1_g2_i1_frame1	KR(p)-PP-KS-DH(p)	2176
RCC1436_7022_c1_g3_i1_frame3	KS(p)-DH(p)	714
RCC1436_7241_c0_g1_i2_frame3	ER-KR-PP-KS-PP	6163
RCC1436_7241_c0_g1_i3_frame1	KR(p)-PP-KS-DH-ER(p)	5221
RCC1436_7241_c0_g2_i1_frame1	KS(p)	669
RCC1436_8310_c0_g1_i1_frame1	KS-KR-DH-ER-PP-TE	7327
RCC1436_8669_c0_g1_i3_frame3	PP-KS-DH-KR(p)	3687

Table S10: Contigs encoding for polyketide synthases retrieved from *Prymnesium parvum* strain RCC-1436, the corresponding domain order and contig length in amino acids.

Contig	Domain order	Length (aa)
PPDW02_10035_c0_g1_i1_frame2r	KS(p)-PP-PP	7825
PPDW02_10358_c0_g1_i4_frame3	PP-KS-DH	2433
PPDW02_12242_c0_g1_i1_frame3	DH-ER-KR-PP-KS-KR-PP-ST-TE-AAT	10540
PPDW02_13277_c0_g1_i3_frame1	PP-PP-PP-KS-DH-PP-KS(p)	4478
PPDW02_13360_c0_g1_i1_frame1	PP-PP-KS(p)	882
PPDW02_13724_c0_g1_i6_frame3	PP-KS-DH	2874
PPDW02_14094_c0_g1_i1_frame2	KS(p)-DH-PP-KS	3114
PPDW02_14094_c0_g3_i1_frame2	KS(p)-DH-KR-PP-KS	3674
PPDW02_14277_c0_g1_i8_frame1r	KR(p)-PP-PP-KS	3793
PPDW02_14856_c0_g1_i1_frame1	PP-KS(p)	1265
PPDW02_14856_c0_g2_i3_frame2	KS(p)-KR-PP-KS(p)	3324
PPDW02_14856_c0_g3_i1_frame1	PP(p)-KS(p)	998
PPDW02_15071_c0_g1_i1_frame3	KS(p)	607
PPDW02_15196_c0_g1_i2_frame1	KS(p)-KR(p)	884
PPDW02_15259_c0_g3_i1_frame2	KR(p)-PP-PP-KS(p)	1456
PPDW02_15259_c0_g3_i2_frame3	KR(p)-PP-PP-KS(p)	1418
PPDW02_15804_c0_g1_i1_frame1r	KS(p)	318
PPDW02_15991_c0_g1_i1_frame3	DH(p)-KR-PP-KS(p)	2786
PPDW02_16274_c0_g1_i1_frame1	KS(p)	516
PPDW02_16274_c0_g1_i2_frame1	KS(p)	1862
PPDW02_20404_c0_g1_i1_frame3	KS(p)	1978
PPDW02_20900_c0_g1_i1_frame3	KS(p)	351
PPDW02_2138_c0_g1_i1_frame1	DH-KR-PP-KS-DH	4722
PPDW02_2138_c0_g1_i4_frame1	DH-KR-ER-KR-PP-KS-DH-KR-PP-KS-KR-PP-ST-TE	13754
PPDW02_21709_c0_g1_i1_frame2r	NRPS-PP-KS(p)	2642
PPDW02_21900_c2_g1_i1_frame1	KS(p)	405
PPDW02_22524_c0_g1_i1_frame2	KS(p)	533
PPDW02_23546_c0_g1_i1_frame2	PP-PP-KS(p)	1330
PPDW02_23951_c0_g1_i1_frame3r	KS(p)	317
PPDW02_24101_c0_g1_i1_frame3r	KS(p)	557
PPDW02_26386_c0_g1_i1_frame3	KS(p)	416
PPDW02_26890_c0_g1_i1_frame2	KR(p)-PP-KS(p)	1323
PPDW02_27112_c0_g1_i1_frame3	PP-PP-PP-KS-DH(p)	3923
PPDW02_27184_c0_g1_i1_frame3	KS(p)	519
PPDW02_28574_c0_g1_i1_frame2	KS(p)-DH	1236
PPDW02_28595_c0_g1_i1_frame1	KR(p)-PP-KS(p)	1010
PPDW02_29468_c0_g1_i5_frame1	KS(p)-DH-KR	2646
PPDW02_30722_c0_g1_i1_frame1	PP-KS(p)	994
PPDW02_30870_c0_g1_i1_frame2	KS(p)	375
PPDW02_31930_c0_g1_i1_frame1	KS(p)	362
PPDW02_3434_c0_g1_i6_frame1	PP(p)-KS-CRO-HMG_CoA	6009

PPDW02_3505_c0_g1_i1_frame2	KR-PP-KS	3716
PPDW02_3505_c1_g1_i2_frame2	KA-DH-ER-KR-PP-KS-DH-KR-PP-KS-DH-KR-MT-KR(p)	13975
PPDW02_35548_c0_g1_i1_frame2	KS(p)	823
PPDW02_36069_c0_g1_i1_frame3	ER-KR-PP-KS-PP-PP(p)	6752
PPDW02_36484_c0_g1_i1_frame1	KS(p)	395
PPDW02_374_c0_g1_i1_frame1	PP-PP-KS-ER-KR-PP-KS-DH-KR-PP-KS-KR-PP-PP-KS	13928
PPDW02_38322_c0_g1_i1_frame1	PP-KS-KR	2906
PPDW02_39067_c0_g1_i1_frame1	KS(p)	312
PPDW02_39167_c0_g1_i1_frame2	KS(p)	521
PPDW02_43544_c0_g1_i1_frame2	KS(p)	315
PPDW02_44762_c0_g1_i1_frame3	KS(p)	503
PPDW02_44908_c0_g1_i1_frame1	KS-KR-ER(p)	2278
PPDW02_44992_c0_g1_i1_frame1	PP-KS(p)	1441
PPDW02_45359_c0_g1_i1_frame3	PP-KS	1920
PPDW02_45641_c0_g1_i1_frame2	KS(p)	355
PPDW02_45852_c0_g1_i1_frame1	KS(p)	396
PPDW02_46628_c0_g1_i1_frame2	KS(p)	357
PPDW02_4705_c1_g1_i1_frame2	KS-AT-KR-DH-KS-KS(p)	8937
PPDW02_47498_c0_g1_i1_frame1	KS(p)	422
PPDW02_50089_c0_g1_i1_frame2	KS(p)	462
PPDW02_50186_c0_g1_i1_frame3	KS(p)	703
PPDW02_50202_c0_g1_i1_frame1	KS(p)	610
PPDW02_50984_c0_g1_i1_frame1	KS(p)	792
PPDW02_51619_c0_g1_i1_frame2	KS(p)	493
PPDW02_5180_c0_g2_i4_frame3	PP-KS-CRO-HMG_CoA-PP-PP-KS-PP-PP	9977
PPDW02_56038_c0_g1_i1_frame2	KS(p)-DH(p)	918
PPDW02_57211_c0_g1_i1_frame1	KS(p)	421
PPDW02_58272_c0_g1_i1_frame1	KS(p)	393
PPDW02_61673_c0_g1_i1_frame1	KS(p)	409
PPDW02_61747_c0_g1_i1_frame3	KS(p)	306
PPDW02_62336_c0_g1_i1_frame3	KS(p)	844
PPDW02_62760_c0_g1_i1_frame2	KS(p)	1044
PPDW02_63438_c0_g1_i1_frame1	KS(p)	311
PPDW02_63755_c0_g1_i1_frame1	PP(p)-KS(p)	963
PPDW02_63848_c0_g1_i1_frame2	KS(p)	547
PPDW02_68531_c0_g1_i1_frame3	KS(p)	511
PPDW02_68676_c0_g1_i1_frame1	PP(p)-KS(p)	817
PPDW02_68909_c0_g1_i1_frame2	KS(p)	640
PPDW02_69098_c0_g1_i1_frame2r	KS(p)	792
PPDW02_69246_c0_g1_i1_frame2	KS(p)	847
PPDW02_8306_c0_g3_i1_frame3	PP(p)-KS(p)	709
PPDW02_8306_c0_g5_i2_frame2	KR(p)-PP-PP-KS-AT(p)	3228
PPDW02_8306_c0_g5_i5_frame2	AT-PP-PP-KS-DH(p)	3771

PPDW02_9755_c0_g1_i4_frame1	PP-KS-DH-ER-KR-PP-KS-KR-PP-DH-KR(p)	11201
PPDW02_9755_c0_g2_i1_frame1	KS(p)-DH-PP-KS-DH-KR-ER(p)-KR(p)	6063

Table S11: Presence (indicated by +) of different prymnesin analogues in the nine *Prymnesium parvum* strains used in this study.

	A-type			B-type			C-type	
	NIES-1812	**PPDW-01**	**UTEX-2797**	**K-0081**	**K-0374**	**UIO-223**	**K-0252**	**NIES-1017**	**RCC-1436**
A-type prymnesins									
PRM-A (2 Cl + DB)	+	+	+						
PRM-A (2 Cl + DB) + pentose		+	+						
PRM-A (2 Cl + O)	+	+							
PRM-A (2 Cl + O) + pentose	+	+							
PRM-A (2 Cl)	+	+	+						
PRM-A (2 Cl) + 2 pentose + hexose		+	+						
PRM-A (2 Cl) + pentose	+	+	+						
PRM-A (3 Cl)	+	+	+						
PRM-A (3 Cl) + 2 pentose + hexose		+	+						
PRM-A (3 Cl) + pentose		+	+						
PRM-A (3 Cl) + pentose + hexose		+	+						
PRM-A (2 Cl + DB)	+	+	+						
PRM-A (2 Cl + O)	+	+							
PRM-A (2 Cl)	+	+	+						
PRM-A (3 Cl)	+	+	+						
B-type prymnesins									
PRM-B (1 Cl + DB)				+	+	+			
PRM-B (1 Cl + DB) + pentose				+	+	+			
PRM-B (1 Cl)				+	+	+			
PRM-B (1 Cl) + 2 hexose									
PRM-B (1 Cl) + hexose				+	+				
PRM-B (1 Cl) + pentose				+	+	+			
PRM-B (1 Cl) + pentose + hexose				+	+	+			
PRM-B (2 Cl)				+	+				
PRM-B (2 Cl) + 2 hexose									
PRM-B (2 Cl) + hexose					+				
PRM-B (2 Cl) + pentose				+	+				
PRM-B (2 Cl) + pentose + hexose				+	+				
PRM-B (1 Cl + DB)				+	+	+			

PRM-B (1 Cl)	+	+	+			
PRM-B (2 Cl)	+	+				
C-type prymnesins						
PRM-C (2 Cl + 2 DB)						
PRM-C (2 Cl + 2 DB) + 2 pentose + hexose						
PRM-C (2 Cl + 2 DB) + pentose						+
PRM-C (2 Cl + 2 DB) + pentose + hexose						+
PRM-C (2 Cl + DB)					+	+
PRM-C (2 Cl + DB) + 2 pentose						+
PRM-C (2 Cl + DB) + hexose + 2 pentose						+
PRM-C (2 Cl + DB) + pentose					+	+
PRM-C (2 Cl + DB) + pentose + hexose						+
PRM-C (2 Cl)				+	+	+
PRM-C (2 Cl) + 2 pentose					+	+
PRM-C (2 Cl) + pentose					+	+
PRM-C (3 Cl + DB)				+	+	+
PRM-C (3 Cl + DB) + 2 pentose				+	+	+
PRM-C (3 Cl + DB) + hexose + 2 pentose						
PRM-C (3 Cl + DB) + pentose				+		+
PRM-C (3 Cl + DB) + pentose + hexose				+	+	+
PRM-C (3 Cl)				+	+	+
PRM-C (3 Cl) + 2 pentose				+	+	+
PRM-C (3 Cl) + 2 pentose + hexose						
PRM-C (3 Cl) + pentose				+	+	+
PRM-C (4 Cl + 3 =O + 3 O)						
PRM-C (4 Cl + 3 =O + 3 O) + pentose						
PRM-C (4 Cl + 3 =O)						+
PRM-C (4 Cl + 3 =O) + pentose						
PRM-C (4 Cl + 3 =O) + pentose + hexose						
PRM-C (4 Cl + DB)				+	+	+
PRM-C (4 Cl + DB) + 2 pentose				+	+	+
PRM-C (4 Cl + DB) + 2 pentose + hexose						

PRM-C (4 Cl + DB) + pentose	+	+	+
PRM-C (4 Cl + DB) + pentose + hexose			+
PRM-C (4 Cl)	+	+	+
PRM-C (2 Cl + 2 DB)			+
PRM-C (2 Cl + DB)			+
PRM-C (2 Cl)	+	+	+
PRM-C (3 Cl + DB)	+	+	+
PRM-C (3 Cl)	+	+	+
PRM-C (4 Cl + 3 =O + 3 O)			
PRM-C (4 Cl + 3 =O)			+
PRM-C (4 Cl + DB)	+	+	+
PRM-C (4 Cl)	+	+	+

Publication III

Distinct physiological and transcriptomic responses of *Prymnesium parvum* under different salinity, phosphorus and cell density conditions

Distinct physiological and transcriptomic responses of *Prymnesium parvum* under different salinity, phosphorus and cell density conditions

Konstantinos Anestis[1*], Sylke Wohlrab[1,4], Elisabeth Varga[2], Per Juel Hansen[3], Uwe John[1,4,*]

[1] Ecological Chemistry, Alfred Wegener Institute, Helmholtz Center for Polar and Marine Research, Am Handelshafen 12, 27570 Bremerhaven, Germany

[2] Department of Food Chemistry and Toxicology, Faculty of Chemistry, University of Vienna, Währinger Straße 40, 1090 Vienna, Austria

[3] Marine Biology Section, University of Copenhagen, Strandpromenaden 5, 3000 Helsingør, Denmark

[4] Helmholtz Institute for Functional Marine Biodiversity at the University of Oldenburg (HIFMB), Ammerländer Heerstraße 231, 26129 Oldenburg

E-mail addresses: kanestis@awi.de (K. Anestis), sylke.wohlrab@awi.de (S. Wohlrab), elisabeth.varga@univie.ac.at (E. Varga), pjhansen@bio.ku.dk (P.J. Hansen), uwe.john@awi.de (U. John)

*corresponding authors

Abstract

The haptophyte *Prymnesium parvum* is known to be responsible for frequent worldwide blooms with negative ecological and financial consequences. The detrimental effects of *P. parvum* blooms are due to its rapid proliferation in combination with the production of toxic compounds with lytic effects on competitors, grazers and fish gills. The secondary metabolites prymnesins have been suggested to be the causative lytic compounds produced by *P. parvum*. These lytic compounds possibly support the mixotrophic character of *P. parvum,* enhancing its nutrient uptake and highlight the complexity of the dynamics behind bloom formation. The detailed relationship between phagotrophy, cell growth and toxicity is however still largely unexplored, because it has only recently been possible to chemically quantify the prymnesins. In the current study, we used controlled physiological experiments, aligned with transcriptomic analysis, to investigate processes related to cell growth, toxicity (cell lysis, prymnesin production and release) and

phagotrophy under different salinities, phosphorus (P) availabilities (P-replete vs P-deplete) and cell densities. Cell lysis was higher at a salinity of 5, compared to a salinity of 30, while P starvation induced higher feeding rates. Additionally, cellular toxin content was higher by an average factor of 10 at high cell densities compared to low cell densities. Transcriptomic analysis suggests distinct gene expression patterns related to cellular energy metabolism and growth, with upregulation of catabolic processing relating to higher growth rates, and lipid metabolism rearrangement for adjustment under the different salinities. Genes involved in phagotrophy, and especially endocytosis, showed higher expression under the P starvation and low salinity conditions, highlighting phagotrophy as evolutionarily conserved response mechanism to different stressors. Polyketide synthase genes, potentially involved in toxin biosynthesis, exhibited distinct expression patterns, with generally higher expression under the high cell density conditions. Our study contributes to a better understanding of the autecology of *P. parvum* by disentangling cellular processes and the influence of environmental parameters on mixotrophy, toxicity, and bloom formation in this ecologically important species.

Introduction

Harmful algal blooms (HABs) are characterized by the rapid proliferation of plankton with detrimental effects on ecosystems. The causes of such plankton blooms are variable and can be of both anthropogenic and environmental origin (Lewitus *et al.*, 2012). Among the best studied driving factors is eutrophication due to the inflow of dissolved nutrients which can be subsequently used from phototrophic plankton (both prokaryotic and eukaryotic) for rapid growth (Heisler *et al.*, 2008). The increasing global occurrence of HABs (Anderson *et al.*, 2012; Gobler *et al.*, 2017) has additionally been suggested to be a consequence of climate change (Gobler, 2020).

Apart from the negative impact of HABs due to their uncontrollable proliferation and subsequent depletion of oxygen in the water, many HAB species are also known to produce toxic compounds. Production and accumulation of toxins is common during algal blooms of these species and many toxins and their corresponding producing species have been studied in detail. The economic losses due to the production of toxins can be considerable (Hallegraeff *et al.*, 2021),

and the accumulation of toxins in shellfish can have direct poisoning effects on humans and animals that consume contaminated seafood (James *et al.*, 2010).

Haptophytes are a diverse group of nanoplankton with worldwide distribution and with an important contribution to primary production and biogeochemical cycles (Edvardsen *et al.*, 2016). Known bloom-forming haptophytes include *Chrysochromulina leadbeateri, Prymnesium polylepis, Prymnesium parvum* and *Phaeocystis spp.*.

Many HAB forming species, including many haptophytes, are mixotrophic, i.e. they are able to combine the two trophic modes of phagotrophy/osmotrophy and phototrophy in order to cover their nutritional needs (Burkholder *et al.*, 2008; Unrein *et al.*, 2013). This is especially the case in eutrophic ecosystems, where growth rates of mixoplanktonic species (as defined by Flynn et al., 2019) can be affected by both the increased dissolved nutrients and the availability of algal and bacterial prey (Burkholder *et al.*, 2008). In addition, mixotrophy can be highly advantageous under low or imbalanced nutrient conditions, as it can be an efficient mechanism to compensate for limiting nutrients (Stoecker *et al.*, 2017). However, it is still not well understood what the potential relationship between toxicity and mixotrophy, the associated costs and contribution to from and sustain algal blooms are.

The HAB species P. parvum is known to produce toxic compounds, collectively called prymnesins. These cause lysis/death of competitors and grazers, as well as lysis of fish gill cells. Prymnesins are large ladder-frame polyketide compound (Igarashi *et al.*, 1999) and three types, A-, B- and C- types, differing in the length of the carbon backbone, have been described (Rasmussen *et al.*, 2016). Most probably, prymnesins are produced by polyketide synthases (PKS) of the modular type I (Anestis *et al.*, 2021). The release of lytic compounds by *P. parvum* into the surrounding water has been shown to assist feeding, via immobilization of the prey and subsequent lysis, which allows the uptake of nutrients through either osmotrophy or phagotrophy (Skovgaard *et al.*, 2003; Tillmann, 2003).

The production of lytic compounds by *P. parvum*, whether studied using bioassays or by actual measurements of prymnesins, are known to be influenced by P availability, light and temperature (Beszteri *et al.*, 2012; Qin *et al.*, 2020; Taylor *et al.*, 2020, 2021). Phosphorus is an essential element for the cellular and metabolic processes of cells, i.e. used for creating the backbone of nucleic acids. Additionally, P is a component for the biosynthesis of phospholipids

and subsequently the maintenance of cell membrane fluidity and resistance, while it also participates in the energy transmission through adenosine phosphate (Dyhrman, 2016). The availability of P in the aquatic ecosystems is in the form of inorganic phosphate, and dissolved organic P in the form of phospho-esters, phosphonates and polyphosphates (Paytan and McLaughlin, 2007). Typical responses to P starvation include higher expression of transporters and proteins involved in scavenging of P from either DOP or cellular sources (Rokitta *et al.*, 2016).

P. parvum typically form blooms in estuaries at low salinity (2-8), despite the fact that this species grows fine in the salinity range of 0.5-45 (Edvardsen and Paasche, 1998; Barone *et al.*, 2010). Why it preferably blooms at low salinities is unknown at present, but could be due input of organic material from freshwaters, or simply because very few species can thrive at these salinities (Brand, 1984). Changes in salinity invokes cellular stress related to the cellular osmotic equilibrium (Parihar *et al.*, 2015). Responses to salinity stress include mechanisms to balance intracellular ion concentration through the expression of ion channels and transporters, the synthesis of organic osmolytes and the adjustment of membrane lipid composition and fluidity (Kirst, 1990; Galinski, 1995; Turk *et al.*, 2004, 2007; Harding *et al.*, 2016, 2017).

In the current study, *P. parvum* strain UIO223 was used to investigate the combinatory effects of typical blooming conditions such as salinity, P availability, and cell density on the cellular toxin content, toxin production and toxin profile, phagotrophy, and general metabolic processes related to adaptation under the different treatments. Different salinity and P availability treatments (salinity of 5 vs salinity of 30 and P-replete vs P-deplete) were applied in order to examine changes in cellular physiology, in combination with two different cell densities (early and late exponential growth). Furthermore, transcriptomics were used to elucidate the underlying cellular processes related to aspects of adaptation under the different conditions, such as energy fluxes, osmotic regulative responses, expression of polyketide synthases and potential to mixotrophy. We hypothesize that *P. parvum* will A) increase its toxin content and production at low salinity, and low medium P concentrations in combination with increased phagotrophy. B) the cellular and metabolic processes deduced from gene expression analyses will depict the corresponding cellular adjustment; C) cell density has an impact on the toxicity, growth rate and associated gene expression as cells getting into rather starvation and need to reallocate resources.

Materials and methods

Experimental set-up, sampling and incubations with prey

Phosphorus replete cultures of *P. parvum* strain UIO-223 were grown in standard K-medium with PO_4^{3-} concentration of 36 µM, while for the P deplete conditions, PO_4^{3-} was added at a final concentration of 2.4 µM. Culture medium with a salinity of 5 was obtained by diluting sterile filtered seawater with MilliQ water. The concentration of inorganic carbon in the low salinity medium was restored by adding 1 M $NaHCO_3$ in 1 mL L^{-1} of medium. Prior to establishing the experimental cultures, the cells were rendered axenic using a cocktail of antibiotics (165 µg mL^{-1} ampicillin, 33,3 µg mL^{-1} gentamicin, 100 µg mL^{-1} streptomycin, 1 µg mL^{-1} chloramphenicol, 10 µg mL^{-1} ciprofloxacin). The treatment with antibiotics lasted 4 days and was performed twice with an interval of one week. The axenicity of the cultures was examined by fluorescence microscopy after staining with 4′,6-diamidino-2-phenylindole (DAPI).

Four replicate cultures were established for each combination of salinity (30 and 5) and phosphorous (P replete and P deplete; 2x2 factorial design) and all cultures were kept in 17 °C in 16:8 light:dark cycle and under a photon flux density of 80 µmol photons m^{-2} s^{-1}. Bubbling was used to avoid carbon deficiency and the pH of the cultures was monitored daily. All cultures were sampled at both low cell density and high cell density.

Cell enumeration was performed using a Multi-Sizer III particle counter (Beckman-Coulter, Fullerton, USA). Mixotrophy was estimated using *Teleaulax acuta* (SCCAP K-1486) as prey, grown under the same condition as *P. parvum*. The initial cell concentration for the incubation was $30*10^3$ cells mL^{-1} and the ratio between *P. parvum* and prey was 1:1, following the recommendation of the existing literature (Lundgren *et al.*, 2016). To estimate phagotrophy, 2 mL of culture were fixed with Lugol (final concentration of 2%, v/v), and inspected in a Sedgewick Rafter chamber under an Axio Vert A1 Microscope equipped with a Colibri 7 (Zeiss) light source.

Physiological parameters: sampling and processing

Samples for inorganic nutrient measurements were taken by filtrating 15 mL of culture using 0.2 µM Millipore filters in order to eliminate cells. The nutrients that were measured included nitrate, nitrite, and phosphate, and were analyzed with a continuous-flow autoanalyzer (Evolution III, Alliance Instruments, Freilassing, Germany). The protocols that were used are

standard for the quantification of nitrite/nitrate (Armstrong, F A J, Stearns and Strickland, 1967) and phosphate (Eberlein and Kattner, 1987) in seawater.

Samples for particulate organic carbon (POC) and particulate organic nitrogen (PON) analysis were collected by filtering 30 mL of culture through pre-combusted glass microfiber filters (Whatman GF/F, Whatman, UK; nominal pore size: 0.7 µm) and were immediately frozen in pre-combusted glass vials until further analysis. The filters were dried at 50 °C overnight, acidified with 300 µL 0.2 N HCl, and again dried overnight at 50 °C. The acidified and dried filters were packed in tin foil and analyzed on a Euro Elemental Analyzer 3000 CHNS-O (HEKAtech GmbH, Germany).

Samples for chlorophyll-*a* (Chl-*a*) concentrations were taken by filtering 15 mL of culture through 22 mm glass microfiber filters (Whatman GF/F, Whatman, Maidstone, UK; nominal pore size: 0.7 µm). The sample filters were frozen immediately at −80 °C until laboratory analysis. Extraction was performed by sonication of filters in 10 mL 90% acetone and then incubated overnight in darkness at 4 °C. The extract was centrifuged at 3020 × g for 10 min, and the fluorescence of the supernatant was determined at 665 nm (TD-700 fluorometer, Turner Designs, Sunnyvale, USA).

Toxin extraction and quantification were performed according to a previously described protocol (Svenssen *et al.*, 2019), with small modifications as described in Anestis et al. (2021). In brief, cells were harvested through 22 mm glass microfiber filters (Whatman GF/F, Whatman, Maidstone, UK; nominal pore size: 0.7 µm). The biomass on each filter was extracted two times with 20 mL MeOH each using an ultrasonic batch for 30 min with a centrifugation step in between (4300 ×g for 15 min at 4 °C). The combined extract (40 mL) was evaporated to dryness using a CentriVap Benchtop Vacuum Concentrator (Labconco Corporation, Kansas City/ MO, USA) at 35 °C. The samples were reconstituted with 1 mL methanol:H_2O (90:10, v:v) and short-time ultrasonic bath treatment. HPLC-FLD measurements were performed after derivatization with the AccQ-Tag Fluor Reagent Kit (Waters Cooperation, Milford/MA, USA) with a 1200 HPLC system (Agilent Technologies, Waldbronn, Germany) using fumonisins B_1 and B_2 as external calibrants due to the lack of standards and the obtained results are an approximation of the prymnesin content in the samples. To confirm the presence of prymnesins and identify the specific prymnesin analogues, HPLC-HRMS-measurements were performed using a 1290 UHPLC system coupled to

a 6550 iFunnel QTOF LC/MS (both from Agilent Technologies). Chromatographic separation was achieved with a Kinetex F5 (2.1 × 100 mm, 2.6 µm, Phenomenex, Aschaffenburg, Germany) column using a water-acetonitrile gradient (eluent A: H_20, eluent B: acetonitrile: H_2O (90:10, v:v)), both eluents contained 1 mM ammoniumformate and 1% formic acid. The mass spectrometer was operated in the positive ionization mode in a scanning range of *m/z* 50 to 1700 with 3 scans per second.

RNA extraction, library construction and sequencing

Cells for RNA extraction were harvested by centrifugation at 1500 × g for 10 min and the cell pellet was transferred to 1 mL pre-chilled TriReagent mixed with glass beads. RNA isolation was performed as described in Wohlrab et al., 2017. Libraries for sequencing were prepared using the Truseq Stranded mRNA Samples Prep LS Protocol (Illumina GmbH, Berlin, Germany) and 1 µg of RNA as input. The paired-end cDNA libraries (2x150 bp) were sequenced on the Illumina Nextseq 500 machine (Illumina, San Diego, USA) and a high-output kit v2 (2 x 150 cycles).

Quality control of sequencing data, *de novo* assembly and annotation

Prior to assembly, the raw reads were pre-processed using Trimmomatic v.0.39 (Bolger *et al.*, 2014) and reads contaminated with adapters or quality scores of <5 were trimmed using the default settings and only paired-end reads were retained. Inspection with FastQC assured the high quality of the reads and absence of adapter contamination before proceeding to the construction of the *de novo* assembly (https://www.bioinformatics.babraham.ac.uk/projects/fastqc/). The reference transcriptome was constructed using Trinity (v2.11.0) with minimum contig length of 300 bp (Haas *et al.*, 2013). To reduce redundancy due to the assembling method, the output contigs were clustered together with a similarity threshold of 0.95 using the cd-hit-est command of CD-hit and the longest representative for each cluster transcript was kept (Fu *et al.*, 2012).

Gene annotation was performed using the Trinotate functional annotation suite (version 3.2.1; Grabherr et al., 2011). Transdecoder (v5.5.0) was used for detecting open reading frames (ORFs) for each gene (https://github.com/TransDecoder/TransDecoder). The gene sequences were aligned against the UniprotKB/Swiss-Prot (release 2021_03) using diamond with BLASTX and BLASTP as an option (blast version 2.10.1) and the best hit for each query was retained with an e value of $<1\ e^{-9}$. Further annotation information, like entries from the Kyoto Encyclopedia of Genes

and Genomes (KEGG) and the assignment of Gene Orthology (GO) terms were retrieved from the UniprotKB database.

Gene expression analysis

Quantification of gene expression was performed by mapping the paired-end reads in CLC Genomics Workbench 20, using the default settings. The resulting gene count matrix was normalized using the variance stabilizing transformation function of the Deseq2 package (Love *et al.*, 2014) and multiple comparison tests with three-way analysis of variance (ANOVA) were performed in order to define the effect of salinity, phosphorus and cell density in gene expression. For genes with significant interactions only, single *t*-tests were applied to identify the conditions causing expression changes. For every gene, a factor was considered to have a significant effect on the expression variance when satisfying an adjusted *p* value threshold of <0.01 and fold change >1.5. *P* values were adjusted by applying the Benjamini-Hochberg false discovery rate for multiple test correction (Yoav Benjamini and Yosef Hochberg, 1995).

Statistical analysis

Statistical analysis was performed using three-way analysis of variance (ANOVA) and the factors salinity, phosphorus and cell density. The normality of the distribution of the residuals was checked with the Shapiro-Wilk test, and an appropriate transformation of the data was applied to achieve $p > 0.05$. Pairwise comparisons were examined using Tukey's HSD (honestly significant difference) test.

Results

Cell growth, physiology and mixotrophy

Growth rates for cultures at low salinity varied from 0.86 to 0.92 μ d^{-1} in comparison to 0.72 to 0.75 μ d^{-1} observed for cells growing at high salinity (p-value < 0.01; Table). Cell growth for the P depleted treatments seemed unaffected compared to P replete cultures until full starvation was reached at day 7 (Figure 1; A and B). The number of cells remained stable for the following 2 days after P starvation (~450,000 cells mL^{-1}) and immediately started growing after P was added at day 9. Addition of P was performed in order to validate that P was the limiting factor and growth

was affected only by its depletion, but POP could not be measured directly to show changes in the cellular stoichiometry.

Particulate organic nutrients (C:N) were measured in order to gain understanding of the elemental composition of the cells under the different treatments. All salinity, phosphorus and cell density treatments had statistically significant effect on the cellular POC content (Table 1). In general, cellular POC was higher in low cell density cultures for all treatments (pairwise comparisons with $p < 0.005$). At low cell densities, the low salinity treatments had the lowest cellular POC content, while at the high cell densities, P-starved cells had a significantly higher cellular POC content. In accordance with the decrease in cellular POC content, a cell density dependent decrease in cellular PON content was also observed (Figure 1; D). Salinity and P as single factors seemed to have no statistically significant effect on cellular PON content; significant differences were, however, observed in interactions of salinity and P. The decrease in cellular PON was higher than in cellular POC, indicated by the cellular C:N stoichiometry; high cell density cultures had a significantly higher C:N ratio ($p <0.001$) compared to low cell density cultures. Cells grown at low salinity, had consistently lower C:N ratios compared to those grown at high salinity. Cellular Chl-*a* content was reduced by ~2.5-fold at the highly dense cultures as compared to low cell density cultures, and this was consistent for all treatments ($p <0.001$). The interaction of P and density also had a significant effect, with highly dense and P starved cells containing higher amount of chl-*a*.

Table 1 Summary of the three-way analysis of variance results. Values marked with * were statistically significant. The tested parameters include particulate organic carbon (POC), nitrogen (PON) and their ratio (C:N), chlorophyll-a (Chl-a) and toxin content per cell.

	POC			PON			C:N ratio			Chl-*a*			Toxin content		
Factor	df	F value	*p*	df	F value	*p*	df	F value	*P*	df	F value	*p*	df	F value	*p*
Salinity	1	15.32	<0.001*	1	0.93	0.34	1	104.17	<0.001*	1	0.74	0.39	1	2.98	0.096
Phosphorus	1	6.45	0.017*	1	0.09	0.76	1	65.24	<0.001*	1	17.3	<0.001*	1	78.9	<0.001*
Density	1	180.39	<0.001*	1	361.91	<0.001*	1	367.6	<0.001*	1	1031.5	<0.001*	1	397.2	<0.001*
Salinity:Phosphorus	1	1.07	0.30	1	12.06	0.002*	1	76.81	<0.001*	1	3.16	0.08	1	3.35	0.079
Salinity:Density	1	23.89	<0.001*	1	11.66	0.002*	1	0.02	0.86	1	0.07	0.78	1	20.8	<0.001*
Phosphorus:Density	1	6.01	<0.02*	1	2.48	0.13	1	36.92	<0.001*	1	35.08	<0.001*	1	52.6	<0.001*
Salinity:Phoshorus:Density	1	0.26	0.61	1	0.12	0.73	1	10.03	<0.001*	1	1.48	0.23	1	10.9	0.0029
Residuals	24			24			24			24			24		

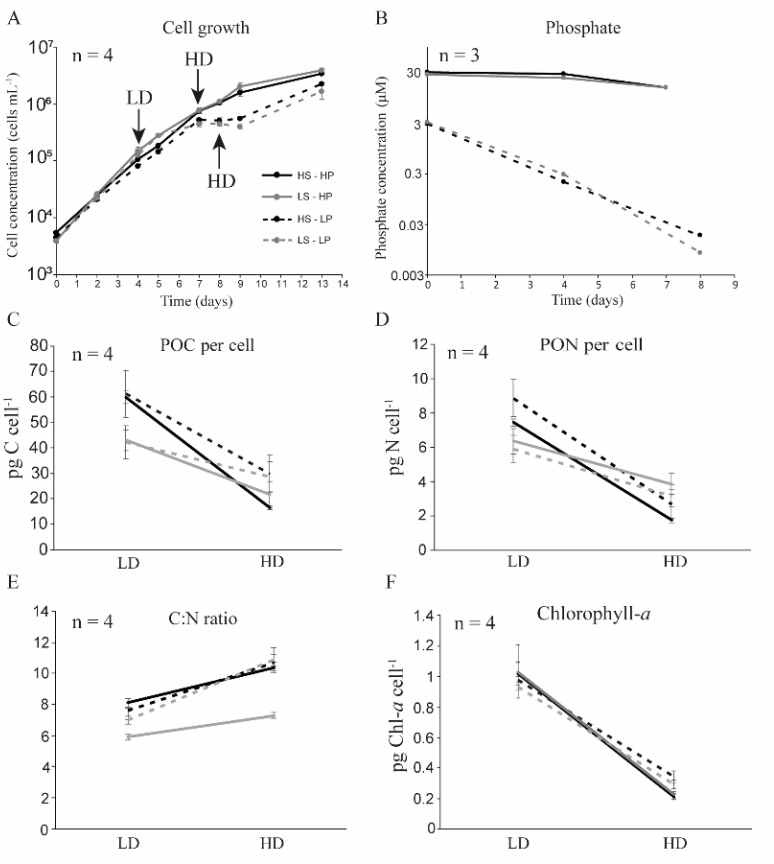

Figure 1 Overview of sample parameters for different time points and treatments (HS = high salinity, LS = low salinity, HP = high phosphorus and LP = low phosphorus). Cell growth (A) and indicated with arrows are the sampling time points for low cell density (LD) and high cell density (HD). Further parameters include phosphate concentration (B); particulate organic carbon (C) and nitrogen (D) and their corresponding ratio (E); chlorophyll-*a* concentration.

Teleaulax acuta was provided as prey and its mortality and phagotrophy by *P. parvum* was measured as the percentage of cells containing food vacuoles after 2 h, 6 h, 24 h, 48 h and 72 h of incubation with the prey. *T. acuta* cells showed higher mortality when incubated with low salinity *P. parvum* cultures, and independently of phosphorus condition, with ~80% being lysed 2 h after the beginning of the incubation with *P. parvum* (Figure 2; c). Change in *T. acuta* concentration at 2 h were observed also under the high salinity condition, but was considerably less extent than in low salinity (Figure 1;c). For the low salinity/P replete treatments, complete prey removal were observed 24 h after the beginning of the incubations, while for the low salinity/P deplete treatments complete prey removal was observed at 72 h (Figure 2; C). For the high salinity treatments, *T. acuta* mortality was lower, but complete prey removal was also observed at 72 h.

Table 2 Growth rates of *Prymnesium parvum* under the different salinity and phosphorous availability conditions under either presence or absence of prey. Values are mean μ d^{-1} ± S.D., n=4.

	In monoculture	Incubated with prey
High salinity – high P	0.75 ± 0.003	0.53 ± 0.029
High salinity – low P	0.72 ± 0.009	0.55 ± 0.077
Low salinity – high P	0.90 ± 0.035	0.85 ± 0.040
Low salinity – low P	0.86 ± 0.031	0.88 ± 0.056

Prymnesium cells containing a food vacuole were first observed 6 h after the beginning of the incubations (Figure 2; d). Phagotrophy was significantly induced in P starved conditions and independently of salinity, with an average of 11 ± 1 % of the total cells containing a food vacuole from 6 h until 48 h. In the P replete treatments , *P. parvum* presented low levels of phagotrophy, with a maximum of < 6 % of the total cells feeding at some time point. The number of cells with a food vacuole considerably decreased for all treatments from 48 h to 72 h and is consistent with the availability of prey, which disappeared at 72 h. Interestingly, even though the highest mortality rates of *Teleaulax* were observed at the low salinity incubations, in the P replete condition, phagotrophy for the percentage of *P. parvum* with food vacuoles was very low. Growth rates recorded for *P. parvum* grown with prey were lower than the growth rates of monocultures for the high salinity treatments; such a difference was not observed at the low salinity treatments (Table 2).

Toxin content and profile

Cellular prymnesin contents in *P. parvum* were significantly higher at high cell density compared to at low cell density for all treatments (Figure 2; A). Cell density and P starvation both had a statistically significant effect in explaining the variance in cellular prymnesin contents ($p < 0.001$), as both factors led to increases in prymnesin content by ~8.3-fold and ~2.4-fold respectively, when high cell densities were compared to low cell densities and low P were compared to high P. Salinity had statistically significant effects only in interaction with P concentration and cell density (Table 1). For low cell density cultures, no significant differences

in toxin contents were observed. The highest amount of cellular toxin content was observed among high density and P starved conditions ($p < 0.005$).

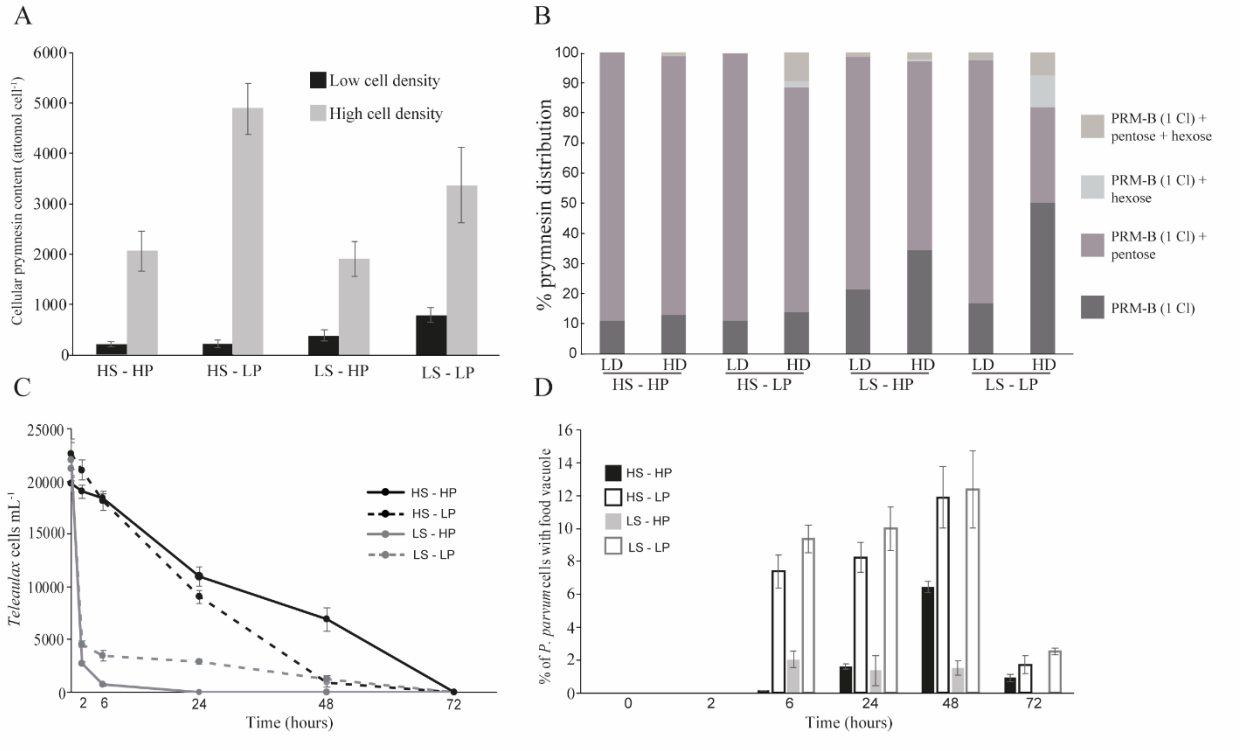

Figure 2 Total cellular prymnesin content (attomol cell^{-1}) and prymnesin analog composition (A and B, respectively) for all treatments (HS = high salinity, LS = low salinity, HP = high phosphorus and LP = low phosphorus) and cell densities (LD = low density and HD = high density). Concentration of *Teleaulax acuta* cells mL$^{-1,}$ when incubated with *Prymnesium parvum* (C), and % of *P. parvum* cells containing a food vacuole (D).

The percentage contribution of the prymnesin analogs to the overall prymnesin quantity, varied among the treatments, and was affected by all factors of the experiment; salinity, P and incubation time (Figure 2; B). The four analogs that were detected differ in presence or absence of attached sugars including a pentose, a hexose or both of these two. The main analog for the majority of time points and treatments was prymnesin containing a pentose, with the exception of the low salinity/P-deplete cells for which the prymnesin without attached sugar accounted for about half of the overall toxins at time point 2. The prymnesin analog without sugar showed a general increasing pattern in the low salinity treatment and especially during the second time point. The prymnesin analog containing both pentose and hexose showed consistently low contribution to the overall prymnesin content, however, it accounted for 9 ± 1 % and 7 ± 2 % for the P starved cells under high salinity and low salinity, respectively. The hexose containing

prymnesin analog was mainly present in the low salinity and P starved cells with a contribution of 11 ± 5 %.

Gene expression analysis

Gene expression differences and generated transcriptomes of the corresponding experimental treatments were analysed for assessing the driving experimental factors for changes in gene expression (Figure 3). Salinity was the main factor, which induced changes in the transcriptome under low cell density. For the high cell density cultures, P-replete and P-deplete culture samples formed two distinct clusters. Salinity explained the expression variance of 3754 transcripts, followed by cell density and phosphorus with 2856 and 1987 genes respectively. The number of DEGs with a KEGG identifier for which salinity had an effect was 324 (Figure 4; A), followed by cell density with 309 (ta 4; B) and P with 225 (Figure 4; C).

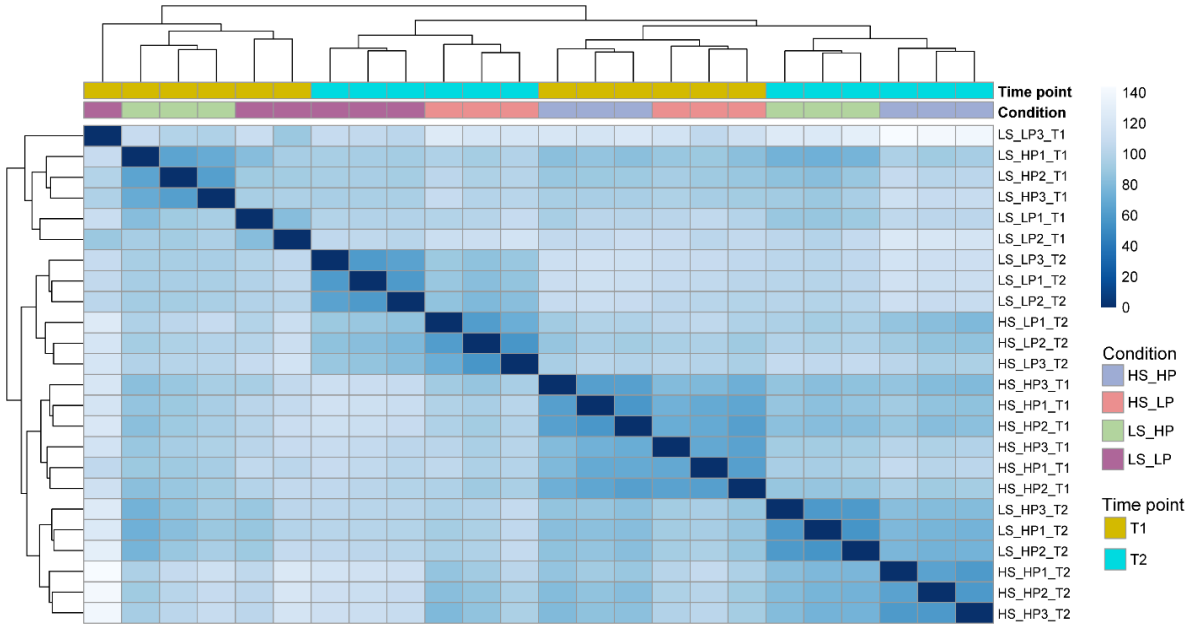

Figure 3 Heatmap of the transcriptome similarities matrix of *Prymnesium parvum* growing under the different salinity and phosphorous availability conditions. The abbreviations correspond to the tested conditions (HS = high salinity, LS = low salinity, HP = high phosphorus, LP = low phosphorus) and time points (T1 = time point 1 and T2 = time point 2). Samples are represented as triplicates (as indicated by the number following the phosphorous abbreviation).

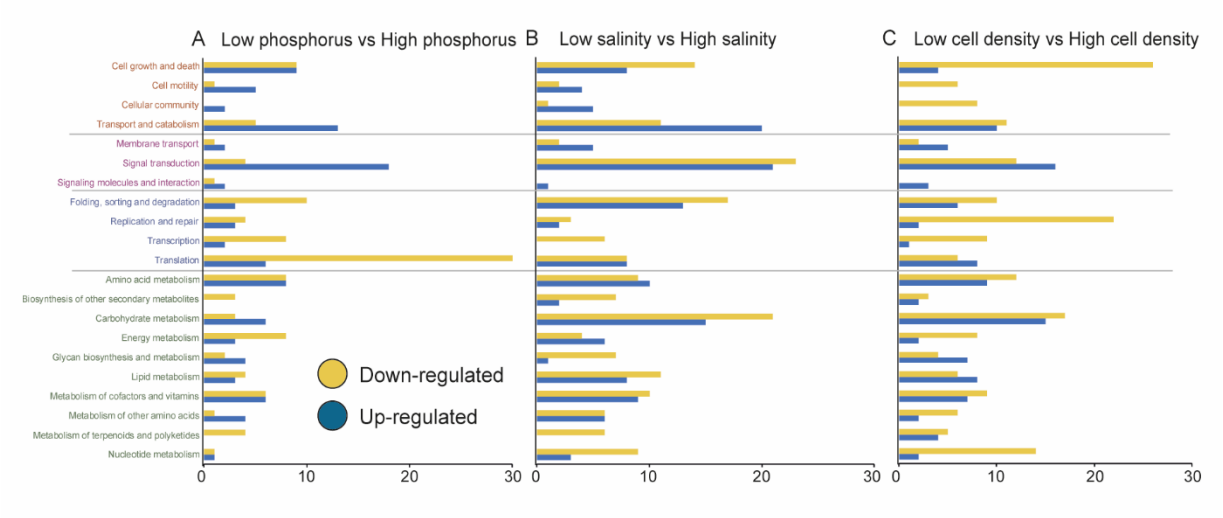

Figure 4 Number of up (blue) and down-regulated (yellow) genes assigned per KEGG category for the different comparison of low phosphorus vs high phosphorus (A), low salinity vs high salinity (B) and low cell density vs high cell density (C).

Signaling and cellular regulation

Signaling and the induced cellular regulative processes involve the reception of signals from the environment conditions including conspecifics. Genes involved in signaling processing and cellular regulation were influenced by all treatments (Figure 5). This functional category consisted of pathways involved in "Signal transduction", "Cell community", "Transcription" and "Translation". Signal transduction processes were mainly up-regulated under P depletion with 18 genes, in comparison to four that were down-regulated (Supplementary Information). Translation was significantly down-regulated at the P-starved cells, with 32 genes in contrast to six up-regulated genes (Figure 5; B and C).

The expression of mitogen-activated protein kinases (MAPKs) was affected by salinity and cell density. A general down-regulation of MAPKs was observed under low salinity and high cell density. Differentially expressed serine/threonine kinases were observed under all treatments and were consistently down-regulated under low salinity and high P. The expression of genes involved in cyclic nucleotide and calcium signaling was mainly affected by salinity and cell density. A cyclic nucleotide gated channel 4 gene (contig DN1719_c0_g1_i15), involved in cAMP signaling, showed 40-fold increase at low salinity.

Ion homeostasis

Low salinity increases osmotic stress and cell membrane fluidity. Genes involved in ion homeostasis involved transporters and channel forming proteins that mainly facilitate the exchange of elements such as potassium, sodium, ammonium and bicarbonate (Supplementary Information). Up-regulated under low salinity were three contigs coding for potassium channels by >2-fold increase, while two magnesium transporters were moderately down-regulated (<2-fold change). A 5.4-fold increase under low salinity was observed for an ion channel-forming bestrophin family protein. In the P-starved cells, a sodium bicarbonate (contig14742_c0_g1_i1) and a sodium/hydrogen exchanger (contig400_c0_g1_i52) were significantly up-regulated by 156-fold and 6.5-fold respectively. Moreover, two ammonium transporters (contig516_c0_g1_i8 and contig10261_c0_g1_i7) were down-regulated by 56-fold and 14-fold respectively.

Carbohydrate and energy metabolism

Carbohydrate metabolism, including anabolic and catabolic processes, are significantly influenced by the salinity treatment (Figure 5; A and B), with genes involved in catabolic processes being significantly up-regulated under low salinity. Significantly overexpressed genes under low salinity included glyceraldehyde 3-phosphate dehydrogenase (contig DN51264_c0_g1_i1) and pyruvate dehydrogenase E1 component (contig DN50014_c0_g1_i1), which showed 31-fold and 30-fold increase respectively (Supplementary Information). Glyceraldehyde 3-phosphate dehydrogenase catalyzes the conversion of glyceraldehyde 3-phosphate to 1,3-bisphosphoglycerate which can subsequently form pyruvate. Pyruvate in turn can be converted to acetyl-CoA and the production of energy in the form of NADH. Acetyl-CoA can subsequently enter the citric acid cycle and produce further energy. Additional overexpressed genes that are involved in glycolysis included pyruvate dehydrogenase E2 component (contig 6111_c0_g1_i19) and glucose-6-phosphate 1-epimerase (contig 1336_c0_g1_i33) with 2-fold and 6-fold increase respectively. Enzymes involved in valine, leucine and isoleucine degradation, such as isovaleryl-CoA dehydrogenase and malonate-semialdehyde dehydrogenase were up-regulated by 77-fold and 46-fold respectively.

On the other hand, malate synthase, which participates in the anabolic process of glyoxylate cycle, showed a 28-fold decrease under low salinity, highlighting the re-arrangement of cellular metabolism in favor of energy production rather than energy storage. Down-regulation under low salinity was also observed for genes encoding for glucokinase (contig9551_c0_g1_i5), phosphoglucomutase (contig10485_c0_g1_i71) and phosphoglycerate kinase (contig4027_c0_g1_i11).

P-starvation and cell density did not induce extensive changes in the expression of genes involved in carbohydrate metabolism (Figure 5; B and C). However, anabolic energy and carbon metabolism related pathways such as photosynthesis were moderately down-regulated in the P-starved and high cell density cultures (Supplementary Information).

Lipid metabolism and fatty acid desaturation

Genes involved in general and specific lipid biosynthesis were mainly influenced by salinity. In the current study, both 3-oxoacyl-acyl carrier protein synthase I (contig1413_c2_g2_i5) and 3-oxoacyl-acyl carrier protein synthase II (contig6027_c0_g1_i10) were up-regulated under low salinity by 23.6-fold and 3.6-fold respectively (Supplementary Information). Moreover, a phosphatidylglycerophosphatase A (contig40746_c0_g1_i1), involved in glycerolphospholipid metabolism, was 59.7-fold up-regulated. Further lipid-related up-regulated genes include arylsulfatase A (contig25_c0_g1_i45) by 7.9-fold, steroyl-CoA desaturase (contig DN7670_c7_g1_i2) by 2.6-fold, aldehyde dehydrogenase (contig37437_c0_g1_i1) by 45.7-fold and alcohol-forming fatty acyl-CoA reductase (contig DN47430_c0_g1_i1) by 129-fold. Down-regulated under low salinity genes included the fatty chain elongation protein 7 (contig 3504_c0_g1_i8) by 6.4-fold.

In P-starved cells, an enoyl-acyl carrier protein reductase I (contig 16503_c0_g1_i3) and a cycloeucalenol cycloisomerase (contig 2347_c0_g1_i3) were down-regulated by 4-fold and 5-fold respectively. Additional up-regulated genes in P-starved cells seem to be involved in glycerolipid and sphingolipid metabolism (Supplementary Information). Under high cell density, the fatty acid degradation enzyme enoyl-CoA hydratase (contig37128_c0_g1_i1) was

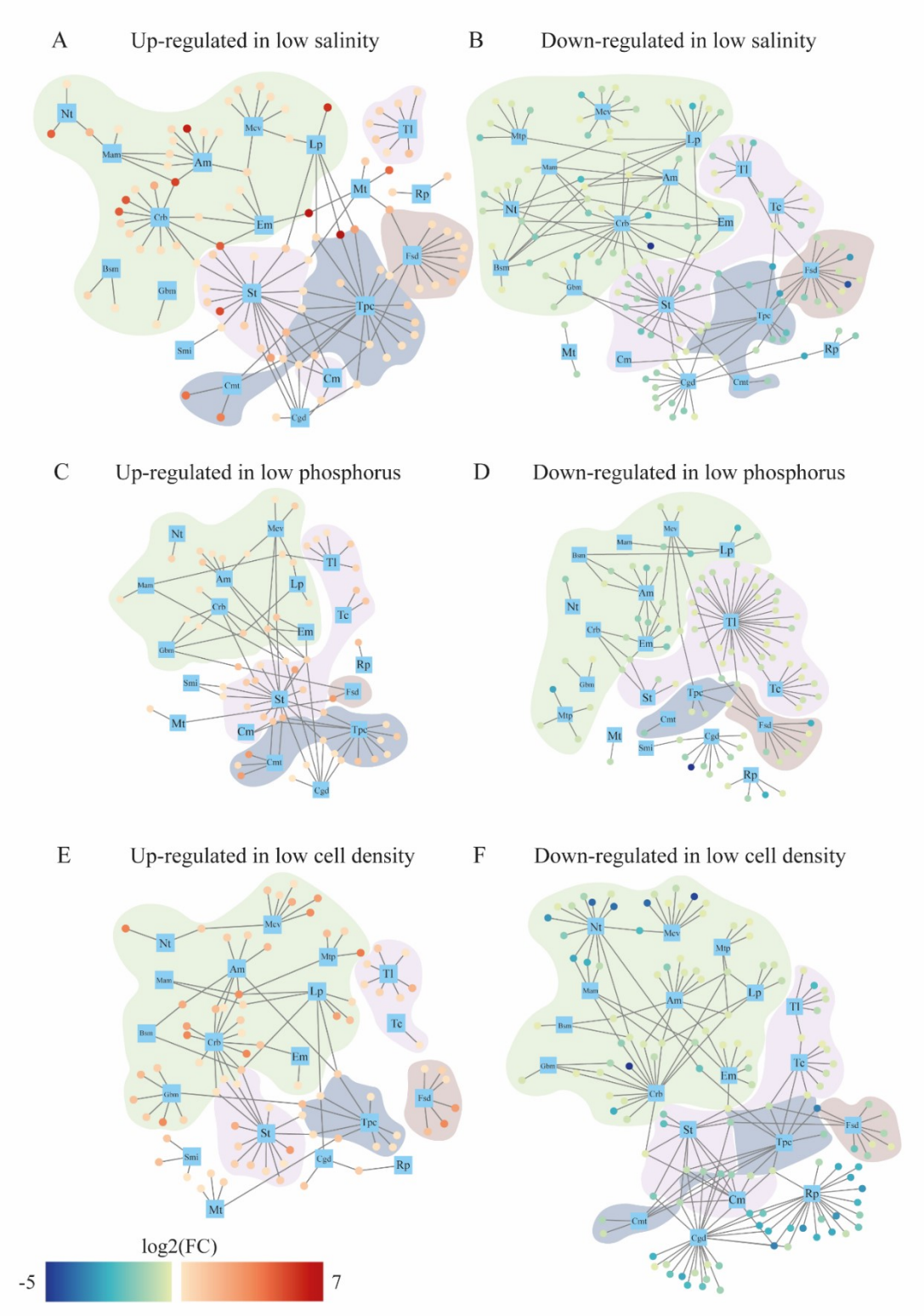

Figure 5 Networks of differentially expressed KEGG identifiers (both up- and down-regulated) for which either salinity (a), phosphorus (b) or time (c) had a statistically significant effect ($p < 0.01$ and FC > 1.5). Shaded are the categories related to general metabolism (light green), signaling and regulation (light pink), mixotrophy (grey) and cellular

secretion (light brown). Abbreviations correspond to the following KEGG categories: Am = amino acid metabolism, Lp = lipid metabolism, Mcv = metabolism of co-factors and vitamins, Crb = carbohydrate metabolism, Nt = nucleotide metabolism, Mtp = metabolism of terpenoids and polyketides, Mam = metabolism of other amino acids, Em = energy metabolism, Bsm = biosynthesis of secondary metabolites, Gbm = glycan biosynthesis, Tl = translation, Tc = transcription, St = signal transduction, Cm = cellular community, Tpc = transport and catabolism, Cmt = cell motility, Fsd = folding, sorting and degradation, Cgd = cell growth and death, Rp = replication and repair, Mt = membrane transport.

up-regulated by 12-fold, while the expression of cycloeucalenol cycloisomerase (affected also by P) was 7-fold higher.

In P-starved cells, an enoyl-acyl carrier protein reductase I (contig 16503_c0_g1_i3) and a cycloeucalenol cycloisomerase (contig 2347_c0_g1_i3) were down-regulated by 4-fold and 5-fold respectively. Additional up-regulated genes in P-starved cells seem to be involved in glycerolipid and sphingolipid metabolism (Supplementary Information). Under high cell density, the fatty acid degradation enzyme enoyl-CoA hydratase (contig37128_c0_g1_i1) was up-regulated by 12-fold, while the expression of cycloeucalenol cycloisomerase (affected also by P) was 7-fold higher.

Endocytosis and Exocytosis

Toxin induced toxicity based on potential endocytosis processes and the release of the toxins. Genes included in the categories of "Transport and catabolism" and "Cell motility" were further investigated in order to assess the cellular processes of mixotrophy. Moreover, the categories of "Folding, sorting and degradation" and "Membrane transport" were analyzed for genes potentially involved in cell secretion. Genes involved in endocytosis were consistently up-regulated under low salinity and P starvation (Supplementary Information). More specifically, 10 genes were up-regulated under either low salinity and P starvation. With regards to cell density, two genes were differentially expressed and all up-regulated in low cell density. The expression of 25 genes involved in phagosome and lysosome formation was affected by one or multiple treatments (Supplementary Information). Two genes involved in flagellar assembly (flgF and flgI) were over-expressed by 22-fold and 17-fold under low salinity. An additional gene involved in flagellar assembly, annotated as RNA polymerase primary sigma

factor (rpoD) showed a 10-fold increase under low P and it was moderated over-expressed (1.5-fold) under low salinity.

In the current study, ATP-binding cassette transporters (ABC transporters) were mainly up-regulated under the low salinity condition (Supplementary Information). A putative nitrate/nitrite transport system ATP-binding protein showed 109-fold up-regulation under low salinity. In addition, the expression of an arginine transport system substrate-binding protein (artI) under low salinity increased by 26-fold, while a phosphonate transport system substrate-binding protein was also up-regulated by 65-fold. A gene putatively involved in secretory systems, annotated as preprotein translocase subunit secA (contig 14630_c0_g1_i1), was found to be up-regulated under both low salinity and low P with 4.5-fold and 9-fold respectively. Furthermore, a modulator of FtsH protease (contig52848_c0_g1_i1), known to inhibit the SecY-degrading activity, was up-regulated by 35-fold at low salinity.

Polyketide synthases

Prymnesins belong to the chemical group of ladder-framed polyketides, which are typically synthetized via polyketide synthase genes. The expression dynamics of PKSs were examined in order to check their expression profile under the different treatments. The expressed PKSs of the analyzed samples formed 10 distinct clusters (Figure 6). Overall, the expression of PKSs was strongly influenced by cell density, showing higher expression values under the high cell density conditions, with the exception of the low salinity and P-replete condition. Clusters D, E, I and J showed the higher overall expression values, and mainly consisted of modular Type I PKSs. The expression of contig UIO223_409_c0_g1_i1 was consistently high across all treatments, but the highest expression value was observed under P-starvation and independently of salinity. This contig is characterized by the presence of a polyketide-type polyunsaturated fatty acid synthase (pfaA), which are involved in the biosynthesis of omega-3 polyunsaturated fatty acids. The effect of P starvation and higher expression of PKSs under this condition was more visible in clusters F and H, and especially for the high salinity treatment. In cluster D, the expression of three contigs (UIO223_7525_c0_g1_i2, UIO223_34765_c0_g1_i1 and UIO40_c0_g1_i4) was higher under P starvation and low cell density.

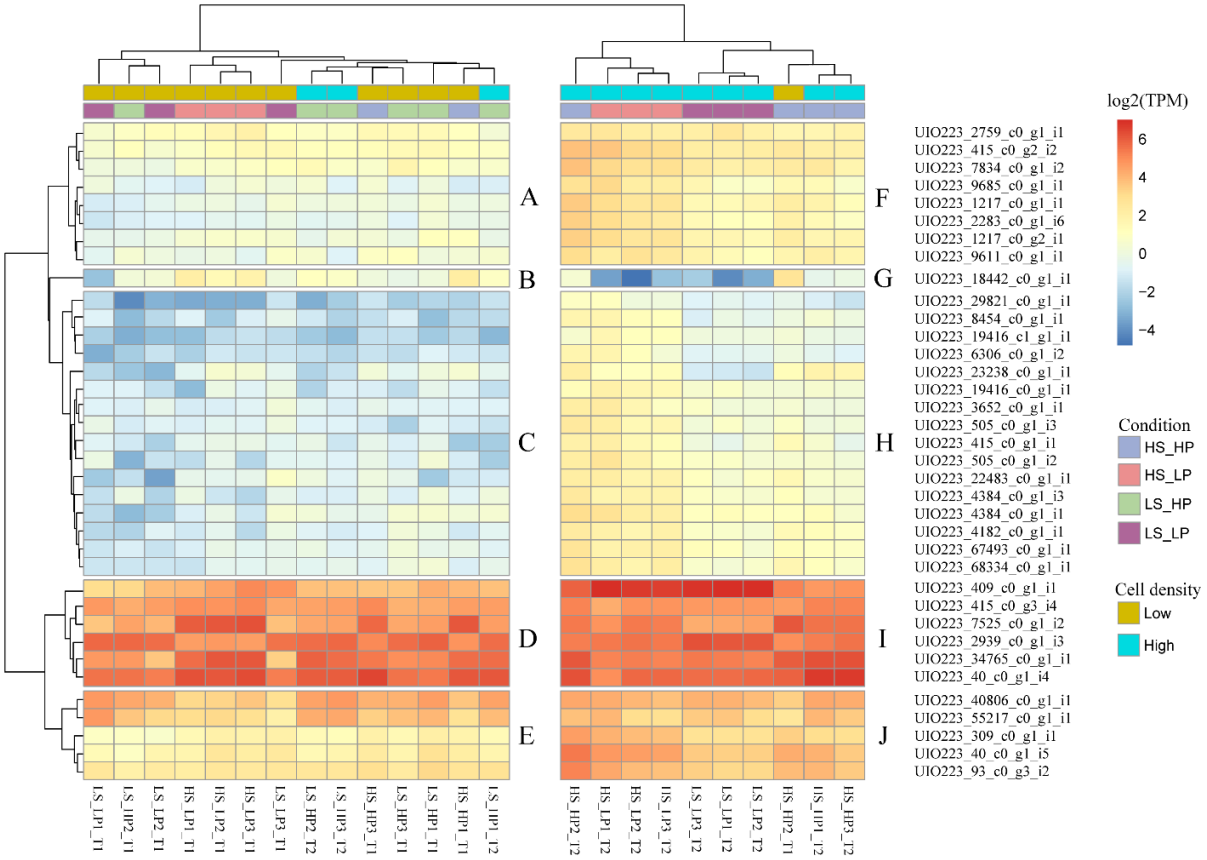

Figure 6 Expression of polyketide synthase genes as log2(TPM)) for all treatments of salinity (HS = high salinity, LS = low salinity), phosphorus availability (HP = high phosphorus and LP = low phosphorus) and cell densities (LD = low density and HD = high density).

Discussion

Cell growth and physiological responses to phosphorus depletion and low salinity

P. parvum is an euryhaline species with the ability to grow in a wide range of salinities from 0.5 to 45 (Edvardsen and Paasche, 1998; Beszteri *et al.*, 2012; Granéli *et al.*, 2012). Blooms of *P. parvum* usually occur in estuaries with low salinity (2-8). but salinity itself does not seem to impact the growth rate to any large extent within the salinity range of 5-30 (Richardson and Patiño, 2021). In the current study, the growth rates for *P. parvum* are consistent with previous findings, with cells growing under low salinity cultures presenting higher growth rates than high salinity cultures.

Cellular POC and PON contents were significantly influenced by cell density, irrespective of salinity and inorganic phosphorous concentration. The general decrease in POC content in high cell density cultures (not nutrient limited) could be attributable to lower dissolved inorganic carbon (DIC) availability due to removal of DIC at the high cell concentration; we did however not measure DIC in this study. However, the decrease in POC was accompanied by a decrease also in PON, suggesting other explanations. Nitrogen is an important structural element of chlorophyll and thus essential for maintaining the functionality of these organelles (Evans and Clarke, 2019). As a result, the observed increase in C:N ratio could be explained by the significant decrease of Chl-*a* at high cell density cultures.

Genes involved in carbohydrate metabolism seemed to be mainly affected by salinity and cell density, suggesting a general re-adjustment of carbon-related pathways under these conditions. The expression pattern of carbohydrate metabolic genes suggests increased carbon turnover related to the growth rates of cells under the different salinity and cell density conditions. To fulfill the energy and carbon units demands, key enzymes involved in glycolysis and pyruvate metabolism were significantly upregulated. On the other hand, carbon storage in the form of glucose via the glyoxylate cycle showed a decrease in gene expression. Carbohydrate rearrangement seems to be a critical factor under different salinity treatments, as it is related to the production of osmolytes, critical for the balance of osmotic pressure in cells (Harding *et al.*, 2016). A prerequisite to adapting to different salinities includes changes in the composition of the cell membrane, which in turn means changes in lipid composition (Russell, 1989). The fluidity of the cell membrane is greatly affected by the content in saturated and un-saturated fatty acids, with increase in un-saturated fatty acids meaning increased fluidity. The expression data suggests the extensive rearrangement of lipid metabolism, with up-regulation of genes involved in the general biosynthesis of fatty acid and metabolism of glycerophospholipids and sphingolipids.

Cell lysis and phagotrophy

Toxins produced by *P. parvum* have been associated with fish-kills, lysis of competitors and grazers as well as toxin-assisted phagotrophy. However, the relationship between prymnesin production, lysis of target cells and phagotrophy still remains unexplored. Lytic

effects of toxins produced by *P. parvum* have been mainly investigated using bioassays, and these investigations have yielded mixed results. Highly toxic *P. parv*um strains have been shown to be able to kill their predators and allowing *P. parvum* to ingest parts of them while less toxic or non-toxic strains were suitable prey (Tillmann, 2003). In a study by Blossom et al. (2014), five strains of *P. parvum* were tested for their toxic effects on a fish species (*Oncorhynchus mykiss*) and a microalga (*Teleaulax acuta*) showing that strains that had a low toxicity towards the microalga were highly toxic towards fish. In another study, *P. parvum* cells were lysed and exposed to fish erythrocytes. Here it was shown that P starved *P. parvum* cells had enhanced lytic toxic effects on the fish erythrocytes (Beszteri *et al.*, 2012).

In the current study, prey mortality was significantly higher at low salinity, irrespectively, of the nutrient conditions. The experimental set-up and results do not allow us to distinguish between potential higher release of prymnesins in the medium at low salinity. Also, we cannot rule out that other unknown compounds may be involved in prey cell lysis. Lastly, the finding that prey cells died rapidly at low salinity could potentially be due to the increased sensitivity of the prey to cell lysis due to osmotic reasons. These aspects deserved further studies.

The highest feeding rates were observed in P-deplete treatments, while the lowest feeding rates were observed in the high salinity and P-replete treatments. At low salinity the rates of prey lysis were initially very high and this could have led low feeding rates because the prey cells had lysed before *P. parvum* had the opportunity to ingest them. Nevertheless, phagotrophy did not seem to boost the growth rate of *P. parvum*, and our data rather supports the idea that phagotrophy in *P. parvum* may be a survival strategy to compensate for nutrient limitation (Skovgaard *et al.*, 2003). Our findings suggest that low salinity is the principal factor that induces higher degree of prey lysis in *P. parvum,* while P starvation seem to induce higher phagotrophy rates.

Phagotrophy involved different steps, starting from the internalization of food via endocytosis and the subsequent formation of a phagosome, which fuses with lysosome for further digestion. Even though transcriptomics were performed in monocultures, gene expression associate to phagotrophy-related processes were induced, indicating that induced mixotrophy is an evolutionary path manifested in *P. parvum* under stress conditions. Genes

involved in endocytosis were consistently up-regulated under low salinity and P starvation, with both treatments inducing strong prey lysis/mortality and feeding in *Prymnesium*. The incubation experiments showed higher phagotrophy under P starvation and independently of salinity. However, potential higher excretion of toxins under low salinity with high efficient lyses of prey may have led to underestimation of phagotrophy or DOM uptake in the experiments. Expression of phagotrophy-related genes has been previously related to ingestion rates in mixotrophic flagellates (McKie-Krisberg *et al.*, 2018). Moreover, factors that influence the expression of such genes include prey availability and light (Lie *et al.*, 2017). In *Alexandrium,* expression of endocytosis genes was more enhanced in a lytic strain in comparison to a non-lytic strain, highlighting also the potential coupling between the processes of lytic toxin production and phagotrophy-related processes (Wohlrab et al., 2016).

Toxin production and polyketide synthases

Recent advances in prymnesin quantification have facilitated our understanding of toxin dynamics and their production and release in the environment. Svenssen et al., 2019 developed an indirect method for the estimation of prymnesin type and found that the majority of the toxin is intracellular. Moreover, the combination of bioassays and biochemical approaches have reinforced the idea that prymnesins are the actual factors behind acute toxicity (Taylor *et al.*, 2020). In the current study, the intracellular toxin content was significantly higher in high cell density cultures, suggesting the occurrence of cell density dependent mechanisms that define the cellular toxin content, with potential implications in ecological level.

Polyketide synthase genes participate in the secondary metabolism and have been extensive studied in marine protists (John et al., 2008; Monroe and Dolah, 2008; Kohli et al., 2016). Many phycotoxins are polyketides, suggesting that PKSs are involved in toxin biosynthesis. The prymnesins can have carbon backbone lengths, varying across the different types, from 83 to 91 carbons (Binzer *et al.*, 2019). The considerable carbon length of toxins highlights the complexity of the underlying molecular biosynthetic mechanisms. Their biosynthesis could potentially involve both PKSs and perhaps partly fatty acid synthases, as it has been previously suggested for the biosynthesis of antibiotics from bacteria (Masschelein *et al.*, 2013). In the currently study, a mixed PKS/FAS transcript was consistently highly

expressed across all conditions. Polyketide synthase genes have been previously reported for *P. parvum* strains that produce different types of prymnesins (Anestis *et al.*, 2021), however, the development of efficient genetic manipulation techniques would be required for better understanding the connection between gene and product. In the current study, the expression of PKSs was strongly influenced by cell density, coinciding with the higher cellular content of prymnesins.

Cell-cell interaction, signaling and cellular regulative responses

Prymnesium cells perceive the environment on different levels. They have to adapt to the changed nutrient and salinity concentrations and also the increased cell density with its associated changes in the culture conditions are absorbed, processed and the cells adjust their cellular functions according to the environment. Genes belonging to signal transduction are usually involved in G-protein pathways, interacting with receptors and leading to downstream effects, such as the increase of important intracellular secondary messengers like diacylglycerol and cyclic guanosine monophosphate. Such processes are considered stress related. In the current study, signal transductions (transduction of signals from the outside of the cell to the inside) in *P. parvum* seems to be operated via MAPKs and serine/threonine kinases. A considerable down-regulation of genes involved in translation was observed under P starvation, suggesting that the final biosynthesis proteins and not gene transcription is mainly affected by P depletion. Moreover, the majority of down-regulated under P starvation genes are involved in the formation of ribosomes, which in turn are related to cell growth (Warner, 1999).

Conclusions

Salinity, phosphorus availability and cell density had important impact on different aspects of *P. parvum* physiology. Prymnesin contents were significantly higher in high cell density cultures, while salinity and P availability influenced the composition of prymnesin analogues. Higher expression of PKSs was observed at high cellular toxin content condition, supporting the involvement of PKSs in prymnesin biosynthesis. Higher rates of prey lysis was observed at low salinity, while P starvation induced higher phagotrophic rates. Phagotrophy did

not increase cell growth, supporting the idea that mixotrophy in *P. parvum* may a survival strategy to cope with nutrient limitation. The gene expression data of the monocultures supports the increased potential to mixotrophy under low salinity and P-starvation conditions, with up-regulation of endocytosis related genes. The regulation of genes involved in carbon and lipid metabolism highlights the increased catabolic processes to sustain high growth rates, while lipid metabolism is readjusted as a response to the need for membrane fluidity adaptation to salinity. Cellular responses are mediated through various signaling pathways, including MAPK, serine/threonine kinases, ABC transporters and cyclic nucleotide signaling.

Funding

This work has been funded by European Union's Horizon 2020 research and innovation programme under grant agreement No. 766327. E.V. received funding of the Austrian Science Fund (FWF) through an Erwin-Schrödinger fellowship [J3895-N28].

Data Accessibility Statement

Raw sequences have been deposited at NCBI (National Center for Biotechnology Information) under the BioProject PRJNA718746.

Competing interests

The authors certify that they have no conflict of interest.

References

Anderson, D.M., Cembella, A.D., and Hallegraeff, G.M. (2012) Progress in understanding harmful algal blooms: Paradigm shifts and new technologies for research, monitoring, and management. *Ann Rev Mar Sci* **4**: 143–176.

Anestis, K., Kohli, G.S., Wohlrab, S., Varga, E., Larsen, T.O., Hansen, P.J., and John, U. (2021) Polyketide synthase genes and molecular trade-offs in the ichthyotoxic species *Prymnesium parvum*. *Sci Total Environ* **795**: 148878.

Armstrong, F A J, Stearns, C.R. and Strickland, J.D.H. (1967) The measurement of upwelling

and subsequent biological process by means of the Technicon Autoanalyzer® and associated equipment. *Deep Sea Res Oceanogr Abstr* **14**: 381–389.

Barone, R., Castelli, G., and Naselli-Flores, L. (2010) Red sky at night cyanobacteria delight : the role of climate in structuring phytoplankton assemblage in a shallow, Mediterranean lake (Biviere di Gela, southeastern Sicily). *Hydrobiologia* **639**: 43–53.

Beszteri, S., Yang, I., Jaeckisch, N., Tillmann, U., Frickenhaus, S., Glöckner, G., et al. (2012) Transcriptomic response of the toxic prymnesiophyte *Prymnesium parvum* (N. Carter) to phosphorus and nitrogen starvation. *Harmful Algae* **18**: 1–15.

Binzer, S.B., Svenssen, D.K., Daugbjerg, N., Alves-de-Souza, C., Pinto, E., Hansen, P.J., et al. (2019) A-, B- and C-type prymnesins are clade specific compounds and chemotaxonomic markers in *Prymnesium parvum*. *Harmful Algae* **81**: 10–17.

Blossom, H.E., Rasmussen, S.A., Andersen, N.G., Larsen, T.O., Nielsen, K.F., and Hansen, P.J. (2014) *Prymnesium parvum* revisited: Relationship between allelopathy, ichthyotoxicity, and chemical profiles in 5 strains. *Aquat Toxicol* **157**: 159–166.

Bolger, A.M., Lohse, M., and Usadel, B. (2014) Trimmomatic: A flexible trimmer for Illumina sequence data. *Bioinformatics* **30**: 2114–2120.

Brand, L.E. (1984) The salinity tolerance of forty-six marine phytoplankton isolates. *Estuar Coast Shelf Sci* **18**: 543–556.

Burkholder, J.A.M., Glibert, P.M., and Skelton, H.M. (2008) Mixotrophy, a major mode of nutrition for harmful algal species in eutrophic waters. *Harmful Algae* **8**: 77–93.

Dyhrman, S.T. (2016) Nutrients and their acquisition: phosphorus physiology in microalgae. In *The physiology of microalgae*. Borowitzka, M.A., Beardall, J., and Raven, J.A. (eds). Dordrecht, The Netherlands: Springer, pp. 155–183.

Eberlein, K. and Kattner, G. (1987) Automatic method for the determination of ortho-phosphate and total dissolved phosphorus in the marine environment turns. *Fresenius' Zeitschrift für Anal Chemie* **326**: 354–357.

Edvardsen, B., Egge, E.S., and Vaulot, D. (2016) Article Diversity and distribution of

haptophytes revealed by environmental sequencing and metabarcoding – a review. **3**: 70176.

Edvardsen, B. and Paasche, E. (1998) Bloom dynamics and physiology of Prymnesium and Chrysochromulina. In *Physiological Ecology of Harmful Algal Blooms*. Anderson, D.M., Cembella, A.D., and Hallegraeff, G.M. (eds). Springer-Verl, Berlin/Heidelberg, Germany, pp. 193–208.

Evans, J.R. and Clarke, V.C. (2019) The nitrogen cost of photosynthesis. *J Exp Bot* **70**: 7–15.

Flynn, K.J., Mitra, A., Anestis, K., Anschütz, A.A., Calbet, A., Ferreira, G.D., et al. (2019) Mixotrophic protists and a new paradigm for marine ecology: Where does plankton research go now? *J Plankton Res* **41**: 375–391.

Fu, L., Niu, B., Zhu, Z., Wu, S., and Li, W. (2012) CD-HIT : accelerated for clustering the next-generation sequencing data. *Bioinformatics* **28**: 3150–3152.

Galinski, E.A. (1995) Osmoadaptation in bacteria. *Adv Microb Physiol* **37**: 273–328.

Gobler, C.J. (2020) Climate change and harmful algal blooms: Insights and perspective. *Harmful Algae* **91**: 101731.

Gobler, C.J., Doherty, O.M., Hattenrath-Lehmann, T.K., Griffith, A.W., Kang, Y., and Litaker, R.W. (2017) Ocean warming since 1982 has expanded the niche of toxic algal blooms in the North Atlantic and North Pacific oceans. *Proc Natl Acad Sci U S A* **114**: 4975–4980.

Grabherr, M.G., Haas, B.J., Yassour, M., Levin, J.Z., Thompson, D.A., Amit, I., et al. (2011) Full-length transcriptome assembly from RNA-Seq data without a reference genome. *Nat Biotechnol* **29**: 644–652.

Granéli, E., Edvardsen, B., Roelke, D.L., and Hagström, J.A. (2012) The ecophysiology and bloom dynamics of *Prymnesium spp*. *Harmful Algae* **14**: 260–270.

Haas, B.J., Papanicolaou, A., Yassour, M., Grabherr, M., Blood, P.D., Bowden, J., et al. (2013) De novo transcript sequence reconstruction from RNA-seq using the Trinity platform for reference generation and analysis. *Nat Protoc* **8**: 1494–1512.

Hallegraeff, G., Enevoldsen, H., and Zingone, A. (2021) Global harmful algal bloom status

reporting. *Harmful Algae* **102**:.

Harding, T., Brown, M.W., Simpson, A.G.B., and Roger, A.J. (2016) Osmoadaptative σtrategy and its molecular signature. **8**: 2241–2258.

Harding, T., Roger, A.J., and Simpson, A.G.B. (2017) Adaptations to high salt in a halophilic protist: Differential expression and gene acquisitions through duplications and gene transfers. *Front Microbiol* **8**: 1–27.

Heisler, J., Glibert, P.M., Burkholder, J.M., Anderson, D.M., Cochlan, W., Dennison, W.C., et al. (2008) Eutrophication and harmful algal blooms: A scientific consensus. *Harmful Algae* **8**: 3–13.

Igarashi, T., Satake, M., and Yasumoto, T. (1999) Structures and partial stereochemical assignments for prymnesin-1 and prymnesin-2: potent hemolytic and ichthyotoxic glycosides isolated from the red tide alga *Prymnesium parvum*. *J Am Chem Soc* 8499–8511.

James, K.J., Carey, B., O'Halloran, J., Van Pelt, F.N.A.M., and Škrabáková, Z. (2010) Shellfish toxicity: Human health implications of marine algal toxins. *Epidemiol Infect* **138**: 927–940.

Kirst, G.O. (1990) Salinity tolerance of eukaryotic marine algae. *Annu Rev Plant Physiol Plant Mol Biol* **41**: 21–53.

Lewitus, A.J., Horner, R.A., Caron, D.A., Garcia-Mendoza, E., Hickey, B.M., Hunter, M., et al. (2012) Harmful algal blooms along the North American west coast region: History, trends, causes, and impacts. *Harmful Algae* **19**: 133–159.

Lie, A.A.Y., Liu, Z., Terrado, R., Tatters, A.O., Heidelberg, K.B., and Caron, D.A. (2017) Effect of light and prey availability on gene expression of the mixotrophic chrysophyte, Ochromonas sp. *BMC Genomics* **18**: 163.

Love, M.I., Huber, W., and Anders, S. (2014) Moderated estimation of fold change and dispersion for RNA-seq data with DESeq2. *Genome Biol* **15**: 1–21.

Lundgren, V.M., Glibert, P.M., Granéli, E., Vidyarathna, N.K., Fiori, E., Ou, L., et al. (2016)

Metabolic and physiological changes in *Prymnesium parvum* when grown under, and grazing on prey of, variable nitrogen:Phosphorus stoichiometry. *Harmful Algae* **55**: 1–12.

Masschelein, J., Mattheus, W., Gao, L.J., Moons, P., van Houdt, R., Uytterhoeven, B., et al. (2013) A PKS/NRPS/FAS hybrid gene cluster from *Serratia plymuthica* RVH1 encoding the biosynthesis of three broad spectrum, zeamine-related antibiotics. *PLoS One* **8**:.

McKie-Krisberg, Z.M., Sanders, R.W., and Gast, R.J. (2018) Evaluation of mixotrophy-associated gene expression in two species of polar marine algae. *Front Mar Sci* **5**: 1–12.

Parihar, P., Singh, S., Singh, R., Singh, V.P., and Prasad, S.M. (2015) Effect of salinity stress on plants and its tolerance strategies: a review. *Environ Sci Pollut Res* **22**: 4056–4075.

Paytan, A. and McLaughlin, K. (2007) The oceanic phosphorus cycle. *Chem Rev* **107**: 563–576.

Qin, J., Hu, Z., Zhang, Q., Xu, N., and Yang, Y. (2020) Toxic effects and mechanisms of *Prymnesium parvum* (Haptophyta) isolated from the Pearl River Estuary, China. *Harmful Algae* **96**: 101844.

Rasmussen, S.A., Meier, S., Andersen, N.G., Blossom, H.E., Duus, J.Ø., Nielsen, K.F., et al. (2016) Chemodiversity of ladder-frame prymnesin polyethers in *Prymnesium parvum*. *J Nat Prod* **79**: 2250–2256.

Richardson, E.T. and Patiño, R. (2021) Growth of the harmful alga, *Prymnesium parvum* (Prymnesiophyceae), after gradual and abrupt increases in salinity. *J Phycol* **57**: 1335–1344.

Rokitta, S.D., von Dassow, P., Rost, B., and John, U. (2016) P- and N-depletion trigger similar cellular responses to promote senescence in eukaryotic phytoplankton. *Front Mar Sci* **3**:.

Russell, N.J. (1989) Adaptive modifications in membranes of halotolerant and halophilic microorganisms. *J Bioenerg Biomembr* **21**: 93–113.

Skovgaard, A., Legrand, C., Hansen, P., and Granéli, E. (2003) Effects of nutrient limitation on food uptake in the toxic haptophyte *Prymnesium parvum*. *Aquat Microb Ecol* **31**: 259–265.

Stoecker, D.K., Hansen, P.J., Caron, D.A., and Mitra, A. (2017) Mixotrophy in the marine plankton. *Ann Rev Mar Sci* **9**: 311–335.

Svenssen, D.K., Binzer, S.B., Medić, N., Hansen, P.J., Larsen, T.O., and Varga, E. (2019) Development of an indirect quantitation method to assess ichthyotoxic b-type prymnesins from *Prymnesium parvum*. *Toxins (Basel)* **11**: 1–15.

Taylor, R.B., Hill, B.N., Bobbitt, J.M., Hering, A.S., Brooks, B.W., and Chambliss, C.K. (2020) Suspect and non-target screening of acutely toxic *Prymnesium parvum*. *Sci Total Environ* **715**: 136835.

Taylor, R.B., Hill, B.N., Langan, L.M., Chambliss, C.K., and Brooks, B.W. (2021) Sunlight concurrently reduces *Prymnesium parvum* elicited acute toxicity to fish and prymnesins. *Chemosphere* **263**: 127927.

Tillmann, U. (2003) Kill and eat your predator: A winning strategy of the planktonic flagellate *Prymnesium parvum*. *Aquat Microb Ecol* **32**: 73–84.

Turk, M., Abramović, Z., and Plemenitaš, Ana, Gunde-Cimerman, N. (2007) Salt stress and plasma-membrane fluidity in selected extremophilic yeasts and yeast-like fungi. *FEMS Yeast Res* **7**: 550–557.

Turk, M., Méjanelle, L., Sentjurc, M., Grimalt, J.O., Gunde-Cimerman, N., and Plemenitaš, A. (2004) Salt-induced changes in lipid composition and membrane fluidity of halophilic yeast-like melanized fungi. *Extremophiles* **8**: 53–61.

Unrein, F., Gasol, J.M., Not, F., Forn, I., and Massana, R. (2013) Mixotrophic haptophytes are key bacterial grazers in oligotrophic coastal waters. **8**: 164–176.

Warner, J.R. (1999) The economics of ribosome biosynthesis in yeast. *Trends Biochem Sci* **0004**: 437–440.

Wohlrab, S., Selander, E., and John, U. (2017) Predator cues reduce intraspecific trait variability in a marine dinoflagellate. *BMC Ecol* **17**: 1–9.

Yoav Benjamini and Yosef Hochberg (1995) Controlling the false discovery rate: A practical and powerful approach to multiple testing. *J R Stat Soc Ser B* **57**: 289–300.

Supplementary information

	Initial concentration	Low cell density	High cell density
High Salinity – High P	32 ± 1.41	29.50 ± 1.8	15.50 ± 5.5
High Salinity – Low P	3 ± 0.12	0.21 ± 0.05	0.02 ± 0.01
Low Salinity – High P	28.7 ± 1.76	24.14 ± 4.44	15.83 ± 1.89
Low Salinity – Low P	3.3 ± 0.13	0.3 ± 0.23	0.01 ± 0.01

Supplementary Table 1: Concentration of PO^{4-} in μM for all treatments and time points including the initial concentration that was measured in the original medium used for the inoculation of the cells.

Transcriptome overview	
Total transcripts	103,051
Total genes	39,197
% GC content	58.46
Contig N50	1901
Median contig length	965
Average contig length	1333.26
Annotation	
KEGG identifiers	10,122
SwissProt hits	15,020

Supplementary Table 2: Overview of the transcriptome features and annotation.

Supplementary Table 3: List of differentially expressed genes involved in mixotrophy and their fold change. In abbreviations are the different treatments of salinity (HS = high salinity, LS = low salinity), phosphorus availability (HP = high phosphorus and LP = low phosphorus) and cell densities (LD = low density and HD = high density).

Contig	KEGG annotation	LS vs HS	LP vs HP	HD vs LD
		FC	FC	FC
Endocytosis				
contig26657_c0_g1_i38	epsin	2.07		
contig5063_c0_g1_i1	programmed cell death 6-interacting protein	1.91		
contig20459_c0_g1_i11	charged multivesicular body protein 3	1.89		
contig671_c0_g1_i17	E3 ubiquitin-protein ligase NEDD4	1.68		
contig25370_c0_g1_i8	Ras-related protein Rab-5C	1.64		
contig5818_c0_g2_i15	Ras-related protein Rab-8A	1.53		
contig20985_c0_g1_i5	Ras-related protein Rab-11A	1.50		
contig2697_c0_g2_i2	charged multivesicular body protein 5		1.58	
contig2656_c0_g1_i8	ubiquitin carboxyl-terminal hydrolase 8		1.65	
contig51441_c0_g1_i1	cell division control protein 42		2.93	
contig21934_c0_g1_i4	heat shock 70kDa protein 1/2/6/8			-1.87
contig6297_c0_g1_i11	vacuolar protein sorting-associated protein 45			-2.37
Phagosome				
contig14934_c0_g1_i1	Ras-related C3 botulinum toxin substrate 1	4.27	3.82	
contig14934_c0_g1_i6	Ras-related C3 botulinum toxin substrate 1	-1.68		
contig9705_c0_g1_i1	NADPH oxidase 2	-1.89	1.95	
contig1980_c0_g2_i2	vesicle transport protein SEC22	-3.30		
contig19580_c0_g1_i2	syntaxin 18		-1.57	
contig15406_c0_g1_i1	tubulin beta			-1.83
contig25576_c2_g1_i4	V-type H+-transporting ATPase subunit E			-1.54
Lysosome				
contig325_c0_g1_i45	arylsulfatase A	7.92		
contig1327_c0_g1_i2	natural resistance-associated macrophage protein 2	2.90	1.99	
contig21737_c0_g1_i32	tripeptidyl-peptidase I	2.77		1.56

contig4362_c0_g1_i222	Niemann-Pick C1 protein	2.13	3.18	1.70
contig9049_c0_g1_i1	lysophospholipase III	1.96		
contig10624_c1_g1_i30	AP-4 complex subunit mu-1	1.82		
contig10624_c1_g1_i6	AP-4 complex subunit mu-1	1.78	1.74	
contig51289_c9_g1_i1	cathepsin D	1.76		
contig13558_c0_g1_i1	legumain	1.70		
contig6804_c0_g1_i3	tartrate-resistant acid phosphatase type 5		-1.79	
contig36033_c0_g1_i1	beta-mannosidase	-1.66		
contig9710_c0_g1_i2	heparan-alpha-glucosaminide N-acetyltransferase	-1.74		
contig4929_c0_g2_i9	ectonucleoside triphosphate diphosphohydrolase 4	-3.65		
contig10624_c1_g1_i28	AP-4 complex subunit mu-1	-4.95		
contig2311_c1_g1_i11	ATP-binding cassette, subfamily A (ABC1), member 2			1.56
contig14499_c0_g1_i2	iduronate 2-sulfatase			3.70
contig4929_c0_g2_i3	ectonucleoside triphosphate diphosphohydrolase 4			-3.25

Supplementary Table 4: List of differentially expressed genes encoding for transporters and their fold change. In abbreviations are the different treatments of salinity (HS = high salinity, LS = low salinity), phosphorus availability (HP = high phosphorus and LP = low phosphorus) and cell densities (LD = low density and HD = high density).

Contig	KEGG annotation	LS vs HS	LP vs HP	HD vs LD
		FC	FC	FC
contig11296_c0_g1_i2	ATP:ADP antiporter, AAA family	1.50		
contig12165_c0_g1_i3	solute carrier family 5 (sodium/myo-inositol cotransporter), member 3	1.73		
contig144_c0_g1_i10	magnesium transporter	-1.66		
contig16185_c4_g1_i2	potassium channel	1.97		
contig16185_c4_g2_i2	potassium channel	3.09		
contig197_c0_g1_i4	solute carrier family 35 (UDP-sugar transporter), member A1/2/3	1.66		
contig2707_c0_g1_i15	ion channel-forming bestrophin family protein	5.35		
contig2707_c0_g1_i22	ion channel-forming bestrophin family protein	2.41		
contig3092_c0_g1_i1	aquaporin TIP	2.89		
contig5280_c0_g1_i10	solute carrier family 12 (potassium/chloride transporter), member 4/5/6	-3.02		
contig14762_c0_g1_i3	potassium channel	2.29		-2.40
contig8900_c0_g1_i2	MFS transporter, MHS family, proline/betaine transporter	1.91		2.59
contig8447_c0_g1_i2	solute carrier family 44 (choline transporter-like protein), member 3	-2.25		
contig14742_c0_g1_i1	solute carrier family 4 (sodium bicarbonate transporter), member 10		15.89	
contig400_c0_g1_i52	solute carrier family 9 (sodium/hydrogen exchanger), member 9		6.42	
contig357_c0_g1_i16	proton-dependent oligopeptide transporter, POT family		2.19	
contig56993_c0_g1_i1	solute carrier family 24 (sodium/potassium/calcium exchanger), member 3		2.05	
contig2570_c0_g1_i8	magnesium transporter		1.74	
contig45654_c0_g1_i1	solute carrier family 35, member C2		1.60	
contig516_c0_g1_i8	ammonium transporter, Amt family		-13.58	
contig10261_c0_g1_i7	ammonium transporter Rh		-56.07	

contig5739_c2_g1_i1	boron transporter	2.10
contig10373_c0_g1_i3	potassium channel	1.91
contig4603_c1_g3_i1	solute carrier family 24 (sodium/potassium/calcium exchanger), member 2	1.83
contig2417_c0_g1_i1	MFS transporter, OPA family, solute carrier family 37 (glycerol-3-phosphate transporter)	-1.72
contig32168_c0_g1_i2	MFS transporter, SP family, sugar porter, other	-1.93

Supplementary Table 5: List of differentially expressed genes involved in metabolism and their fold change. In abbreviations are the different treatments of salinity (HS = high salinity, LS = low salinity), phosphorus availability (HP = high phosphorus and LP = low phosphorus) and cell densities (LD = low density and HD = high density).

Contig	KEGG annotation	LS vs HS	LP vs HP	HD vs LD
		FC	FC	FC
Carbohydrate metabolism				
contig45504_c0_g1_i1	alcohol dehydrogenase (cytochrome c)	32.80		
contig51264_c0_g1_i1	glyceraldehyde 3-phosphate dehydrogenase (phosphorylating)	30.56		
contig50014_c0_g1_i1	pyruvate dehydrogenase E1 component	29.97		
contig1336_c0_g1_i33	glucose-6-phosphate 1-epimerase	5.81		
contig6111_c0_g1_i19	pyruvate dehydrogenase E2 component (dihydrolipoamide acetyltransferase)	1.83		
contig4027_c0_g1_i11	phosphoglycerate kinase	-1.58	-2.03	
contig10485_c0_g1_i71	phosphoglucomutase	-3.71		
contig9551_c0_g1_i5	glucokinase	-3.75		
contig10485_c0_g1_i87	phosphoglucomutase			-1.65
contig1336_c0_g1_i19	glucose-6-phosphate 1-epimerase			-1.96
contig4618_c0_g2_i8	pyruvate carboxylase	1.83		
contig4618_c0_g2_i13	pyruvate carboxylase]	-3.04		
contig5049_c2_g1_i3	methylglyoxal/glyoxal reductase	1.98		
contig1318_c1_g1_i52	methylglyoxal/glyoxal reductase			1.73
contig7939_c0_g1_i2	malate synthase	-3.09		-4.21
contig7939_c0_g1_i24	malate synthase	-8.21		
contig7939_c0_g1_i20	malate synthase	-28.05		-10.61
contig15362_c2_g1_i27	acetyl-CoA carboxylase / biotin carboxylase 2			2.89
contig2678_c0_g1_i47	malate dehydrogenase (decarboxylating)			3.12
contig3475_c0_g2_i3	phosphate acetyltransferase			-2.06
Lipid metabolism				
contig40746_c0_g1_i1	phosphatidylglycerophosphatase A	59.75		
contig9049_c0_g1_i1	lysophospholipase III	1.96		
contig14056_c0_g1_i2	choline/ethanolamine phosphotransferase			1.98

contig6027_c0_g1_i10	3-oxoacyl-[acyl-carrier-protein] synthase II	3.66	2.03	
contig6027_c0_g1_i11	3-oxoacyl-[acyl-carrier-protein] synthase II	2.54		
contig6027_c0_g1_i7	3-oxoacyl-[acyl-carrier-protein] synthase II	1.70		
contig13817_c0_g1_i14	fatty acid synthase, animal type	-3.38		
contig16503_c0_g1_i3	enoyl-[acyl-carrier protein] reductase I		-4.39	
contig36828_c0_g1_i1	3-oxoacyl-[acyl-carrier-protein] synthase I	23.58		
contig1413_c2_g2_i5	long-chain acyl-CoA synthetase			1.70
contig47430_c0_g1_i1	alcohol-forming fatty acyl-CoA reductase	129.07		
contig7670_c7_g1_i2	stearoyl-CoA desaturase (Delta-9 desaturase)	2.69		
contig3504_c0_g1_i25	elongation of very long chain fatty acids protein 7	-6.47		-1.89
contig17156_c0_g1_i1	omega-6 fatty acid desaturase / acyl-lipid omega-6 desaturase (Delta-12 desaturase)		1.78	
contig3504_c0_g1_i8	elongation of very long chain fatty acids protein 7			-1.72
contig7759_c0_g1_i10	acetyl-CoA acyltransferase 1			2.44
contig13138_c0_g1_i1	enoyl-CoA hydratase / long-chain 3-hydroxyacyl-CoA dehydrogenase	-1.54		-1.68
contig21360_c0_g1_i10	3-hydroxyacyl-CoA dehydrogenase	-1.79		-1.79
contig44723_c0_g1_i1	enoyl-CoA hydratase	-1.54		
contig37128_c0_g1_i1	enoyl-CoA hydratase			12.35
contig21360_c0_g1_i9	3-hydroxyacyl-CoA dehydrogenase			-1.63

Supplementary Table 6: List of differentially expressed genes involved in cellular secretion and their fold change. In abbreviations are the different treatments of salinity (HS = high salinity, LS = low salinity), phosphorus

availability (HP = high phosphorus and LP = low phosphorus) and cell densities (LD = low density and HD = high density).

Contig	KEGG annotation	LS vs HS	LP vs HP	HD vs LD
		FC	FC	FC
Membrane transport				
contig14630_c0_g1_i1	preprotein translocase subunit SecA	4.53	9.04	
contig52848_c0_g1_i1	modulator of FtsH protease	34.72		
SNARE interactions in vesicular transport				
contig25835_c0_g1_i13	vesicle-associated membrane protein 7	1.83		
contig20873_c0_g1_i2	vesicle transport through interaction with t-SNAREs	1.53		
contig1980_c0_g2_i2	vesicle transport protein SEC22	-3.30		
ABC transporters				
contig56931_c0_g1_i1	phosphonate transport system substrate-binding protein	65.15		
contig47874_c0_g1_i1	nitrate/nitrite transport system ATP-binding protein	109.06		
contig48378_c0_g1_i1	arginine transport system substrate-binding protein	25.55		
contig245_c0_g1_i8	ATP-binding cassette, subfamily B (MDR/TAP), member 10	2.70		
contig5504_c1_g1_i9	phosphate transport system substrate-binding protein	1.65		
contig426_c0_g1_i19	ATP-binding cassette, subfamily A (ABC1), member 4	-2.24		1.64
contig1_c0_g2_i1	ATP-binding cassette, subfamily G (WHITE), member 2	-2.56		
contig75_c0_g1_i5	ATP-binding cassette, subfamily A (ABC1), member 1		1.94	2.28
contig75_c0_g2_i2	ATP-binding cassette, subfamily A (ABC1), member 4		-2.15	
contig2643_c0_g1_i16	ATP-binding cassette, subfamily C (CFTR/MRP), member 2		-1.10	-2.34
contig13323_c0_g2_i74	ATP-binding cassette, subfamily B (MDR/TAP), member 7			-1.31
contig2770_c0_g3_i8	ATP-binding cassette, subfamily A (ABC1), member 3			1.97

contig2258_c0_g1_i2	ATP-binding cassette, subfamily D (ALD), member 4		3.28
contig13166_c0_g1_i1	ATP-binding cassette, subfamily G (WHITE), member 8 (sterolin 2)		-3.19
contig5504_c1_g1_i4	phosphate transport system substrate-binding protein		1.71
Glycosyltransferases			
contig57435_c0_g1_i1	glucosyl-3-phosphoglycerate synthase	115.48	
contig2340_c0_g1_i18	[Skp1-protein]-hydroxyproline N-acetylglucosaminyltransferase	1.81	
contig2302_c0_g1_i3	probable glucuronoxylan glucuronosyltransferase IRX7		3.70
contig36616_c0_g1_i2	putative beta-1,4-xylosyltransferase IRX10		1.79
contig3422_c0_g3_i1	hydroxyproline O-galactosyltransferase 2/3/4/5/6		1.62

Supplementary Table 7: List of differentially expressed genes involved in signal transduction and their fold change. In abbreviations are the different treatments of salinity (HS = high salinity, LS = low salinity), phosphorus availability (HP = high phosphorus and LP = low phosphorus) and cell densities (LD = low density and HD = high density).

Contig	KEGG annotation	LSvs HS	LP vs HP	HD vs LD
		FC	FC	FC
MAP kinases				
contig4400_c1_g1_i7	mitogen-activated protein kinase kinase 1	2.12		-2.64
contig4400_c0_g1_i2	mitogen-activated protein kinase kinase 1	-1.98		
contig4400_c0_g2_i3	mitogen-activated protein kinase kinase 9	-2.70		
contig2199_c0_g1_i1	mitogen-activated protein kinase 7/14	-4.63		
contig4400_c1_g1_i15	mitogen-activated protein kinase kinase 1			-1.87
contig4400_c1_g1_i10	mitogen-activated protein kinase kinase 1			-2.07
contig4400_c1_g1_i5	mitogen-activated protein kinase kinase 1			-2.19
Serine/threonine kinases				
contig806_c0_g1_i4	serine/threonine kinase 4	-2.48		
contig4779_c0_g2_i10	cyclin-dependent kinase 2	-1.83		-2.79
contig22208_c0_g1_i31	serine/threonine-protein kinase CTR1		2.79	
contig22208_c0_g1_i20	serine/threonine-protein kinase CTR1		2.52	
contig22208_c0_g1_i43	serine/threonine-protein kinase CTR1		2.17	
contig4400_c2_g1_i1	serine/threonine-protein kinase ULK2		2.50	
contig10782_c0_g1_i1	serine/threonine-protein kinase CTR1			2.48
Cyclic nucleotide and calcium signaling				
contig4865_c1_g1_i4	P-type Ca2+ transporter type 2A			1.51
contig8488_c0_g1_i3	phosphatidylinositol phospholipase C, beta			-1.56
contig1641_c0_g1_i25	inositol 1,4,5-triphosphate receptor type 2			-2.36
contig2956_c1_g1_i2	hyperpolarization activated cyclic nucleotide-gated potassium channel 4			2.85
contig2956_c1_g1_i4	hyperpolarization activated cyclic nucleotide-gated potassium channel 4			1.84
contig1916_c0_g1_i21	phosphatidylinositol phospholipase C, epsilon			1.65

contig1719_c0_g1_i133	cyclic nucleotide gated channel alpha 4			-3.44
contig14934_c0_g1_i1	Ras-related C3 botulinum toxin substrate 1	4.27	3.82	
contig4520_c3_g1_i3	solute carrier family 8 (sodium/calcium exchanger)	-1.69		
contig4865_c1_g1_i3	P-type Ca2+ transporter type 2A	-2.54		
contig1719_c0_g1_i15	cyclic nucleotide gated channel alpha 4	39.83		
contig14934_c0_g1_i6	Ras-related C3 botulinum toxin substrate 1	-1.68		
contig15366_c0_g1_i2	calcium/calmodulin-dependent protein kinase I	-3.83		2.69
contig5616_c0_g1_i2	aspartate beta-hydroxylase			4.15
contig2540_c1_g1_i1	phosphatidylinositol phospholipase C, delta			1.64

Publication IV

Retention of prey genetic material by the kleptoplastidic ciliate *Strombidium* cf. *basimorphum*

frontiers in Microbiology

ORIGINAL RESEARCH
published: 28 July 2021
doi: 10.3389/fmicb.2021.694508

Retention of Prey Genetic Material by the Kleptoplastidic Ciliate *Strombidium* cf. *basimorphum*

Maira Maselli[1], Konstantinos Anestis[2†], Kerstin Klemm[2†], Per Juel Hansen[1] and Uwe John[2,3]*

[1] Marine Biological Section, Department of Biology, University of Copenhagen, Helsingør, Denmark,
[2] Alfred-Wegener-Institute, Helmholtz Center for Polar and Marine Research, Bremerhaven, Germany, [3] Helmholtz Institute for Functional Marine Biodiversity, Oldenburg, Germany

Many marine ciliate species retain functional chloroplasts from their photosynthetic prey. In some species, the functionality of the acquired plastids is connected to the simultaneous retention of prey nuclei. To date, this has never been documented in plastidic *Strombidium* species. The functionality of the sequestered chloroplasts in *Strombidium* species is thought to be independent from any nuclear control and only maintained via frequent replacement of chloroplasts from newly ingested prey. Chloroplasts sequestered from the cryptophyte prey *Teleaulax amphioxeia* have been shown to keep their functionality for several days in the ciliate *Strombidium* cf. *basimorphum.* To investigate the potential retention of prey genetic material in this ciliate, we applied a molecular marker specific for this cryptophyte prey. Here, we demonstrate that the genetic material from prey nuclei, nucleomorphs, and ribosomes is detectable inside the ciliate for at least 5 days after prey ingestion. Moreover, single-cell transcriptomics revealed the presence of transcripts of prey nuclear origin in the ciliate after 4 days of prey starvation. These new findings might lead to the reconsideration of the mechanisms regulating chloroplasts retention in *Strombidium* ciliates. The development and application of molecular tools appear promising to improve our understanding on chloroplasts retention in planktonic protists.

Keywords: kleptoplasty, ciliates, *Strombidium*, mixotrophy, plankton

OPEN ACCESS

Edited by:
Jean-David Grattepanche, Temple University, United States

Reviewed by:
Ravi Toteja, University of Delhi, India
Jun Gong, Sun Yat-sen University, China

****Correspondence:***
Maira Maselli
maira.maselli@bio.ku.dk

† These authors have contributed equally to this work

Specialty section:
This article was submitted to Aquatic Microbiology, a section of the journal Frontiers in Microbiology

Received: *13 April 2021*
Accepted: *30 June 2021*
Published: *28 July 2021*

Citation:
Maselli M, Anestis K, Klemm K, Hansen PJ and John U (2021) Retention of Prey Genetic Material by the Kleptoplastidic Ciliate Strombidium cf. basimorphum. Front. Microbiol. 12:694508. doi: 10.3389/fmicb.2021.694508

INTRODUCTION

Kleptoplasty is the non-permanent acquisition of chloroplasts from a photosynthetic organism by an otherwise heterotrophic organism (De Vries and Archibald, 2018). The phenomenon is common among marine ciliates (Stoecker et al., 1987; Stoecker et al., 2009). Since they acquire phototrophy from prey, plastidic ciliates are termed non-constitutive mixotrophs, or non-constitutive mixoplankton referring to planktonic species (Mitra et al., 2016; Flynn et al., 2019). Acquired phototrophy gives mixotrophic ciliates a competitive advantage over purely heterotrophic species when prey concentrations are low and light is available (Dolan and Pérez, 2000; Schoener and McManus, 2017).

Kleptoplastidic species in the *Mesodinium rubrum* species complex are known to only exploit chloroplasts from cryptophytes within the *Teleaulax/Plagioselmis/Geminigera* clade, from which they also retain the nuclei (process known as karyoklepty) and other prey organelles (Hansen et al., 2012; Johnson et al., 2016; Kim et al., 2017). The retention of prey nuclei allows the host to maintain some genetic control of the acquired chloroplasts through the transcription of plastid-related genes

from the kleptokaryon. Other than the ability to photosynthesize, *Mesodinium rubrum* acquires from the prey the potential to metabolize several essential compounds including amino acids and vitamins (Altenburger et al., 2020). This enables *Mesodinium* species to retain fully functional plastids and live as a complete autotroph for about four generations in the absence of prey (Smith and Hansen, 2007). Such phenomena of kleptoplasty and karyoklepty have been also recorded in some dinoflagellates (Onuma and Horiguchi, 2015; Onuma et al., 2020).

Kleptoplastidic ciliates in the genera *Laboea*, *Strombidium*, and *Tontonia* can instead exploit chloroplasts derived from a much wider range of algal groups, including chlorophytes, haptophytes, cryptophytes, and heterokonts (Laval-Peuto and Febvre, 1986; Johnson and Beaudoin, 2019). These ciliates have much higher prey ingestion rates than *Mesodinium rubrum* and, thus, potentially a fast turnover of sequestered prey plastids. Photosynthesis contributes much less to the total carbon uptake compared to *M. rubrum*, and they cannot grow autotrophically when prey is not available (Schoener and McManus, 2012; Maselli et al., 2020). Transmission electron microscopy studies on kleptoplastidic ciliates in the genera *Laboea*, *Strombidium*, and *Tontonia* have never revealed the retention of any algal prey nuclei (Laval-Peuto and Febvre, 1986; Stoecker et al., 1988). The function of the sequestered chloroplasts in these ciliates is thus currently thought to depend on their innate robustness and ability to survive inside the ciliate host. Based on studies on the kleptoplastidic *Strombidium rassoulzadegani*, kleptoplastidic ciliates in the genus *Strombidium* are thought to depend on more frequent reacquisition of prey plastids compared to *M. rubrum* because they do not express genes related to plastid maintenance and replication (Santoferrara et al., 2014; Mcmanus et al., 2018).

Strombidium basimorphum is a worldwide distributed species, first morphologically described in Canadian waters (Martin and Montagnes, 1993) and then reinvestigated through molecular systematic in a Chinese population (Liu et al., 2011). It has been shown to significantly contribute to grazing on photosynthetic picoeukaryotes in a north Pacific ocean region (Orsi et al., 2018), but the retention of functional chloroplasts in this species has only recently experimentally ascertained on an isolate of *Strombidium* cf. *basimorphum* from Danish coastal waters (Maselli et al., 2020).

This ciliate seems to more efficiently exploit chloroplasts for photosynthesis when ingestion is suppressed by the unavailability of prey. Chlorophyll *a*-specific photosynthetic rates increase from about 2 pg C pg chl-a^{-1} day^{-1} when the ciliate actively ingest prey, to 6–8 pg C pg chl-a^{-1} day^{-1} when the prey gets depleted (Maselli et al., 2020; Hughes et al., 2021). Photosynthetic rates are kept relatively higher and constant during at least 5 days of prey starvation (Maselli et al., 2020). *Strombidium* cf. *basimorphum* can thus maintain chloroplasts functionality unaltered for several days when chloroplasts are not replaced via the ingestion of prey. To get some insight into the molecular mechanisms that stand behind the retention of functional chloroplasts, here, we tested the ability of the Danish isolate of *Strombidium* cf. *basimorphum* to also retain prey genetic material. We studied this in well-fed cells and in cells that had been starved for 1–7 days. Molecular techniques such as quantitative polymerase chain reaction (qPCR), fluorescence *in situ* hybridization (FISH) and single-cell transcriptomics were applied. Quantitative PCR and FISH, as applied in here on cultures, were recently developed to detect the presence of prey genetic material in *Mesodinium* cf. *major* in field samples (Herfort et al., 2017).

MATERIALS AND METHODS

Culture Conditions and Experimental Design

Cultures of *S.* cf. *basimorphum* were established from single cells isolated from natural seawater samples from Roskilde fjord (Denmark). The isolate was identified and cultured as described in Maselli et al. (2020) and maintained for about 1 year feeding it the cryptophyte *Teleaulax amphioxeia* (SCCAP, K-1837). The experiment was conducted in *f*/20 media (a 1:10 dilution of the standard *f*/2 media from Guillard, 1975), at a salinity of 15, at 15°C, with a photon flux density of 100 μmol photons m^{-2} s^{-1} in a light/dark cycle of 14:10 h. Ciliates were allowed to grow exponentially for 5 days in borosilicate bottles (3.5 L of culture in 5-L flasks), by daily restoring the prey concentration that saturates their growth (*T. amphioxeia:* 1.0 × 10^4 cell mL^{-1}, as in Maselli et al., 2020). At the fifth day, ciliates were fed for the last time and split in three replicates of 1-L into 2-L Blue Cap glass flasks (VWR, Darmstadt, Germany). Cells were harvested for DNA extraction and FISH the day after, when prey was still available (T0); after 48 h, when prey was depleted (T2); and after 5 and 7 days, during prey starvation (T5 and T7).

DNA Extraction

S. cf. *basimorphum* cells were collected from 200 mL of the experimental cultures onto Nitex nylon filters (Millipore by Merck, Darmstadt, Germany) with a mesh size of 10 μm, allowing the separation of the ciliates from prey (*T. amphioxeia* length, ∼5 μm). Filters were subsequently rinsed with clean culture media to make sure that no *T. amphioxeia* cells were retained. Samples of *T. amphioxeia* triplicate monocultures were collected on 0.2-μm polycarbonate filters (Whatman Nuclepore, Cytiva, Freiburg, Germany). DNA from both ciliates and prey samples was extracted using the NucleoSpin Soil DNA isolation kit (Macherey-Nagel, Düren, Germany), following the manufacturer's instructions. Elution was performed using a small volume (35 μL) of the elution buffer provided by the kit. The concentration of the DNA was estimated using a NanoDrop spectrophotometer (ND-1,000 Peqlab, Erlangen, Germany).

Quantitative PCR

T. amphioxeia nuclear 28S ribosomal RNA (rDNA) D2 Unique Sequence Element (USE) primers (TxD2 1F and TxD2 USE 2R) and nucleomorph 28S rDNA D2 USE primers (TxNm 1F and TxNm 1R) were used in qPCR assays to detect the presence of prey genetic material in DNA extracted from ciliates and provide a semiquantitative estimation of its concentration over time, following prey depletion and starvation. The primers (**Supplementary Table 1**) were designed and checked for their

specificity by Herfort et al. (2017). All qPCR assays were run in technical triplicates on a StepOnePlus Real-Time PCR system (Applied Biosystems, Foster City, CA, United States). One nanogram of ciliate DNA was added to the following PCR mixture: 5 μL FAST SYBR Green Master Mix (Applied Biosystems by Thermo Fisher Scientific, Bremen, Germany), 0.125 μL of each primer (final concentration, 125 nM), and nuclease free water to a final volume of 10 μL.

Technical triplicate assays of each of the *T. amphioxeia* DNA replicate were run at the same DNA concentration as for the ciliate DNA. Quantitative PCR reactions were run as follows: 40 cycles of 95°C for 3 s and 60°C for 30 s, followed by a melting curve protocol (95°C for 15 s, 60°C for 1 min, and 0.3°C increments with a 15-s hold at each step). Control assays as a general control for extraneous nucleic acid contamination were also subjected to qPCR amplification with purified water in place of DNA.

Fluorescence *in situ* Hybridization

To investigate the potential transcriptional activity of prey nuclear material in *S.* cf. *basimorphum*, ciliates were hybridized a FISH probe for the *T. amphioxeia* nuclear-encoded 28S rRNA D2 USE (TxD2 RNA, **Table 1**) designed by Herfort et al. (2017). Twenty milliliters of experimental cultures in the different growth phases (T0, T2, T5, and T7) were fixed in paraformaldehyde (4% final concentration) and stored at 4°C for 1 h, prior to the collection of the ciliates on 3-μm polycarbonate filters (Whatman Nuclepore). Filters were incubated for 1 h in 1 mL of 50% dimethylformamide (DMF) to reduce chloroplast autofluorescence (Groben and Medlin, 2005). Filters were subsequently hybridized for 3 h at 37°C in a buffer with 30% formamide according to Herfort et al. (2017), washed for 10 min at the same temperature with a second buffer [1 × SET buffer: 150 mM NaCl, 1 mM ethylenediaminetetraacetic acid (EDTA), 20 mM Tris/HCL], and counterstained with 4′,6-diamidino-2-phenylindole (DAPI). Samples were inspected using the Olympus BX50 microscope equipped with a CoolLED pE-300 light source on 400 × magnification with appropriate wavelengths for DAPI (excitation, 350 nm; emission, 450 nm), Alexa488 (excitation, 480 nm; emission, 530 nm), and chloroplast fluorescence (excitation, 600 nm; emission, 650 nm). Images were acquired by an Olympus DP71 camera using the software CellSense. *S.* cf. *basimorphum* samples from cultures fed with the green alga *Nephroselmis rotunda* were treated in the same way and used as negative control to check for the specificity of the probes.

Single Cell Transcriptomics

To further validate the presence of prey transcripts in the ciliate as an indicator of active nuclei, nucleomorph, and/or plastid genome, single-cell transcriptomics was performed. Eight single cells were isolated from the experimental cultures after 4 days of prey starvation. Each cell was individually picked with a drawn Pasteur pipette, washed three times by transferring it in clean drops of sterile filtered media, and then transferred in the Lysis buffer provided by the extraction RNAqueous^{TM}-Micro Total RNA Isolation Kit (Thermo Fisher Scientific, Bremen, Germany). The complementary DNA (cDNA) libraries were generated using the SMART-Seq v4 Ultra Low Input RNA Kit for Sequencing (Takara Bio Europe SAS, Saint-Germain-en-Laye, France), and cDNA was quantified using the Agilent High Sensitivity Kit (Agilent Technologies Germany GmbH & Co. KG, Waldbronn, Germany). Adapter and index ligation was done using the Nextera® XT DNA Library Preparation Kit (Illumina GmbH, Berlin, Germany). The raw sequences were demultiplexed with bcl2fastq, and their quality and potential contamination with adapters were checked using FastQC. Reads were trimmed using TrimGalore with the default settings, and rRNA was removed with SortMeRNA (Kopylova et al., 2012). The final reads were mapped toward the reference transcriptome of *T. amphioxeia* generated by Altenburger et al. (2020), using the kallisto software (Bray et al., 2016). The reference assembly included the functional annotation of the transcripts with assigned Kyoto Encyclopedia of Genes and Genomes (KEGG) orthologs. To consider a *T. amphioxeia* transcript present in the ciliate, a threshold of ≥ 50 reads summed from all eight cells was set. The raw read sequences have been deposited at the National Center for Biotechnology Information (NCBI) under the BioProject PRJNA718746.

TABLE 1 | Average cycle threshold (Ct) values for prey nuclear and nucleomorph 28S genes in qPCR assays conducted on prey DNA (*T. amphioxeia* monoculture) and DNA extracted from the ciliate (*S.* cf. *basimorphum*) at different time points (corresponding to different nutritional stages of the ciliate culture).

	Nuclear 28S rDNA		Nucleomorph 28S rDNA	
	No. of replicates	Average Ct	No. of replicates	Average Ct
T. amphioxeia monoculture	9	20 ± 0.4	9	20.7 ± 0.6
T0, *S.* cf. *basimorphum*	9	29.2 ± 0.4	9	27.4 ± 0.4
T2, *S.* cf, *basimorphum*	9	34.1 ± 1.3	8	33.5 ± 1.7
T5, *S.* cf. *basimorphum*	7	35.5 ± 0.8	5	32.9 ± 1.4

Ct values are reported as average ± standard deviation.

RESULTS

The *Strombidium* cf. *basimorphum* cultures decline in cell concentration immediately after prey was depleted. Ciliates concentration changed from ∼130 to 110 cells mL^{-1} during the two first days of the incubation to further decrease to ∼85 cells mL^{-1} after 3 days of prey starvation (T5) and to ∼60 cells mL^{-1} after 5 days of prey starvation (T7) (**Supplementary Figure 1**).

Despite the differences in harvested amount of cells at each time point, the yield of DNA extraction was similar ranging between 7.7 and 5.2 ng μL^{-1}. However, 1 ng of template DNA extracted from ciliates that were actively feeding (T0) was sufficient to detect *T. amphioxeia* nuclear and nucleomorph 28S rDNA using the qPCR assays. The relative concentration of these prey genes appears to be lower in DNA extracted from ciliates subjected to prey deprivation, and only very low residual signals were detected after 3 days of starvation based on the average cycle threshold (Ct, **Table 1**). The amplification products of DNA

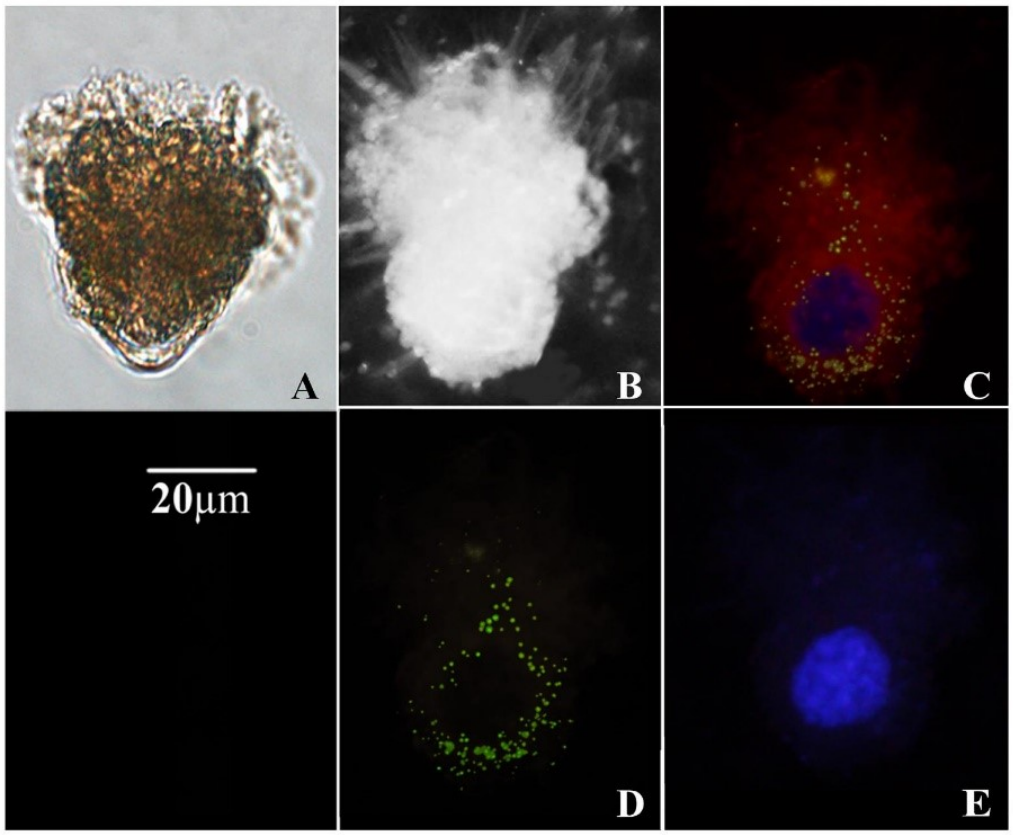

FIGURE 1 | Micrographs of *Strombidium* cf. *basimorphum*. **(A)** Light microscopy of a *S.* cf. *basimorphum* cell in liquid suspension (prior the collection on filter). **(B)** Bright field micrograph of a *S.* cf. *basimorphum* cell on filter. **(C)** Micrograph of the same cell on filter, acquired with combined light channels: the cell is hybridized with the probe for the prey rRNA (green) and counterstained with DAPI (blue). Sequestered chloroplasts are visible in red. **(D)** Micrograph of the same cell acquired with a single light channel for the FISH probe, showing prey rRNA. **(E)** Micrograph of the same cell acquired with a single light channel for DAPI, showing *S.* cf. *basimorphum* macronucleus.

extracted from ciliates at T7 were not reliable, so results of the qPCR assays for this time point are not shown. The reliability of the amplification products was assessed inspecting the melt curve of each of the replicate. Replicates that displayed multiple or shifted peaks in their melt curve have been omitted. The average cycle threshold (Ct) values for the nuclear 28S rDNA range between 29.2 ± 0.4 at T0 and 35.5 ± 0.8 at T5, while average Ct for the nucleomorph 28S rDNA is 27.4 ± 0.4 at T0 and 32.9 ± 1.4 at T5 (**Table 1**).

Average cycle thresholds (Cts) of the nuclear and nucleomorph genes are significantly different in *S.* cf. *basimorphum* at T0 ($p < 0.0001$), while they are not different in the *T. amphioxeia* monoculture.

The morphology of ciliates collected on filters was quite well preserved (**Figure 1**). The fluorescent signal obtained upon hybridization with *T. amphioxeia* rRNA probe was clearly detectable within the ciliate cytoplasm (**Figures 1C,D**, **2A–H**).

Prey rRNA is quite spread inside the ciliate cells, but the fluorescent signal is more intense around the ciliate nuclei (**Figures 1C,D**, 2B,C) or in localized clusters within the ciliate cytoplasm (**Figures 2A,E**). The fluorescent signal of the prey rRNA probe could be detected in ciliates at all-time points (**Figure 2**), and its intensity seems comparable among individuals sampled at different time points (**Figures 2E–H**). Individual cells that contained labeled rRNA as wells as individual cells that did not were found in all samples. However, the percentage of positive hybridized cells (over total cell numbers) was not determined. Negative controls of *S.* cf. *basimorphum* fed with a different prey item (*N. rotunda*) did not show any signal of hybridization, confirming the specificity of the probes.

The transcriptomic analysis of the ciliate single cells revealed the presence of transcripts of prey nuclear origin. For each ciliate cell, an average of ∼17 million reads were generated and mapped against the reference transcriptome of *T. amphioxeia*. The mapping revealed the presence of 282 transcripts of prey nuclear and chloroplast origin (**Supplementary Table 2**). Among the 100 most expressed genes of prey origin, there were 11 transcripts of chloroplast origin and six transcripts encoding ribosomal proteins (**Figure 3**). Chloroplast genes included photosystems I and II apoproteins, subunits, and cytochromes. Moreover, we detected prey nuclear-encoded genes involved in amino acid biosynthesis and degradation. Genetic information pathways included genes related to the transcription and translation of the prey nucleus within the host. A detailed list of the retrieved

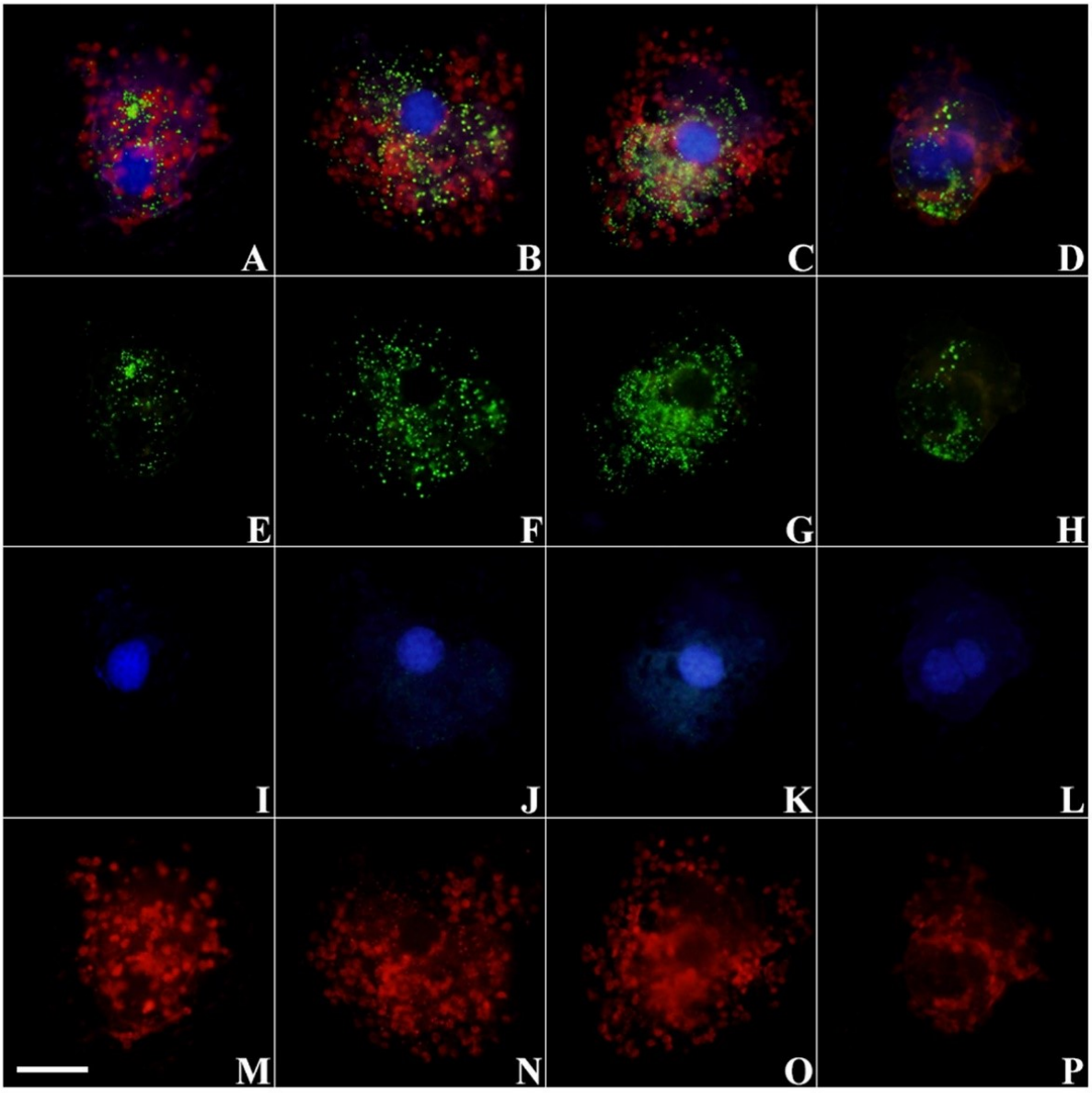

FIGURE 2 | Micrographs of *S.* cf. *basimorphum* cells hybridized with the probe for the prey rRNA (Alexa Fluor 488 dye labeled) and counterstained with DAPI at different time intervals. Combined light channels: **(A)** T0, actively feeding cells; **(B)** T2, prey depleted; **(C)** T5, prey starved; **(D)** T7, prey starved. Single light channels are shown below each cell: **(E–H)** light channel for the FISH probe, showing prey rRNA; **(I–L)** light channel for DAPI, showing ciliates nuclei; and **(M–P)** light channel for chlorophyll autofluorescence, showing chloroplasts. The scale bar in the left bottom corner is 20 μm and refers to all panels. Blue, ciliates nuclei; green, prey RNA; red, chloroplasts.

transcripts and their functional annotation is provided in the **supplementary material**.

DISCUSSION

The retention of prey genetic material is here documented for the first time in a kleptoplastidic *Strombidium* species through the use of specific molecular markers and single-cell transcriptomics. *Strombidium* cf. *basimorphum* is shown to retain genetic material from prey nuclei and nucleomorphs. The observation of prey rRNA and other transcripts of prey nuclear origin suggests that prey genetic material is transcriptionally active inside the ciliate.

Quantitative PCR results suggest that prey DNA disappears quite quickly after ingestion in *S.* cf. *basimorphum*, contrarily to what has been observed in *Mesodinium rubrum*, which is able to retain prey nuclei for up to 10 weeks (Johnson and Stoecker, 2005; Kim et al., 2017).

The relative concentration of the prey nucleomorph gene was higher compared to that of the prey nuclear gene (lower Ct values) in DNA-extracted *S.* cf. *basimorphum* but not in the DNA extracted from the prey monoculture, suggesting that prey

FIGURE 3 | Heatmap representing the 100 most expressed transcripts of prey origin and their corresponding pathways according to the Kyoto Encyclopedia of Genes and Genomes. The expression values are provided for each separate cell and are shown as transcripts per million (TPM). Transcripts that have not been detected are represented in gray. Transcripts of ribosomal and chloroplast origin are highlighted with blue and green asterisks, respectively. The figure was generated using the R package ggplot2.

nucleomorphs are better preserved in the ciliates compared to the prey nuclei. The reason for that may be attributed to the location of the nucleomorph in between the membranes of the chloroplasts of *T. amphioxeia* (Garcia-Cuetos et al., 2010). The location of the nucleomorph in between chloroplasts membranes would eventually preserve it from degradative processes in the ciliate cytoplasm. The presence of the nucleomorph could actually render *Teleaulax* chloroplasts favorable in comparison to other chloroplast types (Altenburger et al., 2020).

The strong fluorescent signal obtained upon hybridization with the prey rRNA probe proves the presence of prey ribosomes within the ciliate. It is not unequivocally proven that those ribosomes are being actively transcribed from the prey nuclear gene. Indeed, ribosomes could have been sequestered from the prey together with chloroplasts, although the general turnover rates make this not the most likely scenario. It is possible that rRNA clusters visualized with FISH in some of the ciliate cells are in fact food vacuoles. However, the fluorescent signal was persistent and diffuse all over the ciliate cytoplasm even after 5 days of prey starvation, suggesting that prey ribosomes are at least somehow maintained in the ciliate and are not only contained concentrated in food vacuoles. Nevertheless, a fraction of cells (not quantified) did not show any fluorescence upon hybridization. This can be ascribed to a dilution of the sequestered genetic material due to cell division, as has been described before in *Mesodinium rubrum* (Kim et al., 2017).

The transcriptional activity of the prey genetic material is proven by the results of the ciliate single-cell transcriptomics. The functional annotation of prey transcripts found in *S.* cf. *basimorphum* revealed the presence of genes of nuclear and chloroplast origin, involved in metabolic processes related to photosynthesis as well as to processes related to transcription and translation. All these processes argue for an active transcription of at least partially remained nuclei of the prey. These results will deserve further and extensive studies to elucidate the responses of the host toward functions related to the kleptoplasts (Uzuka et al., 2019) and the presence of photosynthesis-related genes (and eventually their evolutionary origin) within the genome of the host (Hongo et al., 2019; Hehenberger et al., 2019; Mansour and Anestis, 2021).

The fact that *S.* cf. *basimorphum*, unlike *Mesodinium*, is not able to grow as pure autotroph in the absence of prey could be explained by its need to incorporate nutrients other than carbon through ingestion. Further investigations of its transcriptome and the transcriptional activity of prey genetic material would provide further insight on the metabolism and potential dependence to prey metabolites of this ciliate.

Our study demonstrates the retention of prey genetic material in a *Strombidium* species; to which extent this is true for all plastidic *Strombidium* spp. is presently unknown. If retention of prey genetic material is indeed found in all plastidic *Strombidium* species, it would indicate that it is essential for the survival of plastids inside these ciliates. The ability (or lack of) to retain prey genetic material may also explain why kleptoplasts are not found in all *Strombidium* species and other ciliate groups living in the photic zone of the sea. To get deeper understandings, the same techniques would have to be employed on a natural specimen, and probes for different algal preys would have to be developed.

DATA AVAILABILITY STATEMENT

The datasets presented in this study can be found in online repositories. The names of the repository/repositories and accession number(s) can be found below: https://www.ncbi.nlm.nih.gov/, PRJNA718746.

AUTHOR CONTRIBUTIONS

MM, KA, KK, and UJ did the data acquisition and analysis. PH contributed to data interpretation and draft the manuscript. All authors contributed and commented on earlier versions of the manuscript and approved the final version of the manuscript, and involved in conceiving the study.

FUNDING

This work was supported by the European Union's Horizon 2020 research and innovation program under grant agreement No. 766327. Further financial support was provided by the POF4 subtopic 6.2 research program of the Helmholtz society and the Alfred-Wegener-Institute for Polar and Marine Research and by the project CoCliME. Project CoCliME is part of ERA4CS, an ERA-NET initiated by JPI Climate, and funded by EPA (IE), ANR (FR), BMBF (DE), UEFISCDI (RO), RCN (NO), and FORMAS (SE), with cofunding by the European Union (Grant No. 690462).

ACKNOWLEDGMENTS

We thank Michele Laval-Peuto for her insightful opinions on the interpretation of the experimental results.

SUPPLEMENTARY MATERIAL

The Supplementary Material for this article can be found online at: https://www.frontiersin.org/articles/10.3389/fmicb.2021.694508/full#supplementary-material

REFERENCES

Altenburger, A., Cai, H., Li, Q., Drumm, K., Kim, M., Zhu, Y., et al. (2020). Limits to the cellular control of sequestered cryptophyte prey in the marine ciliate Mesodinium rubrum. *ISME J.* 15, 1056–1072.

Bray, N. L., Pimentel, H., Melsted, P., and Pachter, L. (2016). Near-optimal probabilistic RNA-seq quantification. *Nat. Biotechnol.* 34, 525–527.

De Vries, J., and Archibald, J. M. (2018). Plastid autonomy vs nuclear control over plastid function. 1st ed. elsevier ltd. *Adv. Bot. Res.* 85, 1–28. doi: 10.1016/bs.abr.2017.11.011

Dolan, J. R., and Pérez, M. T. (2000). Costs, benefits and characteristics of mixotrophy in marine oligotrichs. *Freshw. Biol.* 45, 227–238. doi: 10.1046/j.1365-2427.2000.00659.x

Flynn, K. J., Mitra, A., Anestis, K., Anschütz, A. A., Calbet, A., Ferreira, G. D., et al. (2019). Mixotrophic protists and a new paradigm for marine ecology: where does plankton research go now? *J. Plankton Res.* 41, 375–391. doi: 10.1093/plankt/fbz026

Garcia-Cuetos, L., Moestrup, O., Hansen, J., Daugbjerg, N., Hansen, P. J., and Daugbjerg, N. (2010). The toxic dinoflagellate *Dinophysis acuminata* harbors permanent chloroplasts of cryptomonad origin, not kleptochloroplasts. *Harmful Algae* 9, 25–38. doi: 10.1016/j.hal.2009.07.002

Groben, R., and Medlin, L. (2005). *In situ* hybridization of phytoplankton using fluorescently labeled rRNA probes. *Methods Enzymol.* 395, 299–310. doi: 10.1016/S0076-6879(05)95018-0

Guillard, R. R. L. (1975). *Culture of Phytoplankton for Feeding Marine Invertebrates. Culture of Marine Invertebrate Animals*. Boston, MA: Springer, 29–60.

Hansen, P. J., Moldrup, M., Tarangkoon, W., Garcia-Cuetos, L., and Moestrup, O. (2012). Direct evidence for symbiont sequestration in the marine red tide ciliate *Mesodinium rubrum*. *Aquat. Microb. Ecol.* 66, 63–75. doi: 10.3354/ame01559

Hehenberger, E., Gast, R. J., and Keeling, P. J. (2019). A kleptoplastidic dinoflagellate and the tipping point between transient and fully integrated plastid endosymbiosis. *Proc. Natl. Acad. Sci.* 116, 17934–17942. doi: 10.1073/pnas.1910121116

Herfort, L., Zuber, P., Maxey, K., Voorhees, I., Simon, H. M., Grobler, K., et al. (2017). Use of highly specific molecular markers reveals positive correlation between abundances of *Mesodinium* cf . *major* and its preferred prey, *Teleaulax amphioxeia*, during red water blooms in the Columbia river estuary. *J. Eukaryot. Microbiol.* 64, 740–755. doi: 10.1111/jeu.12407

Hongo, Y., Yabuki, A., Fujikura, K., and Nagai, S. (2019). Genes functioned in kleptoplastids of *Dinophysis* are derived from haptophytes rather than from cryptophytes. *Sci. Rep.* 9, 1–11. doi: 10.1038/s41598-019-45326-5

Hughes, E. A., Maselli, M., Sørensen, H., and Hansen, P. J. (2021). Metabolic reliance on photosynthesis depends on both irradiance and prey availability in the mixotrophic ciliate. *Strombidium* cf. *basimorphum*. *Front. Microbiol.* 12:1577. doi: 10.3389/fmicb.2021.642600

Johnson, M. D., and Beaudoin, D. J. (2019). The genetic diversity of plastids associated with mixotrophic oligotrich ciliates. *Limnol. Oceanogr.* 64, 2187–2201. doi: 10.1002/lno.11178

Johnson, M. D., and Stoecker, D. K. (2005). Role of feeding in growth and photophysiology of *Myrionecta rubra*. *Aquat. Microb. Ecol.* 39, 303–312. doi: 10.3354/ame039303

Johnson, M. D., Beaudoin, D. J., Laza-Martinez, A., Dyhrman, S. T., Fensin, E., Lin, S., et al. (2016). The genetic diversity of *Mesodinium* and associated cryptophytes. *Front. Microbiol.* 7:2017. doi: 10.3389/fmicb.2016.02017

Kim, M., Drumm, K., Daugbjerg, N., and Hansen, P. J. (2017). Dynamics of sequestered cryptophyte nuclei in *Mesodinium rubrum* during starvation and refeeding. *Front. Microbiol.* 8:423. doi: 10.3389/fmicb.2017.00423

Kopylova, E., Noé, L., and Touzet, H. (2012). SortMeRNA: Fast and accurate filtering of ribosomal RNAs in metatranscriptomic data. *Bioinformatics* 28, 3211–3217. doi: 10.1093/bioinformatics/bts611

Laval-Peuto, M., and Febvre, M. (1986). On plastid symbiosis in *Tontonia appendiculariformis* (Ciliophora, Oligotrichina). *Biosystems* 19, 137–158.

Liu, W., Yi, Z., Warren, A., Al-Rasheid, K. A., Al-Farraj, S. A., Lin, X., et al. (2011). Taxonomy, morphology and molecular systematics of a new oligotrich ciliate, *Williophrya maedai* gen. nov., sp. nov., with redescriptions of *Strombidium basimorphum* and *Pseudotontonia simplicidens* (Protozoa, Ciliophora, Oligotrichia). *Syst. Biodivers.* 9, 247–258.

Mansour, J. S., and Anestis, K. (2021). Eco-evolutionary perspectives on mixoplankton. *Front. Mar. Sci.* 8:666160. doi: 10.3389/fmars.2021.666160

Martin, A. J., and Montagnes, D. J. (1993). Winter ciliates in a British Columbian fjord: six new species and an analysis of ciliate putative prey. *J. Eukaryot. Microbiol.* 40, 535–549.

Maselli, M., Altenburger, A., Stoecker, D. K., and Hansen, P. J. (2020). Ecophysiological traits of mixotrophic *Strombidium* spp. *J. Plankton Res.* 42, 485–496. doi: 10.1093/plankt/fbaa041

Mcmanus, G. B., Liu, W., Cole, R. A., Biemesderfer, D., and Mydosh, J. L. (2018). Strombidium rassoulzadegani: a model species for chloroplast retention in Oligotrich ciliates. *Front. Mar. Sci.* 5:205. doi: 10.3389/fmars.2018.00205

Mitra, A., Flynn, K. J., Tillmann, U., Raven, J. A., Caron, D., Stoecker, D. K., et al. (2016). Defining planktonic protist functional groups on mechanisms for energy and nutrient acquisition: incorporation of diverse mixotrophic strategies. *Protist* 167, 106–120. doi: 10.1016/j.protis.2016.01.003

Onuma, R., and Horiguchi, T. (2015). Kleptochloroplast enlargement, karyoklepty and the distribution of the cryptomonad nucleus in *Nusuttodinium* (= Gymnodinium) *aeruginosum* (Dinophyceae). *Protist* 166, 177–195.

Onuma, R., Hirooka, S., Kanesaki, Y., Fujiwara, T., Yoshikawa, H., and Miyagishima, S. Y. (2020). Changes in the transcriptome, ploidy, and optimal light intensity of a cryptomonad upon integration into a kleptoplastic dinoflagellate. *ISME J.* 14, 2407–2423.

Orsi, W. D., Wilken, S., del Campo, J., Heger, T., James, E., Richards, T. A., et al. (2018). Identifying protist consumers of photosynthetic picoeukaryotes in the surface ocean using stable isotope probing. *Environ. Microbiol.* 20, 815–827.

Santoferrara, L. F., Guida, S., Zhang, H., and McManus, G. B. (2014). *De novo* transcriptomes of a mixotrophic and a heterotrophic ciliate from marine plankton. *PLoS One* 9:7. doi: 10.1371/journal.pone.0101418

Schoener, D. M., and McManus, G. B. (2012). Plastid retention, use, and replacement in a kleptoplastidic ciliate. *Aquat. Microb. Ecol.* 67, 177–187. doi: 10.3354/ame01601

Schoener, D. M., and McManus, G. B. (2017). Growth, grazing, and inorganic C and N uptake in a mixotrophic and a heterotrophic ciliate. *J. Plankton Res.* 39, 379–391. doi: 10.1093/plankt/fbx014

Smith, M., and Hansen, P. J. (2007). Interaction between *Mesodinium rubrum* and its prey: Importance of prey concentration, irradiance and pH. *Mar. Ecol. Prog. Ser.* 338, 61–70. doi: 10.3354/meps338061

Stoecker, D. K., Johnson, M. D., De Vargas, C., and Not, F. (2009). Acquired phototrophy in aquatic protists. *Aquat. Microb. Ecol.* 57, 279–310. doi: 10.3354/ame01340

Stoecker, D. K., Michaels, A. E., and Davis, L. H. (1987). Large proportion of marine planktonic ciliates found to contain functional chloroplasts. *Nature* 326, 790–792.

Stoecker, D. K., Silver, M. W., Michaels, A. E., and And Davis, L. H. (1988). Obligate mixotrophy in *Laboea strobila* a ciliate which retains chloroplasts. *Mar. Biol.* 99, 415–423. doi: 10.1007/Bf 02112135

Uzuka, A., Kobayashi, Y., Onuma, R., Hirooka, S., Kanesaki, Y., Yoshikawa, H., et al. (2019). Responses of unicellular predators to cope with the phototoxicity of photosynthetic prey. *Nat. Commun.* 10, 1–17. doi: 10.1038/s41467-019-135686

Conflict of Interest: The authors declare that the research was conducted in the absence of any commercial or financial relationships that could be construed as a potential conflict of interest.

Publisher's Note: All claims expressed in this article are solely those of the authors and do not necessarily represent those of their affiliated organizations, or those of the publisher, the editors and the reviewers. Any product that may be evaluated in this article, or claim that may be made by its manufacturer, is not guaranteed or endorsed by the publisher.

Supplementary information

Table S1: Primers and probes used in this study as designed by Herfort et al. 2017

Assay	Gene region	Primer/probe	Sequence (5´–3´)
qPCR	T. amphioxeianuclear 28S rDNAD2	TxD2 1F	TGAAAAAGGGCCTGAAATTG
		TxD2 2R	ATCATTCACTCGCATGCCCC
	T. amphioxeianucleomorph28S rDNAD2	TxNm 1F	ATCCTGGCGCGTGCTTAAAT
		TxNm 1R	CTTCCGTCCGTCCTAAGAACA
FISH	T. amphioxeia nuclear-encoded 28S rRNA D2	TxD2 rRNA	Alexa488AACACACGAGTTAAGATACC AATGGATCATTCACTCGCATGCCC

Table S2: Number of *T. amphioxeia* transcripts found in *S.* cf. *basimorphum* and their functional annotation according to KEGG

KEGG pathway	Number of transcripts
Brite Hierarchies	**94**
Protein families: genetic information processing	72
Protein families: metabolism	1
Protein families: signaling and cellular processes	23
Cellular Processes	**60**
Cell growth and death	24
Cell motility	7
Cellular community – eukaryotes	7
Cellular community – prokaryotes	2
Transport and catabolism	15
Environmental Information Processing	**21**
Membrane transport	3
Signal transduction	18
Genetic Information Processing	**44**
Folding, sorting and degradation	10
Replication and repair	2
Transcription	9
Translation	23
Metabolism	**50**
Amino acidmetabolism	14
Carbohydratemetabolism	6
Energy metabolism	20
Glycanbiosynthesis and metabolism	1
Lipidmetabolism	2
Metabolism of cofactors and vitamins	2
Metabolism of other amino acids	2
Nucleotidemetabolism	1
Not Included in Pathway or Brite	**5**
Unclassified: genetic information processing	2
Unclassified: metabolism	3
Organismal Systems	**11**
Development	1
Digestive system	3
Endocrine system	5
Excretory system	2

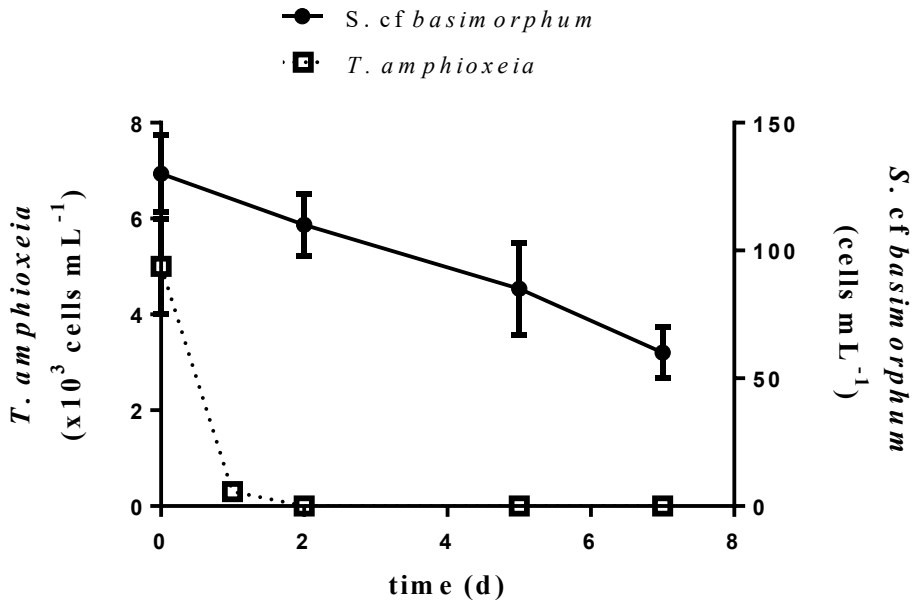

Figure S1: Changes in cell concentrations of *S.*cf. *basimorphum* and *T. amphoxeia* in the experiment. Errors bars represent standard deviation among the three biological replicates.

Synthesis

Mixoplankton and evolution

The meticulous literature review presented in this thesis (**Publication I**) highlights the critical role of phagotrophy in shaping the evolution of life. The two groups of constitutive (CM) and non-constitutive mixoplankton (NCM) have the major common trait of performing phagotrophy and a major difference in the way they perform photosynthesis. The CMs harbor and use plastids innately as the principal and under most circumstances sufficient nutritional mode, while the NCMs need to acquire photosynthetic ability by feeding and subsequently use plastids for carbon fixation. The ability to perform phagotrophy or phototrophy shows plasticity, with multiple observed cases of losses and reacquisition of these two processes by organisms, which further highlights the occurrence of evolutionary constraints that define the success of using either mode of nutrition.

Factors that influence phagotrophy include environmental parameters like light, nutrients and temperature (Li et al., 1999; Hansen, 2011b; Wilken et al., 2013; Anderson et al., 2018b). Phagotrophy is the basis for receiving the subsequent benefits, which in the case of the CMs involve the full digestion of food and subsequent use of the released micro- and macronutrients (Ward et al., 2011; Mitra et al., 2014; Ward and Follows, 2016; Flynn et al., 2018). On the other hand, the partial digestion of food by NCMs allows them to not only receive direct nutrients from the digested prey but also sequester organelles (prevalently plastids) and use them for obtaining carbon from photosynthesis or other essential metabolic products such as lipids and vitamins (Patron et al., 2006; Gawryluk et al., 2019; Hongo et al., 2019; Altenburger et al., 2021).

Mixoplanktonic species are ideal model organisms for studying the evolution of life in the oceans (Jones, 2000; Johnson, 2011; Archibald, 2015). The establishment of photosynthetic capability in eukaryotes is widely accepted to originate from the uptake and integration of a photosynthetic cyanobacterium by an eukaryote, a process known as “primary endosymbiosis” (Cavalier-Smith, 1987; Zimorski et al., 2014). This primary event to date at least – 900 Ma ago and resulted to a primary plastid, which is surrounded by to membranes (Parfrey et al., 2011;

Shih and Matzke, 2013). The subsequent engulfment of primary plastid-bearing organisms by heterotrophs resulted spreading plastids in many lineages through similar secondary or tertiary events (Larkum et al., 2007; Howe et al., 2008; Keeling, 2013).

In addition to the classical theory of endosymbiosis being the main driving factor behind permanent plastid establishment, kleptoplasty has been suggested to have also played a critical role (Bodył, 2018). This is highlighted by the high diversity and complex origin of photosynthesis related genes in both pure photosynthetic and kleptoplastidic organisms. The "shopping bag model" has indeed provided insights on the dynamics of the acquisition of photosynthetic genes, suggesting the uptake and integration of cytosolic DNA from endosymbionts (Larkum et al., 2007; Howe et al., 2008). The presence of photosynthetic genes of various phylogenetic origin in the kleptoplastidic *Dinophysis sp.* supports the "shopping bag model", while studies from the Ross Sea Dinoflagellate stress the importance of the establishment of efficient transcription mechanisms (Hehenberger et al., 2019; Hongo et al., 2019). As presented in **Publication I**, the current evidences from genomic studies in kleptoplastidic and endosymbiotic mixoplankton support the idea that mixoplankton are ideal organisms for studying the dynamics behind the establishment of photosynthesis in eukaryotes.

Key messages:

- ✓ The plasticity in the gain and loss of photosynthetic ability and phagotrophy highlights the occurrence of evolutionary constraints and the important of the environment.
- ✓ The study of mixoplankton can provide with substantial insights on the evolution of permanent plastids as it represents the full gradient from plastid steeling heterotrophs and endosymbiotic mixoplankton (NCM) to grazing phototroph (CMs).

Exploring the potential molecular mechanisms of prymnesin biosynthesis

Prymnesins are chemically classified as polyketides and are known to be produced by *Prymnesium parvum*. **Publication II** reports the presence of multiple polyketide synthases (PKSs) in nine strains of *P. parvum.* The selection of strains that produce different prymnesin types allowed me to identify potential similarities and differences in PKS related to the type of prymnesin. In addition, eight modular type I PKSs were found to be present in all strains, while the expression variance of two contigs was explained by the toxin content, providing promising

candidates for further studying toxin biosynthesis. Out of all PKS domains, the ketosynthase (KS) domain is the most evolutionary conserved and is therefore used for constructing phylogenies. In general, the retrieved KS domains from *P. parvum* fell into the group of haptophytes, in accordance to the topology of phylogenies from known protists (John et al., 2008; Kohli et al., 2016). Moreover, the phylogenetic analysis of KS domains in **Publication II** indicates a relaxed selection pressure leading to highly diverse domains driven by evolutionary processes such as gene duplications and domain shuffling (Beedessee et al., 2019). Sub-clades of *P. parvum* KS sequences were found within the general haptophyte clade (**Publication II**) and were mainly characterized by the converseness of their active sites which play an important role in the functionality of the KS domains (Kwon et al., 1998).

In **Publication II**, longer and higher number of modular type I PKSs were retrieved from the highly toxin producing type B strains. The relationship between toxicity and numbers of PKSs in different species have given mixed results. Larger contigs and a higher number of modular PKS transcripts were retrieved from a highly toxic strain of *Gambierdiscus sp*. compared to a non-toxic one (van Dolah et al., 2020). In another study, PKS transcripts were higher expressed in a toxic strain of *G. balechii* as compared to a non-toxin one (Wu et al., 2020). Other studies have suggested no differences in terms of total number of PKSs transcripts when toxic and non-toxic species or strains of the same species were used, suggesting their constitutive presence in the genome of the organisms (Verma et al., 2019; Vingiani et al., 2020).

The expression pattern of PKS under various salinities, phosphorus (P) availabilities and cell densities was investigated in **Publication III**. The expressed PKSs formed 10 distinct clusters, suggesting changes in expression dynamics influenced by the treatments. Overall, the expression of PKSs was higher under the high cell density conditions, with the exception of the low salinity and P-replete treatment. However, additional cluster were observed, for which the expression of PKSs was higher in P starved cultures. The considerable carbon length of this group of toxins highlights the complexity of the underlying molecular biosynthetic mechanisms and their biosynthesis could potentially involve both PKSs and perhaps partly FAS, as it has been previously described for the biosynthesis of antibiotics from bacteria (Masschelein et al., 2013). A mixed PKS/FAS transcript was consistently highly expressed across all conditions investigated in **Publication III**.

Key messages:

- ✓ Numerous polyketide synthases are reported for nine *P. parvum* strains.
- ✓ The phylogenetic analysis of the KS domains suggests the presence of both mixed haptophyte and *P. parvum* specific clades and provided prevalent candidate genes involved in prymnesin biosynthesis.
- ✓ Expression dynamics of PKSs are mainly influenced by cell density, with higher expression under high cell density conditions.

Mixotrophy and toxin production

The study presented herein (**Publication III**) suggests the occurrence of density dependent mechanisms that regulate toxin production in *P. parvum*, with increasing prymnesin content induced by higher cell densities. Interestingly, cell lysis of *Teleaulax acuta* cells incubated with *P. parvum* was considerably faster under the low salinity conditions. The connection between toxin production and mixotrophy still remains elusive. Toxin production by microalgae has evolved in many groups and can serve for outcompeting grazers and competitors (Selander et al., 2006; Donk and Ianora, 2011). The presence of strains of variable toxin production in the environment suggests the involvement of community related functions with ulterior purpose being the survival of the species. In *P. parvum*, less lytic strains are favored by the lysis of competitors or prey caused by the more lytic strains (Driscoll et al., 2013; John et al., 2015).

In *P. parvum*, toxin production can have direct implications for its fitness as it facilitates capture and subsequent engulfment of motile prey (Skovgaard and Hansen, 2003; Tillmann, 2003). Increased allelopathy (in terms of hemolytic activity) and a subsequent increase in engulfment of bacteria has been previously observed in *P. parvum* growing under P replete condition (Legrand et al., 2001; Beszteri et al., 2012). Additional evidences for toxin-assisted mixotrophy come from *Karlodinum armiger* (Berge et al., 2012) and *Karlodinium veneficum* (Adolf et al., 2006; Sheng et al., 2010). Moreover, another mechanism includes the release of mucus, such as in *Dinophysis sp.* and *Alexandrium pseudogonyaulax* and the formation of traps

which are suggest to stabilize the lytic compounds and capture the prey for subsequent consumption (Blossom et al., 2012; Mafra et al., 2016; Ojamäe et al., 2016).

The evolutionary constraints of mixotrophy include the related metabolic trade-offs, as the use of both photosynthetic and phagotrophic machineries imply certain costs (Raven, 1984, 1997). In the study presented here (**Publication II**), gene expression data was compared to the intracellular toxin content in order to gain insights on the expression pattern of metabolic genes in a gradient of toxin content. The results suggest the generalized down-regulation of metabolic genes with increasing toxin content, while no clear correlation was observed between toxin content and growth rates.

Key messages:

- ✓ Toxin content in *P. parvum* is significantly increased at high cell density conditions.
- ✓ Cell lysis of prey was considerably faster in incubations with *P. parvum* growing under low salinity.
- ✓ Gene expression analysis across a gradient of toxin content in nine *P. parvum* strains suggests the downregulation of metabolic processes with increasing toxin content.

The benefits of mixotrophy under nutrient availability changes

In the study presented herein (**Publication III**), enhanced phagotrophy in *P. parvum* was observed under P starvation and it was independent of the salinity of the cultures. In the experiments presented herein, the growth rates of *P. parvum* feeding on prey seem to not be affected by the increased phagotrophy, supporting the idea of mixotrophy in *P. parvum* is rather a survival strategy than an active way to increase proliferation when compared to pure phototrophic growth (Skovgaard and Hansen, 2003). However, slight increases in growth rate can have enormous effects of the population growth for plankton population due to its high number of individual cells and therefore small change can dramatically multiply the population cell number, but these mild changes are hard to detect statistically in culture experiments with few replicates (Collins and Bell, 2006). The availability of nutrients and light are important prerequisites for autotrophic growth. In nutrient limited environments, mixotrophy is advantageous as it is an efficient mechanism to compensate for missing nutrients either by the

formation of symbiotic relationships or consumption of prey (Stoecker et al., 2017; Hörstmann et al., 2021).

The impact on phagotrophy on the growth rate of mixotrophic species is highly variable and present high diversity among protist groups (Stoecker, 1999). Phagotrophy, at first place, can be ubiquitous or inducible under unfavorable environmental conditions. Dinoflagellates are a good example of the diversity in the degree in which species can engage to mixotrophy. Some dinoflagellate species can grow as pure autotrophs under nutrient-rich medium, while others require the consumption of prey to sustain their growth (Hansen, 2011a). Additionally, induction of phagotrophy due to nutrient limitation is a common phenomenon, highlighting the role of mixotrophy as a survival mechanism (Smalley et al., 2003; Johnson, 2015; Anderson et al., 2018b).

Nutrient limitation can show different degrees ranging from initial nutrient limitation to full cellular nutrient starvation. Changes in cellular nutrient availability would been a significant impact of a certain nutrient in the elemental stoichiometry of a cell. Previous studies in *P. parvum*, have shown that P or N availability can indeed have variable effects on cellular C:N:P stoichiometry (Lindehoff et al., 2009; Lundgren et al., 2016). However, contrary to the results from publication III, no relationship between P limitation and feeding on eukaryotic prey by *P. parvum* was observed, which was attributed to the possibility that no cellular starvation was accomplished (Skovgaard et al., 2003; Lundgren et al., 2016). On the other hand, increased phagotrophy has been observed in P-starved *P. parvum* cells feeding on bacteria (Legrand et al., 2001). In the same study, cellular P content in the P starved *P. parvum* cells increased after the addition of bacteria and became similar to P replete cultures. In the study presented herein (**Publication III**), the measurement of cellular organic POP was not feasible, but it can be assumed that similar compensation mechanisms have occurred.

Key messages:

- ✓ Phosphorus limitation enhanced toxicity and phagotrophy in *P. parvum.*
- ✓ No significant effect on growth rates was observed in *P. parvum* cells feeding on prey.

Kleptokaryon retention in *Strombidium* cf. *basimorphum*

Strombidium cf. *basimorphum* is a non-constitutive mixotroph (NCM) and needs to feed and steal plastids for its prey in order to sustain its growth (Maselli et al., 2020; Hughes et al., 2021). I have used *S.* cf. *basimorphum* (grazer) and *Teleaulax amphioxeia* (prey) as a model system to study the potential control of the prey plastid by either the grazer or the prey nucleus (kleptokaryon). In **Publication IV**, the presence of 282 transcripts of prey origin is reported for *Strombidium* cf. *basimorphum*, using single-cell transcriptomics. This is, to my knowledge, the first known example of nuclei retention in an oligotrich ciliate. The expressed transcripts of *Teleaulax amphioxeia* in the ciliate have nuclear, ribosomal or chloroplast origin (**Publication IV**). The presence of photosynthesis related genes expressed by the prey nucleus suggests that the kleptokaryon could indeed be involved in the maintenance of the kleptoplasts (**Publication IV**). Additionally, supporting evidences for the transcriptional activity of the prey nuclei include the presence of prey genes involved in transcription and translation. Much of the existent knowledge on the dynamics of kleptokaryon retention and transcriptional activity comes from *Mesodinium sp.* (Altenburger et al., 2021). In *Mesodinium sp.*, the long rentention of kleptoplasts of cryptophyte origin is achieved by the significant transcriptional activity of the prey nucleus, which can account for about half of the total transcriptome of the cell (Johnson et al., 2007; Kim et al., 2016; Altenburger et al., 2021). The expressed kleptokaryon genes in *Mesodinium sp.* are involved in the biosynthesis of metabolites and maintenance of the plastids, pathways for which the ciliate lacks the genetic toolkit (Lasek-Nesselquist et al., 2015; Kim et al., 2016). It can thus be concluded that nuclei retention from prey is an effective mechanism to assure the longevity of the kleptoplasts and their efficient functioning in the host cell.

Key messages:

- ✓ The oligotrich ciliate *S.* cf. *basimorphum* retains genetic material from the cryptophyte prey.
- ✓ The expression of prey genes involved in transcription and translation suggest that the kleptokarya remain transcriptionally active within the host

Conclusions

The study of mixoplankton is an emerging topic in marine biology, as more and more research is trying to shed light to the underlying processes of mixoplankton in ecosystem functionality. Even though certain patterns can be observed in terms of phagotrophic rate and environmental parameters such as light, temperature and nutrients, the responses of mixoplankton are strongly species-specific. The rapid development on genomic-based approaches has tremendously contributed to a better understanding of the evolution of life. The application of genomics and transcriptomics in the study of mixoplankton species has provided substantial insights on the dynamics of permanent organelle establishment. Such studies have also revealed the variable degree of integration of the kleptoplasts/endosymbionts in the host, which is further depicted on their various level of genetic connection.

The production of toxins by many CMs is indicative of the different strategies involved in phagotrophy. In the herein presented studies, the potential genes underlying the biosynthesis of prymnesin presented high diversity in different strains of *Prymnesium parvum*, and their phylogenetic analysis shows the presence of general haptophyte and *P. parvum* specific clades. The gene expression analysis of *P. parvum* strains of various toxin content highlights the downregulation of basic metabolic processes with increasing toxin content. Moreover, cell density-dependent mechanisms occur in the biosynthesis of toxin, while transcriptomic data shows distinct patterns related to traits of *P. parvum* ecophysiology such as growth rate, toxin production and adaptation to the different stressors of salinity and phosphorus. Feeding in *Prymnesium parvum* was enhanced under phosphorus limitation, while growth rates seemed unaffected when growing under mixotrophic conditions, supporting the idea that mixotrophy in *P. parvum* is a survival strategy and efficient way to compensate for the lack of macronutrients. However, prey mortality was higher at low salinity, suggesting that prey lysis and phagotrophy are independent and influenced differently by salinity and phosphorus. The measurement of toxin quantity in the medium was not possible in the current studies, and could help in better understanding the dynamics between toxin production and release in the environment.

The ciliate *Strombidium* cf. *basimorphum* is documented as the first oligotrich ciliate to retain transcriptionally active prey genetic material. This suggests the existence of a certain degree of genetic connection between the ciliate and the kleptoplasts, and the occurrence of

molecular mechanisms involved in the maintenance of the kleptoplasts. The presence of genes involved in transcription and translation supports the idea that the kleptokaryon remains active within the ciliate.

Future Perspectives

Over the past few years, an increasing number of studies have reinforced the idea that many mixoplankton species can offer important new knowledge about the evolution of permanent organelles. Isolating and culturing new mixoplankton species with various degree of kleptoplast integration and retention efficiency is critical, as subsequent genomic and physiological studies could contribute to understanding the different stages from pure heterotroph to pure autotroph.

Given the variable responses of mixoplankton to environmental parameters, the combination of multiple treatments and field experiments are prerequisites for better understanding the functionality of mixoplankton in a community context.

The exact role of many toxins produced by mixoplankton still remains elusive, and so are their biosynthetic mechanisms. The development and improvement of next generation sequencing techniques have revolutionized research and their further implementation to generate reference genomes for toxic microalgae seems crucial. The generated reference genomes could assist not only the retrieval of genes potentially involved in toxin biosynthesis, such as polyketide synthases, but provide with a more solid base for future comparative transcriptomic studies. In the case of toxins, it is important to combine genomics/transcriptomics and biochemistry in order to find the connection between gene and product. Moreover, the improvement of chemical approaches to measure prymnesins in the water will assist towards understanding the dynamics of toxin biosynthesis and secretion.

Even though the first evidences for prey nuclei retention in *Strombidium* cf. *basimorphum* are reported, the further investigation of the transcriptome of the ciliate and the contribution of the prey transcriptome to the total cell transcriptome are the first next steps for better understanding the modes of molecular communication between the ciliate and the prey. Moreover specifically, further questions concern the presence of photosynthesis related genes in the genome of the ciliate. New information will help towards placing *S.* cf. *basimorphum* in the spectrum of known plastid control mechanisms known in kleptoplastidic and karyokleptic mixoplankton species.

References

Adolf, J. E., Stoecker, D. K., and Harding, L. W. (2006). The balance of autotrophy and heterotrophy during mixotrophic growth of *Karlodinium micrum* (Dinophyceae). 28, 737-751 doi:10.1093/plankt/fbl007.

Akbar, M. A., Yusof, N. Y. M., Tahir, N. I., Ahmad, A., Usup, G., Sahrani, F. K., et al. (2020). Biosynthesis of saxitoxin in marine dinoflagellates: An omics perspective. *Mar. Drugs* 18, 1–24. doi:10.3390/md18020103.

Altenburger, A., Cai, H., Li, Q., Drumm, K., Kim, M., Zhu, Y., et al. (2021). Limits to the cellular control of sequestered cryptophyte prey in the marine ciliate *Mesodinium rubrum*. *ISME J.* 15, 1056–1072. doi:10.1038/s41396-020-00830-9.

Andersen, K. H., Aksnes, D. L., Berge, T., Fiksen, Ø., and Visser, A. (2015). Modelling emergent trophic strategies in plankton. *J. Plankton Res.* 37, 862–868. doi:10.1093/plankt/fbv054.

Anderson, D. M., Cembella, A. D., and Hallegraeff, G. M. (2012). Progress in understanding harmful algal blooms: Paradigm shifts and new technologies for research, monitoring, and management. *Ann. Rev. Mar. Sci.* 4, 143–176. doi:10.1146/annurev-marine-120308-081121.

Anderson, D. M., Fensin, E., Gobler, C. J., Hoeglund, A. E., Hubbard, K. A., Kulis, D. M., et al. (2021). Marine harmful algal blooms (HABs) in the United States: History, current status and future trends. *Harmful Algae* 102, 101975. doi:10.1016/j.hal.2021.101975.

Anderson, R., Charvet, S., and Hansen, P. (2018a). Mixotrophy in chlorophytes and haptophytes - effect of irradiance, macronutrient, micronutrient and vitamin limitation. *Front Microbiol* 9, 1704. doi:10.3389/FMICB.2018.01704.

Anderson, R., Charvet, S., and Hansen, P. J. (2018b). Mixotrophy in chlorophytes and haptophytes-effect of irradiance, macronutrient, micronutrient and vitamin limitation. *Front. Microbiol.* 9, 1704. doi:10.3389/fmicb.2018.01704.

Anderson, R., Jürgens, K., and Hansen, P. J. (2017). Mixotrophic phytoflagellate bacterivory field measurements strongly biased by standard approaches : A case study. 8, 1–12.

doi:10.3389/fmicb.2017.01398.

Archibald, J. M. (2015). Endosymbiosis and eukaryotic cell evolution. *Curr. Biol.* 25, R911–R921. doi:10.1016/j.cub.2015.07.055.

Barone, R., Castelli, G., and Naselli-Flores, L. (2010). Red sky at night cyanobacteria delight : the role of climate in structuring phytoplankton assemblage in a shallow, Mediterranean lake (Biviere di Gela, southeastern Sicily). *Hydrobiologia* 639, 43–53. doi:10.1007/s10750-009-0016-2.

Beisner, B. E., Grossart, H.-P., and Gasol, J. M. (2019). A guide to methods for estimating phago-mixotrophy in nanophytoplankton. *J. Plankton Res.* doi:10.1093/plankt/fbz008.

Berge, T., Poulsen, L. K., Moldrup, M., Daugbjerg, N., and Hansen, P. J. (2012). Marine microalgae attack and feed on metazoans. *ISME J.*, 1926–1936. doi:10.1038/ismej.2012.29.

Beszteri, S., Yang, I., Jaeckisch, N., Tillmann, U., Frickenhaus, S., Glöckner, G., et al. (2012). Transcriptomic response of the toxic prymnesiophyte *Prymnesium parvum* (N. Carter) to phosphorus and nitrogen starvation. *Harmful Algae* 18, 1–15. doi:10.1016/j.hal.2012.03.003.

Binzer, S. B., Svenssen, D. K., Daugbjerg, N., Alves-de-Souza, C., Pinto, E., Hansen, P. J., et al. (2019). A-, B- and C-type prymnesins are clade specific compounds and chemotaxonomic markers in *Prymnesium parvum*. *Harmful Algae* 81, 10–17. doi:10.1016/J.HAL.2018.11.010.

Blossom, H. E., Daugbjerg, N., and Juel, P. (2012). Toxic mucus traps : A novel mechanism that mediates prey uptake in the mixotrophic dinoflagellate *Alexandrium pseudogonyaulax*. *Harmful Algae* 17, 40–53. doi:10.1016/j.hal.2012.02.010.

Blossom, H. E. (2018). Mixotrophy and toxicity in harmful microalgae. Department of Biology, Faculty of Science, University of Copenhagen.

Bodył, A. (2018). Did some red alga-derived plastids evolve via kleptoplastidy? A hypothesis. *Biol. Rev.* 93, 201–222. doi:10.1111/brv.12340.

Brunson, J. K., McKinnie, S. M. K., Chekan, J. R., McCrow, J. P., Miles, Z. D., Bertrand, E.

M., et al. (2018). Biosynthesis of the neurotoxin domoic acid in a bloom-forming diatom. *Science (80).* 361, 1356–1358. doi:10.1126/science.aau0382.

Burkholder, J. A. M., Glibert, P. M., and Skelton, H. M. (2008). Mixotrophy, a major mode of nutrition for harmful algal species in eutrophic waters. *Harmful Algae* 8, 77–93. doi:10.1016/j.hal.2008.08.010.

Burns, J. A., Pittis, A. A., and Kim, E. (2018). Gene-based predictive models of trophic modes suggest Asgard archaea are not phagocytotic. *Nat. Ecol. Evol.* 2, 697–704. doi:10.1038/s41559-018-0477-7.

Cane, D. E., Walsh, C. T., and Khosla, C. (1998). Harnessing the biosynthetic code: Combinations, permutations, and mutations. *Science (80).* 282, 63–68. doi:10.1126/science.282.5386.63.

Cavalier-Smith, T. (1987). The simultaneous symbiotic origin of mitochondria, chloroplasts, and microbodies. *Ann. N. Y. Acad. Sci.* 503, 55–71. doi:10.1111/j.1749-6632.1987.tb40597.x.

Chan, Y. F., Chiang, K. P., Ku, Y., and Gong, G. C. (2019). Abiotic and biotic factors affecting the ingestion rates of mixotrophic nanoflagellates (Haptophyta). *Microb. Ecol.* 77, 607–615. doi:10.1007/s00248-018-1249-2.

Collins, S., and Bell, G. (2006). Evolution of natural algal populations at elevated CO2. *Ecol. Lett.* 9, 129–135. doi:10.1111/j.1461-0248.2005.00854.x.

Donk, E. Van, and Ianora, A. (2011). Induced defences in marine and freshwater phytoplankton: a review. *Hydrobiologia* 668, 3–19. doi:10.1007/s10750-010-0395-4.

Driscoll, W. W., Espinosa, N. J., Eldakar, O. T., and Hackett, J. D. (2013). Allelopathy as an emergent, exploitable public good in the bloom-forming microalga *Prymnesium parvum*. *Evolution (N. Y).* 67, 1582–1590. doi:10.1111/evo.12030.

Edvardsen, B., and Paasche, E. (1998). “Bloom dynamics and physiology of Prymnesium and Chrysochromulina,” in *Physiological Ecology of Harmful Algal Blooms*, eds. D. M. Anderson, A. D. Cembella, and G. M. Hallegraeff (Springer-Verl, Berlin/Heidelberg, Germany), 193–208.

Ferrer, J. L., Jez, J. M., Bowman, M. E., Dixon, R. A., and Noel, J. P. (1999). Structure of chalcone synthase and the molecular basis of plant polyketide biosynthesis. *Nat. Struct. Biol.* 6, 775–784. doi:10.1038/11553.

Flöder, S., Hansen, T., and Ptacnik, R. (2006). Energy-dependent bacterivory in ochromonas minima - a strategy promoting the use of substitutable resources and survival at insufficient light supply. *Protist* 157, 291–302. doi:10.1016/j.protis.2006.05.002.

Flynn, K. J., and Mitra, A. (2009). Building the "perfect beast": Modelling mixotrophic plankton. *J. Plankton Res.* 31, 965–992. doi:10.1093/plankt/fbp044.

Flynn, K. J., Mitra, A., Anestis, K., Anschütz, A. A., Calbet, A., Ferreira, G. D., et al. (2019). Mixotrophic protists and a new paradigm for marine ecology: Where does plankton research go now? *J. Plankton Res.* 41, 375–391. doi:10.1093/plankt/fbz026.

Flynn, K. J., Mitra, A., Glibert, P. M., and Burkholder, J. A. M. (2018). "Mixotrophy in harmful algal blooms: by whom, on whom, when, why, and what next," in *Global Ecology and Biogeography*, eds. P. M. Glibert, E. Berdalet, M. A. Burford, G. C. Pitcher, and M. Zhou (Springer), 113–132.

Flynn, K. J., Stoecker, D. K., Mitra, A., Raven, J. A., Glibert, P. M., Hansen, P. J., et al. (2013). Misuse of the phytoplankton-zooplankton dichotomy: The need to assign organisms as mixotrophs within plankton functional types. *J. Plankton Res.* 35, 3–11. doi:10.1093/plankt/fbs062.

Freitag, M., Beszteri, S., Vogel, H., John, U., Freitag, M., Beszteri, S., et al. (2011). Effects of physiological shock treatments on toxicity and polyketide synthase gene expression in *Prymnesium parvum* (Prymnesiophyceae). *Eur. J. Phycol.* 46, 193–201. doi:10.1080/09670262.2011.591438.

Gawryluk, R. M. R., Tikhonenkov, D. V., Hehenberger, E., Husnik, F., Mylnikov, A. P., and Keeling, P. J. (2019). Non-photosynthetic predators are sister to red algae. *Nature* 572, 240–243. doi:10.1038/s41586-019-1398-6.

Gobler, C. J. (2020). Climate change and harmful algal blooms: Insights and perspective. *Harmful Algae* 91, 101731. doi:10.1016/j.hal.2019.101731.

Gobler, C. J., Doherty, O. M., Hattenrath-Lehmann, T. K., Griffith, A. W., Kang, Y., and

Litaker, R. W. (2017). Ocean warming since 1982 has expanded the niche of toxic algal blooms in the North Atlantic and North Pacific oceans. *Proc. Natl. Acad. Sci. U. S. A.* 114, 4975–4980. doi:10.1073/pnas.1619575114.

González-Olalla, J. M., Medina-Sánchez, J. M., and Carrillo, P. (2019). Mixotrophic trade-off under warming and UVR in a marine and a freshwater alga. *J. Phycol.* 55, 1028–1040. doi:10.1111/jpy.12865.

Green, B. J., Fox, T. C., and Rumpho, M. E. (2005). Stability of isolated algal chloroplasts that participate in a unique mollusc/kleptoplast association. *Symbiosis* 40, 31–40.

Hallegraeff, G., Enevoldsen, H., and Zingone, A. (2021a). Global harmful algal bloom status reporting. *Harmful Algae* 102. doi:10.1016/j.hal.2021.101992.

Hallegraeff, G. M., Anderson, D. M., Belin, C., Bottein, M.-Y. D., Bresnan, E., Chinain, M., et al. (2021b). Perceived global increase in algal blooms is attributable to intensified monitoring and emerging bloom impacts. *Commun. Earth Environ.* 2. doi:10.1038/s43247-021-00178-8.

Hansen, P. J. (2011a). The role of photosynthesis and food uptake for the growth of marine mixotrophic dinoflagellates. *J. Eukaryot. Microbiol.* 58, 203–214. doi:10.1111/j.1550-7408.2011.00537.x.

Hansen, P. J. (2011b). The Role of Photosynthesis and Food Uptake for the Growth of Marine Mixotrophic Dinoflagellates1. *J. Eukaryot. Microbiol.* 58, 203–214. doi:10.1111/j.1550-7408.2011.00537.x.

Hansen, P. J., Anderson, R., Stoecker, D. K., Decelle, J., Altenburger, A., Blossom, H. E., et al. (2019). Mixotrophy among freshwater and marine protists. Elsevier Ltd. doi:10.1016/B978-0-12-809633-8.20685-7.

Hansen, P. J., Nielsen, L. T., Johnson, M., Berge, T., and Flynn, K. J. (2013). Acquired phototrophy in *Mesodinium* and *Dinophysis* – A review of cellular organization, prey selectivity, nutrient uptake and bioenergetics. *Harmful Algae* 28, 126–139. doi:10.1016/J.HAL.2013.06.004.

Hansen, P. J., Ojamäe, K., Berge, T., Trampe, E. C. L., Nielsen, L. T., Lips, I., et al. (2016). Photoregulation in a kleptochloroplastidic dinoflagellate, *Dinophysis acuta*. *Front.*

Microbiol. 7, 785. doi:10.3389/fmicb.2016.00785.

Haroardóttir, S., Wohlrab, S., Hjort, D. M., Krock, B., Nielsen, T. G., John, U., et al. (2019). Transcriptomic responses to grazing reveal the metabolic pathway leading to the biosynthesis of domoic acid and highlight different defense strategies in diatoms. *BMC Mol. Biol.* 20, 1–14. doi:10.1186/s12867-019-0124-0.

Hehenberger, E., Gast, R. J., and Keeling, P. J. (2019). A kleptoplastidic dinoflagellate and the tipping point between transient and fully integrated plastid endosymbiosis. *Proc. Natl. Acad. Sci.* 116, 17934–17942. doi:10.1073/PNAS.1910121116.

Heisler, J., Glibert, P. M., Burkholder, J. M., Anderson, D. M., Cochlan, W., Dennison, W. C., et al. (2008). Eutrophication and harmful algal blooms: A scientific consensus. *Harmful Algae* 8, 3–13. doi:10.1016/j.hal.2008.08.006.

Hongo, Y., Yabuki, A., Fujikura, K., and Nagai, S. (2019). Genes functioned in kleptoplastids of *Dinophysis* are derived from haptophytes rather than from cryptophytes. *Sci. Rep.* 9, 1–11. doi:10.1038/s41598-019-45326-5.

Hörstmann, C., Buttigieg, P. L., John, U., Raes, E. J., Wolf-gladrow, D., Bracher, A., et al. (2021). Microbial diversity through an oceanographic lens : refining the concept of ocean provinces through trophic-level analysis and productivity-speci fi c length scales. 00. doi:10.1111/1462-2920.15832.

Howe, C. J., Barbrook, A. C., Nisbet, R. E. R., Lockhart, P. J., and Larkum, A. W. D. (2008). The origin of plastids. *Philos. Trans. R. Soc. B Biol. Sci.* 363, 2675–2685. doi:10.1098/rstb.2008.0050.

Hughes, E. A., Maselli, M., Sørensen, H., and Hansen, P. J. (2021). Metabolic Reliance on Photosynthesis Depends on Both Irradiance and Prey Availability in the Mixotrophic Ciliate, Strombidium cf. basimorphum. *Front. Microbiol.* 12. doi:10.3389/fmicb.2021.642600.

Igarashi, T., Satake, M., and Yasumoto, T. (1999). Structures and partial stereochemical assignments for prymnesin-1 and prymnesin-2: potent hemolytic and ichthyotoxic glycosides isolated from the red tide alga *Prymnesium parvum*. *J. Am. Chem. Soc.*, 8499–8511. doi:10.1021/ja991740e.

James, K. J., Carey, B., O'Halloran, J., Van Pelt, F. N. A. M., and Škrabáková, Z. (2010). Shellfish toxicity: Human health implications of marine algal toxins. *Epidemiol. Infect.* 138, 927–940. doi:10.1017/S0950268810000853.

Jenke-Kodama, H., Sandmann, A., Müller, R., and Dittmann, E. (2005). Evolutionary implications of bacterial polyketide synthases. *Mol. Biol. Evol.* 22, 2027–2039. doi:10.1093/molbev/msi193.

John, U., Beszteri, B., Derelle, E., Van de Peer, Y., Read, B., Moreau, H., et al. (2008). Novel insights into evolution of protistan polyketide synthases through phylogenomic analysis. *Protist* 159, 21–30. doi:10.1016/j.protis.2007.08.001.

John, U., Beszteri, S., Glöckner, G., Singh, R., Medlin, L., Cembella, A. D., et al. (2010). Genomic characterisation of the ichthyotoxic prymnesiophyte *Chrysochromulina polylepis*, and the expression of polyketide synthase genes in synchronized cultures. 45, 215–229. doi:10.1080/09670261003746193.

John, U., Tillmann, U., Hülskötter, J., Alpermann, T. J., Wohlrab, S., and Van de Waal, D. B. (2015). Intraspecific facilitation by allelochemical mediated grazing protection within a toxigenic dinoflagellate population. *Proc. R. Soc. B Biol. Sci.* 282. doi:10.1098/rspb.2014.1268.

Johnson, M. D. (2011). The acquisition of phototrophy: Adaptive strategies of hosting endosymbionts and organelles. *Photosynth. Res.* 107, 117–132. doi:10.1007/s11120-010-9546-8.

Johnson, M. D. (2015). Inducible Mixotrophy in the Dinoflagellate Prorocentrum minimum. *J. Eukaryot. Microbiol.* 62, 431–443. doi:10.1111/jeu.12198.

Johnson, M. D., Oldach, D., Delwiche, C. F., and Stoecker, D. K. (2007). Retention of transcriptionally active cryptophyte nuclei by the ciliate *Myrionecta rubra*. *Nature* 445, 426–428. doi:10.1038/nature05496.

Jones, R. I. (2000). Mixotrophy in planktonic protists: An overview. *Freshw. Biol.* 45, 219–226. doi:10.1046/j.1365-2427.2000.00672.x.

Keeling, P. J. (2013). The number, speed, and impact of plastid endosymbioses in eukaryotic evolution. *Annu. Rev. Plant Biol.* 64, 583–607. doi:10.1146/annurev-arplant-050312-

120144.

Keller, M. D., Shapiro, L. P., Haugen, E. M., Cucci, T. L., Sherr, E. B., and Sherr, B. F. (1994). Phagotrophy of fluorescently labeled bacteria by an oceanic phytoplankter. *Microb. Ecol.* 28, 39–52. doi:10.1007/BF00170246.

Kim, G. H., Han, J. H., Kim, B., Han, J. W., Nam, S. W., Shin, W., et al. (2016). Cryptophyte gene regulation in the kleptoplastidic, karyokleptic ciliate Mesodinium rubrum. *Harmful Algae* 52, 23–33. doi:10.1016/j.hal.2015.12.004.

Kohli, G. S., John, U., Van Dolah, F. M., and Murray, S. A. (2016). Evolutionary distinctiveness of fatty acid and polyketide synthesis in eukaryotes. *ISME J.* 10, 1877–1890. doi:10.1038/ismej.2015.263.

Kwon, H., Smith, W. C., Scharon, A. J., Hwang, S. H., Kurth, M. J., and Shen, B. (1998). C-O Bond formation by polyketide synthases. *Science (80-.).* 297, 1327–1330.

Larkum, A. W. D., Lockhart, P. J., and Howe, C. J. (2007). Shopping for plastids. *Trends Plant Sci.* 12, 189–195. doi:10.1016/j.tplants.2007.03.011.

Lasek-Nesselquist, E., Wisecaver, J. H., Hackett, J. D., and Johnson, M. D. (2015). Insights into transcriptional changes that accompany organelle sequestration from the stolen nucleus of Mesodinium rubrum. *BMC Genomics* 16, 1–14. doi:10.1186/s12864-015-2052-9.

Legrand, C., Johansson, N., Johnsen, G., Borsheim, K. Y., and Granéli, E. (2001). Phagotrophy and toxicity variation in the mixotrophic Prymnesium patelliferum (Haptophyceae). *Limnol. Oceanogr.* 46, 1208–1214. doi:10.4319/lo.2001.46.5.1208.

Lewitus, A. J., Horner, R. A., Caron, D. A., Garcia-Mendoza, E., Hickey, B. M., Hunter, M., et al. (2012). Harmful algal blooms along the North American west coast region: History, trends, causes, and impacts. *Harmful Algae* 19, 133–159. doi:10.1016/j.hal.2012.06.009.

Li, A., Stoecker, D. K., and Adolf, J. E. (1999). Feeding, pigmentation, photosynthesis and growth of the mixotrophic dinoflagellate Gyrodinium galatheanum. *Aquat. Microb. Ecol.* 19, 163–176. doi:10.3354/ame019163.

Lindehoff, E., Graneli, E., and Graneli, W. (2009). Effect of tertiary sewage effluent additions

on Prymnesium parvum cell toxicity and stable isotope ratios. 8, 247–253. doi:10.1016/j.hal.2008.06.004.

Lundgren, V. M., Glibert, P. M., Granéli, E., Vidyarathna, N. K., Fiori, E., Ou, L., et al. (2016). Metabolic and physiological changes in *Prymnesium parvum* when grown under, and grazing on prey of, variable nitrogen:Phosphorus stoichiometry. *Harmful Algae* 55, 1–12. doi:10.1016/j.hal.2016.01.002.

Mafra, L. L., Nagai, S., Uchida, H., Tavares, C. P. S., Escobar, B. P., and Suzuki, T. (2016). Harmful effects of Dinophysis to the ciliate Mesodinium rubrum : Implications for prey capture. *Harmful Algae* 59, 82–90. doi:10.1016/j.hal.2016.09.009.

Maselli, M., Altenburger, A., Stoecker, D. K., and Hansen, P. J. (2020). Ecophysiological traits of mixotrophic Strombidium spp. *J. Plankton Res.* 42, 485–496. doi:10.1093/plankt/fbaa041.

Masschelein, J., Mattheus, W., Gao, L. J., Moons, P., van Houdt, R., Uytterhoeven, B., et al. (2013). A PKS/NRPS/FAS hybrid gene cluster from *Serratia plymuthica* RVH1 encoding the biosynthesis of three broad spectrum, zeamine-related antibiotics. *PLoS One* 8. doi:10.1371/journal.pone.0054143.

Meire, L., Mortensen, J., Meire, P., Juul-Pedersen, T., Sejr, M. K., Rysgaard, S., et al. (2017). Marine-terminating glaciers sustain high productivity in Greenland fjords. *Glob. Chang. Biol.* 23, 5344–5357. doi:10.1111/gcb.13801.

Mitra, A., Flynn, K. J., Burkholder, J. M., Berge, T., Calbet, A., Raven, J. A., et al. (2014). The role of mixotrophic protists in the biological carbon pump. *Biogeosciences* 11, 995–1005. doi:10.5194/bg-11-995-2014.

Mitra, A., Flynn, K. J., Tillmann, U., Raven, J. A., Caron, D., Stoecker, D. K., et al. (2016). Defining planktonic protist functional groups on mechanisms for energy and nutrient acquisition: incorporation of diverse mixotrophic strategies. *Protist* 167, 106–120. doi:10.1016/j.protis.2016.01.003.

Ojamäe, K., Hansen, P. J., and Lips, I. (2016). Mass entrapment and lysis of Mesodinium rubrum cells in mucus threads observed in cultures with Dinophysis. 55, 77–84. doi:10.1016/j.hal.2016.02.001.

Onuma, R., Hirooka, S., Kanesaki, Y., Fujiwara, T., Yoshikawa, H., and Miyagishima, S. ya (2020). Changes in the transcriptome, ploidy, and optimal light intensity of a cryptomonad upon integration into a kleptoplastic dinoflagellate. *ISME J.* doi:10.1038/s41396-020-0693-4.

Orr, R. J. S., Stüken, A., Murray, S. A., and Jakobsen, K. S. (2013). Evolution and distribution of saxitoxin biosynthesis in dinoflagellates. *Mar. Drugs* 11, 2814–2828. doi:10.3390/md11082814.

Parfrey, L. W., Lahr, D. J. G., Knoll, A. H., and Katz, L. A. (2011). Estimating the timing of early eukaryotic diversi fi cation with multigene molecular clocks. 108, 13624–13629. doi:10.1073/pnas.1110633108.

Park, M. G., Kim, M., and Kim, S. (2014). The acquisition of plastids/phototrophy in heterotrophic dinoflagellates. *Acta Protozool.* 53, 39–50. doi:10.4467/16890027AP.14.005.1442.

Patron, N. J., Waller, R. F., and Keeling, P. J. (2006). A tertiary plastid uses genes from two endosymbionts. *J. Mol. Biol.* 357, 1373–1382. doi:10.1016/j.jmb.2006.01.084.

Pillet, L., and Pawlowski, J. (2013). Transcriptome analysis of foraminiferan elphidium margaritaceum questions the role of gene transfer in kleptoplastidy. *Mol. Biol. Evol.* 30, 66–69. doi:10.1093/molbev/mss226.

Rasmussen, S. A., Meier, S., Andersen, N. G., Blossom, H. E., Duus, J. Ø., Nielsen, K. F., et al. (2016). Chemodiversity of ladder-frame prymnesin polyethers in *Prymnesium parvum*. *J. Nat. Prod.* 79, 2250–2256. doi:10.1021/acs.jnatprod.6b00345.

Raven, J. A. (1984). A COST-BENEFIT ANALYSIS OF PHOTON ABSORPTION BY PHOTOSYNTHETIC UNICELLS. *New Phytol.* 98, 593–625. doi:10.1111/j.1469-8137.1984.tb04152.x.

Raven, J. A. (1997). Phagotrophy in phototrophs. *Limnol. Oceanogr.* 42, 198–205. doi:10.4319/lo.1997.42.1.0198.

Rein, K. S., and Borrone, J. (1999). Polyketides from dinoflagellates: origins , pharmacology and biosynthesis. *Comp. Biochem. Physiol.* 124, 117–131. doi:doi: 10.1016/s0305-0491(99)00107-8.

Roelke, D. L., Barkoh, A., Brooks, B. W., Grover, J. P., Hambright, K. D., Laclaire, J. W., et al. (2016). A chronicle of a killer alga in the west: Ecology, assessment, and management of *Prymnesium parvum* blooms. *Hydrobiologia* 764, 29–50. doi:10.1007/s10750-015-2273-6.

Roelke, D. L., Grover, J. P., Brooks, B. W., Joanglass, Davidbuzan, Southard, G. M., et al. (2011). A decade of fish-killing *Prymnesium parvum* blooms in Texas: Roles of in flow and salinity. *J. Plankton Res.* 33, 243–253. doi:10.1093/plankt/fbq079.

Selander, E., Thor, P., Toth, G., Pavia, H., and Ety, S. (2006). Copepods induce paralytic shellfish toxin production in marine dinoflagellates. *Proc. R. Soc. B Biol. Sci.* 273, 1673–1680. doi:10.1098/rspb.2006.3502.

Selosse, M. A., Charpin, M., and Not, F. (2017). Mixotrophy everywhere on land and in water: the grand écart hypothesis. *Ecol. Lett.* 20, 246–263. doi:10.1111/ele.12714.

Serôdio, J., Cruz, S., Cartaxana, P., and Calado, R. (2014). Photophysiology of kleptoplasts: Photosynthetic use of light by chloroplasts living in animal cells. *Philos. Trans. R. Soc. B Biol. Sci.* 369. doi:10.1098/rstb.2013.0242.

Sheng, J., Malkiel, E., Katz, J., Adolf, J. E., and Place, A. R. (2010). A dino fl agellate exploits toxins to immobilize prey prior to ingestion. 107, 1–6. doi:10.1073/pnas.0912254107.

Shih, P. M., and Matzke, N. J. (2013). Primary endosymbiosis events date to the later Proterozoic with cross-calibrated phylogenetic dating of duplicated ATPase proteins. 110, 12355–12360. doi:10.1073/pnas.1305813110.

Skovgaard, A. (1996). Mixotrophy in Fragilidium subglobosum (Dinophyceae): Growth and grazing responses as functions of light intensity. *Mar. Ecol. Prog. Ser.* 143, 247–253. doi:10.3354/meps143247.

Skovgaard, A., and Hansen, P. J. (2003). Food uptake in the harmful alga *Prymnesium parvum* mediated by excreted toxins. *Limnol. Oceanogr.* 48, 1161–1166. doi:10.4319/lo.2003.48.3.1161.

Skovgaard, A., Legrand, C., Hansen, P., and Granéli, E. (2003). Effects of nutrient limitation on food uptake in the toxic haptophyte *Prymnesium parvum*. *Aquat. Microb. Ecol.* 31, 259–265. doi:10.3354/ame031259.

Smalley, G., Coats, D., and Stoecker, D. (2003). Feeding in the mixotrophic dinoflagellate Ceratium furca is influenced by intracellular nutrient concentrations. *Mar. Ecol. Prog. Ser.* 262, 137–151. doi:10.3354/meps262137.

Smayda, T. J. (1997). Bloom dynamics : Physiology , behavior , trophic e : ffects. 1132–1136.

Staunton, J., and Weissman, K. J. (2001). Polyketide biosynthesis: A millennium review. *Nat. Prod. Rep.* 18, 380–416. doi:10.1039/a909079g.

Stoecker, D. K. (1999). Mixotrophy among dinoflagellates. *J. Eukaryot. Microbiol.* 46, 397–401. doi:10.1111/j.1550-7408.1999.tb04619.x.

Stoecker, D. K., Hansen, P. J., Caron, D. A., and Mitra, A. (2017). Mixotrophy in the marine plankton. *Ann. Rev. Mar. Sci.* 9, 311–335. doi:10.1146/annurev-marine-010816-060617.

Stoecker, D. K., Johnson, M. D., De Vargas, C., and Not, F. (2009). Acquired phototrophy in aquatic protists. *Aquat. Microb. Ecol.* 57, 279–310. doi:10.3354/ame01340.

Tillmann, U. (2003). Kill and eat your predator: A winning strategy of the planktonic flagellate *Prymnesium parvum*. *Aquat. Microb. Ecol.* 32, 73–84. doi:10.3354/ame032073.

Wagstaff, B. A., Hems, E. S., Rejzek, M., Pratscher, J., Brooks, E., Kuhaudomlarp, S., et al. (2018). Insights into toxic *Prymnesium parvum* blooms: the role of sugars and algal viruses. *Biochem. Soc. Trans.* 0, BST20170393. doi:10.1042/BST20170393.

Wagstaff, B. A., Vladu, I. C., Barclay, J. E., Schroeder, D. C., Malin, G., and Field, R. A. (2017). Isolation and characterization of a double stranded DNA megavirus infecting the toxin-producing haptophyte *Prymnesium parvum*. *Viruses* 9. doi:10.3390/v9030040.

Ward, B. A., Dutkiewicz, S., Barton, A. D., and Follows, M. J. (2011). Biophysical aspects of resource acquisition and competition in algal mixotrophs. *Am. Nat.* 178, 98–112. doi:10.1086/660284.

Ward, B. A., and Follows, M. J. (2016). Marine mixotrophy increases trophic transfer efficiency, mean organism size, and vertical carbon flux. *Proc. Natl. Acad. Sci. U. S. A.* 113, 2958–2963. doi:10.1073/pnas.1517118113.

Weissman, K. J. (2015). Uncovering the structures of modular polyketide synthases. *Nat. Prod. Rep.* 32, 436–453. doi:10.1039/c4np00098f.

Wilken, S., Huisman, J., Naus-Wiezer, S., and Van Donk, E. (2013). Mixotrophic organisms become more heterotrophic with rising temperature. *Ecol. Lett.* 16, 225–233. doi:10.1111/ele.12033.

Wright, J., and Cembella, A. (1998). "Ecophysiology and biosynthesis of polyether marine biotoxins," in *Physiological Ecology of Harmful Algal Blooms*, ed. G. Anderson, DM, Cembella, AD, Hallegraef (Springer-Verlag), 427–451.

Zimorski, V., Ku, C., Martin, W. F., and Gould, S. B. (2014). Endosymbiotic theory for organelle origins. *Curr. Opin. Microbiol.* 22, 38–48. doi:10.1016/j.mib.2014.09.008.